GEOCHEMICAL INVESTIGATION OF COMPOSITE BODIES INVOLVING INTERMEDIATE MEMBERS OF THE ALKALI BASALT - TRACHYTE SUITE

by

W.W. Boyd Jr., B.Sc.

Thesis presented for the DEGREE OF DOCTOR OF PHILOSOPHY of the UNIVERSITY OF EDINBURGH in the FACULTY OF SCIENCE

1974

CONTENTS

SUMMARY

The geochemistry of the intermediate members (hawaiites, mugearites, benmoreites) of the alkali-olivine basalt-trachyte suite occurring as composite bodies is reviewed.

Typically, but not invariably, the porphyritic unit is hawaiite and the nearly aphyric unit a mugearite or benmoreite.

The four suites studied represent composite flows in both Tertiary and Carboniferous volcanics as well as composite sills and dykes ranging in age from Pre Cambrian to Pleistocene.

The hawaiite members of the composite bodies contain a wide range of plagioclase phenocryst composition; from bytownite to andesine. They may be accompanied by phases interpreted as originating in the immediate parental liquids at higher pressures. At least part of the variability in trace element distribution may be attributed to the polybaric fractionation of the phases observed.

Mugearites and benmoreites show less variability in their phenocryst composition, but an equally variable trace element distribution. This is not inconsistent with their postulated origin by crystal fractionation at relatively low pressures from hawaiites, themselves displaying a highly variable trace element content.

Ba, Sr, Zr, Zn, and Y all increase in passing from hawaiites to the mugearites; Rb is highly variable in content, but also shows an increase. The content of Nb increases, but at a much slower rate. Ni shows a marked decrease.

The content of Ba, Zr and possibly Zn, rises in passing from the mugearites to the benmoreites; the content of Sr

and Ni decreases. Rb, Y and Nb are highly variable; the content either rises very slowly or remains steady.

The field, mineralogical and geochemical data are consistent with the various crystal fractionation models proposed to explain the genesis of such bodies. Most of the bodies are believed to have developed in high level, compositionally zoned magma chambers. The composite flows represent the relatively rapid extrusion of lavas from such chambers; the various intrusive bodies represent either the serial tapping of such chambers to fill high level subadjacent cavities, or planar sections through such chambers exposed by erosion.

CHAPTER 1

AIMS AND OBJECTIVES OF PRESENT STUDY

The close field association of porphyritic and nearly aphyric members of the alkali-olivine basalt-trachyte suite has long been recognized by geologists. Flows of hawaiitic and mugearitic composition are abundant in the late stages of development in many alkaline or "transitional" (to tholeiitic) volcanic series. These flows frequently show the distinctive textural feature noted above: the hawaiites being porphyritic, with predominating plagioclase phenocrysts, and the mugearites being aphyric, or nearly so.

The association has been recognized in a number of well studied sequences: Ben More on Mull, Mauna Kea on Hawaii, Nandewar in Australia, as well as the suites studied in the present thesis. This association not only occurs as successive flows, in which a substantial time interval separates the eruptive events, but as composite flows or intrusions where the time interval is minimal or non-existent. Commonly, but not invariably, the porphyritic member is the more basic unit.

This phenomenon, then, is directly linked to rapidly changing magmatic compositions erupting at any one volcanic centre. The evidence from most of these composite bodies indicates early ascent of the less basic, more alkaline unit, followed abruptly or gradationally by the more basic and porphyritic unit.

It is the primary aim of this study to investigate such composite bodies and to present detailed data on their geochemistry with the object of further understanding their genesis.

Fig. 1.1

Sketch map of locations referred to in the text.

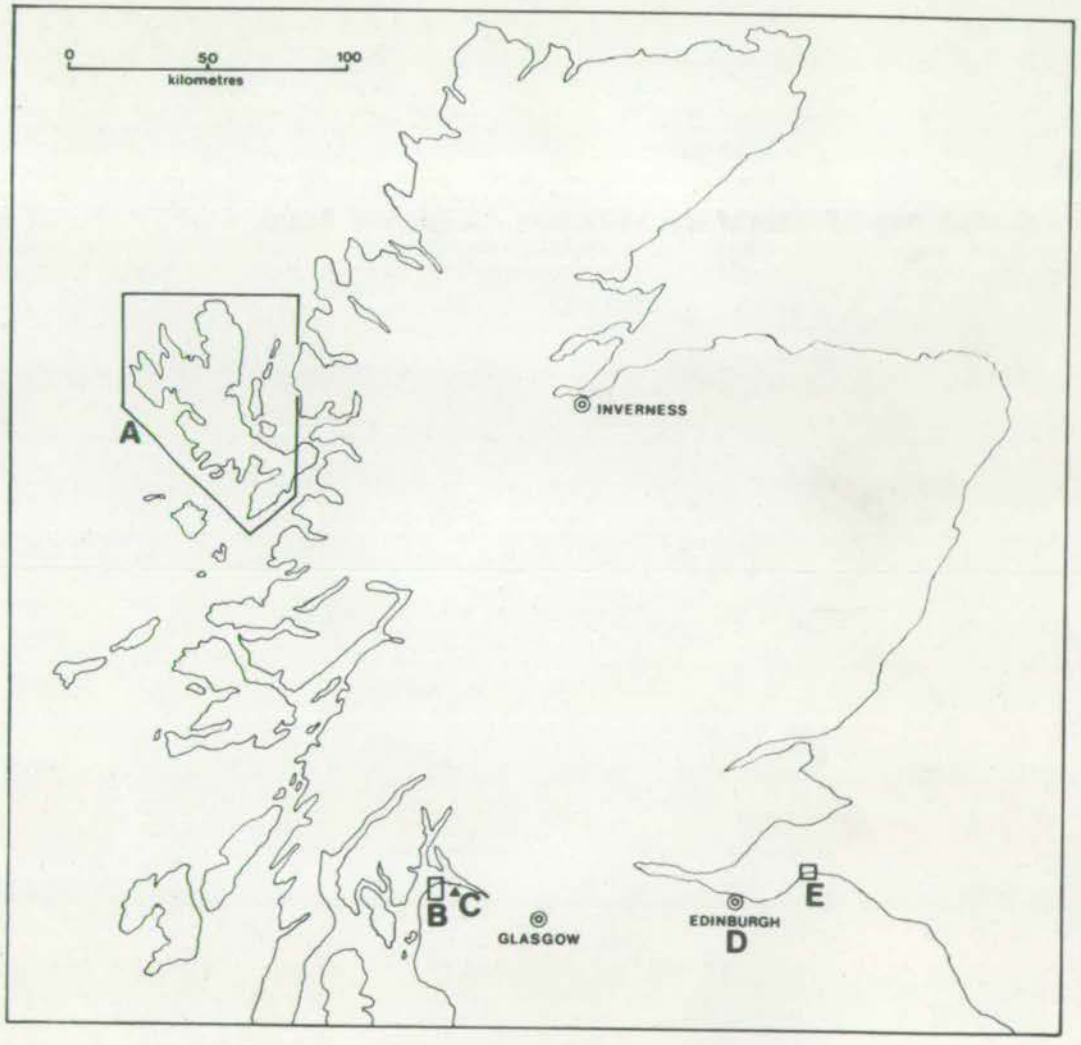
0
50
100
kilometres
A
INVERNESS
B
C
GLASGOW
EDINBURGH
D
E

Four suites were chosen for study:

A. Three localities on North Skye, in the Tertiary Volcanics of the Hebridean Province: Talisker, Roineval and Drum na Criche (Fig. 1.1, A).

B. Three localities within the Carboniferous volcanics of the Scottish Midland Valley: individual flows at North Berwick promontory; intrusions (the Dasses, St. Leonard's Sill) at the Royal Park, Edinburgh; the two compositie flows near Greenock, western Scotland. (Fig. 1.1; localities E, D, B, C).

C. A selected group of Pre-Cambrian "Big Feldspar Dykes" (BFDs) from SW Greenland.

D. An 8 metre thick sill exposed on the flanks of the Pliocene/Pleistocene volcano, Piton des Neiges, on the island of Réunion.

The first two suites include the localities from which composite flows were first recognized and described; they are easily accessible and the salient features well displayed. Material from suites C and D was collected by Dr. B.G.J. Upton.

The phenomenon of composite flows is not restricted to either oceanic or continental volcanic centres; nor is it, apparently, restricted in geologic time. The mechanism involved in their genesis may be relevant to the broader problems involved in the genesis of bimodal volcanic provinces, of which this may be a very specific and limited manifestation.

Previous work

Tyrrell (1912) noted the similarity of the association Markle (hawaiite)-mugearite in the Carboniferous lavas of the Midland Valley to some Tertiary "sills" described by

Harker (1904) from Skye.

Kennedy (1931) realized that these "sills" were probably flows similar in nature to flows he had mapped in the Carboniferous lavas of western Scotland.

MacDonald (1967) described in detail the chemical variation within a single Markle (hawaiite) basalt flow. He believed the variation in chemical composition to be too great to result from crystal fractionation alone. He adopted a suggestion of Hamilton (1956) in which the partial fusion of a gabbroic parent, with liquids withdrawn at appropriate intervals, would provide the requisite variation.

Upton and Wadsworth (1967) described an 8 metre thick composite sill from the Piton des Neiges volcano, Réunion. While the range in composition was far greater than that found in the composite flows of the Midland Valley or N. Skye, the phenomenon was analogous. No composite flows were noted in the vicinity although hawaiites and mugearites are common as discrete flows within the contemporaneous extrusive sequence.

Bridgwater and Harry (1968) described in detail a number of composite dykes from SW Greenland ("BFDs"). Again, there was a wider range in composition than that present in composite flows. The mechanism for their origin was worked out in detail, differing from classical crystal fractionation mechanisms in that fractionation of liquids was proposed as the primary mechanism.

Abbott (1969) described a sequence of plagioclase-phyric hawaiites, mugearites and benmoreites from a Miocene shield volcano in eastern Australia. Numerous chemical data are

given for both phenocrysts and bulk rock compositions, facilitating comparisons with the present study.

The association of plagioclase-phyric hawaiites with nearly aphyric mugearites is common enough to imply that the generic mechanism responsible is a common phenomenon; it suggests the coexistence, possibly in a single chamber, of liquids of contrasting composition.

This supposition is supported by the change in composition of lavas erupted during a single eruptive cycle, usually spanning several weeks. Murata and Richter (1966) noted that the lavas erupted during the 1959-1960 eruption of Kilauea (Hawaii) became progressively more basic with time. Jakobsson et al. (1973) describe a progressive change from mugearitic to hawaiitic composition over several weeks during the 1973 eruption of Heimaey (Iceland).

The present study starts with the assumption that magma chambers can contain liquids of different composition, possibly with compositional gradients. It has been argued previously that this is due to processes other than crystal fractionation (Bridgwater and Harry, 1968; Hamilton, 1965) and that such gradients and contrasting compositions can co-exist without homogenization by convection.

Terminology and classification

The basaltic compositions dealt with belong, for the most part, in the category of transitional (Coombs, 1963) basalts; that is, they contain CIPW normative hypersthene and olivine. This category does include basalts with minor amounts of normative nepheline or quartz as well. The effect

of modal minerals and post extrusive alteration upon the CIPW molecular combination conventions results in a blurring of the boundaries for transitional basalts. These effects are discussed more fully in the chapter on Classification; only the outline of the terminology and classification scheme is given below (Table 1.1).

Compositions frequently referred to throughout the text are defined as follows:

Table 1.1.

Rock name	Thornton-Tuttle Index*	CIPW normative feldspar
Alkali-olivine basalt	< 20 to 30	An_{65-50}
Hawaiite	30 to 45-50	An_{50-30}
Mugearite	45-50 to 65	An_{30-15}
Benmoreite	65 to 75	An_{15-5}

* CIPW normative qz + ab + or + ne + lc + ks (Differentiation Index (D.I.)).

Graphically, these categories may be shown (Fig. 2.1) upon a modification of Tilley's (1950) alkalis versus silica diagram, used by Upton and Wadsworth (1972). The Thornton-Tuttle indices are superimposed as a grid upon the plot; the diagram is further subdivided by lines dividing silica-saturated and undersaturated compositions, or alkali and tholeiitic basalts for three provinces - the Gardar, Hebridean and Hawaiian.

In dealing with the transitional basalts from the Carboniferous volcanics of the Midland Valley of Scotland, comparisons

Fig. 2.1

Total alkalis plotted against silica; diagram after Tilley (1950), modified by Upton & Wadsworth (1972). The solid lines marked Gardar, Hebridean and Hawaiian separate silica-saturated and undersaturated rocks in these provinces. The dashed lines separate compositional fields of the rocks noted by means of the differentiation index.

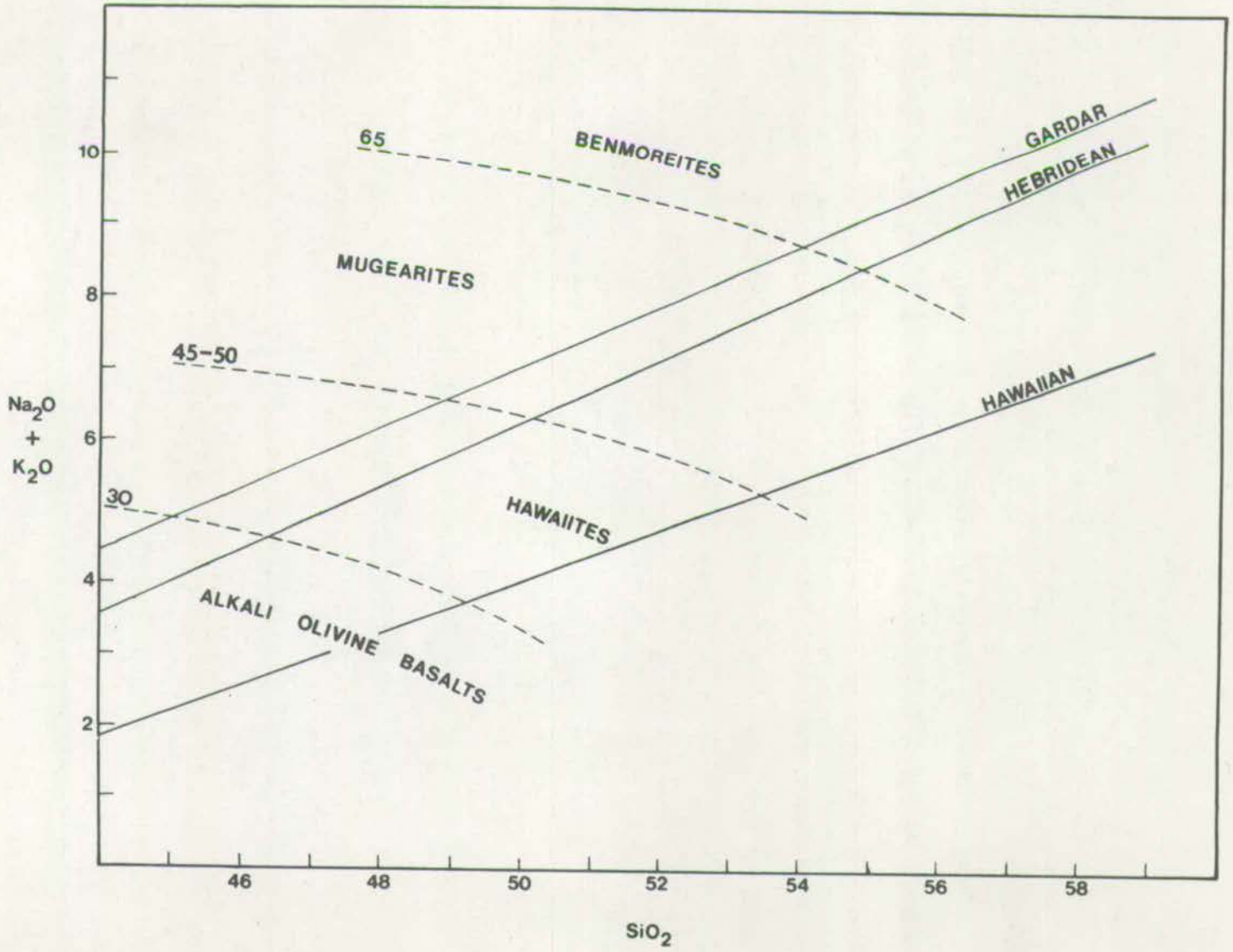
65
BENMOREITES
GARDAR
HEBRIDEAN
MUGEARITES
45-50
HAWAIITES
HAWAIIAN
30
ALKALI OLIVINE BASALTS
10
8
6
4
2
Na2O + K2O
46
48
50
52
54
56
58
SiO2

with previous work are facilitated if MacGregor's (1928) terminology can be related to the classification used above. MacGregor's terminology is reproduced below (Table 2.1) with approximately equivalent terms in brackets. There is, it should be noted, only limited equivalence of terminology. The terms should be equated with caution; Markle basalts, for instance, include both hawaiites and alkali-olivine basalts. In general, however, the use of hawaiite in place of "Markle basalt" is justifiable.

Table 2.1
(after Tomkeieff, 1937)

Macro-porphyritic	Craiglockhart (olivine, Cpx)	Dunsapie (alkali-olivine basalt) plag, Cpx, Ol	Markle (hawaiite) Plag + Ol
Micro-porphyritic	Hillhouse (Ol ± Cpx)	Dalmeny (alkali-olivine basalt) Ol ± Plag ± Cpx	Jedburgh (hawaiite) Plag + Ol
SiO_2 range	42.4 - 46.6	47.7 - 46.9	44.5 - 47.7

CHAPTER 2

FIELD RELATIONS

Hebridean Province: Northern Skye

Introduction

Anderson and Dunham (1966) have divided the 600-1300 M. of Eocene, predominantly alkaline lavas into five groups:

5. Osdale Group. Mugearites and basalts.
4. Bracadale Group. Mugearites and trachytes.
3. Beinn Totaig Group. Mugearites and alkali-olivine basalts.
2. Ramascaig Group. Porphyritic and non-porphyritic basalts, with a mugearite flow at the top.
1. Beinn Edna Group. Basalts, with a mugearite flow at the top.

The outcrop areas of the different groups, as well as localities referred to throughout the text are shown in Fig. 1.2;2.2. Extrusion of the lavas from vents or fissures appears to have commenced in the east and migrated to the west. The spatial relationship of the lavas in each group with dykes of the same general composition has suggested to many workers that the dykes served as feeders for the flows.

Although there are limited data on the distribution of compositional types in the province, the general impression from field observations is that the intermediate members (hawaiite, mugearite) of the series alkali-olivine basalt-trachyte predominate, or at least do not show the minima frequently shown by compositionally similar suites on oceanic islands (Chayes, 1963) or certain continental associations

Fig. 1.2

Distribution of basalt groups on North Skye after Anderson & Dunham (1966).

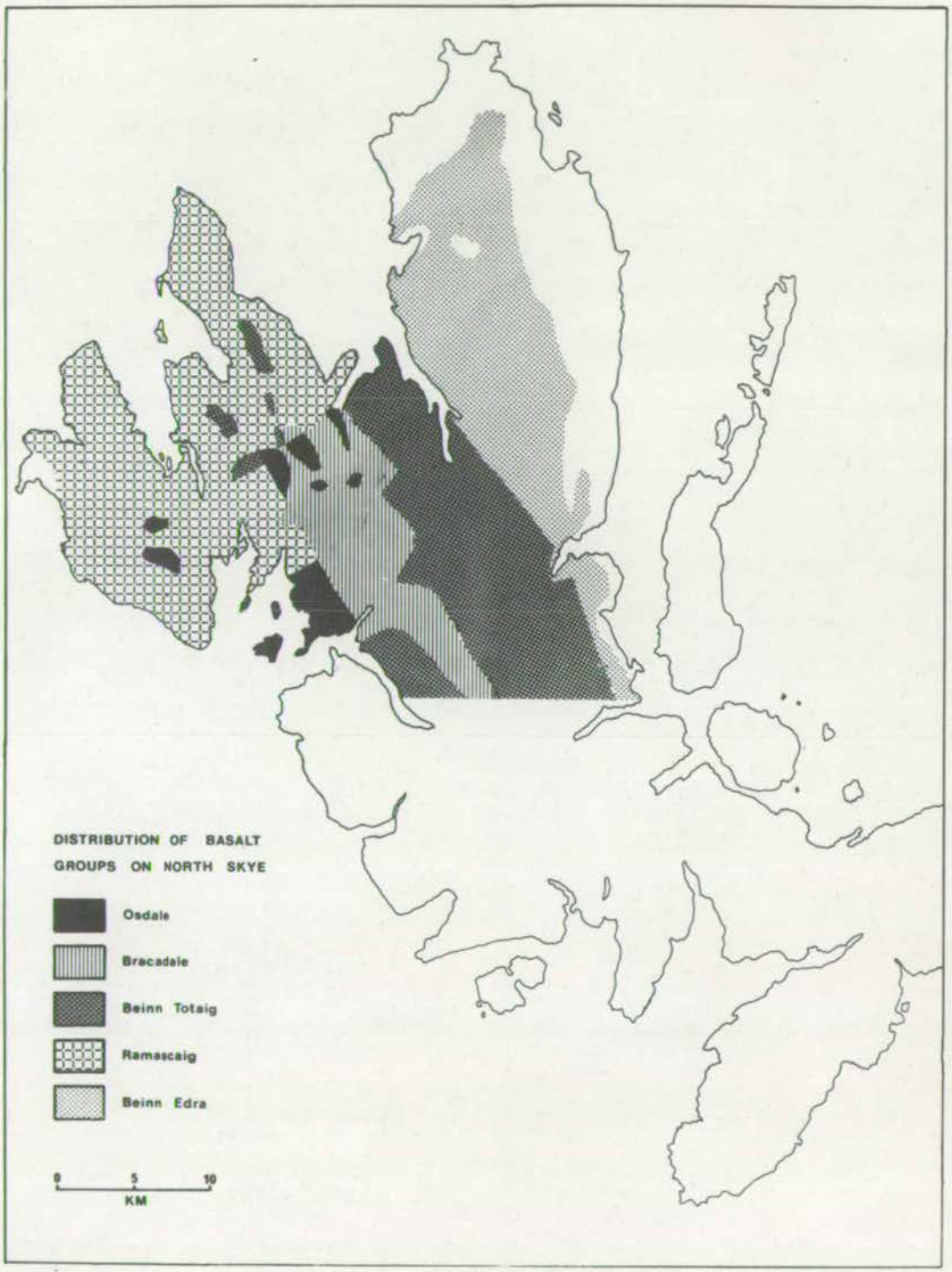
DISTRIBUTION OF BASALT
GROUPS ON NORTH SKYE
Osdale
Bracadale
Beinn Totaig
Ramascaig
Beinn Edra
0
5
10
KM

Fig. 2.2

Sketch map showing localities in North Skye referred to in the text.

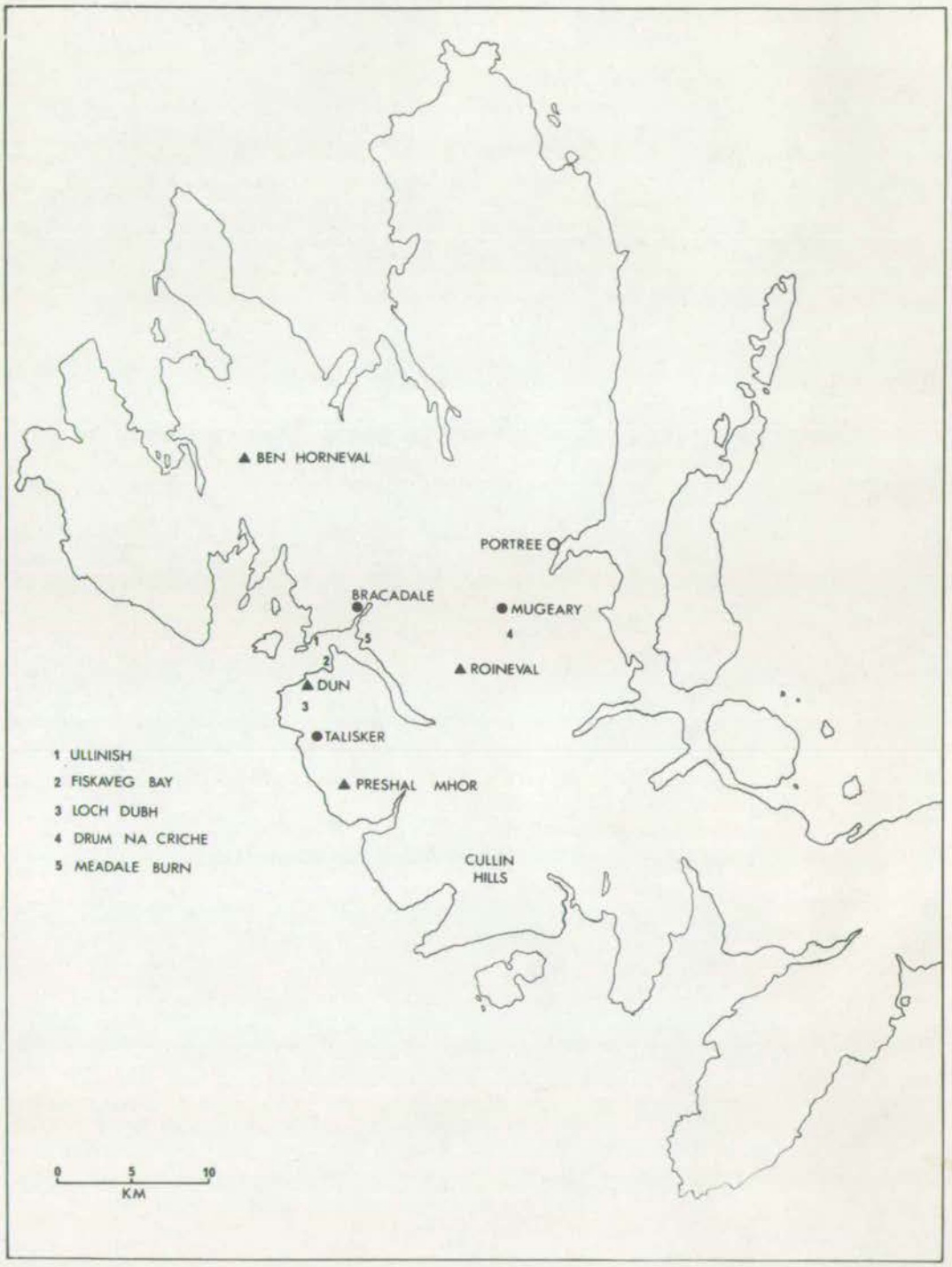
▲ BEN HORNEVAL
PORTREE
BRACADALE
● MUGEARY
4
5
1
2
▲ ROINEVAL
▲ DUN
3
● TALISKER
▲ PRESHAL MHOR
CULLIN HILLS
1 ULLINISH
2 FISKAVEG BAY
3 LOCH DUBH
4 DRUM NA CRICHE
5 MEADALE BURN
0 5 10
KM

PLATE 1.2

Fig. 1.

The composite flow at the "Dun" lies in the background, behind the first exposure of the underlying alkali-olivine basalt. The low hill to the left of the "Dun" is an outcrop of the lower nearly aphyric hawaiite. View to the N.W. Outcrop in foreground is 1.5m high.

Fig. 2.

View from the "Dun", looking eastwards; the division between porphyritic and aphyric members is marked by the first grassy break in slope on the outcrop.

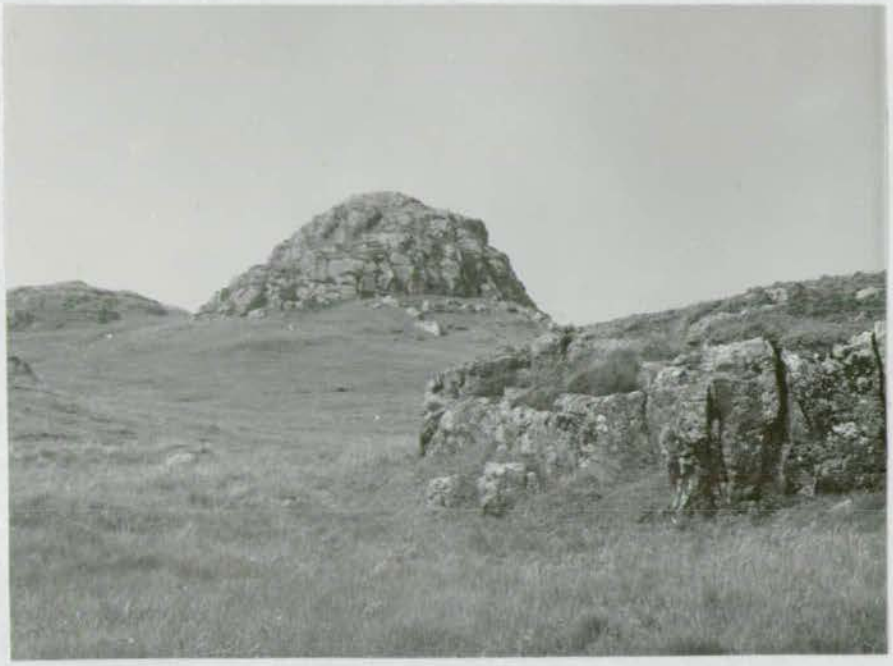

(Cox et al., 1969).

The composite flows of Drum na Criche and Roineval appear in the upper part of the Beinn Totaig Group; that of Talisker probably belongs to the Ramascaig Group (Thompson et al., 1972). Individual porphyritic hawaiite and mugearite flows are common in the area from Mugeary north to Edinbain and Beinn Bhreac (Anderson and Dunham, 1966).

Harker (1904) first described the composite flows at Roineval, Drum na Criche and Talisker. The first two are very similar to one another, but the flow at Talisker is distinctive in that the underlying non-porphyritic member is not more evolved compositionally than the groundmass of the overlying porphyritic hawaiite.

Individual composite flows

Talisker. The composite flow is exposed over several square kilometres, in outcrops extending from Talisker north to the "Dun" SSW of Fiskaveg Bay (Fig. 2.2; Plate 1.2, Figs. 1 and 2). The best exposure is on the hill of the "Dun" itself, with a section including at least 7 m. of porphyritic hawaiite, overlying 3-5 m. of sparsely porphyritic or aphyric hawaiite. Immediately to the west is a lower rounded knob with 4 m. of porphyritic hawaiite overlying approximately 10 m. of an essentially aphyric hawaiite. A NW trending fault with a minor vertical displacement is inferred to run between the two sections. In this second, westernmost exposure, more of the aphyric rock is exposed, and a section of some 17 m. thickness has been compiled.

Approximately 12 m. below the lowest exposure of aphyric hawaiite in the first or easternmost section, there are outcrops of an alkali-olivine basalt. No contact with the lower

member of the composite flow is exposed, so that 17 m. should be considered as a minimum estimate of the thickness.

One kilometre to the south and due east of Loch Dubh (Fig. 2.2) another section, lacking the aphyric lower member, was sampled. An alkali-olivine basalt exposed 15 m. below the lowest exposure of the porphyritic rock was analyzed, and appears compositionally identical with the alkali-olivine basalt from the section to the north.

Harker (1904) noted an essential difference in phenocryst distribution between the composite flow at Talisker and those at Roineval and Drum na Criche: the boundary between the units at Talisker is diffuse, while those at Roineval and Drum na Criche are sharper.

At Talisker over distances varying from 20 cm. to as much as 80 cm. the proportion of plagioclase phenocrysts diminishes from 18–20% to less than 10% by volume. The junction between the two units shows no evidence of brecciation or chilled surfaces. There does not appear to be a marked concentration of phenocrysts at the lower border of the upper unit.

Drum na Criche. The composite flow of Drum na Criche lies about 8 km. WSW of Portree (Fig. 2.2) and 1.6 km. SSE of Mugeary.

Harker (1904) described four craigs as being composite in composition; only the two easternmost were sampled, probably the same locality sampled and analyzed by Muir and Tilley (1961). The lower mugearites were sampled in a series up to the junction from the lowest exposures, but the porphyritic upper member was sampled from a loose block at the bottom of the low scarp.

Its exact position in relation to the section is not known, but it is believed to be halfway between the lower contact with the aphyric unit and the top of the knob. Harker (1904) suggests that the maximum thickness of the upper porphyritic member is at least 30-35 m., but in the sections sampled it does not exceed 10 m. The rock is deeply weathered; relatively fresh samples could only be obtained from an isolated knob to the west and from loose blocks lying at the base of the outcrop.

Only 3.5 to 4 m. of the lower, aphyric mugearite are exposed. This is a minimum thickness, since no contact with an underlying flow is exposed. The mugearite has a characteristic fissile or platy appearance, yellow brown on weathered surfaces, grey-black on fresh. The contact with the overlying porphyritic hawaiite, as in the flow at Talisker, shows no brecciation or chilled surfaces. In contrast with Talisker, however, the junction between the two units is very sharp, generally less than 10 cm. and essentially planar.

Roineval. The composite flow at Roineval lies 2.4 km. SW of Drum na Criche (Figs. 2.2,). There are minor, but significant differences, however. The division between the two units is more diffuse, the zone being 10-20 cm. thick in the main massif itself. On the small outlier to the east, however, phenocrysts are present throughout the exposed portion of the mugearite (2-2.5 m. thick). Moreover, the upper porphyritic unit has a minimum thickness of 30-35 m. The lower aphyric mugearite has a minimum thickness of 4 to 4½ m. - again with no lower contact exposed. Harker (1904)

did not find the lower aphyric (mugearitic) part of the flow on the NE side of the massif, suggesting that the flow units may vary rapidly in thickness over very short distances.

Specimens were collected from a cliff face on the west side of the massif, about 10 m. south from the small valley dividing the massif from a smaller outlier to the north. The aphyric mugearite was easily sampled but specimens of the overlying porphyritic unit were only obtained from near the top of the section and from exposures 30-40 m. to the north, in what appeared to be the middle of the upper unit.

All of the composite flows appear to be of limited areal extent - less than 10 km^2. The volume, then, is close to a maximum of 3 km^3 in the instance of Roineval, considerably less for Drum na Criche, and possibly equal to that for Talisker.

Intrusions and non-composite flows, N. Skye.

Introduction

A number of dykes at localities near the composite flows were sampled and analyzed, especially on the western coast of Skye, near the composite flows of Talisker and Roineval. In general they were of little aid, other than in giving a very general picture of the compositional range present. The dykes mapped as "mugearite" on the North Skye sheet of the Geological Survey would not be so classified in terms of the definitions used in this study.

Isolated flows of hawaiites were analyzed to provide background statistical information on the range of compositions defined by the term "hawaiite". These proved of considerable

value to the study as a whole.

Fiskavaig Bay

A small inlet NE of the composite flow exposure of the "Dun" (cf. Talisker) has at least six dykes exposed, cutting a series of hawaiite flows. The flows and dykes are stratigraphically below the Talisker composite flow horizon by at least 100 m. One dyke (Analyses 1-4 Table 1C) contains fragments (10-15 cm. in length) of anorthosite (Analysis 5) along the margins of the dyke.

The other dykes investigated (Analyses 6-7, Table 1C) are similar in composition to the flows exposed in cliffs surrounding the inlet, and may have served as possible feeders for the flows.

Their chronologic relationship to the upper part of the section where the composite flow occurs is not known, as the area over which the composite flow is exposed is limited and nowhere is there evidence of it being cut by dykes.

Ullinish Point

Due north from Fiskavaig Bay, across Loch Harport, one mugearite dyke (marked X^{M}) and several tholeiitic dykes (marked K^{D}) are shown on the 1" Geol. Survey North Skye Sheet. These are exposed on the foreshore, below the Hotel (Ullinish) pasturelands.

The dyke mapped as "mugearite" by Harker (1904) is at least 3 m. wide, with abundant plagioclase phenocrysts (Analyses 8-9, Table 1C). Smaller, phenocryst-free dykes are associated with it, possibly as apophyses of the large dyke itself (Analysis 10, Table 1C). Smaller dykes nearby

(Analyses 11-12, Table 1C) are tholeiitic.

Vidigill Burn

Harker (1904) and Anderson and Dunham (1966) described what appears to be a composite dyke with a mugearite in the central part, and a basalt containing large plagioclase ($An_{55\pm5}$) phenocrysts on the sides, exposed in the small Burn SE of Summerdale River.

The precise relationship of the units is not clear, as the critical contacts are obscure. The relationship of more evolved central part with basic margins is the reverse of other composite bodies studied.

Summerdale River

Summerdale River lies ENE, across Loch Harport, from the Dun Hill of the Talisker flow; it empties into Loch Harport on its eastern shore just to the south of the small promontory on the southern edge of Gesto Bay. Vidigill Burn, described above, empties into it, about 2 km. east of its opening on Loch Harport.

The hawaiite flow exposed in the roadcut on the main road to Bracadale, where it crosses Vidigill Burn, and a porphyritic hawaiite dyke exposed in the stream bed were both analyzed (Analyses 15-16, Table 1C). Analysis 16 is of a non-porphyritic marginal facies; the porphyritic portions of the dyke appeared too altered to be of value. The dyke itself is 3-4 m. wide, with 0.5-0.75 m. of phenocryst-free margins and a central zone where phenocrysts constitute 20-25% of the rock.

The other dykes analyzed are from Ardtreck Point, the

northernmost point on the peninsula that the Talisker composite flow is found on. Both are tholeiitic (Analyses 17-18, Table 1C); no sample of the large dyke mapped as mugearite (X^M) could be obtained.

The large massif at Preshal More was analyzed to provide data on what R.N. Thompson (pers.comm., 1968) suggested as a very primitive composition (Analyses 19-20). It occurs in a series of alkali-olivine basalts and hawaiites (Analyses 25-28); its exact relationship to the sequence as a whole is not known. Its possible relationship in low to intermediate pressure fractionation models is discussed in the section on Petrogenesis.

Analyses of 3 gabbroic dykes (Analyses 32-34, Table 1C) from the small burn east of Balmeanach were made to provide data on the range of compositions involved; Drever (1969) has suggested that such dykes are the cumulates formed during the evolution of the hawaiites and mugearites.

The Midland Valley of Scotland

Introduction

Lavas were erupted at a large number of centres throughout and adjacent to the Midland Valley during Lower Carboniferous times. Compositions ranged from alkali-olivine basalts to quartz trachytes and rhyolites (cf. Francis, 1967); MacGregor's (1928) terminology for the basic lavas has been widely used in later work related to the area. Table 2.1 of the first chapter presented his classification, with the roughly equivalent terminology of the present classification scheme.

Early Carboniferous tectonic activity was associated with the rejuvenescence of the Devonian rift valley and mildly alkaline volcanism at centres within the Midland Valley and bordering it. Two large volcanic fields are of special interest to the present study. The first, emanating from a line of volcanoes parallel to the boundary faults of the Midland Valley, extended in the west from Dunbarton rock to the Kilsyth Hills (Clyde Plateau lavas). The other, of similar volcanics, lay to the east. These latter volcanics are exposed on both limbs of the Midlothian syncline, i.e. in the vicinity of Edinburgh and near North Berwick. Suites from the western field (viz. the composite flow near Greenock) and from both sides of the syncline in the eastern field (namely in the Royal Park and at North Berwick) have been examined in the present thesis. These suites are believed representative of the widespread association of porphyritic hawaiite and mugearite in the Clyde Plateau and Lothian lavas.

Tomkeieff (1937) in his compilation of the distribution of rock types in the Midland Valley, has Markle basalts occupying 58% (by volume) of the succession, mugearites (12%), alkali-olivine basalts (17%) and more silicic rocks (trachyandesite, trachyte, rhyolite) as 7.5%. Locally, the individual lava successions appear to vary randomly in constitution.

There is no indication that in the Midland Valley province, as a whole, that geographical differences in the distribution of lava types existed, at least during the lower Carboniferous, nor was there any systematic migration of the site(s) of

volcanic activity within the Midland Valley.

Tomkeieff (1937) estimated that the lava succession in the western part of the Midland Valley (which includes the Campsie, Kilpatrick and Renfrewshire Hills, Kintyre Peninsula and the island of Arran in Scotland, and Antrim in Ireland) comprised 87% of the total volume for the province as a whole. Several detailed recent studies have been made of individual sections in the Clyde Plateau lavas (Hamilton, 1956; MacDonald, 1965). Both these later works and Tyrrell's (1912) earlier compilation suggest that the bulk of the rocks are hawaiitic rather than basaltic in composition.

McAdam et al., (1971) estimate a total of 520 metres of volcanics in the eastern volcanic field, of which 160 m. are trachytic, the remainder being basalts, basaltic tuffs, hawaiites and mugearites.

In the Midland Valley province and adjacent volcanic fields, the association of porphyritic hawaiite-mugearite is common in the lavas of the Clyde Plateau and the Lothians, but not in Arran, Antrim, Kintyre, Fyfe or the Kelso region.

The individual suites studied are considered in detail below.

North Berwick promontory (Fig. 3.2.)

Three flows are exposed at the north end of the promontory, dipping 7-10° WSW.

The uppermost of the three flows is approximately 15 m. thick, with abundant plagioclase and altered olivine phenocrysts. The flow top is vesicular and slaggy; sparse vesicles are present throughout the flow.

Fig. 3.2

Sketch map showing localities on the promontory at North Berwick, East Lothian. Flows dip 7-10° W.S.W. LWM is Low Water Mark; HWM is High Water Mark.

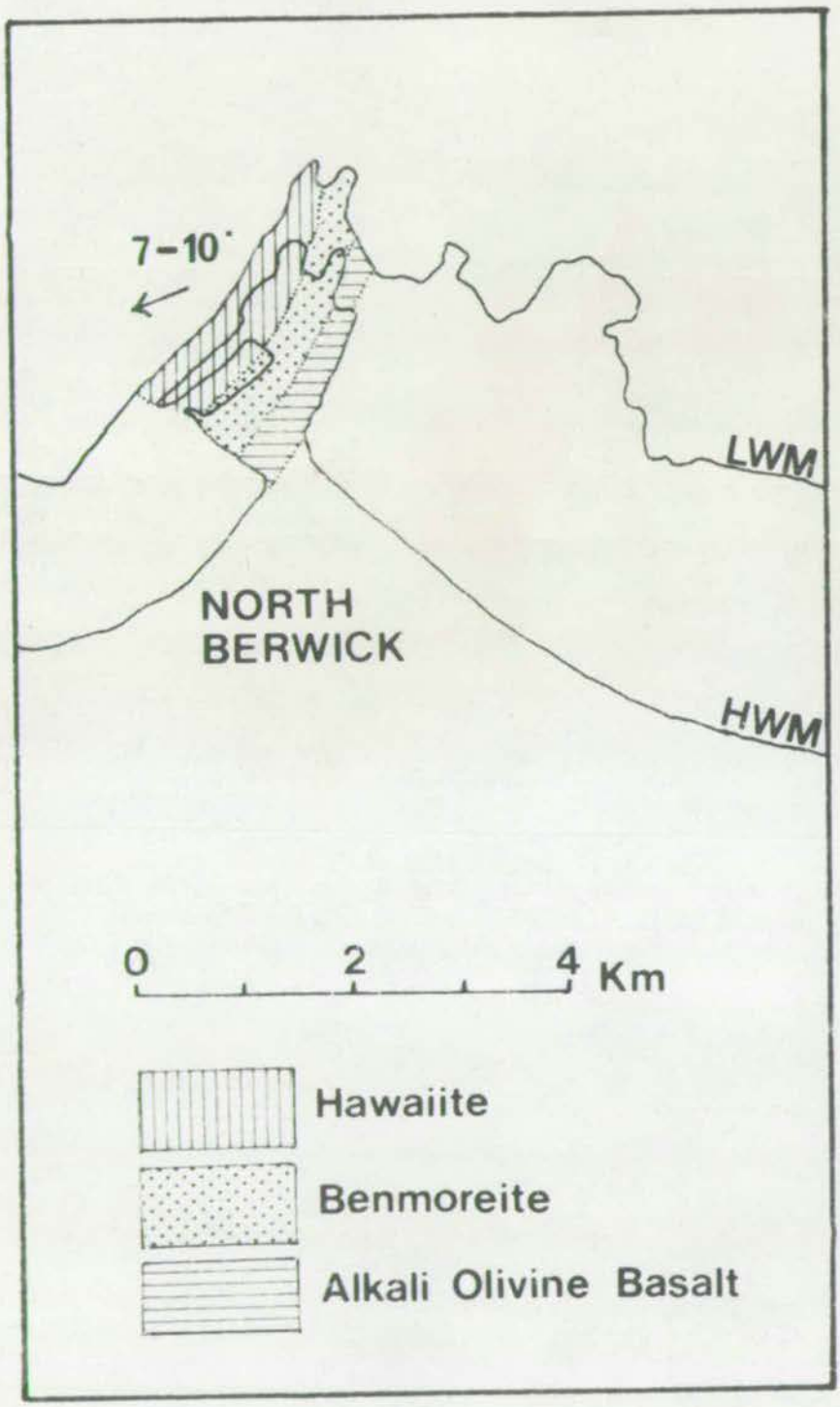
7–10°
LWM
NORTH
BERWICK
HWM
0
2
4 Km
Hawaiite
Benmoreite
Alkali Olivine Basalt

Upper margin of the Dasses, The Royal Park, Edinburgh. Arthur's Seat in the background. (photo graph courtesy of Dr. B. G. J. Upton)

The 8 m. thick underlying benmoreite (mugearite of Clough et al., 1910; Day, 1930) is extensively weathered, with a brecciated, vesicular top of 1 to 3 m. thickness.

Below the benmoreite flow is an alkali-olivine basalt, 6.5-7.0 m. thick, containing small gabbroic inclusions and feldspar phenocrysts.

The section exposed on the North Berwick promontory and foreshore is from the lower part of the succession in East Lothian; a similar sequence of flows appear further inland, but are thicker (McAdam et al., 1971). The feature of primary interest here is the succession of hawaiite overlying the less basic, more evolved benmoreite. This section of three flows lies above a sequence of tuffs and agglomerates, which appear to have accumulated in shallow lagoons and mark the opening of volcanic activity in the area.

The Royal Park, Edinburgh

Introduction

Within the volcanic complex of Arthur's Seat in the Royal Park, Edinburgh, there are three exposed composite intrusions: the Dasses, Girnal Craig, and St. Leonard's Sill (Fig. 4.2). The first two intrusions are probably different exposures of the same body. Only the Dasses and St. Leonard's Sill have been utilized in the present study. They correspond in compositional range to the lavas of the succession at Arthur's Seat. This succession shows a very definite progression with time from more basic lavas (ankaramites, alkali-olivine basalts) to more evolved (mugearite) flows at the top of the succession.

The intrusions cover the compositional range alkali-olivine basalt-hawaiite (the Dasses) and alkali-olivine basalt-benmoreite (St. Leonard's Sill), with an ill-defined junction between the two units. The textural contrast between the two units is much greater in St. Leonard's Sill for here the marginal facies is very nearly aphyric. The Dasses, on the other hand, shows very little change in the amount of plagioclase phenocrysts present. Both intrusions have been extensively altered.

The Dasses

The intrusion occurs as a series of discontinuous outcrops; the southernmost is a thin (≃ 1.5 m.) sheet of feldspar-phyric hawaiite ("Markle") which is again present in the other outcrops as irregular patches, although it is probably a continuous sheet. Three separate masses overlie this unit; they are texturally indistinguishable from it, but compositionally they are more basic, ranging in composition from hawaiite to alkali olivine basalt.

Oertel (1952) first recognized the composite nature of the sill, terming the marginal hawaiite Basalt I and the interior unit of hawaiite-alkali-olivine basalt Basalt II. His division was based solely on the alignment of plagioclase phenocrysts to define "flow planes". Oertel reasoned that because the flow planes of Basalt I were distorted in the southernmost and middle of the three discontinuous masses and that the flow planes of Basalt II were almost vertical in the same area, this marked the site of intrusion of Basalt II into position. Since there is no evidence of chilled margins

or brecciation, both units were emplaced within a very short time interval.

St. Leonard's Sill

In contrast to the Dasses, St. Leonard's Sill has a distinct aphyric and porphyritic facies, although the border between them is diffuse.

The sill is composite in a limited area only; in three dimensions, the central, approximately 7 m. thick porphyritic facies is oval, surrounded by a 2 m. thick envelope of highly altered, nearly aphyric rock. This marginal facies has a diffuse border as much as 50 cm. thick with the central porphyritic facies; the rock becomes less oxidised in the vicinity of this diffuse zone.

The sill was sampled at the locality described by MacGregor (1936, p.324) as being at or near "Jeanie Dean's Cottage" - although this landmark no longer exists. Good exposures are available, but both facies are highly altered.

The Western Midland Valley of Scotland

The composite flow south of Greenock

The Lower Carboniferous volcanics in western Scotland are divided into a lower group of feldsparphyric hawaiites and nearly aphyric mugearites, and an upper group of alkali-olivine basalts, mugearites and trachytes (Kennedy, 1932).

Two different examples of composite flows are described from the lower group of volcanics. The first, from exposures near Loch Thom, was described by Kennedy (1931) in a paper which first pointed out the general nature of the phenomenon.

The second occurrence has a distinctly different character, in that a more evolved flow lies either within a single mugearite flow or between two individual mugearite flows. It is noted here because it is believed to be a part or byproduct in the genesis of hawaiite-mugearite composite bodies, and represents a stage that is rarely observed.

Loch Thom

The first composite flow occurs near the village of Inverkip, on the Firth of Clyde, south of Greenock (Locality B, Fig. 1.1).

Both units were sampled in the vicinity of Kennedy's locality H (Fig. 5.2) where they are well exposed and stratigraphically above exposures of underlying mugearites (Table 1E, Analysis 20). The thickness of each unit is variable; either may thicken or thin at the expense of the other, or even disappear entirely. In contrast to the sequences on North Skye, no alkali-olivine basalts occur immediately below the composite flow in the succession, which consists almost solely of mugearites with rare hawaiites. There is, moreover, no evidence that composite flows occur elsewhere in the sequence; indeed, although Kennedy writes of "composite flows", it is not certain that there is more than one flow unit present even at the top of the succession.

The porphyritic upper member of the composite flow is dark red to deep purple with prominent (1-1.5 cm.) feldspar phenocrysts. It overlies an almost aphyric unit of the same colour. At the locality in which the flow was sampled the upper unit is nearly 5 meters thick, the lower unit at least

Fig. 5.2 (after Kennedy, 1931)

Sketch map of the composite flow south of Greenock. The extent of the flow is shown by hachures in the vicinity of Dunrod Hill. Kennedy's described localities at D, H, I; the specimens analyzed in the present study are from location H.

Fig. 4.2

Sketch map of the Royal Park, Edinburgh, showing sample localities for the Dasses: marginal facies (A), central facies (B); St. Leonard's Sill, both facies (D); Jenny Dean's Cottage (C).

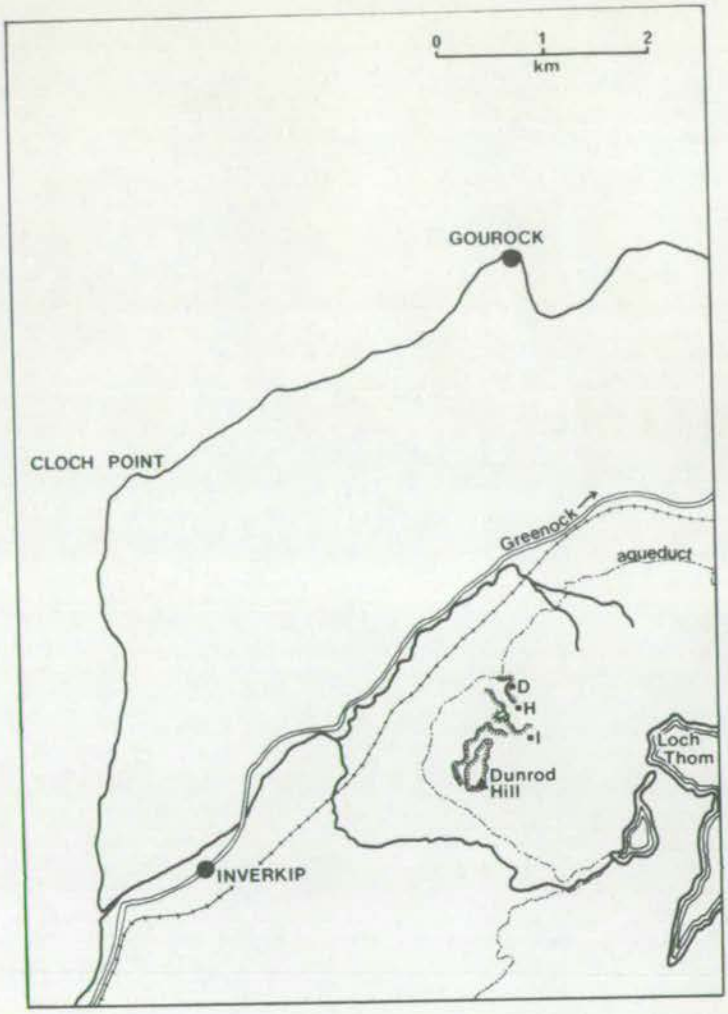
0
1
2
km
GOUROCK
CLOCH POINT
Greenock
aqueduct
D
H
I
Dunrod
Hill
Loch
Thom
INVERKIP

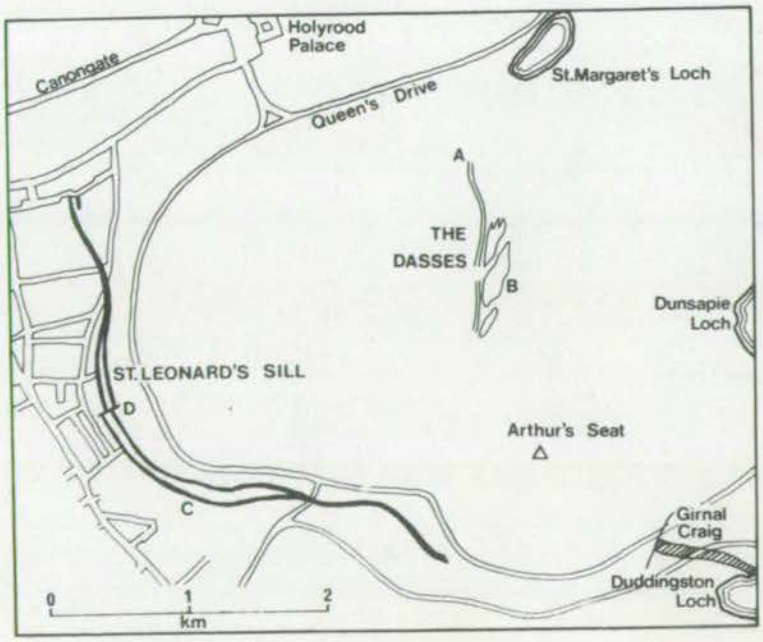
Holyrood
Palace
Canongate
Queen's Drive
St.Margaret's Loch
A
THE
DASSES
B
Dunsapie
Loch
ST.LEONARD'S SILL
D
Arthur's Seat
C
Girnal
Craig
Duddingston
Loch
0
1
2
km

a meter thick. No lower contact was exposed. There is no evidence of chilling or brecciation at the junction of the two units, but the junction is sharp (within 10 cm.) and the surface, in two dimensions, appears planar.

Craigmarloch Wood

Even though the rocks are altered and the exposures poor, the second occurrence is of interest in that a more siliceous, porphyritic rock ("trachyandesite") lies within or between mugearite flow(s) (Fig. 6.2).

Kennedy (1932) described this second composite flow, of benmoreite ("trachyandesite")-mugearite composition, from two exposures to the northeast of the first locality, and lying to the south of Port Glasgow (locality C, Fig. 1.1).

Kennedy considered the best exposure to be in Craigmarloch Wood, below the triangulation point (marked 519 (elevation in feet) on topographical maps). The other exposure, south of the Gryffe Valley, does not show the internal contacts as clearly.

The flow occurs interbedded in a sequence of mugearites and porphyritic hawaiites. The lower mugearite is not more than 3.5 m. thick, the upper one approximately 7 m. thick; the benmoreite facies between varies from 3.5 to 9 m. in thickness. There is no evidence of chilling at either the upper or lower contact of the benmoreite; the contact zone is gradational over 60-80 cm., with rounded, resorbed xenoliths of mugearitic material dispersed throughout. The mugearite, in a zone 50-60 cm. thick adjacent to the contact zone has a network of leucocratic veins; the platy structure

Fig. 6.2

Diagrammatic sketch of composite flow at Craigmarloch Wood showing transition zone between the central benmoreite facies and mugearite.

Fig. 7.2

Diagrammatic sketch of distribution of compositional facies in the S.W. Greenland composite dykes.

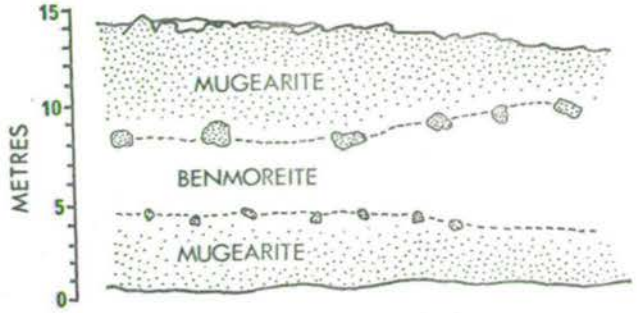
15
10
5
0
METRES
MUGEARITE
BENMOREITE
MUGEARITE

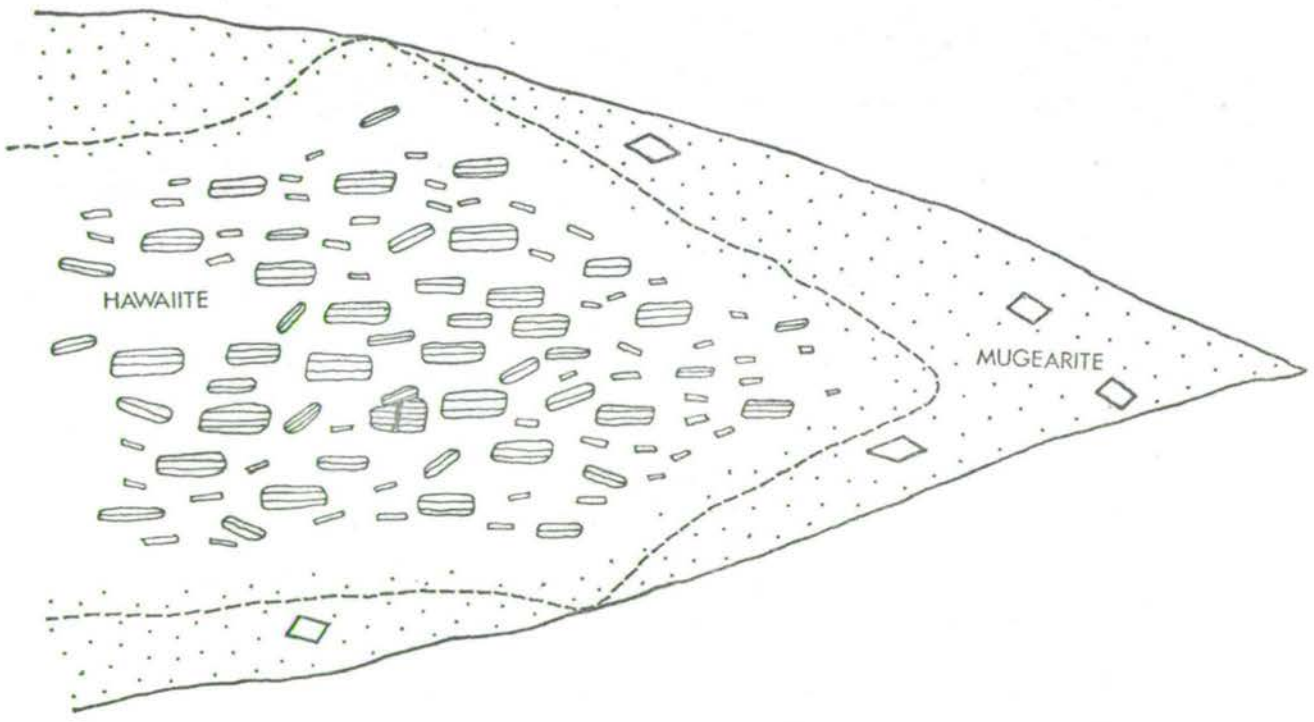
HAWAIITE
MUGEARITE

in the vicinity is contorted (Kennedy, 1932). Locally, the benmoreite has broken through the mugearite and displays a vesicular upper surface. Where it is in contact with the overlying porphyritic hawaiite, the latter shows no evidence of veining or alteration by the benmoreite.

Field evidence suggests rapid, successive emplacement of both units; the usual correlation of the porphyritic member with a more basic composition is no longer valid. It is of interest that the mugearite is here also nearly aphyric, although it is the more basic unit.

South-west Greenland

Introduction

The Gardar Province in the Pre-Cambrian (1300-1000 m.y. B.P.) of southwest Greenland includes both an extrusive alkali-olivine basalt-trachyte lava succession with compositionally related dyke swarms and "central-type" alkalic intrusive complexes.

The tectonic setting and nature of volcanism in the area are in many aspects analogous to those of the Midland Valley of Scotland. In both, the volcanism was in a cratogenic continental setting of block faulting, although on a larger scale in the Gardar Province.

The dyke suites studied were collected by Drs. B.G.J. Upton and D. Bridgwater from (A) a concentrated zone of ENE-WSW dykes lying along the Tugtotôq-Ilimaussaq axis and (B) in the vicinity of Isortoq (Fig. 8.2).

The earliest dykes in the Tugtutôq-Ilimaussaq region include "giant dykes" of troctolitic gabbros, syenogabbros

Fig. 8.2.

Sketch map of locations in SW Greenland referred to in Appendix A and the text.

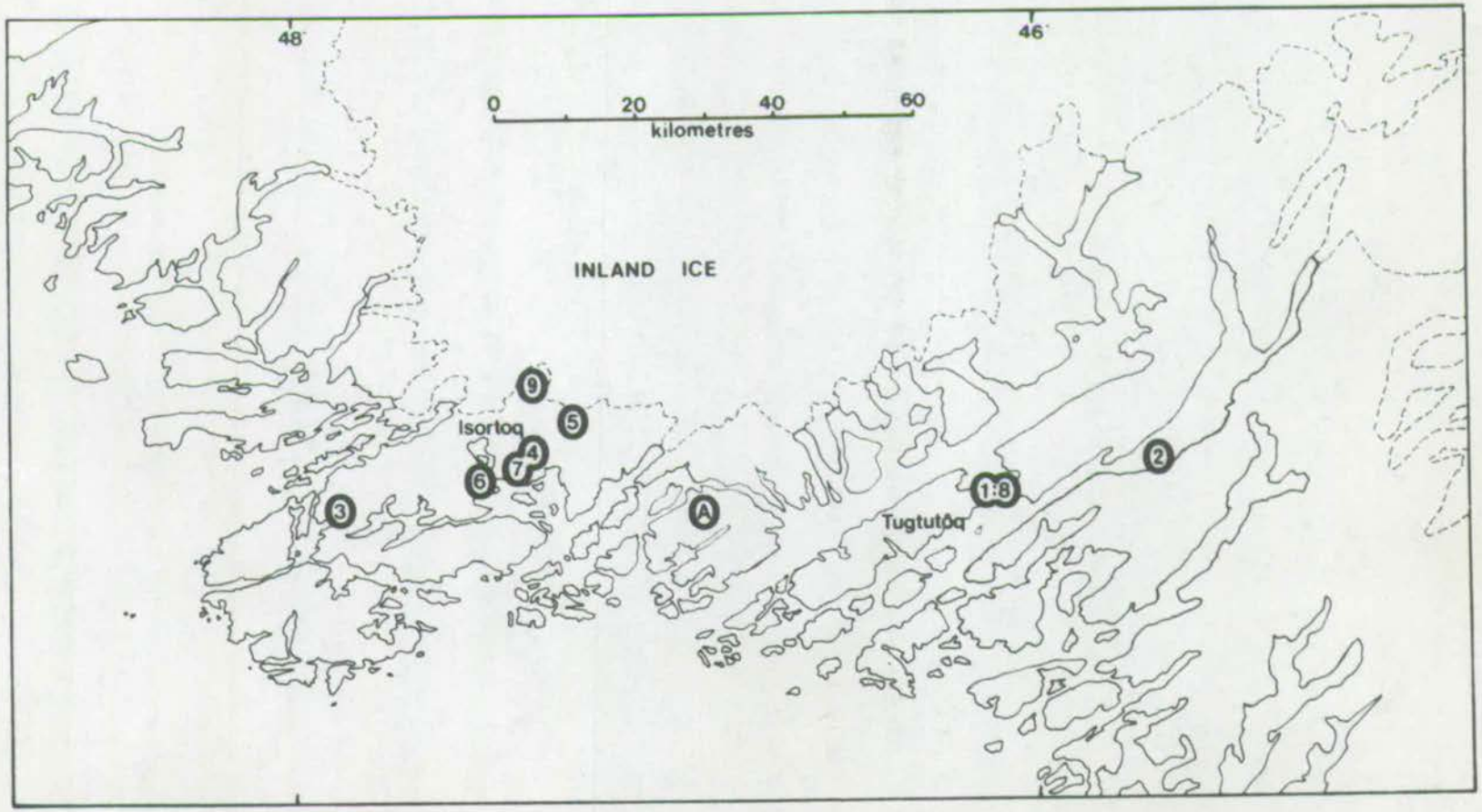
48°
46°
0
20
40
60
kilometres
INLAND ICE
Isortoq
Tugtutôq
9
5
4
7
6
3
A
1:8
2

and syenites. These dykes are, in part, composite, with syenite centres and more basic margins. They are followed by a group of dykes that range in composition from alkali-olivine basalt to benmoreite, which are typically composite in nature, with porphyritic, basic centres and more evolved, nearly aphyric margins. The basic central facies is characterised by its content of anorthosite xenoliths and plagioclase megacrysts. This second group of dykes was succeeded by a suite of more evolved composition including trachytes, comendites and phonolites.

For the purposes of the present study, the second group of composite dykes, termed "Big Feldspar Dykes" (BFD) by the field workers, are of particular relevance.

It has been suggested (Upton, 1970) that some of the extrusive basalts in the vicinity of Ilimaussaq may have been erupted from the giant gabbroic dykes and that the later, plagioclase-phyric flows higher in the sequence may have erupted from the BFDs. These latter volcanics have been described by Stewart (1964).

The Big Feldspar Composite Dykes

These have the following distinctive features:(Fig.7.2)

(1) Relatively aphyric margins, containing some pinkish alkali feldspar phenocrysts.

(2) a central, predominantly plagioclase-phyric facies with or without anorthositic inclusions,

(3) a junction between the two units that is gradational; very rarely is the central unit chilled against the outer facies, or are inclusions of the marginal facies included in the central unit.

Centre of 5 m. wide B.F.D. dyke,Niaquonag Island, near Tugtutoq.(photograph courtesy of Dr.B.G.J.Upton)

Contact zone of B.F.D. dyke,SW Greenland;small islet between Kangue and Tugtutoq.(photograph courtesy of Dr. B.G.J.Upton)

The range in composition may be as great as from alkali -olivine basalt to benmoreite, but the majority of dykes studied appear to be more limited in their compositional range, i.e. from hawaiite to mugearite.

Bridgwater and Harry (1968) noted that the BFD dykes in the western part of the province (i.e., in the vicinity of Isortoq) tend to be oversaturated, dominantly potassium rich, whereas those in the eastern part are undersaturated and soda-rich.

Individual dykes vary in total width as well as showing relative variation in the width of the two units. Dykes on Qaersuarssuk (A on Fig. 9.2) are 10-17 m. wide, with marginal facies of 2.5-3 m. width grading into the central porphyritic unit over 5 cm. (Watt, 1968). The gradational zone varies from 2-3 m. to as little as 5 cm., but seems more commonly to vary between 5-30 cm. (Bridgwater and Harry, 1968, pp.141). Both these latter authors and Upton (1962, p.34) stress the lack of uniformity in the width of margins relative to the central facies of dykes. Where single dykes can be followed over any distance the marginal unit may predominate or disappear; usually it is the central facies that disappears, however.

In some instances there is evidence that the marginal facies solidified before the emplacement of the central unit; Bridgewater and Harry (1968, p.51) note that the centre intruded through the margin and chilled against the country rock, and that inclusions of the marginal facies do occur within the central unit. Although the marginal facies shows

only rare inclusions of feldspathic material, the central zone shows a gradual increase in the amount of inclusions as the centre of the dyke is approached. These are aligned parallel to the sides of the dyke; where the dykes are widest, the inclusions are larger and less altered.

Réunion

Introduction

The geology of Réunion, in the western Indian Ocean, has been described by Lacroix (1936), Bussière (1959) and Upton and Wadsworth (1972).

The older of the two shield volcanoes comprising the island, Piton des Neiges (Fig. 9.2) is composed of two compositionally distinct lava sequences (Upton and Wadsworth, 1970).

(A) Oceanite Series: Olivine rich transitional basalts.

(B) Differentiated Series: alkali-olivine basalts, hawaiites, mugearites, trachytes with contemporaneous compositionally equivalent intrusions.

The analogy with evolutionary stages in Hawaiian volcanoes is relatively straightforward; the Oceanite series constitutes the shield-building stage in the volcanoes' evolution. The Differentiated Series represents the declining stage during which more alkalic and presumably lower temperature lavas were erupted.

Although the extrusive Differentiated Series and their supposed contemporaneous intrusive rocks are compositionally similar, they differ slightly in their phenocryst assemblages. Olivine is invariably present in the lavas, but it is lacking

Fig. 9.2

Sketch map of Reunion showing the location of the Bras Rouge sill and the two volcanic peaks.

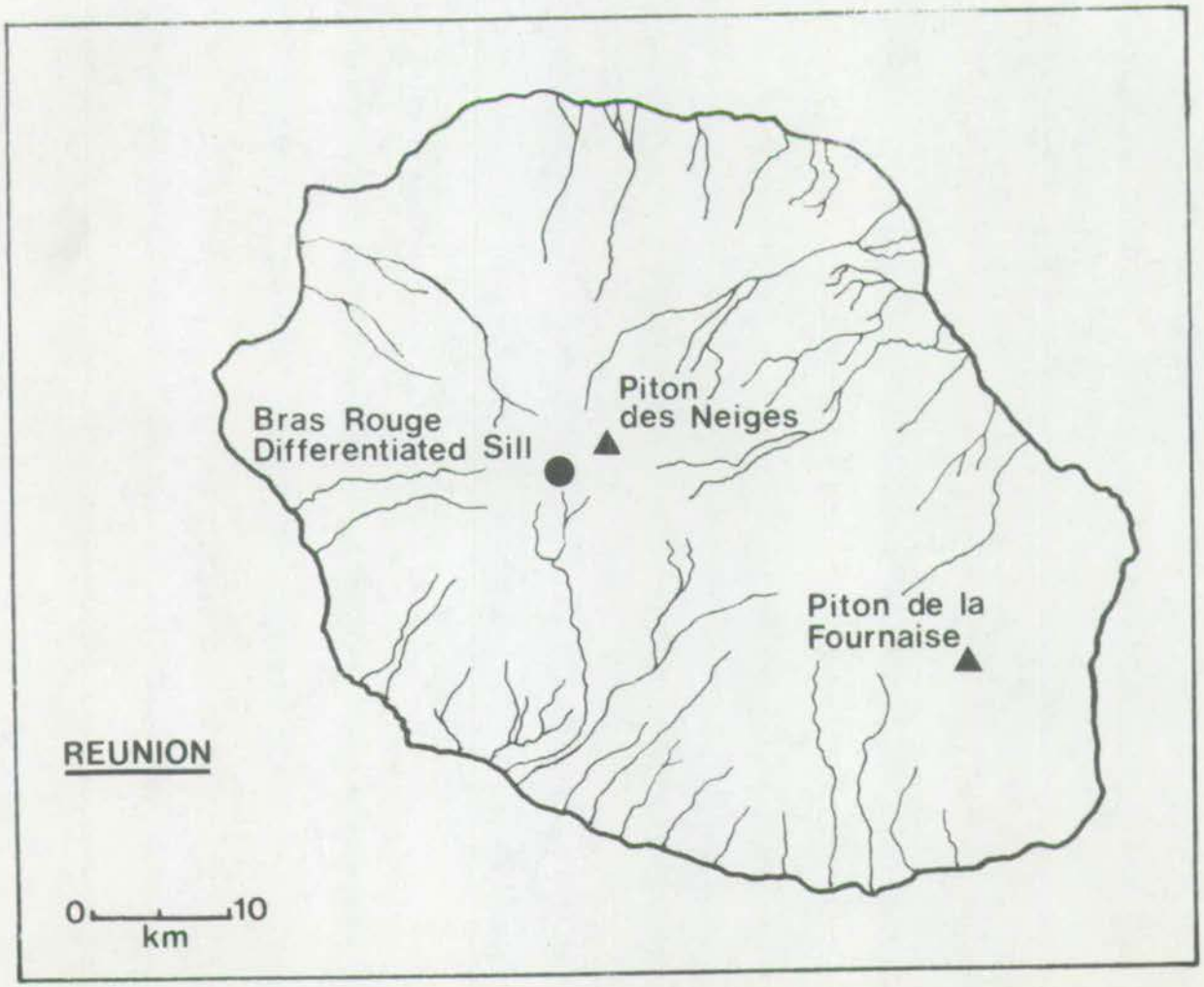
Bras Rouge
Differentiated Sill
Piton
des Neiges
Piton de la
Fournaise
REUNION
0
10
km

or scarce and strongly resorbed in the intrusives. Both contain relatively abundant phenocrysts of clinopyroxene, plagioclase and an amphibole. Upton and Wadsworth (1972) summarized the difference between the extrusives and intrusives as due to crystallization under dry and wet conditions respectively.

The intrusives may be divided (Upton and Wadsworth, 1970) into two main groups:

(A) Various intrusives equivalent in age to the Oceanite series; these include olivine dolerites, picrites and olivine gabbros.

(B) Intrusives equivalent in age to the Differentiated Series. These are a complex assemblage of younger basaltic, hawaiitic and mugearitic sheets. The syenitic sheet of the Cirque de Cilaos is one of the youngest intrusive events, but it is cut by thin glassy sheets of yet later intrusives.

Cirque de Cilaos complex sill (Bras Rouge Sill)

The sill was described by Upton and Wadsworth (1967); it shows a range in composition from alkali-olivine basalt to mugearite with segregation veins in the upper part of benmoreitic composition.

Sampling was based on a field division into several easily defined units. The contacts are black and flinty; these grade into the main body of the sill which has been divided into two parts: a lower, 6 meter thick dark portion overlain by 2 meters of a lighter coloured rock. The junction between the two parts is gradational over two to

Fig. 10.2

Diagrammatic cross-section of the Bras Rouge sill showing distribution of analysed samples.

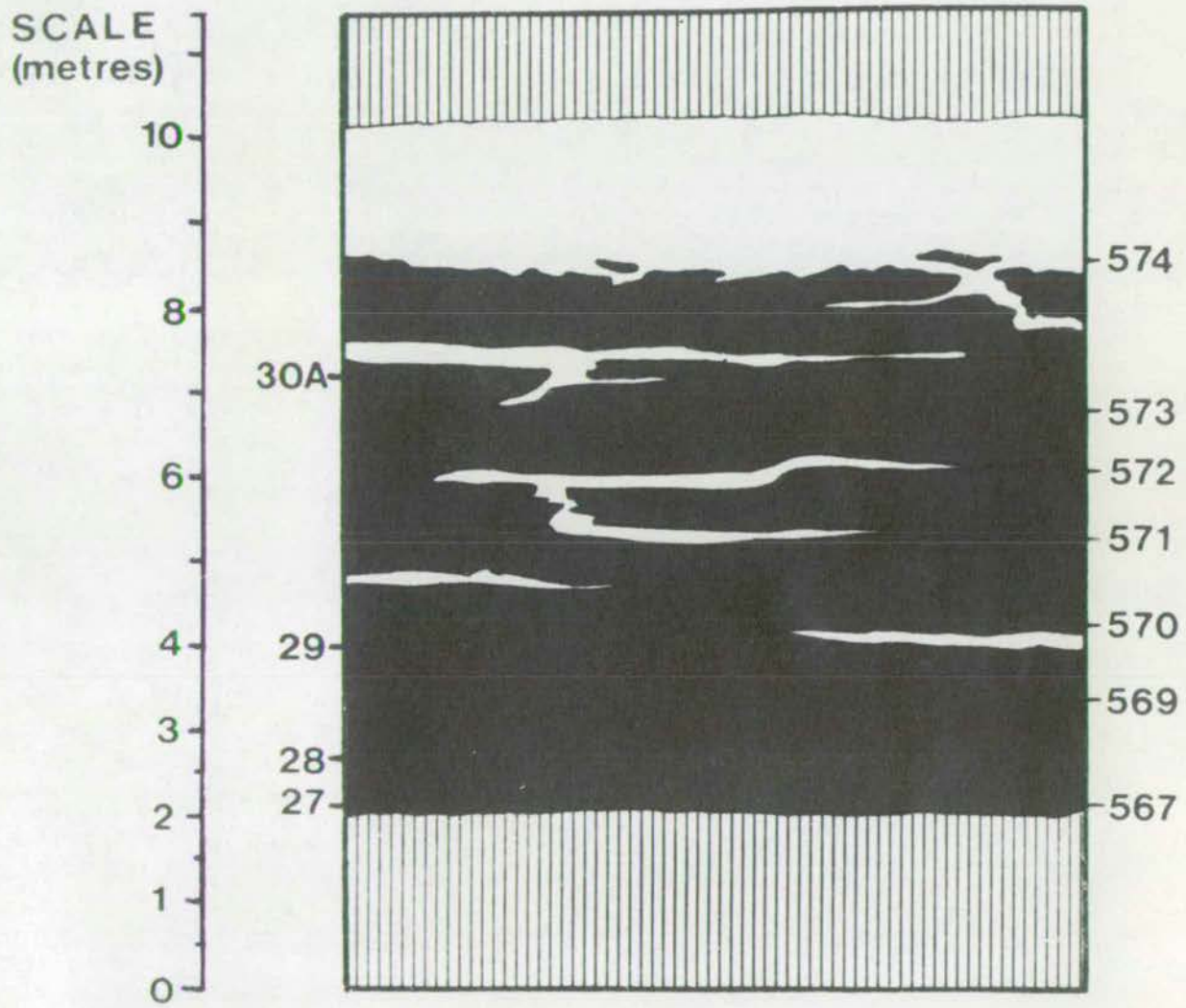
SCALE
(metres)
10
8
6
4
3
2
1
0
30A
29
28
27
574
573
572
571
570
569
567

Fig. 11.2.

Diagramatic sketch showing the location of samples collected from hawaiite flow on Piton des Neiges.

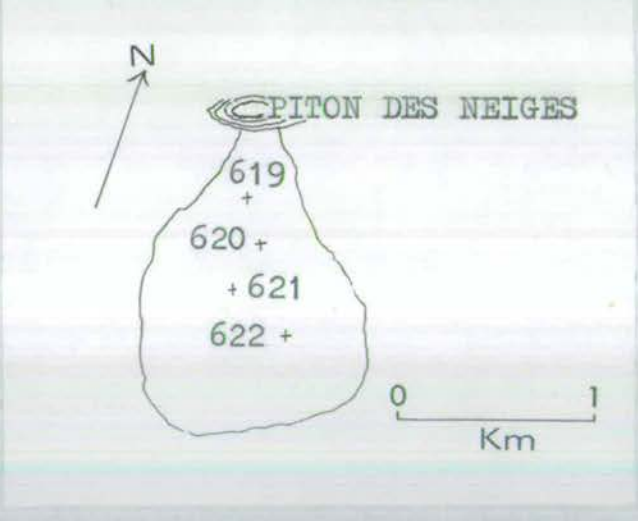

three centimeters; it is slightly irregular but approximately parallel with the contacts. Fragments of the lower part are incorporated within the upper facies; subhorizontal leucocratic veins are present throughout the lower dark zone, becoming more abundant and thicker near the junction with the lighter upper portion and appear continuous with it. There is no evidence of chilling against the more basic rocks.

Upton and Wadsworth interpreted the field evidence as indicating that the in situ "fractional crystallization of a basaltic magma...resulted in the upward segregation of an alkalic residue, which locally reinjected its complimentary basic fraction, and itself differentiated further to give the leucocratic veinlets in the upper part of the sill". (pp.1479-80). Their diagrammatic sketch of the sill (p.1479) is reproduced here (Fig. 10.2) showing the location of newly analyzed specimens.

Upton and Wadsworth in their interpretation of the data suggested that the sill was derived by successive topping of a zoned magma chamber. The initial injection of mugearite was thus followed by progressively more basic magmas.

Analyses of a single hawaiite flow, regarded as the youngest lava emitted from the summit crater of Piton des Neiges, were made to see whether it was derived from a similar, zoned magma chamber. The flow forms an extensive block lava flow that travelled SE from the summit area; the specimens were collected from widely spaced points along the length of the flow to ensure that as much of the presumed chamber would be sampled.

CHAPTER 3

PETROGRAPHY

Hebridean Province; Northern Skye

Introduction

General descriptions of the petrography of the composite flows at Drum na Criche, Roineval and Talisker were given by Harker (1904, p.264). He noted the similarities between the Drum na Criche and Roineval flows, but contrasted them with the flow at Talisker, which he suggested was more basic.

Muir and Tilley (1961) supplemented Harker's earlier description of the underlying mugearite by a detailed mineralogical investigation.

The present chapter describes the petrography of each of the three flows separately; their differences and similarities are summarized at the end.

Talisker

The junction between the two units is diffuse over some 80 cm.; the amount of phenocrysts in the lower unit never exceeds 3% whereas in the upper hawaiite they constitute between 18 and 25% (Table 1.3; Fig. 1.3). Less than 1% olivine (Fo_{55}) and titanomagnetite microphenocrysts are present. The plagioclase phenocrysts may be separated into two generations on morphological evidence: (A) one of ovoid, or ovoid with euhedral overgrowths (Plate 1.3, Figs. 1 and 2) and (B) a generation of phenocrysts which usually lack twinning, are embayed and frequently display sieve texture

PLATE 1.3

Fig. 1.

Ovoid phenocryst (Group A) with inclusions in margin.

Crossed polarizers. 30x.

Fig. 2.

Rounded microphenocryst (Group A) with euhedral overgrowth.

Crossed polarizers. 50x.

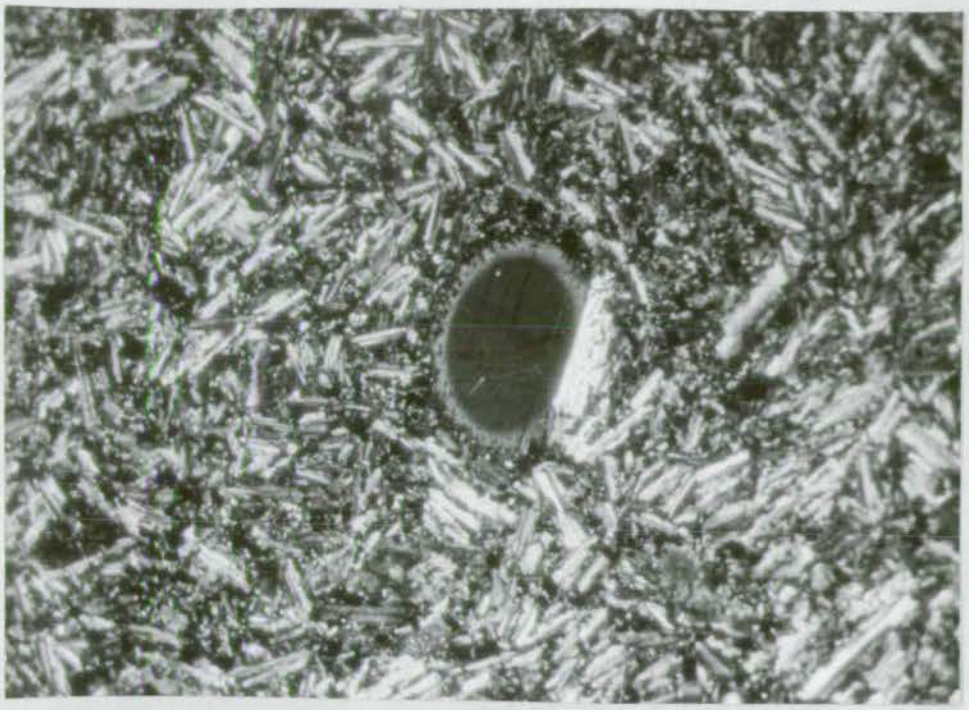

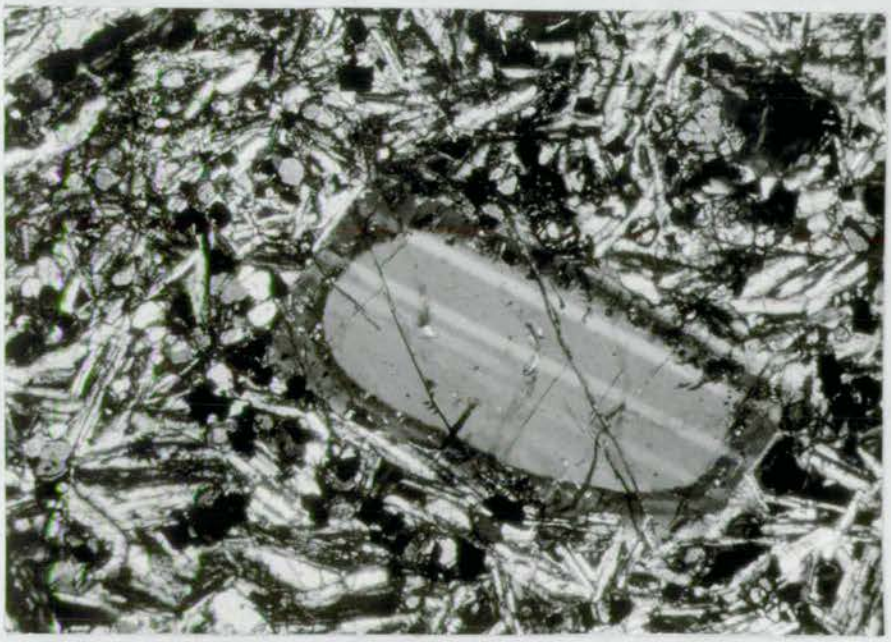

Table 1.3

Petrography of the composite flows, N. Skye

	Phenocrysts (volume %)			Groundmass					
TALISKER	PLAG	OL	OXIDES	PLAG	CPX	OL	Fe-Ti OXIDES	APATITE	BIOTITE, CHLORITE
Upper unit	18-25	1	1	+	+	+	+	+	+
lower unit	3	1	1	+	+	+	+	+	+
DRUM NA CRICHE									
Upper unit	20-27	1	1	+	+	+	+	+	+
Lower unit	1	1	1	+	+	+	+	+	+
ROINEVAL									
upper unit	28	1	1	+	+	+	+	+	+
lower unit[a]	1	1	1	+	+	+	+	+	+

[a] contains 1% amphibole pseudomorphs as phenocrysts

Fig. 1.3

Distribution of phenocrysts with height in the Talisker composite flow.

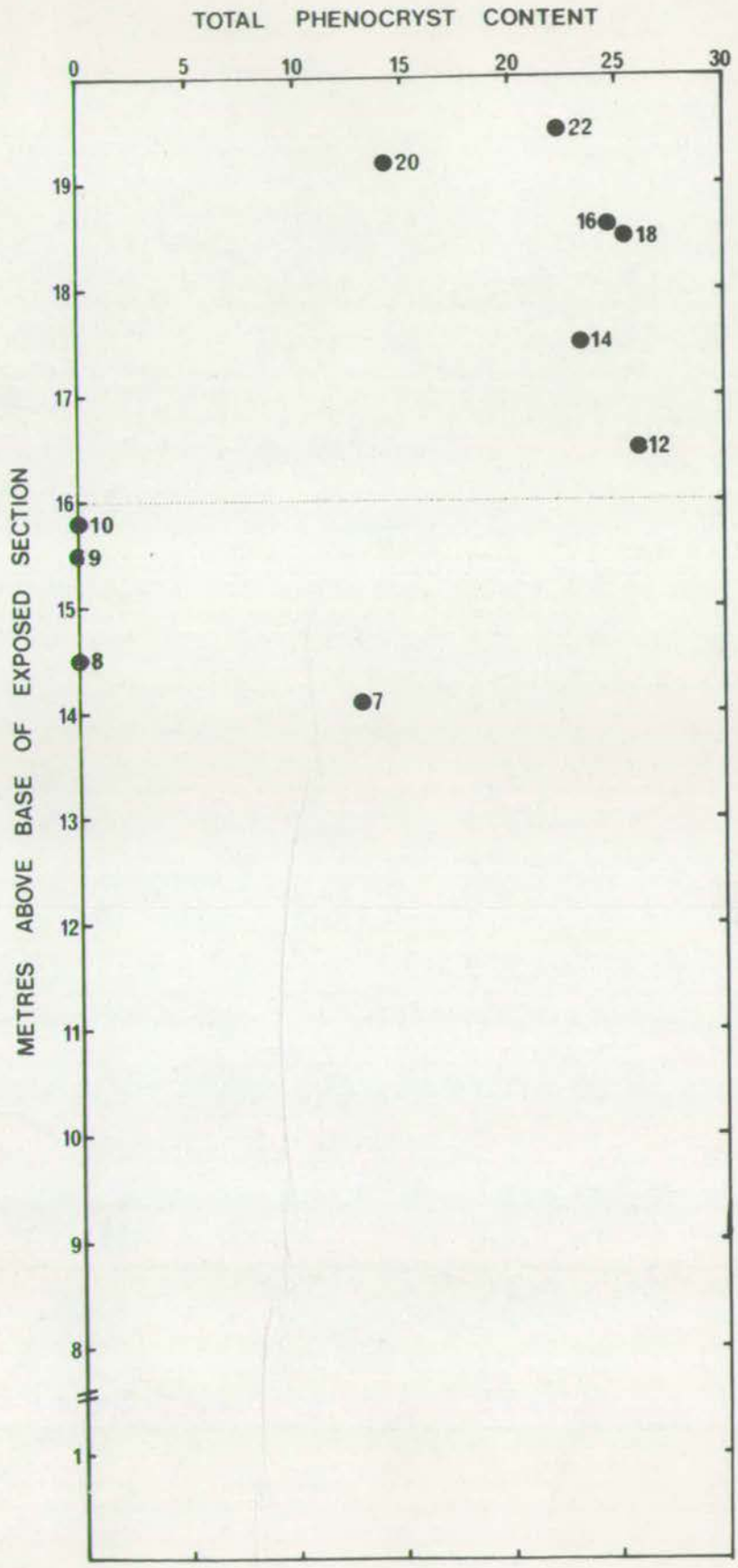
TOTAL PHENOCRYST CONTENT
0
5
10
15
20
25
30
METRES ABOVE BASE OF EXPOSED SECTION
19
18
17
16
15
14
13
12
11
10
9
8
1
22
20
16
18
14
12
10
9
8
7

(Plate 2.3, Fig. 1). The majority of phenocrysts belong to Group A; less than 1% are in Group B.

Group A phenocrysts have chemically homogeneous cores of labradorite surrounded by narrow more calcic rims, themselves jacketed by an outer rim which is zoned outwards to andesine. Inclusions (≪ 0.1 mm.) are concentrated in a zone between the calcic rim and the outer jacket.

Group B phenocrysts lack zoning and inclusions; they appear to be homogeneous andesines.

The size distribution of the phenocrysts in Group A appears distinctly bimodal (Plate 2.3, Fig. 2); there are "microphenocrysts" ranging from 0.8 mm. to 2 mm. and a population of larger crystals ("phenocrysts") ranging in size from 3 mm. up to 2 cm. in length. There is no apparent variation in the amount of either population with distance above the junction of the two units.

Rare phenocrysts of opaque spinel are present either as embayed crystals (1-8 mm. in length) with titanomagnetite rims or as inclusions within Group A plagioclase phenocrysts.

The groundmass of the porphyritic hawaiite has small (< 0.1 mm.) disoriented andesine laths, granular olivine, ophitic to subophitic titanoaugite, a scarce brown amphibole, abundant chlorite, clear patches of analcite and homogeneous titanomagnetite, sometimes surrounded by ilmenite granules.

Near the junction of the two units the hawaiite groundmass has a very pronounced trachytoid texture, with fewer plagioclase phenocrysts. The pyroxenes, olivines and titanomagnetites occur as very small granules (≪ 0.1 mm.) in the pre-

PLATE 2.3

Fig. 1.

Group B phenocryst, showing sieve-like texture.

Crossed polarizers. 15x.

Fig. 2.

Size range of phenocrysts and microphenocrysts in upper porphyritic unit.

Crossed polarizers. 30x.

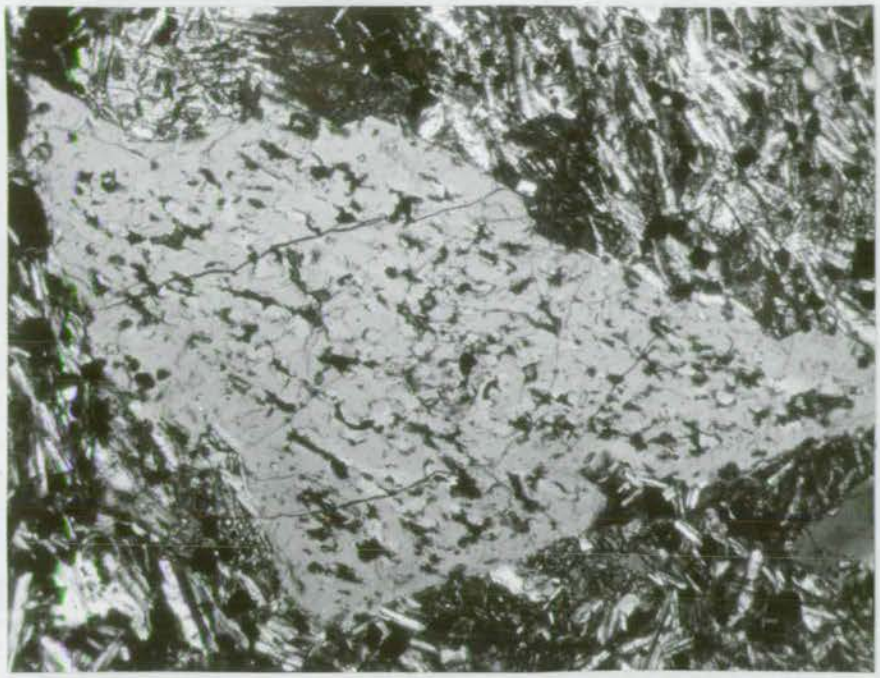

PLATE 3.3

Fig. 1.

Plagioclase phenocryst in lower hawaiite showing ovoid form, and rim of inclusions.15×

Fig. 2.

Cleavage fragments of ovoid phenocrysts showing no evidence of subsequent resorbtion after rupture.15×

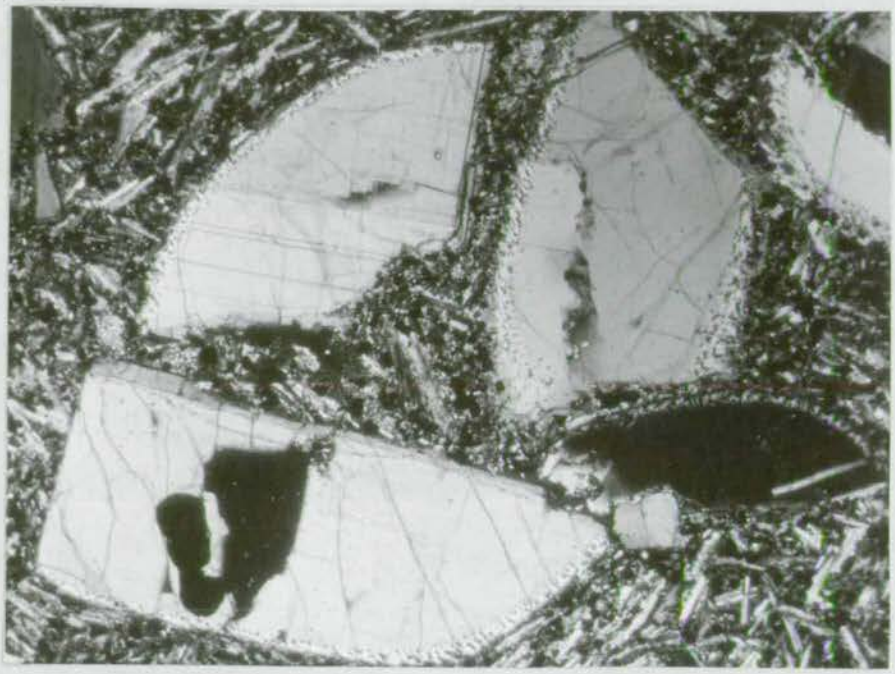

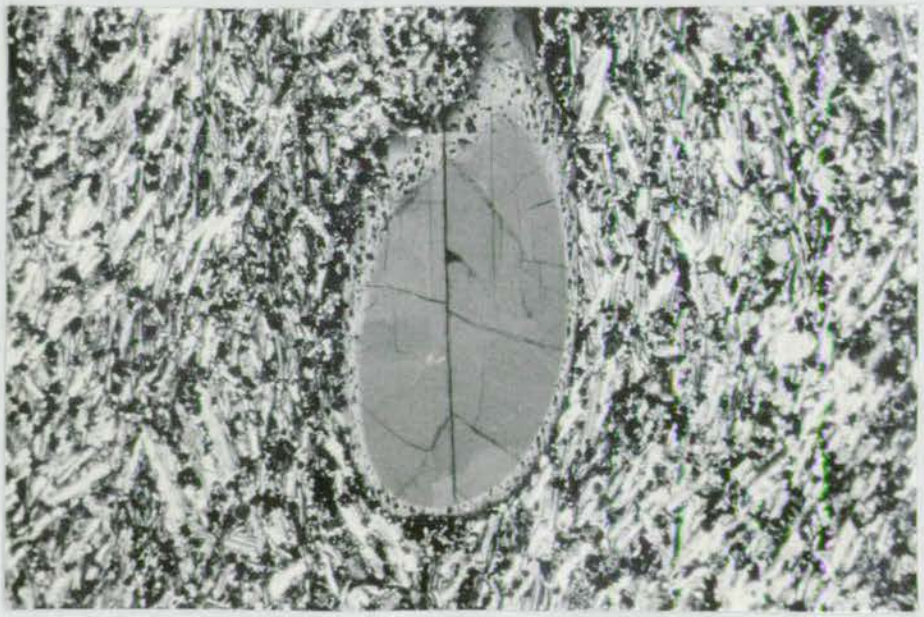

dominantly andesine matrix. The scarce phenocrysts of Group A plagioclase are almost invariably ovoid (Plate 3.3, Fig. 1) and generally lacking in euhedral overgrowths.

The aphyric hawaiites of the lower unit show a progressive decrease in grain-size below and away from the junction with the upper unit. The groundmass mineralogy and texture is similar to that of the lower part of the upper unit. Locally it may contain a much higher percentage of homogeneous titanomagnetites. An aggregate total of less than 1% microphenocrysts of sodic labradorite, olivine and titanomagnetite are present. Ovoid phenocrysts of plagioclase, similar to group A of the upper unit do occur throughout the lower unit, but they constitute less than 1% of the rock.

The alkali-olivine basalts lying below the composite flow contain 15-20% microphenocrysts of olivine, with occasional labradorite and titanomagnetite microphenocrysts. The groundmass contains plagioclase laths with rounded, altered olivines and subophitic to ophitic clinopyroxenes and chlorite replacing an original glassy mesostasis. Magnetite grains appear homogeneous; ilmenite is rare.

Drum na Criche

The upper porphyritic hawaiite has 20-27% andesine phenocrysts, embayed microphenocrysts of titanomagnetite and pseudomorphed olivine. Morphologically there appears to be only one generation of plagioclase phenocrysts although there are differences in composition of up to 6% An between individuals. The phenocrysts are euhedral, or rarely embayed; crystal fragments are common. There appears to be

a distinct bimodal distribution in phenocryst size; microphenocrysts ranging from 0.6 to 1 mm. and larger phenocrysts from 5 to 8 mm.

The groundmass is predominantly zoned plagioclase with granules of clinopyroxene, olivine pseudomorphs and very abundant, homogeneous titanomagnetites. Ilmenite occurs as scarce discrete grains, or rods; biotite, acicular apatite and a brownish amphibole are accessories.

The junction with the underlying mugearite is accomplished within several centimetres. The mugearite has a trachytoid texture; scarce microphenocrysts (0.8-1 mm.) of oligoclase have narrow rims of an alkali feldspar. The groundmass oligoclases are zoned outwards to alkali feldspar. Clinopyroxene and olivine occur as granules; titanomagnetite granules with occasional ilmenite lamellae, but no discrete ilmenite grains are present in amounts up to 12%. Acicular apatite, biotite and an amphibole are accessory minerals; pyrite and/or chalcopyrite as well as pseudobrookite (Muir and Tilley, 1961) occur as scarce discrete blebs.

Roineval

Petrographically and chemically the composite flow at Roineval is similar to that of Drum na Criche. The porphyritic hawaiite has phenocrysts of sodic labradorite with narrow, more calcic outer rims and an ill defined outer jacket of andesine which merges with the groundmass. There are occasional altered microphenocrysts (0.7 mm.) of olivine and relatively unaltered titanomagnetites (0.5-1 mm.). The plagioclase phenocrysts are euhedral, or rarely, slightly

embayed. Fragmented phenocrysts are common. There is, as at Drum na Criche, a pronounced bimodal distribution in the size of the phenocrysts: phenocrysts 0.5 to 1.2 mm. in length, and larger phenocrysts 3 to 20 mm. in length.

The petrography of the underlying mugearite is similar to that of the Drum na Criche mugearite, although the groundmass contains a higher percentage of chlorite(s). There are occasional microphenocrysts of an altered olivine, plagioclase, amphibole pseudomorphs, and titanomagnetites. Locally, the amount of plagioclase phenocrysts may approach 15% (i.e. the small outlier to the east); these are more calcic than the scarce microphenocrysts of andesine to oligoclase.

The groundmass oligoclases are strongly zoned, to alkali feldspar. Clinopyroxene granules are usually unaltered, but the titanomagnetites are largely altered to maghemite or haematite. Acicular apatite, biotite and amphibole occur as accessories.

Summary:

The similarities between the three flows may be summarized as follows:

1. All three upper units have the phenocryst assemblage plagioclase + olivine + titanomagnetite.
2. All three upper units appear to have a bimodal distribution of plagioclase phenocryst sizes.
3. All three flows have lower units that are nearly aphyric; these contain (a) phenocrysts similar in composition to the upper unit but show little or no resorption and (b) microphenocrysts that are more sodic in composition than (a).

Roineval and Drum na Criche have relatively minor differences; the flow at Talisker, however, differs from the others in that:

1. It contains the additional phenocryst phases of an opaque spinel and andesine.
2. The labradorite phenocrysts are frequently ovoid, with inclusion filled margins; the phenocrysts of Drum na Criche and Roineval are euhedral with no inclusions.

Roineval differs from Drum na Criche primarily in the wider, less well defined junction between the two units. Locally, the mugearite may contain sporadic phenocrysts throughout. The mugearite at Roineval also contains rare pseudomorphs after what appears to be amphibole.

The Midland Valley of Scotland

North Berwick, East Lothian.

The uppermost of the three flows exposed on the promontory at North Berwick pier is a plagioclase-phyric hawaiite. Phenocrysts of labradorite (6-8 mm.) constitute 17-20% of the rock; microphenocrysts of pseudomorphed olivine (2 mm.) contribute less than 3%. The groundmass is predominantly sodic labradorite, with granules of clinopyroxene, Fe-Ti oxides and needles of apatite in a chloritic matrix. The plagioclase phenocrysts are euhedral to subhedral, rarely showing any signs of corrosion. Narrow rims, normally zoned to An_{50}, are usually present. The olivine pseudomorphs are either chlorite(s) with opaque rims, or a mixture of chlorites plus calcite.

The underlying flow is a nearly aphyric benmoreite

(mugearite of Clough et al., 1910) with scarce microphenocrysts (1-1.5mm.) of andesine in a trachytoid groundmass of oligoclase zoned to alkali feldspar, granular clinopyroxene, haematite and maghemite. There are no apparent variations in the amount of plagioclase phenocrysts within the flow.

Lowest of the three flows is an alkali-olivine basalt ("Dunsapie type") with 18 to 21% calcic labradorite phenocrysts, 8-11% clinopyroxene phenocrysts and 6 to 8% of pseudomorphed olivine microphenocrysts. The plagioclase phenocrysts are euhedral to subhedral with occasional embayments, and usually show narrow normally zoned rims which only rarely contain inclusions. The clinopyroxene phenocrysts are optically homogeneous and frequently deeply embayed. There are possibly two generations; one more severely corroded, the other relatively unaltered, but no compositional difference between the two groups has been noted. In addition, there are occasional small gabbroic xenoliths (labradorite plus clinopyroxene and altered olivine) up to 1.5 cm. across.

The groundmass is sodic labradorite, granular clinopyroxenes and opaques, with probable olivine pseudomorphs, subordinate apatite and abundant chlorite(s).

Both the gabbroic xenoliths and the two possible generations of clinopyroxene phenocrysts have been noted in analogous basalts elsewhere in the Carboniferous volcanics of the Midland Valley (cf. Clark, 1956; MacDonald, J.G., 1965).

The Royal Park, Edinburgh

The Dasses Sill

The thickest portions of the Dasses Sill have a central facies of porphyritic alkali-olivine basalt ("Dunsapie type") with a marginal facies of porphyritic hawaiite (Markle); there is a gradational textural and compositional junction between the two. The differentiation between the facies was first made on structural grounds (Oertel, 1952) and later on a petrographic basis (Rutledge, 1952).

Oertel's (1952) division was based on the orientation and dispersion of phenocryst phases - notably plagioclase. Rutledge noted that although both facies have 20-28% plagioclase phenocrysts, augite was only present in the central, more basic component (Table 2.3 summarizes his petrographic observations).

The hawaiitic (outer) facies has 25-28% andesine zoned normally to oligoclase phenocrysts, less than 3% pseudomorphs after olivine microphenocrysts and less than 1% pseudomorphs after opaque microphenocrysts. The plagioclase phenocrysts are euhedral to subhedral, extensively altered, but with occasional clear, unaltered areas. Rutledge (1952) gives the average phenocryst size as 1-2 mm. with a maximum size of 14 x 10 mm. The outer rims frequently have zones of inclusions (opaque minerals plus stubby apatite crystals).

The pseudomorphs after olivine microphenocrysts average 1-1.5 mm. in diameter. The less abundant euhedral pseudomorphs are now largely haematite with some leucoxene or anatase.

The groundmass of the hawaiite consists of relatively

fresh andesine zoned to an alkali feldspar, altered clinopyroxenes and opaque minerals in an ophitic to subophitic texture. The opaque minerals occur as euhedral octahedra and granules. Acicular apatite crystals are common.

The central, alkali olivine basalt facies has phenocrysts of plagioclase, clinopyroxene, pseudomorphs after olivine and microphenocrysts of Fe-Ti oxides. The basalt is considerably less altered than the hawaiite. The plagioclase occurs as euhedral to subhedral phenocrysts, averaging 4-6 mm., but not exceeding 7 mm. in length. They show narrow, more calcic rims than cores, with inclusions of opaque minerals, clinopyroxene and possibly olivine pseudomorphs. The volume of phenocrysts (20-27%) overlaps the range found in the hawaiite.

Titanaugite occurs as euhedral to subhedral phenocrysts, pale brown with a faint purplish tinge. The crystals range from 1.0 to 3.0 mm. across, and show but minor alteration, along fractures or cleavage planes, usually to chlorite(s). The average content of titanaugite phenocrysts is 6%.

The olivine pseudomorphs are similar in size to the clinopyroxene phenocrysts, but more abundant, averaging 8%. The pseudomorphs are largely calcite with rims and zones of chlorite(s) and opaque minerals.

Fe-Ti oxides occur as euhedral microphenocrysts, usually less than 1.5 mm. They are altered to haematite, or maghemite, or occasionally even more altered to a mixture of leucoxene and rutile.

The groundmass of the alkali-olivine basalt is less altered than that of the hawaiite; it is predominantly andesine zoned to an alkali feldspar, with clinopyroxene

granules and prisms, olivine pseudomorphs and granules of opaque minerals. Chlorite, analcite, apatite and biotite are present, but less abundant.

Locally the rocks are intensively altered. Rutledge (1952), in discussing the sequence of alteration, considered that it occurred in several definite stages: (A) analcimisation of the groundmass and plagioclase phenocrysts; (B) Chloritisation of the ferromagnesian phenocrysts and groundmass minerals. Both Clark (1956) and Rutledge (1952) believed that the feldspars, in particular, had been altered from more calcic compositions to albite throughout both stages (analcitisation and chloritisation). The last stage involved emplacement of calcite and quartz in veins filling fractures.

St. Leonard's Sill

In contrast to the Dasses Sill, St. Leonard's Sill has a well defined porphyritic central facies of alkali-olivine basalt and a nearly aphyric marginal facies of benmoreite composition. The marginal facies is extensively altered whereas the central facies shows relatively little alteration, with the exception of the groundmass and microphenocrysts of Fe-Ti oxides which are now maghemite and haematite.

The central alkali olivine basalt ("Dunsapie-type") has 17-20% euhedral to subhedral labradorite phenocrysts 5% titanaugite and 1% of pseudomorphed olivine microphenocrysts. Microphenocrysts of Fe-Ti oxides constitute less than 1%. The plagioclase phenocrysts are slightly altered, with homogeneous cores and normally zoned rims; the titanaugite

TABLE 2.3

	PHENOCRYST (Volume %)				GROUNDMASS						
	PLAG	CPX	OL	Fe-Ti OXIDES	PLAG	OL	CPX	OXIDES	APATITE	BIOTITE	CHLORITE
DASSES											
Outer facies	25-28	-	3-3	1	+	?	+	+	+	+	
Inner facies	20-27	6	8	1	+	+	+	+	+	+	
ST. LEONARDS											
Outer facies	2	-	-	-	+	?	+	+	+	+	
Inner facies	17-20	5	1	1	+	+	+	+	+	+	

phenocrysts are euhedral with slight zones of alteration along the margins and fractures. Although they appear optically homogeneous, analyses indicate that they are zoned. It should be noted that there are no corroded clinopyroxenes as in the analogous central basalt zone of the Dasses or in the alkali olivine basalts of the extrusive sequence (Clarke, 1956).

The groundmass is predominantly (≃ 40%) andesine with subophitic or granular clinopyroxene (12%), olivine pseudomorphs (3%), opaque minerals, now largely haematite or maghemite (6%) and a matrix of analcite and chlorite(s).

The very altered outer facies has scarce microphenocrysts of oligoclase averaging less than 1.5 mm. in length. The groundmass has a trachytoid texture, predominantly oligoclase zoned to an alkali feldspar with granules of opaque minerals, and clinopyroxenes.

The junction between the two facies is quite diffuse; an average width measured at the locality where the samples were collected was 110 cm.

MacGregor (1928) considered all three composite intrusions (The Dasses, Girnal Craig, St. Leonard's Sill) to be representative of a single intrusive event. The petrography of the three intrusions suggests that whereas the Dasses and Girnal Craig might be parts of a single intrusion, St. Leonard's Sill should be considered as a separate intrusion.

The Composite Flow south of Greenock.

The upper, plagioclase-phyric hawaiite (Markle basalt of Kennedy (1931)) contains 15-22% plagioclase phenocrysts

Fig. 2.3

Phenocryst distribution with height in the Greenock composite flow.

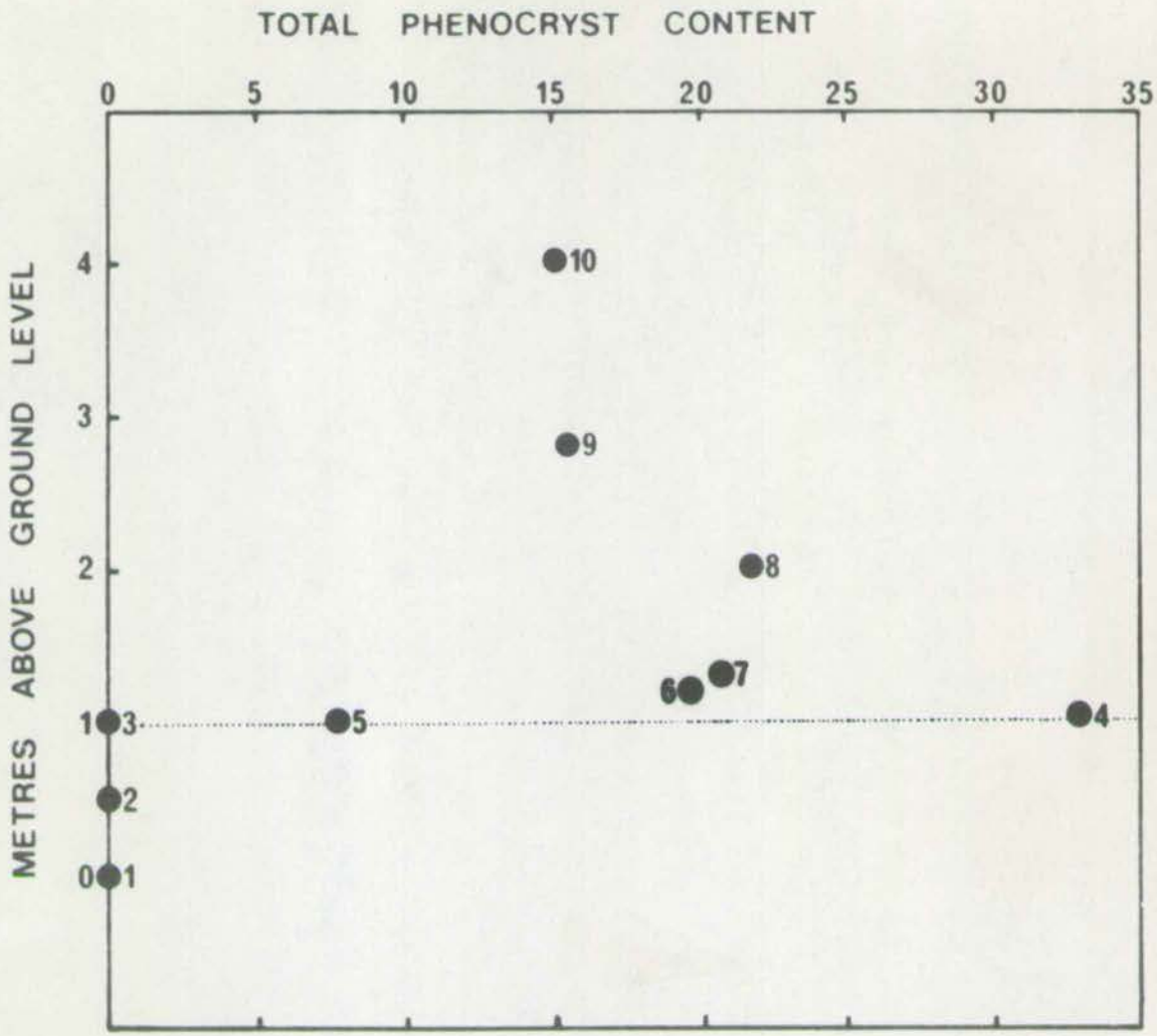
TOTAL PHENOCRYST CONTENT
0
5
10
15
20
25
30
35
METRES ABOVE GROUND LEVEL
4
3
2
1
0
10
9
8
7
6
5
4
3
2
1

PLATE 4.3

Fig. 1.

Zoned microphenocrysts in upper porphyritic Hawaiite, Greenock Composite flow.

Crossed polarizers. 30x.

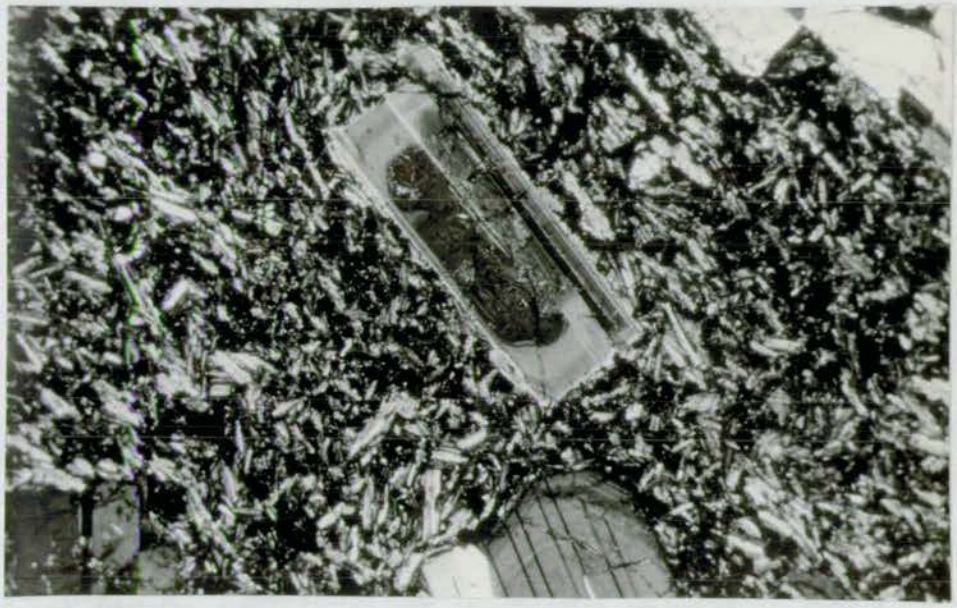

with less than 1% clinopyroxene and titanomagnetite microphenocrysts. The amount of phenocrysts increases from 15% to a maximum of 22% (Table 2.3, Fig. 2.3) 1 metre above the junction with the underlying mugearite. The phenocrysts are generally euhedral with continuous rims around a complexly zoned core (Plate 4.3, Fig. 1) of bytownite. The phenocrysts show a distinct bimodal size distribution: (A) microphenocrysts ranging from 0.8 to 2 mm., and (B) phenocrysts ranging in size from 6 mm. up to 10 mm. and occasionally as large as 20 mm. The rare microphenocrysts (2-2.5 mm.) of clinopyroxene and titanomagnetite tend to be glomeroporphyritic as do the larger plagioclase phenocrysts.

The groundmass of the upper porphyritic unit has the distinctive lack of a trachytoid texture in common with the hawaiites of the N. Skye composite flows. Plagioclase laths predominate, with granules of clinopyroxene, amorphous haematite or maghemite after titanomagnetite, olivine pseudomorphs and stubby apatite crystals. Kennedy (1931) noted the presence of quartz xenocrysts with clinopyroxene reaction rims, as being present in both parts of the flow, but none was noted in the present study.

The underlying, nearly aphyric mugearite contains scarce euhedral microphenocrysts of andesine (0.9-2 mm.) with narrow rims zoned to oligoclase. Kennedy (1931) also noted scarce phenocrysts of bytownite in the upper part of the mugearite which he believed were derived from the overlying porphyritic unit. These were not present more than 80 cm. below the junction in the specimens examined during the present study. Microphenocrysts ($\simeq$ 1 mm. in length) of clinopyroxene are

Table 3.3

	PHENOCRYSTS (Volume %)			GROUND MASS					
	PLAG	CPX	Fe-Ti-OXIDES	PLAG	CPX	OL	Fe-Ti-OXIDES	APATITE	BIOTITE, CHLORITE
GREENOCK									
Upper Unit	15-22	1	1	+	+	+	+	+	+
Lower Unit	1	1	1	+	+	+	+	+	+

also present.

The groundmass has a pronounced trachytoid texture with predominant oligoclase zoned to alkali feldspar (0.08-0.25 mm.), subophitic clinopyroxene, olivine pseudomorphs, amorphous haematite (after titanomagnetite ?), acicular apatite and scarce biotite and a brownish amphibole.

Craigmarloch Wood

In contrast to the other composite flows studied, the possible composite flow at Craigmarloch Wood has a more evolved (benmoreite) porphyritic unit between nearly aphyric, less evolved (mugearite) unit(s).

The central porphyritic benmoreite contains euhedral or slightly embayed and rounded phenocrysts of andesine (4 to 8 mm.) largely altered to sericite. These tend to be glomeroporphyritic. Euhedral to subhedral microphenocrysts of clinopyroxene and olivine pseudomorphs (1 to 3 mm.) are also present.

The groundmass has an orthophyric texture with predominant oligoclase laths, granular clinopyroxene and haematite or maghemite (after titanomagnetite ?), stubby apatite crystals and a mesostasis of alkali feldspar.

The nearly aphyric mugearite has a groundmass with a distinctive trachytoid texture, dominated by zoned andesine laths (0.15 - 0.2 mm.) with an alkali feldspar in the interstices. Granular clinopyroxene, olivine pseudomorphs, haematite and accessory acicular apatite with scarce biotite flakes comprise the rest of the groundmass.

Transition zones (see Fig. 6.2) 50 to 80 cm. wide occur between the central benmoreite flow and the mugearites.

Kennedy's (1932) descriptions suggest that the mugearite was at least partially solidified when the benmoreite was intruded; rounded, embayed fragments of mugearite predominate. Veins of benmoreite penetrate the mugearite, the internal structure of which is severely distorted.

The occurrence suggests that more evolved compositions than mugearites may occur within composite flows. Texturally, the roles are reversed, with the more evolved member being porphyritic, and instead of almost simultaneous eruption, more time had elapsed before intrusion of the second unit. The next occurrence discussed shows a similar association, but it is one in which the textural analogy with composite flows is more exact, and in which there was a longer period between eruption of the contrasting flow units.

South-west Greenland

The central facies of the composite dykes contains from 20 to 40% sodic labradorite or andesine phenocrysts, usually rounded, but rarely embayed. They are accompanied by up to 4% of other phenocrysts, listed below in order of abundance:

(A) Euhedral to subhedral Fe-Ti oxides, frequently displaying resorption features.

(B) subhedral clinopyroxenes 2-3 mm. across.

(C) Pseudomorphs (after olivine ?)

(D) Euhedral, colourless, apatite prisms frequently associated with the Fe-Ti oxides.

The groundmass of the central facies is predominantly andesine zoned to alkali feldspar. Clinopyroxene (frequently chloritised), amphibole, biotite, opaque minerals and acicular

Anorthosite and plagioclase megacryst fragments in B.F.D. dyke from the south coast of eastern Tugtutoq.(photograph courtesy of Dr.B.G.J.Upton)

apatite complete the assemblage.

Bridgwater and Harry (1968) make a distinction between what are called plagioclase phenocrysts here, which are included within the group they prefer to call plagioclase "megacrysts", and a series of xenoliths, possibly cognate.

The term "megacrysts" avoids genetic implications; it includes large feldspar crystals of two likely origins: (a) phenocrysts (which have never settled and aggregated) and (b) cognate xenocrysts from an early formed anorthositic cumulate. Their observations suggest that the anorthosite xenoliths represent the earliest stage of fractionation products followed by the "megacrysts", although precipitation of the latter, overlaps the formation of the anorthosites and extends to include the phenocrysts formed as the last generation of plagioclases in the magma.

Phenocrysts may be distinguished from the (cognate) xenocrysts derived from the disaggregated anorthosites on the basis of the following criteria, based upon Bridgwater and Harry's (1968) data:

(A) Deformation textures. Plagioclases in the anorthosites invariably are granulated, ruptured or at the very least show deformation of twin planes. Phenocrysts are not granulated, although they may show some distortion of the optical indicatrix. In only one instance has anorthosite that is free of deformation been noted (Upton, 1964).

(B) Composition. The anorthosite plagioclases are generally more calcic ($\geq An_{60}$) than the phenocrysts in the composite dykes (An_{50}-An_{35}).

(C) Inclusions. Plagioclases from the anorthosites only rarely show inclusions; when present, these are almost invariably concentrated along the crystal boundaries. Phenocrysts may not always contain inclusions, but when present, they tend to be scattered throughout the crystal or concentrated in a marginal zone surrounding an inclusion free core.

Deformation of the anorthosite xenoliths obscures the textures of the plagioclases and included mafic minerals. Upton (1964) believes that plagioclase alone was the phenocryst phase at the time of the anorthosite formation from a liquid parental to the composite dykes. It should be noted, however, that there are included within the anorthosites the following phases:

Olivine + Fe-Ti oxides + orthopyroxene + clinopyroxene. Whether they are cumulus phases (with the plagioclase) is in question.

The marginal more evolved facies contains 1-5% of alkali feldspar phenocrysts, typically rhomb-shaped, 2-20 mm. in length. Locally they may form "rafts" (Bridgwater and Harry, 1968) and include phenocrysts of Fe-Ti oxides. The phenocryst assemblage in the marginal facies is:

Alkali feldspar + opaques + olivine pseudomorphs + clinopyroxene pseudomorphs + apatite.

Microphenocrysts of apatite, and both olivine and clinopyroxene pseudomorphs are scarce.

The groundmass of the marginal rocks is predominantly zoned equidimensional alkali feldspar, ophitic to subophitic clinopyroxene, apatite needles, chlorite and biotite. The

groundmass near the chilled margin has a poorly defined trachytoid texture, which becomes progressively more equigranular away from margin.

Within the transition zone between the two facies both alkali feldspar and plagioclase (usually severely altered) phenocrysts may occur. Clinopyroxene, olivine pseudomorphs, Fe-Ti oxides, scarce apatite are also present as phenocryst phases. As in the central facies, the apatite and Fe-Ti oxides are frequently associated. Biotite may surround the Fe-Ti oxides, which usually show resorption features.

The groundmass is equidimensional with predominant plagioclase zoned to an alkali feldspar, and clinopyroxene, chlorites, opaques and apatite needles. Patches of carbonate and epidote are frequently present.

Réunion: Bras Rouge Sill

The petrography of the sill in the gorge of the Bras Rouge has been described by Upton and Wadsworth (1967). A new suite of specimens has been analyzed, and the following account draws primarily on Upton and Wadsworth's description with additional minor details from the new suite. Table 3.3 summarizes the petrography of both suites; it is based in part upon Table 1 of Upton and Wadsworth.

The lower chilled margin contains a maximum of 5% of microphenocrysts; these are predominantly a sodic andesine, corroded alkali feldspars, and scarce bytownite. Clinopyroxene, Fe-Ti oxides and a brown basaltic hornblende occur more rarely. The semi-opaque groundmass has scattered calcite-filled ocelli.

With increasing height above the base of the sill, grain

TABLE 3.3A

SUMMARY OF PETROGRAPHY OF THE BRAS ROUGE SILL

Based on Data from Upton and Wadsworth's (1967) Table 1, with additional data for the samples analyzed in this study. Numbers throughout the text refer to the sample numbers given in this table and in Appendix A.

MODAL PERCENTAGES

	Feldspar	cpx	ore	chlorite + biotite	amphibole	quartz	calcite	olivine pseudom.
Re 574	55.1	24.3	14.8	2.1	-	-	3.7	-
Re 30A	52.0	22.0	12.4	3.4	-	-	5.0	5.1
Re 573	48.9	24.2	13.1	9.3	-	0.2	4.3	-
Re 572	57.1	17.9	11.1	10.6	-	-	3.3	-
Re 571	55.2	17.1	14.2	10.2	-	-	3.3	-
Re 570	56.1	12.1	15.9	11.2	0.5	-	4.2	-
Re 29	59.3	6.5	12.9	13.2	1.6	0.7	5.8	trace
Re 569	61.3	4.2	13.1	14.1	-	0.5	4.9	-
Re 28	67.3	1.3	8.4	-----	16.2 -----	0.5	6.2	-
Re 5670	16.1	1.5	1.4	-	-	-	-	-
Re 5671	5.6	0.8	1.2	-	-	-	-	-
Re 27	4.5	0.7	0.7	-	trace	-	-	-
	2.0	0.5	1.3	—	—	—	—	—
Re 619	21.2	2.0	0.6					1.9
620	19.7	0.5	0.6					2.1
621	16.9	1.0	0.5					1.6
622								

size increases and distinction between phenocryst (or xenocryst) and groundmass becomes difficult. Relatively large plagioclases in the lower 2 m. of the sill (28,569) have distinctive zones of sieve texture separating oligoclase cores from more andesine outer rims; these have been interpreted as possible phenocrysts by Upton and Wadsworth. Within less than a metre's distance above this, the amount has decreased and the cores are labradorite with more calcic rims. No other phases have been interpreted as being phenocrysts in the central part of the sill, although one of the two generations of titanomagnetites probably is. These are 0.8-1.5 mm. across and usually altered.

The groundmass is predominantly plagioclase, which increases both in amount and anorthite content upwards. Plagioclase core compositions range from andesine (28) to labradorite (29,574), and Upton and Wadsworth report bytownite for a specimen from the central, most basic zone (30A). The plagioclases are zoned normally outwards to an alkali feldspar which merges with the mesostasis. Towards the centre of the sill ophitic to subophitic clinopyroxene coexists (572) or takes the place of (573,574) amphibole and chlorite(s). Upton and Wadsworth report pseudomorphs after olivine (30A) in the centre of the sill. Biotite, chlorite(s), titanomagnetites, ilmenite and acicular apatite are present throughout. Zoned amphiboles (28,29,569-572) partially replaced by chlorite are present in the lower parts of the sill. Patches of calcite and to a lesser extent quartz are present, although no quartz is found in the most basic rocks. A smaller

generation of Fe-Ti oxides are relatively unaltered (as contrasted with the possible microphenocryst generation, which are extensively altered); both chalcopyrite and pyrrhotite are present as discrete rounded grains in the groundmass, but rarely included within the Fe-Ti oxides.

The Hawaiite flow (Fig. 11.2)

With the exception of a specimen from the uppermost part of the flow (619), the flow has abundant (18-22%) euhedral labradorite, 1-2% clinopyroxene and olivine phenocrysts as well as 0.5-1% Fe-Ti oxide microphenocrysts in a trachytoid groundmass of plagioclase, clinopyroxene granules and Fe-Ti oxides, set in a matrix of semi-opaque glass. There are less abundant euhedral to subhedral bytownite microphenocrysts, slightly corroded, present in at least one specimen (619).

The petrography for both the sill and flow is summarized in Table 3.3).

CHAPTER 4

MINERALOGY

Introduction

The phenocryst assemblages and some groundmass minerals from the composite bodies have been analyzed by electron microprobe. For some plagioclase phenocrysts these data are supplemented by XRF data for trace elements. All analyses are presented in Appendix C and summarized in figures throughout this section. Reference to individual analyses within the tables of Appendix C is made by bracketed figures. Discussion of the analytical statistics as well as the recalculation procedures precede the analyses in the Appendix.

In this section the mineral assemblages are described for each composite body in the following order: (a) phenocrysts, in order of abundance, (b) groundmass minerals.

FELDSPARS

North Skye; Talisker

As discussed in the petrography section, the plagioclase phenocrysts were subdivided into Groups A and B. Group A phenocrysts are typically ovoid or ovoid with a varying amount of euhedral overgrowths. The cores are chemically homogeneous, $An_{52}Ab_{47}Or_1$ (1) surrounded by a thin (< 0.03 mm.) crenulated zone of $An_{60}Ab_{39}Or_1$ (2). Peripheral to this zone and the discontinuous outer zone, which may be in part a euhedral overgrowth, are small (< 0.01 mm.) inclusions (Plate 1.4; Figs. 1,2) of clinopyroxene, opaques and possibly

Fig. 1.4.

The composition and structural state of plagioclase phenocrysts from the North Skye composite flows plotted on Uruno's (1963) diagram. The dashed lines are Uruno's measure of Al-Si order based on optical parameters. The most ordered ("low") plagioclases would plot on the left hand side of the diagram. Solid lines (running NNW-ESE) are lines of equal An content. The solid symbols represent phenocryst cores, the unfilled symbols, the rims. XX(α α) and YY ($\beta\beta$) are the total angular distance measured across the trace of (010) on the stereographic net.

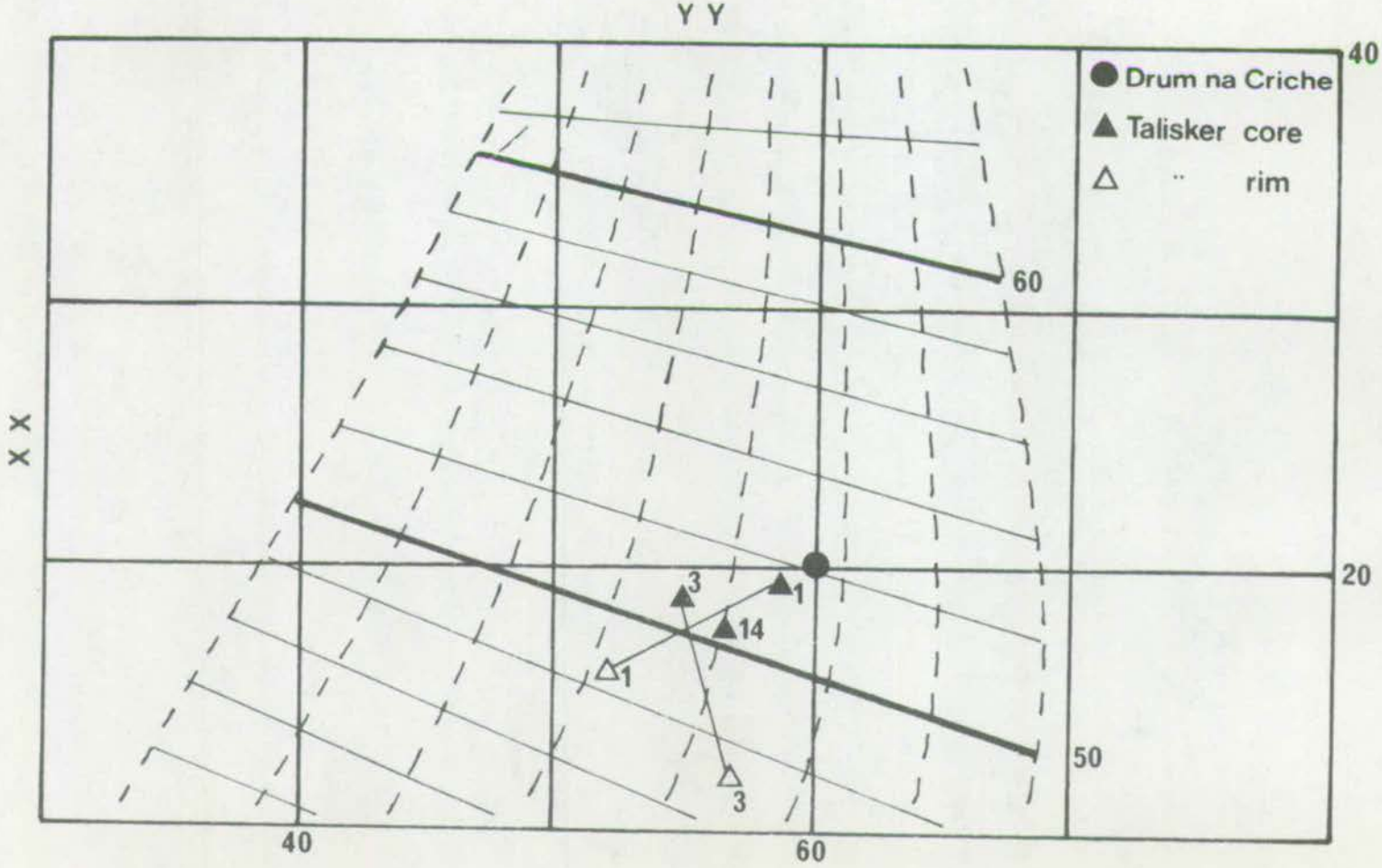
Y Y
X X
Drum na Criche
Talisker core
rim
40
60
20
50
40
60
3
1
14
1
3

zircons. This zone grades outward from $An_{45}Ab_{54}Or_1$ to $An_{34}Ab_{63}Or_3$(3,4) with scarce patches of anorthoclase.

The scarcer Group B phenocrysts are irregular in shape, embayed, or showing incipient sieve texture; and are chemically homogeneous - $An_{32}Ab_{64}Or_4$ (5). In contrast to the phenocrysts of Group A, which usually have abundant twin lamellae, the phenocrysts of Group B are apparently untwinned, with irregular, patchy extinction.

Optical determinations of the composition and structural state of the phenocrysts of Group A were made using a universal stage and plotting the Köhler angle (the difference in degrees between the α and β of adjacent twin lamellae on a diagram first presented by Uruno (1963) (Fig. 1.4).

On the basis of the optical determinations, supplemented by XRD data (Table 5C of Appendix C), the phenocrysts of Group A have an intermediate structural state, typical of plagioclase phenocrysts in volcanic rocks (Stewart et al., 1966). There are some differences between the parameters given by Bambauer et al. (1967) for plagioclases of this composition and the present data. Part of the difference is certainly due to the fact that the powders used in the XRD traces are bulk phenocryst including up to 5% of plagioclase with a different composition and possibly structural state. It is not known what scatter in the data is usually found, but the differences are small enough to suggest that they are not significant.

Bulk phenocryst separates (6,7) from different levels in the upper hawaiite were analyzed by XRF (Table 1.4), Sr ($\simeq$ 1100 ppm) and Ba ($\simeq$ 50 ppm) contents are similar to the

PLATE 1.4

Fig. 1.

Cathodoluminescence of plagioclase phenocryst in porphyritic hawaiite near Talisker. The central portion (An_{52}) is uniform in colour, except for light patches possibly due to impurities. The more calcic rim (An_{62}) is darker. Light blue areas in groundmass are a more sodic plagioclase (An_{40-35}). Orange patches are apatite; Fe-Ti oxides, clinopyroxenes, olivine and chlorite are black. 3×

Fig. 2.

Similar to Fig. 1, but showing faint dark striations in the central area, due possibly to compositional variations. Dark areas in the groundmass feldspars are due to a combination of the red-infrared plus blue spectral peaks typical for alkali feldspars. 3×

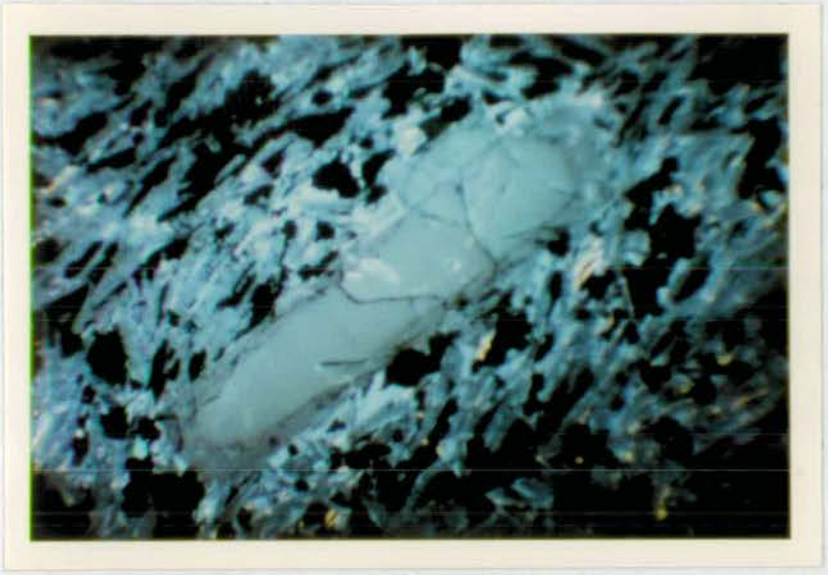

levels present in plagioclases (An_{55-50}) tabulated by Corlett and Ribbe (1967). Rough estimates of Sr zoning by microprobe traverses gave 640-980ppm in the centre, 900-1100ppm in the outer jacket. The high levels of Zr and Ni in the phenocrysts are probably due to the inclusions from the outer part of the Ca-rich zone.

Cathodo luminescence of the calcic plagioclases of the hawaiites is characterized by two broad spectral peaks (Sippel and Spencer, 1970) at ≈5590Å (green) and ≈4500Å (blue). A third peak, at ≈7100Å (red-infrared) appears in more sodic feldspars, which lack the green peak. The position of both the green and blue peaks is not sensitive to composition; the activator ions responsible for the luminescence are not known, but in the case of the green peak Sippel and Spencer concluded that some ion replacing calcium in the plagioclase structure was responsible. Plagioclases of different generations in lavas have been distinguished on the basis of their spectra (D.J. Marshall, pers.comm. 1972) but there was no apparent difference in the spectra of Groups A and B phenocrysts. It is known that iron diminishes the effect (Kastner, 1971) of luminescence; hence the high iron content of the Talisker groundmass may inhibit the effect. Group A phenocrysts (Plate 1.4, Figs. 1 and 2) show distinctive colour changes in the compositionally different cores and rims, as explained in the figure captions.

The groundmass plagioclase laths are zoned from An_{45} through $An_{34}Ab_{63}Or_1$ to $An_5Ab_{73}Or_{22}$ (8,9), similar to the range reported by Keil et al., (1973) for hawaiites from

PLATE 2.4

Fig. 1.

Ovoid phenocryst of Group A with homogeneous core, more calcic rim (dark zone) and ragged outer jacket. Inclusion zone lies partly in calcic rim and partly in the outer jacket.
Magnification: 30x; crossed polarizers.

Fig. 2.

Detail of ovoid phenocryst showing elongate "worm trails" reaching almost to the outer rim. The crenulate nature of the border between the core and outer jacket is visible, marked by a lighter shade of grey.
Magnification: 30x; crossed polarizers.

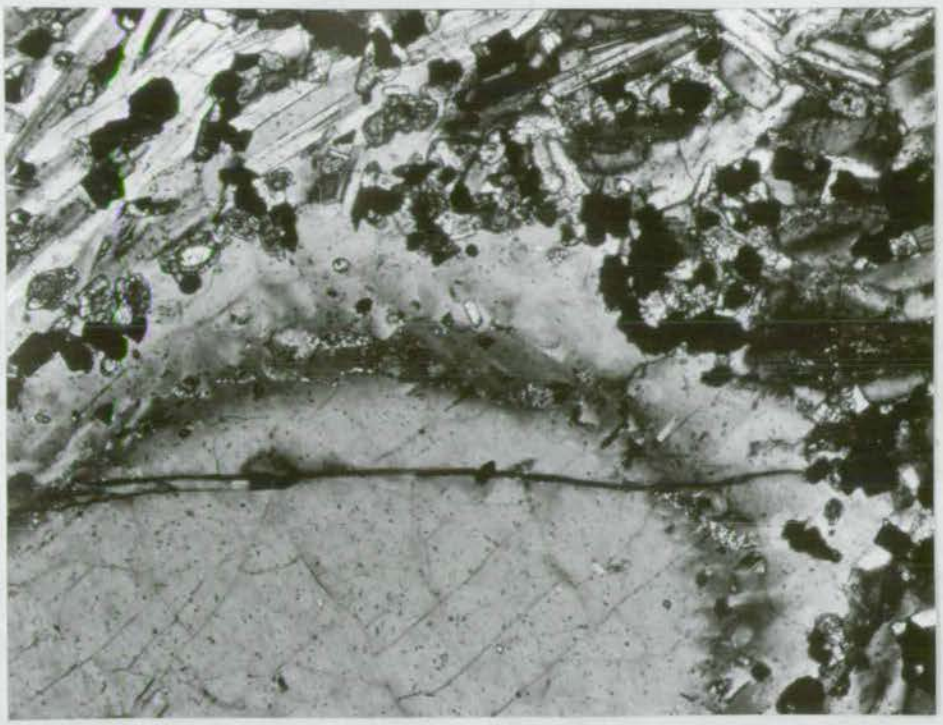

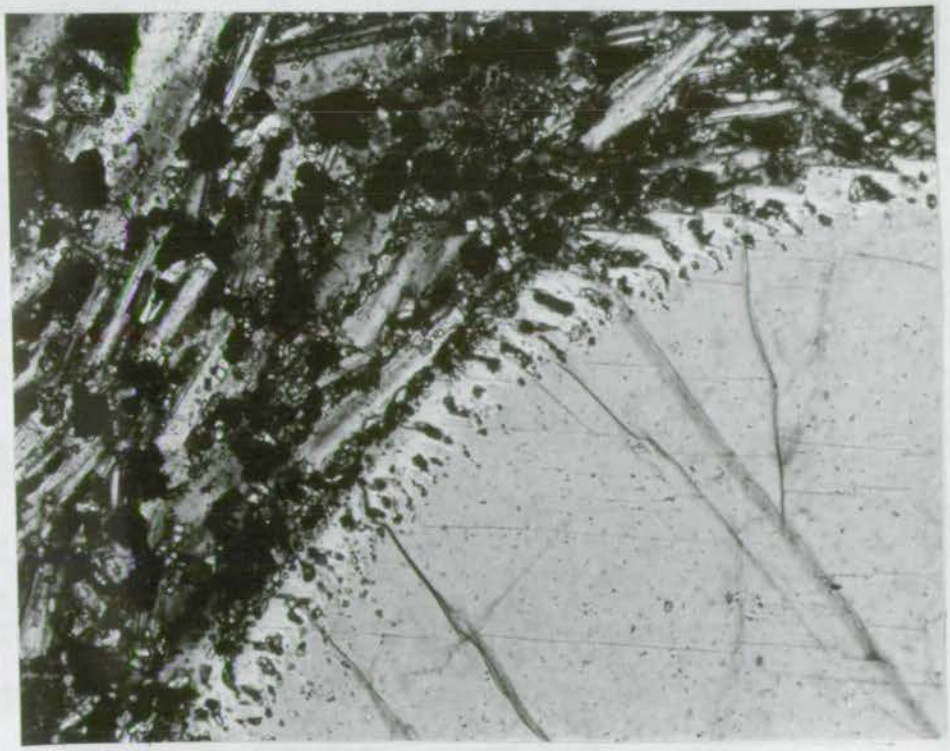

Haleakala and West Maui. It is not sure whether there exists a compositional gap (as reported by Keil et al.) for the groundmass feldspars from An_{34} to anorthoclase or whether there is a continuum of compositions. There are irregular, clear patches of analcime (10); these are probably the last phase to crystallize from the residuum, rather than anorthoclase, as implied by Keil et al., 1973.

The lower, essentially aphyric unit contains scarce ovoid phenocrysts (Plate 2.4; Fig. 2) similar to those of Group A in the upper unit but very rarely having any overgrowths. Optical determination of composition (An_{52}) suggests they are possibly the same group of phenocrysts. Euhedral microphenocrysts of plagioclase are very scarce (< 2%) but significantly more basic ($An_{58}Ab_{41}Or_1$) (11) as are the cores of the groundmass plagioclase ($An_{51}Ab_{47}Or_2$) (12).

The underlying alkali-olivine basalts have plagioclase microphenocrysts up to 1 mm. long, apparently homogeneous ($An_{72}Ab_{27}Or_1$)(13). The groundmass consists largely of disoriented plagioclase laths (An_{70}) with rounded, altered olivine grains, subophitic clinopyroxenes and homogeneous titanomagnetites.

Drum na Criche

The plagioclase phenocrysts differ from those of Talisker by their euhedral form with little or no evidence of resorption, a more sodic composition of the core and a lack of reversed zoning on the margins.

The core compositions range from An_{43} to An_{49} (14-17); but morphologically there appears to be only one generation of phenocrysts. There is no apparent correlation of composition

with size in what appears to be a bimodal population as far as size is concerned.

The phenocrysts have narrow rims, normally zoned to An_{42}, but lack the anorthoclase rims noted on the Talisker phenocrysts.

The contents of Sr (1450 ppm) and Ba (342 ppm) are significantly higher than those of the Talisker phenocrysts (Table 1.4). Comparison with Corlett and Ribbe's (1967) data (Table 1.4) for plagioclases of similar (An_{44}) composition, shows that these levels are higher by up to 30%.

The groundmass plagioclases have core compositions of An_{49} to An_{46}, thus overlapping the range of composition in the phenocrysts. The rims show normal zoning to an alkali feldspar. Analcime is rarely present.

The underlying mugearite has been studied in detail by Muir and Tilley (1961). Their analyses were based on separated mineral fractions supplemented by XRD data. Much of the following description is based on their data.

The scarce microphenocrysts of plagioclase have cores of An_{45}, zoned to calcic anorthoclase margins. Muir and Tilley (1961) note that the most sodic portions still displaying obvious twinning are An_{30}, but these zone out to calcium-rich anorthoclase in which very fine scale albite-pericline twinning is detectable; this anorthoclase forms the bulk of the groundmass feldspar. The XRD data of Muir and Tilley were interpreted as indicative of a "high" structural state for the cores of the plagioclase microphenocrysts. The interpretation was based on a limited number of reflections between 20 and $28^{o}2\theta$, and on comparison of this data with

known patterns of feldspars, quenched at high temperatures.

The groundmass feldspars have cores as calcic as An_{30}, but, according to Muir and Tilley, with significant potassium in solid solution ("potash oligoclase" or "potash andesine"). These grade outwards into calcic-anorthoclase.

Roineval

The porphyritic hawaiite of the upper unit has euhedral, rarely embayed, but frequently fragmented phenocrysts with homogeneous cores ($An_{53}Ab_{45}Or_2$) (22) very rarely with narrow more calcic rims (An_{60}-optical determination) and an outer jacket zoned from $An_{51}Ab_{47}Or_2$ to An_{40} (optical determ.) which merges with the groundmass feldspar.

Analyses by XRF of bulk plagioclase phenocrysts show an unusually high level of Sr (1860 ppm) for a bulk composition (25) similar to that of Drum na Criche (26) (Table 1.4).

The groundmass plagioclases appear to be of similar composition to those of Drum na Criche:- $An_{49}Ab_{49}Or_2$ to An_{40} with outer rims zoned to an alkali feldspar.

The lower unit locally contains up to 15% plagioclase phenocrysts of similar composition to those in the upper unit (An_{52-50}). These are more calcic than scarce microphenocrysts of plagioclase (An_{40}).

The groundmass feldspars' composition, based on optical determinations are similar to those of the mugearite at Drum na Criche.

Fig. 2.4

Plot of analyzed feldspar compositions for the Talisker, Roineval and Drum na Criche composite flows; data for the Bras Rouge sill includes the previous data of Upton & Wadsworth (1967).

A: North Skye Composite Flows
B: Greenock Composite Flow
C: Greenland Composite Dykes
D: Bras Rouge Composite Sill

• phenocrysts
---- range of composition in groundmass feldspars.

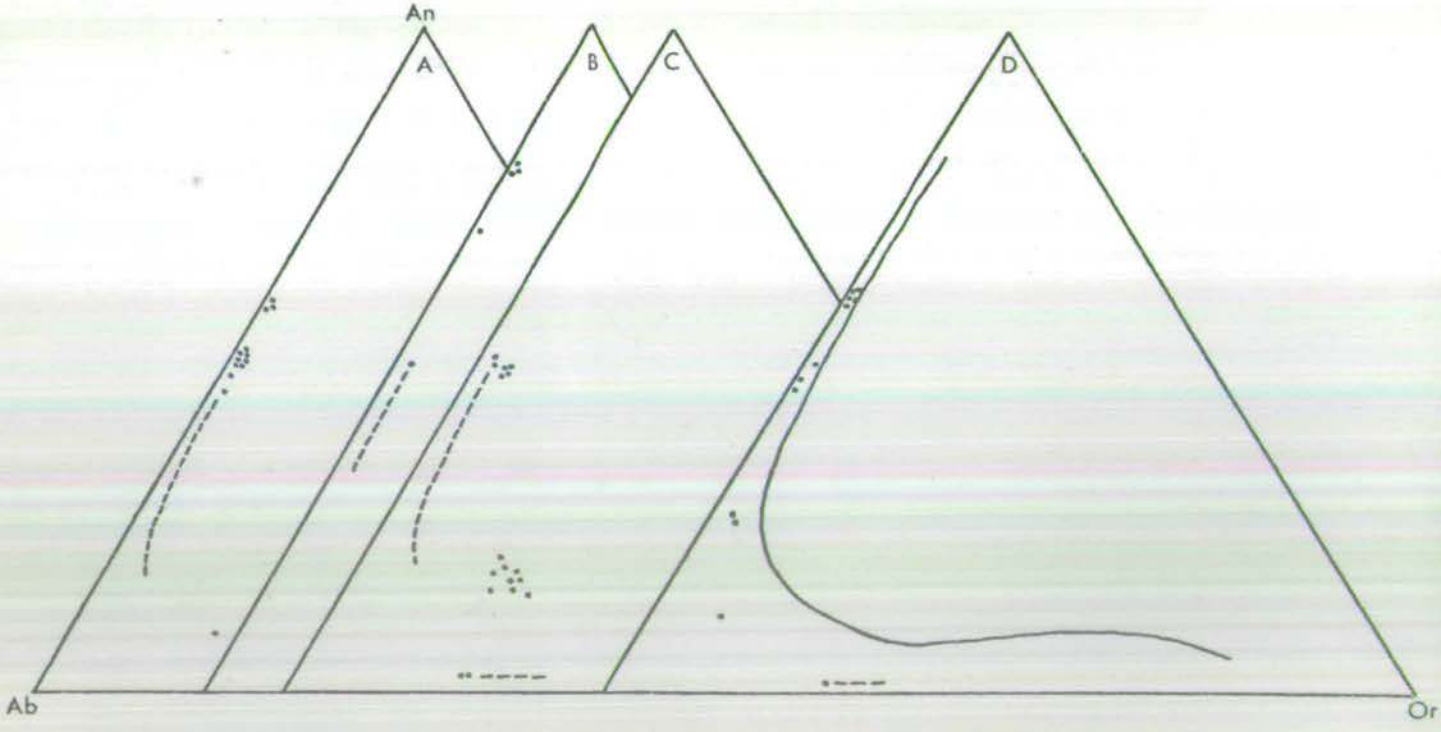

Solid line represents limit of ternary solid solution in natural feldspars (Smith and MacKenzie, 1958)

Midland Valley of Scotland

North Berwick

The uppermost flow, of hawaiite, contains euhedral to subhedral plagioclase phenocrysts (An_{62-60}) with narrow rims zoned to An_{50}. The groundmass is predominantly feldspar (An_{55} zoned to An_{30}).

The underlying benmoreite has scarce microphenocrysts with homogeneous cores of An_{40}, strongly zoned outwards to an alkali feldspar. Muir and Tilley (1961) describe the bulk of the groundmass feldspar in a similar flow just south of North Berwick as being a sodic sanidine with minor amounts of anorthoclase (Fig. 2.4). This also appears to be true of the flow at North Berwick.

The lowest of the three flows is an alkali-olivine basalt with euhedral to subhedral plagioclase phenocrysts with homogeneous cores of An_{63} (10) with narrow, slightly more calcic (An_{64}) (11) rims jacketed by plagioclase zoned to An_{55}.

The groundmass feldspar have cores of An_{55} zoned to An_{50-45}.

The occasional small gabbroic xenoliths contain plagioclases of An_{65-60}.

The Royal Park, Edinburgh

The Dasses

The hawaiitic (outer) facies contains largely sericitized and analcimised phenocrysts normally zoned from An_{45-30}. The extensive alteration of the phenocrysts is not confined to any specific zone; its pervasiveness does not permit a more accurate determination of the composition range.

The groundmass feldspars (An_{35} zoned to an alkali feldspar (?)) are relatively unaltered. The mesostasis lacks analcime, which is abundant in the central (alkali-olivine basalt) facies. This suggests that it may not necessarily be the result of late stage alteration.

The inner alkali-olivine basalt facies has relatively unaltered phenocrysts of An_{49} zoned to An_{47} (12,13). Rutledge (1952) reported a compositional range of An_{75} (cores) to An_{50} (margin). This is closer in compositional range to the plagioclases found in rocks of similar composition at Arthur's Seat (Clark, 1956) and North Berwick (this study) although Clark (p.46) notes a similar range (bytownite-andesine). The phenocrysts are frequently altered to analcime along cleavage cracks and their margins.

The groundmass feldspar is normally zoned from An_{45-30}. Rutledge, on the basis of more samples, reported An_{52} to An_{28}; he noted abundant analcime in the groundmass, but not replacing the groundmass feldspars, as it does the phenocrysts.

St. Leonard's Sill

The central porphyritic facies (alkali-olivine basalt) is similar in composition to that of the Dasses; it does not, however, show as wide a range in plagioclase composition. The slightly altered phenocrysts have cores of An_{55-50}, normally zoned to An_{40}.

The groundmass plagioclase is zoned from An_{40-35} to An_{20-15}; MacGregor (1936) noted that in some samples an alkali feldspar was present.

The marginal, benmoreitic facies has scarce microphenocrysts

TABLE 1.4

Trace element content of plagioclase phenocryst separates; sample numbers refer to the groundmass analyses in the Tables of Appendix A. Trace element content of the groundmass, with the Distribution coefficient are presented in Table 2.6.

Sample No.		Ba	Sr	Rb	Zr	Zn	Ni	Composition
Talisker (1A)	23	96	1132	8	188	21	6	An_{52-50}
"	21	35	1147	5	171	24	57	"
"	19	56	1155	3	156	26	30	"
"	17	6	1100	2	152	26	32	"
"	15	65	1097	3	168	22	26	"
"	13	87	1130	4	170	26	32	"
"	11	140	1115	9	15	<5	9	"
Drum na Criche (1B)	7	342	1454	2	207	34	17	An_{45}
Roineval (1B)	18	328	1864	16	153	24	<5	An_{45}
Dasses (1D)	13	370	640	30	83	55	<5	ca. An_{40}
"	14	450	795	35	120	47	<5	"
"	15	2080	672	44	165	75	<5	"
Greenock (1E)	17	160	953	18	<5	5	<5	An_{78-75}
"	15	225	985	22	<5	44	<5	"
"	13	180	1010	21	<5	40	<5	"
"	11	91	984	8	182	42	45	"
"	9	380	822	36	<5	68	<5	"
"	7	360	807	40	<5	86	<5	"
"	5	260	940	26	<5	41	<5	"
SW Greenland (1G)*		1942	2222	18	332	45	34	An_{45}
B.G.J. Upton: T49 IV		3525	1860	-	-	-	-	$An_{28}\ Ab_{64}\ Or_{8}$
" T49 III		4175	1680	176	-	-	-	$An_{18}\ Ab_{68}\ Or_{14}$
" T526		4375	107	74	-	-	-	$An_{9}\ Ab_{66}\ Or_{25}$

* Trace element analysis for groundmass of Analysis 21, Table 1G in Table 2.6.

TABLE 1.4 (contd.)

(Data from Corlett and Ribbe (1967))

Specimen No.	Ba	Sr	An content
130	-	800	43.2
94	100	300	43.3
239	150	500	44.3
37	150	1100	44.5
54	100	900	44.5
212	35	1800	44.7
147	-	700	51.1
243	150	1000	"
30	150	900	"
Avg 251,253	130	1250	52.1
Avg 24, 213	200	900	≃54
Avg 247, 246, 267	150	750	56.5

of An_{35-30} zoned to an alkali feldspar. The groundmass feldspar has cores of An_{30-25} zoned to an alkali feldspar. By analogy with rocks of similar composition at North Berwick and Congalton Mains the alkali feldspar should be sodic sanidine with minor amounts of anorthoclase. This is not suggested by a plot of the normative feldspar in the rock (Fig. 3.4), but this is due primarily to the extensive alteration.

The Western Midland Valley of Scotland

Composite Flow south of Greenock

The porphyritic upper unit has phenocrysts with complexly zoned cores ranging in composition from An_{78-68} (1-3, 5). These are surrounded by narrow normally zoned rims of An_{70-58}(4,6), although Kennedy (1931) noted rims of An_{30} contiguous with the groundmass. Analyses of bulk phenocryst separates (8,9) gives an average composition of An_{74}. The wide range in phenocryst core compositions (3 versus 5) is a feature first noted in the phenocrysts of Drum na Criche; here, however, the phenocrysts are considerably more basic than found in the other composite flows studied.

Sr and Ba contents of the bulk separates (Table 1.4) are higher than those for plagioclases of similar composition analyzed by Corlett and Ribbe (Table 1.4).

The groundmass laths have cores of $An_{55}Ab_{44}Or_1$ (7) zoned normally to An_{30}. A plot of normative feldspar in the groundmass of the hawaiites suggests (Fig. 3.4) that the amount of alkali feldspar is volumetrically less significant than in hawaiites from Drum na Criche and Roineval.

Fig. 3.4

Plot of normative feldspar composition for rocks of the Dasses, St. Leonard's Sill, Greenock composite flow and the Craigmarloch Wood composite flow.

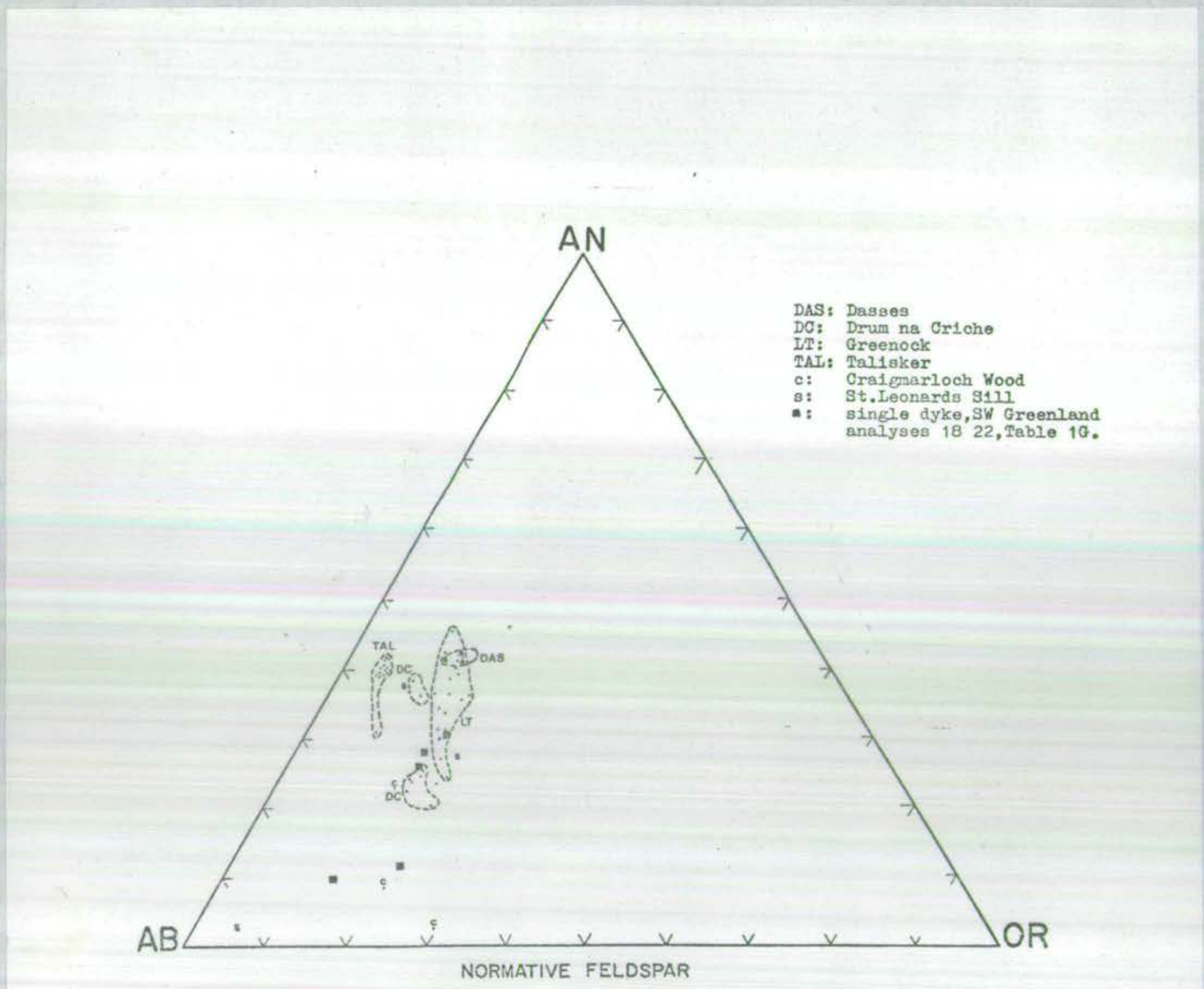

Two groups of plagioclase phenocrysts are present in the lower, mugearitic unit: (a) strongly zoned microphenocrysts of plagioclase (An_{55} to An_{28}), and (b) more basic plagioclases of An_{76-70}, which are present only in the upper 80 cm. The groundmass feldspars are strongly zoned from An_{40} to An_{28}; Kennedy (1931) noted small patches of analcime in the mesostasis, but no alkali feldspar, although a plot of the normative feldspars (Fig. 3.4) might suggest that anorthoclase is present.

Craigmarloch Wood

The central porphyritic facies contains phenocrysts of plagioclase with cores (An_{35}) zoned normally to An_{25}. The tabular groundmass feldspars have cores of An_{25-20} with rims zoned to an alkali feldspar. The normative feldspar (Fig. 3.4) suggests that this is mainly anorthoclase with minor amounts of sodic sanidine.

The nearly aphyric mugearite does not appear to contain plagioclase phenocrysts; the groundmass feldspar has cores of An_{40-35} zoned to An_{20-15}; the margins merge with an alkali feldspar present intersertally.

South-west Greenland

Reference is made throughout this section to feldspars analyzed in the present study; as in the preceding sections these are followed by the analysis number in brackets. Note is made throughout the section to optical determinations given by Bridgwater and Harry (1968).

The central porphyritic facies contains plagioclase with apparently homogeneous cores of An_{45} with narrow, discontinuous rims of An_{48}(1-8). The range in phenocryst

compositions does not appear to be wide within the central unit of the dykes examined; Bridgwater and Harry note that phenocrysts may have rims of an alkali feldspar (p.138) and that the range in compositions may extend from An_{58} to An_{35}. Cognate xenocrysts were not found in the suite of dykes examined; according to Bridgwater and Harry these are generally more calcic ($\geq An_{60}$) than the phenocrysts present in the central facies.

Bulk separates of the plagioclase phenocrysts (from sample GGU 86052) have 2222 ppm of Sr and 1942 ppm of Ba, levels higher than found for plagioclases of this composition by Corlett and Ribbe (1967) or for the Roineval and Drum na Criche separates (Table 1.4). These high levels seem to be true of both plagioclases and alkali feldspars from dykes in the vicinity (B.G.J. Upton; unpub. data).

Refined XRD data for the same plagioclase separate give unit cell parameters that are significantly smaller than those of Bambauer et al. (1967) for "low" plagioclases of similar composition. The parameters should be slightly higher due to the higher Or content; this suggests that the plagioclases may be disordered.

The plagioclase of the groundmass is zoned from An_{40} through An_{25} to albite away from the margin, but close to the margin may be zoned from An_{30} to anorthoclase.

The alkali feldspar phenocrysts of the marginal facies are usually micro- or cryptoperthitic; the extent and coarseness of the exsolution increasing away from the margins. The cores of the phenocrysts are typically polysynthetically twinned anorthoclase (11-16) zoned outwards to sodic sanidine

(17,18). Within the narrow gradational zone between the two facies both plagioclase ($An_{35-30(?)}$) and either sanidine or anorthoclase (19-22) may coexist. The plagioclase in this junction zone, however, is usually too altered to determine its composition.

None of the coarsely exsolved alkali feldspars on the border of the junction zone was analyzed. Similar anorthoclases from the rhomb porphyries of the Oslo region have been described by Harnik (1969) as having cores micro- to cryptoantiperthitically unmixed, with the antiperthitic host comprising more than 90% of the volume. The alkali feldspar present is usually unmixed again to form either (a) pure albite or sanidine, or (b) form another series of antiperthite or perthite. The rims are more Ab, Or rich, with larger domains of exsolved plagioclase. Both cores and rims are structurally disordered ("high" to "intermediate").

The groundmass feldspars in the marginal facies are either wholly alkali feldspar (anorthoclase and/or sanidine) near the chilled margin or plagioclase (An_{50} to An_{30}) zoned outwards to an alkali feldspar. Bridgwater and Harry (1968, p.141) note that although total alkalis fall, soda may increase away from the margin, suggesting that there is a progressive decrease in K, Na-rich alkali feldspars towards Na rich plagioclase away from the margins.

Réunion

Upton and Wadsworth (1967) have given a description of the mineralogy of an earlier suite of specimens from the Bras Rouge Sill. Their descriptions are given below with

reference to figure 10.2 augmented by a series of analyses on another suite of specimens, and the mugearite flow on Piton des Neiges.

Bras Rouge Sill

The lower chilled margin contains at least three feldspars, given in order of abundance: (a) plagioclase (An_{30}), (b) coarsely perthitic alkali feldspar with albite (1,2) and an altered K-feldspar, and (c) xenocryst plagioclase of An_{79-68}.

Away from the chilled margin, the groundmass plagioclase shows increasingly cores (An_{47} at Re 28; An_{61} at Re 29; An_{81} at Re 30A) which are normally zoned towards an alkali feldspar. Na-K analyses of feldspar fractions from Re 28 suggested a range of $An_{40}Ab_{55}Or_5$ to $An_{10}Ab_{60}Or_{30}$ (Fig. 2.4).

In the lower part of the sill (Re 28,29; see Fig. 10.2), plagioclase phenocrysts with a distinctive zone of sieve texture separating a sodic core from a more calcic outer rim occur.

In Re 28 the core compositions range from An_{41} to An_{21} with outer ring zoned from An_{47} to alkali feldspar.

In Re 29 they are fewer in number, with more basic (An_{50}) cores; the outer rims were zoned from An_{61} to an alkali feldspar.

At the highest level sampled in the lower part of the sill (Re 574) none of the distinctive plagioclase phenocrysts are present. The feldspars are strongly zoned from An_{62} through to $An_1Ab_{71}Or_{28}$(1-12), Fig. 2.4.

Hawaiite flow, Piton des Neiges

Two plagioclases are present in glassy, sparsely porphyritic sample (Re 619) from close to the source of the eruption; (a) plagioclase of An_{55-52}, and (b) less abundant phenocrysts of An_{72}

The other specimens collected further away from the source (Re 620-22) show only one feldspar (An_{55-50}) with complex zoning throughout the phenocryst. The groundmass feldspars have cores of An_{45-40} zoned normally outwards to An_{30-25}.

Summary

Feldspar forms the predominant phenocryst phase in all of the composite bodies studied; it is likely that it was the predominant fractionating phase as well. A review of the most significant features are given below.

In the three composite flows on Skye, despite a near identity of composition in the porphyritic units (hawaiites) there is considerable variation in the composition of the phenocrysts. Talisker is quite distinct from Roineval and Drum na Criche, in that:

(A) Two morphological and chemically distinct plagioclases are present, Group A phenocrysts with compositions of An_{52}, Group B phenocrysts with compositions of An_{32}. Few of the phenocrysts in Group A are euhedral; they are either ovoid, or show rounded, anhedral forms.

(B) In contrast, the phenocrysts of Drum na Criche and Roineval are euhedral, rarely rounded; they are of one group morphologically and chemically, although there is

a wider compositional range in this one group - An_{50} to An_{43}.

(C) The Talisker phenocrysts almost invariably have a narrow, more calcic zone on the outer margin, with a thin band of inclusions on its outer border. Drum na Criche and Roineval rarely have inclusion-filled borders, or reversed zoning.

Phenocrysts in the three units contain distinctly different levels of Sr and Ba.

There appears to be a bimodal population of phenocryst sizes in each of the three porphyritic units.

Each of the nearly aphyric units contains two groups of plagioclase phenocrysts: (1) a group with compositions analogous to that found in the overlying, porphyritic unit, and (2) microphenocrysts of more basic composition (Talisker) or less basic (Drum na Criche and Roineval) than those of group (1).

Phenocrysts of group (1) are present sporadically throughout the lower unit, usually, though, they are more numerous near the junction of the two units. The microphenocrysts of group (2) are present, in minor amounts throughout the lower unit.

Comparison of phenocrysts from individual flows, such as the hawaiite at North Berwick with the compositionally analogous porphyritic hawaiite of the Talisker shows that those of the former are almost 10% more basic. The underlying benmoreite is more evolved than any of the aphyric units in the composite flows, with microphenocrysts more sodic than those found as microphenocrysts in the mugearites.

The composite bodies in the Royal Park, Edinburgh, have alkali-olivine basalt as a central, porphyritic unit, with phenocrysts of variable composition. In the Dasses, Rutledge's (1952) optical determinations of An_{75} to An_{50} indicate a far greater compositional range than the microprobe analyses of An_{49} to An_{47}; the former are more typical of the compositions found in alkali-olivine basalts. The central facies of St. Leonard's Sill, however, also has phenocrysts in almost the same range (An^{55-30}).

The outer facies are:

(A) porphyritic hawaiite (the Dasses) with phenocrysts of An_{45-40} zoned to An_{30}; these appear to fall in the lower part of the compositional range found so far for hawaiites.

(B) nearly aphyric benmoreite with scarce microphenocrysts of An_{35-30} (St. Leonard's Sill).

The hawaiite of the Greenock composite flow has phenocrysts with a range of An_{78} to An_{58}, far more basic than any other unit studied. Similarly, the mugearite has more basic (An_{55-50}) compositions than those of the flows on N. Skye.

The central porphyritic facies of the flow at Craigmarloch Wood (benmoreite) has phenocrysts with compositions (An_{35}) similar to those of the benmoreites at N. Berwick and the Royal Park. The aphyric mugearite is devoid of phenocrysts.

The porphyritic central facies (hawaiites) of Greenland contain phenocrysts of An_{50} to An_{45}, or compositions near the average for the hawaiites studied. The range of compositions noted by Bridgwater and Harry (1968) for both their megacrysts and cognate xenocrysts covers the range of compositions found in hawaiites.

In the marginal facies, the feldspars enter the two feldspar field with a sodic sanidine and a plagioclase ($An_{35-30(?)}$) precipitating. This also appears in the Bras Rouge Sill (Réunion) where the marginal facies contains a coarsely exsolved perthite and plagioclase of An_{30}. In the Greenland rocks, the plagioclase was clearly the unstable phase, in the Bras Rouge Sill, the alkali feldspar (of unknown bulk composition) appears unstable.

The plagioclases in the Bras Rouge Sill span the entire range found elsewhere in the composite bodies (An_{80} to alkali feldspars).

The hawaiites in the rocks studied display a wide variety of plagioclase compositions (An_{78} - An_{43}); the range in more evolved rocks, becomes progressively narrower: mugearites (An_{55-40}), benmoreites (An_{35-30}).

Spinels

Spinel (magnetite) occurs as microphenocrysts forming less than 3% of total phenocrysts in all of the hawaiites of the composite bodies studied, but less commonly in the more evolved rocks. Ilmenite is present rarely in the groundmass, never as phenocrysts. The porphyritic hawaiite at Talisker is unique in that scarce phenocrysts of hercynite are also present.

The analyses are presented in Table 1.2C (Appendix C); for convenience, the spinels from all the composite bodies are discussed as a group. Bracketted numbers, as before, refer to the number of the analysis in Table 1.2C. Recalculation of the analyses follows the procedure given by Carmichael (1967);

this results in very minor differences in the amount of Fe_2O_3 as calculated by Anderson's (1968) method.

Examination by reflected light showed that only the titanomagnetites of the composite flows on N. Skye were almost devoid of alteration to maghemite, haematite or even limonite except on the borders of the phenocrysts and along cracks.

The microphenocrysts (1,4,5,6) in the Talisker porphyritic hawaiite, relative to the groundmass titanomagnetites (2,3) show the following characteristics:

(A) lower TiO_2, higher MgO.

(B) Al_2O_3 is usually lower

(C) A lower content of Ulvöspinel.

Prévot and Mergoil (1973) noted similar relationships for TiO_2 and MgO in a hawaiite from the Massif Central (France) over at least three generations of titanomagnetites. Trends in the Talisker hawaiite are not as clearly defined, for the TiO_2 increase is only 1%; Prévot et al., suggested that this was a result of decreasing oxygen fugacity. Data from other alkaline lavas shows similar small variations in TiO_2 (Anderson, 1968; Carmichael, 1967).

Both Anderson (1968) and Prévot et al. (1973) noted an increase in ulvöspinel content as crystallization proceeds. This is at variance with the conclusion of Carmichael and Nicholls (1967) that the ulvöspinel contents should decrease as the Fe_2O_3/FeO increases in the magma.

The same trends do not hold for the titanomagnetite phenocryst in the Roineval hawaiite (7,8) as compared with groundmass titanomagnetites (9), but both phenocryst and

PLATE 3.4

Fig. 1.

Phenocryst of hercynite (light grey) with spineliferous titanomagnetite border (white) in the upper unit of the composite flow near Talisker, N. Skye.
Magnification: 30x; reflected light.

groundmass are more extensively altered than those of Talisker. Prèvot and Mergoil (1973) have noted that low temperature alteration (i.e. maghemitization) alters the cation ratios; Fe/Ti may decrease by as much as 30%.

The typically altered appearance (in reflected light) of titanomagnetite in all of the other composite bodies suggested that analyses of these would prove of little value.

The lavas and composite bodies in the Midland Valley of Scotland are either altered to haematite (the composite flow near Greenock, Craigmarloch Wood) or maghemite plus haematite with ilmenite lamellae (the composite bodies of the Royal Park, the flows at North Berwick).

The porphyritic central facies of the composite dykes of S.W. Greenland have up to 2% of large phenocrysts of opaque minerals. These show a wide range in alteration, from haematite and maghemite with numerous ilmenite lamellae to haematite plus leucoxene or anatase. Analyses of a large phenocryst (10,11) represent an average of some twenty spot analyses; the variability in the analyses is too great to consider the analyses as more than qualitative.

Similarly, the phenocrysts of opaque minerals in the Bras Rouge Sill are altered to haematite and/or maghemite. The groundmass titanomagnetites (12) appear to be less altered, but provide no evidence of compositional trends.

The hercynite phenocrysts in the Talisker porphyritic unit show little variation in composition (13-15) and are comparable to those found by Binns et al. (1970) and interpreted as xenocrysts in a basanite (16). They are surrounded by a border (Fig. 1, Plate 3.4) of spineliferous titanomagnetite

(17-19) similar in composition to phenocrysts found by Aoki (1966) in more evolved rocks ("trachyandesites"). They are not compositionally homogeneous but show considerable compositional differences across the width of the border (Fig.1; PLATE 3.4)

Clinopyroxenes

Introduction

The clinopyroxene analyses are presented in Table 1.3C Appendix D, and are referred to throughout by the bracketted numbers. Recalculation of the total Fe into Fe^{3+} and Fe^{2+} has been done by alotting an equal amount of Fe^{3+} to the molecular amount of Na + K present in the analyses (Carmichael, 1962). Hamm and Vieten (1971) have proposed recalculation to 4 metal cations, but with the present data this led to either an excess of Fe^{3+} over Fe^{2+} or else to none at all. Direct estimates of the Fe^{3+}/Fe^{2+} ratio by the relative intensities of the L_α and L_β lines (Albee and Chodos, 1970) were consistent with the amounts derived by the present method of recalculation in the few instances where it was attempted.

The method used to calculate Fe^{3+}/Fe^{2+} ratios will influence the amount of Al allotted to the Z position of the idealized pyroxene formula; in almost all analyses there is sufficient Al and Si to fill the position. Where there is not (1), the deficiency is made up with Ti.

Both Aoki (1964) and Le Bas (1962) have noted a decrease in the amount of Al + Ti in the Z position of clinopyroxenes with evolution of the host rock. This accords with the data

from the present series in passing from the alkali-Olivine basalts to hawaiites.

Calculation of the end member molecules theoretically present in the clinopyroxenes follows the method outlined by Kushiro (1962). Jadeite is not calculated for the pyroxenes; Kushiro suggested that this component is usually absent from igneous clinopyroxenes. Where comparisons are made with analyses of other authors their analyses have been recalculated by Kushiro's method to give a consistent basis for comparison.

Clinopyroxene occurs as a phenocryst phase in the composite flow south of Greenock and near Craigmarloch Wood, but is lacking in those of N. Skye, where it is present only in the groundmass. It occurs as phenocrysts in the alkali-olivine basalt central facies of the Dass es and St. Leonard's Sill, as well as the alkali-olivine basalt at North Berwick. It is usually present, in amounts less than 3%, in both facies of the Greenland composite dykes. It is lacking in the chilled marginal facies of the Bras Rouge Sill, but is common throughout the lower part of the sill as ophitic to subophitic grains; the hawaiite flow contains between 2-5% as phenocrysts.

North Skye

The ophitic to subophitic groundmass titanaugites ($Ca_{46}Mg_{36}Fe_{18}$) (1,2) in the Talisker porphyritic hawaiite are similar in composition and content of Acmite ($\simeq$ 5%) and Ca-Tschermak's molecule (0.1-0.5%) to the groundmass clino-pyroxene (3) of the Kyogle hawaiite, N.S.W. (Wilkinson, 1969).

The clinopyroxenes present in the groundmass of the Drum

na Criche mugearite (4) contain considerable Acmite (17.6%) and Ca-Tschermak's molecule (4.7%). Increase of the latter molecule is a function of decreasing temperature (Hytönen and Schairer, 1961) and/or increasing pressure (Clark et al., 1962; Kushiro, 1962). It departs from the trend shown by Aoki (1964) for the groundmass clinopyroxenes of a compositionally similar rock series, in which the main substitution of Ca Fe^{2+} for Ca Mg is followed by Na Fe^{3+} for Ca Mg Fe^{2+}. Stephenson (1972) found that in the pyroxenes from the nepheline syenites of the South Qôroq Centre (S. Greenland), the Na Fe^{3+} enrichment became dominant at about Na^{2+}-Mg = -0.1, later than occurs in the trend for the N. Skye series.

The Midland Valley of Scotland

The alkali-olivine basalt at North Berwick contains 2 groups of phenocrysts, one corroded, the other relatively unaltered. Compositionally there is little difference between them except in their Al_2O_3 content (5,6). Both are similar to the phenocrysts in the central facies of St. Leonard's Sill (7,8) but quite dissimilar to clinopyroxene in the compositionally similar central facies of the Dasses (9). These differences are reflected in the amounts of Ca-Tschermak's molecule (Table 1.3C):

(A) the phenocrysts in the North Berwick flow and St. Leonard's Sill contain amounts (7.3-10%) similar to those noted by Kushiro (1962) for clinopyroxenes associated with olivine nodules in basalts and in Kaersutite bearing alkali-olivine basalts.

(B) the clinopyroxene in the Dasses contains 50-70% less

(3.7%) which may be indicative of a lower P,T origin.

The clinopyroxene phenocrysts in the hawaiite at Greenock (10,11) are slightly less iron-rich than that of the Dasses ($Ca_{42}Mg_{44}Fe_{14}$ versus $Ca_{38}Mg_{45}Fe_{17}$) but similar in content of end member molecules.

Kennedy (1932) reported microphenocrysts of clinopyroxene ($Ca_{52}Mg_{44}Fe_4$ - optical determination) in the benmoreite of Craigmarloch Wood; these seem surprisingly iron-poor and Ca-rich by comparison with the trends observed for less evolved rocks. Huckenholz (1962), for instance, gives phenocryst composition of ca. $Ca_{44}Mg_{40}Fe_{16}$ for compositionally similar rocks from the Eifel region.

S.W. Greenland

The clinopyroxene phenocryst from the central facies (12,13) are more iron-rich ($Ca_{44}Mg_{35}Fe_{21}$) than those noted by Bridgwater and Harry (1968) as occurring with the anorthosite inclusions (ca. $Ca_{35}Fe_{28}Mg_{35}$ - optical determination). They contain more Acmite (ca. 18%) than the clinopyroxene phenocrysts analyzed in compositionally similar rocks from the other composite bodies.

Réunion

Groundmass clinopyroxenes in the upper basaltic part of the Bras Rouge Sill are zoned (14,15) from Fe,Ti rich centres to Ca,Mg,Al rich margins. The clinopyroxene phenocryst in the hawaiite flow on the Piton des Neiges (16) is similar in composition to that of the marginal zone in the Bras Rouge Sill groundmass clinopyroxene. They are similar in compositional range to the clinopyroxenes from the alkali-

olivine basalts of the Midland Valley of Scotland, and those noted by Aoki (1964) from alkali-olivine basalts, hawaiites and mugearites.

Summary

The clinopyroxenes show a relatively restricted compositional range, similar to those reported from analogous rock suites elsewhere. Only the clinopyroxene in the groundmass of the mugearite at Drum na Criche and the phenocryst present in the central facies of the S.W. Greenland composite dykes deviate from this trend, being more iron and soda-rich.

The variation in Ca-Tschermak's molecule in phenocrysts from compositionally similar alkali-olivine basalts may be a function of crystallisation at different pressures and not simply a decrease in temperature as appears to be a reasonable explanation for the high amount in the clinopyroxene of the Drum na Criche mugearite. The content of Ca-Tschermak's molecule in basaltic rocks (both tholeiites and alkali-olivine basalts) is an average of 1.7% (Kushiro, 1962), but Aoki noted that the suite of rocks similar in compositional range to those studied here contained an average of 2.7% for both groundmass and phenocrysts. The average for the phenocrysts in the present suites is still higher (ca. 5.0%) but because the amount varies both with temperature and pressure, assignment of the variation as a function of one or the other is difficult.

There is little variation in the Acmite content of the clinopyroxenes in the suite from the Midland Valley alkali-olivine basalts and hawaiites; Abbott (1969) attributes a

similar lack of variation in the Nandewar clinopyroxenes as a result of low oxygen fugacities. The increase in Acmite from ca. 5% to 18% in passing from the hawaiites to the mugearites in the composite flows of N. Skye would thus be interpreted as crystallization under conditions of rising oxygen fugacity.

Olivine

The olivine phenocrysts in the porphyritic hawaiites of Talisker and Roineval show slight zoning (Fo_{55-52}) with narrow rims of iddingsite (1-4). The composition is more iron-rich than compositions noted in hawaiites elsewhere: Fo_{85}-Fo_{78} (Huckenholz, 1965b); Fo_{74}-Fo_{71} (Baxter, 1973). Both olivine and clinopyroxene are present in the groundmass of the hawaiites, with clinopyroxene dominant.

Olivine is predominant over clinopyroxene in the groundmass of the mugearites at Drum na Criche and Roineval, ranging in composition from Fo_{63}-Fo_{42} (Muir and Tilley, 1961). The scarce microphenocrysts show a similar compositional range. Huckenholz (1965b) found a similar (Fo_{65}-Fo_{40}) compositional range in the microphenocrysts and groundmass olivines of the Eifel.

The alkali-olivine basalt at Talisker contains at least two generations of phenocryst, morphologically and chemically distinct (Fo_{79} and Fo_{73})(5,6). These are similar to olivines noted in alkali-olivine basalts elsewhere as phenocrysts: Fo_{81} (Hughes and Brown, 1972); Fo_{85} (Huckenholz, 1965b).

The hawaiites of the other suites studied usually contain olivine pseudomorphs, as noted in the section on Petrography.

Clarke (1956) determined the composition optically of olivines in the alkali-olivine basalts of the Royal Park, Edinburgh as Fo_{86}. By analogy with the basalts discussed above this would seem too magnesian.

The marginal and central facies of the Greenland composite dykes both contain pseudomorphs after olivine; the compositions can only be inferred by comparison with the compositional range noted for analogous rocks. Bridgwater and Harry (1968) noted olivines of Fo_{73} to Fo_{43} in association with plagioclase "megacrysts" (cf. Petrography) and Fo_{73} to Fo_{52} for the olivines associated with the anorthosite (cognate) xenoliths.

Olivine is absent in the lower part of the Bras Rouge Sill, except for serpentine pseudomorphs in rocks interpreted as accumulitic by Upton and Wadsworth (1967). Partial analyses (Fe,Mg) of olivine phenocrysts in the hawaiite flow on the Piton des Neiges indicate a composition of Fo_{70}.

Comparison of the analyses with olivines of similar composition given by Simkin and Smith (1970) shows no distinctive features; the content of CaO is within the range typical of volcanic olivines (0.28-0.56). Simkin and Smith (1970) stress that there is a "remarkable correlation with crystallisation environment of the host rock", and suggest that the content of CaO is not dependent on host rock chemistry but more on the PT environment or cooling rate of the lava.

Summary

Comparison of olivine phenocryst compositions determined

in the present study with those in analogous rock suites elsewhere indicates that:

(A) Alkali-olivine-basalts have a relatively narrow range from Fo_{85} to Fo_{73}.

(B) Hawaiites show a very wide range, from Fo_{85} to Fo_{52}.

(C) Mugearites have a slightly more restricted range: Fo_{65} to Fo_{40}.

Apatite occurs in the groundmass of most of the hawaiites, mugearites and benmoreites examined, but is not always present in the alkali-olivine basalts. It only occurs as phenocrysts in the central facies of the Greenland composite dykes. The phenocrysts are colourless and inclusion-free; they may be present in the marginal (mugearitic or even benmoreitic) facies and the transition zone between the two facies.

Amphibole occurs as phenocrysts in the marginal rocks of the Bras Rouge Sill (basaltic hornblende), and as a probable pseudomorph in the mugearite at Roineval.

Muir and Tilley (1961) and Bryan (1970) comment on an amphibole in the groundmass of mugearites which is possibly a member of the arfvedsonite-richterite series. Upton and Wadsworth (1967) noted the presence of a second amphibole ("lanéite") zoned outwards to riebeckite-arfvedsonite in the Bas Rouge Sill, with a third amphibole present in the upper portion of the sill. Lanéite (α pale cinnamon brown, β light brown, γ light apple green) may be similar in composition to the cores of the zoned amphiboles (ferrohastingsite and arfvedsonite rims) described by Aoki (1964) and Stull (1973) from alkaline volcanics and granites.

CHAPTER 5

CLASSIFICATION

The scheme of classification and terminology presented in the first chapter is developed in more detail below. Two aspects are discussed: (A) the nomenclature and classification of hawaiites, mugearites and benmoreites, and (B) the effect that modal mineralogy has on the broader division into silica saturated or undersaturated and transitional basaltic compositions.

Classification and Terminology

Hawaiites were originally defined by Iddings (1913) on a chemical basis and mugearites by Harker (1904) on a mineralogical basis. Hawaiite was redefined, and restricted, by MacDonald (1960) to rocks mildly undersaturated whose K_2O:Na_2O ratio is less than 1:2, carrying modal and normative andesine. Mugearites contain a similar K_2O:Na_2O ratio but contain modal and normative oligoclase; very typically the K_2O rich oligoclase is rimmed by a greater proportion of alkali feldspar than the feldspar of the hawaiites (Muir and Tilley, 1961). Classification of hawaiite and mugearite using the Differentiation Index (D.I.) of Thornton and Tuttle (1960), if restricted to a specific number (Thompson et al., 1972) results in discrepancies with classifications based on the original definitions. The boundaries are approximately fixed at a D.I. of about 30 for the division between hawaiites and alkali-olivine basalts and 45-50 for the division between hawaiites and mugearites.

The wide variety of terms used to classify compositions intermediate to mugearite and trachyte led to the definition of Benmoreite (Tilley and Muir, 1964); these rocks typically have K_2O:Na_2O ratios greater than those of mugearites, with normative feldspar compositions of An_{15-5} (Coombs and Wilkinson, 1969; Thompson et al., 1972). The division between benmoreites and mugearites is about 65; that between the benmoreites and trachytes at around 75.

These definitions of hawaiite, mugearite and benmoreite are in general use. Keil et al. (1972) question the validity of usage in the definition and classification of hawaiites and mugearites of the modal feldspar. Microprobe analyses of the groundmass feldspars in both this study and Keil et al.'s (1972) indicate that the range in composition is considerably more on specimens chemically classified as hawaiites and mugearites. Rocks chemically classified as hawaiites in this thesis contain groundmass feldspars with rare compositions ranging from labradorite to calcic andesine; similarly, Keil et al. (1972) found that in rocks chemically classified as hawaiites, the groundmass feldspar was labradorite, presumably in the core zones. In a similar fashion, Keil et al. (1972) found that the groundmass feldspars in rocks chemically classified as mugearites was andesine and not oligoclase. The type mugearite of Drum na Criche does have at least some strongly zoned, groundmass feldspars with core zones of sodic andesine, but these are not the predominant feldspar, as noted by Muir and Tilley (1961).

The point made by both this study and Keil et al. (1972)

is that the modal feldspar in hawaiites ranges in composition from labradorite to andesine; that in the mugearites ranges from andesine to oligoclase

Keil et al. (1972) note that in hawaiites and mugearites the normative feldspar is very different from the modal feldspar, due partly to the presence of interstitial analcime, anorthoclase and sandine. Recalculation of normative nepheline, if the rock shows no modal nepheline, as feldspar, and allotment of the correct amount of Al_2O_3 to normative clinopyroxenes results in closer approximation of normative to modal feldspar.

The classification scheme utilized in this study involves all of these criteria reviewed above: normative and modal feldspar, K_2O:Na_2O ratios and the Differentiation Index. The scheme is conveniently depicted in the plot of alkalis versus silica (Fig. 1.5) as modified by Upton and Wadsworth (1972).

The composite bodies studied are plotted on the diagram; with the exception of the composite flow at Drum na Criche they all plot parallel or subparallel to the trends typically controlled by ferromagnesia fractionation trends. The trend for Drum na Criche appears to involve an entirely different mechanism of evolution or fractionation controlled by variation of alkalis, alone. These mechanisms of evolution are discussed in detail in the Petrogenesis section; it should be noted, however, that the phenocryst assemblage in Drum na Criche is not significantly different than that of the composite flow at Roineval.

It was noted in the first chapter that the compositions

Fig. 1.5

Distribution of analyses from composite bodies referred to in the text.

TAL: Talisker composite flow.

DC: Drum na Criche composite flow

R: Roineval composite flow

LT: Greenock composite flow

GR: Greenland composite dyke(analyses 18-22,Table 1G)

Reunion analyses are shown by filled circles.

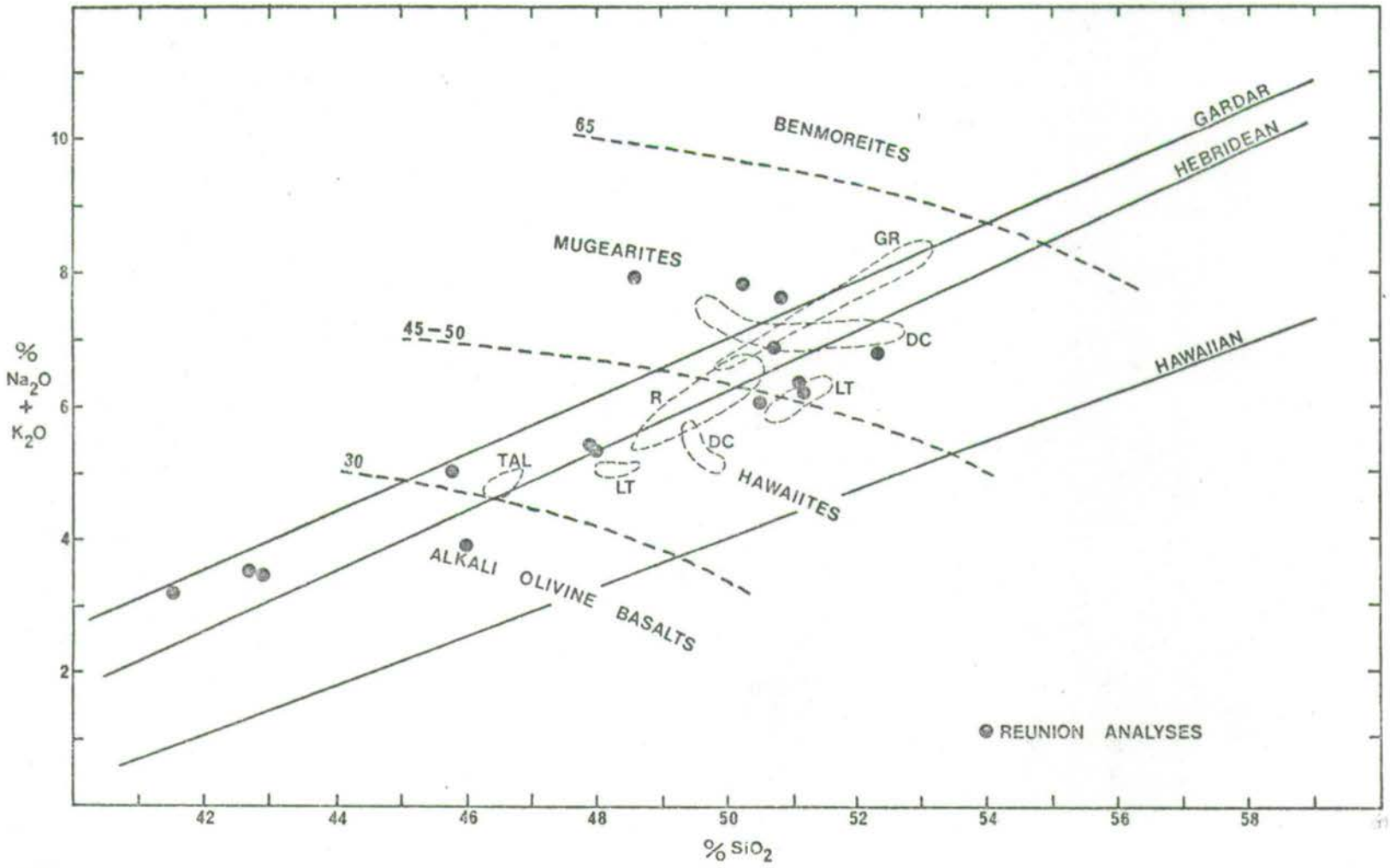
65
BENMOREITES
GARDAR
HEBRIDEAN
MUGEARITES
GR
45–50
DC
HAWAIIAN
R
LT
DC
30
TAL
LT
HAWAIITES
ALKALI OLIVINE BASALTS
REUNION ANALYSES
% Na2O + K2O
% SiO2
10
8
6
4
2
42
44
46
48
50
52
54
56
58

dealt with are transitional, that is they contain normative olivine plus hypersthene or usually less than 5% of either nepheline or quartz, although the more evolved members may show as much as 15% quartz. Lack of conformity in the composite bodies to fit within the normative bounds of the group is due largely to the disparity of composition between modal and normative minerals. Coombs and Wilkinson (1969) note that there are at least four ways in which normative ne is altered in relation to modal nepheline:

(A) clinopyroxenes in alkalic basalts typically have several percent ne in their norms, and could contribute as much as two percent to the normative ne of the bulk rock.

(B) Modal titanomagnetites contain MgO, Al_2O_3 and may contain excess FeO as ulvöspinel (Fe_2TiO_4); in the calculation of the normative minerals these are combined with silica, increasing ne at the expense of ab.

(C) if modal nepheline is present, and assuming that it is stoichiometric, approximately 20% is represented as normative or.

(D) the presence of oxidized iron increases normative ab, then hy at the expense of ne and ol respectively.

In addition, as noted above in the discussion of normative and modal feldspars, normative an is increased relative to ab by the aluminous nature of the groundmass clinopyroxenes typical of alkali-olivine basalts, hawaiites and mugearites.

CHAPTER 6

GEOCHEMISTRY

Introduction

Major oxide and selected trace-element analyses, with CIPW normative minerals for all the composite bodies studied are presented in Appendix A. The analyses referred to within the text are contained in the order given below.

TABLE 1A: Talisker composite flow and the underlying alkali-olivine basalts.

TABLE 1B: The composite flows of Drum na Criche, Roineval and individual hawaiite flows.

TABLE 1C: Individual hawaiite flows and dykes in N. Skye.

TABLE 1D: East Lothian, the Royal Park and Craigmarloch Wood.

TABLE 1E: Greenock composite flow.

TABLE 1G: SW Greenland.

TABLE 1H: Piton des Neiges, Reunion: Bras Rouge Sill and hawaiite flow.

This chapter discusses the distribution, content and variation of major and minor elements in the composite bodies. comparisons are made with element distribution in compositionally analogous rocks from Reunion (Upton and Wadsworth, 1972), Mauritius (Baxter, 1973) and the Comores (Flower, 1973 and Strong, 1970).

Where the $Fe_2O_3/FeO + Fe_2O_3$ ratio of the analyses in Appendix A exceeds 0.26, the ratio has been adjusted to this figure for calculation of the CIPW normative minerals.

Elimination of oxidation effects on the normative minerals is an arbitrary procedure, based either upon the lowest ratio found for the suite of rocks studied, or adjustment of the Fe_2O_3 content to a fixed level, representative of what are believed to be the least altered in the specific suite of rocks studied. The procedure adopted follows the first option; the ratio is based upon the average of the lowest ratios found in recent hawaiite and mugearite flows from Hawaii (MacDonald, 1968) and somewhat older flow from Reunion (Upton and Wadsworth, 1972) and Mauritius (Baxter, 1973).

Distribution of elements

Two aspects of element distribution in the composite bodies are usually apparent from the correlation matrices (Appendix D); these are:

(A) The variation of elements as a function of distance from the boundaries of the flow or intrusion, and

(B) Correlation between major and trace elements follows the usual pattern (Cf. Taylor, 1965) and is usually explicable in terms of groups of major elements which form the predominant mineral assemblages of the rocks.

Several statistical terms are used in the text; although familiar, they are defined below to avoid any misunderstanding:

A. Standard Deviation $\sigma = ((X-\bar{X})^2/M)^{\frac{1}{2}}$ represents the average dispersion of X on either side of the mean $\bar{X}$ for M samples. It is assumed that σ is normally distributed.

B. Coefficient of variation. $V = (\sigma)(100)/\bar{X}$, or the standard deviation given as a percentage of the mean value.

C. Correlation coefficient. The "degree" of linear relation-

ship between two variables. Pearson's r has values ranging from 0 (no correlation) to -1 or +1 (for perfect negative or positive correlation). It should be noted that non-linear relationships might be overlooked; all of the data has been plotted versus height or distance from the borders of the bodies and a non-linear relationship was not apparent. In every instance, it is the null hypothesis that we test against (no correlation between elements). The correlation coefficient, r, is quoted in the text and tables. To set confidence limits for the value of correlation in the hypothetical population from which the sample is taken, r is transformed to Z, given in the tables of standard statistical texts (Cf. Krumbein and Greybill, 1965).

Chayes (1964) has repeatedly emphasized the effect that the summation to 100% in rock analyses has on correlation coefficients between the major oxides. Closure increases negative but decreases positive covariance in a given analysis. In the context of the present study, these effects are recognized; it is primarily the value of the correlation coefficient between SiO_2, Al_2O_3, CaO and Fe which are affected. The values of most interest in the present study are, then, correlation coefficients between trace elements and major elements and the correlation between various elements and distance from the borders of the composite bodies.

The trace-elements analyzed for were chosen for two reasons: (a) to give a broad geochemical picture of the intermediate members of the alkali-olivine basalt-trachyte suite and (b) to provide some indication of the specific phases

being fractionated in the magma. These provide useful guides in evaluating the least-squares subtraction models discussed in Petrogenesis.

The Distribution coefficient (the ratio: (amount of element in the solid phase/amount of element in liquid)) is used to approximate the partition of the trace-element between crystals and magma in equilibrium. This coefficient varies in a regular fashion as a function of crystal composition, and must approach some limiting value, which is not known with certainty. In general, the formation of phenocrysts must vary between equilibrium and fractional crystallization. The general discussions for individual composite bodies that follow do not attempt to predict element distributions but attempt a general analysis of mass balance between liquids and fractionated crystals.

There have been several recent discussions following different approaches to the question of what the Distribution coefficient represents. Greenland (1970) generalized the logarithmic (Rayleigh) fractionation law, which assumes perfect fractionation of the phenocrysts, to allow a varying Distribution coefficient and/or varying proportions of the fractionating phases. The boundary conditions, however, necessitate a closed system fractionation model; estimates of the proportion of the original magma now remaining in equilibrium with each batch of crystal fractionates has to be made, and for the bodies considered in this study with the possible exception of the Bras Rouge Sill, this is not possible. His approach approximates the distribution of trace element data from a sill quite closely.

Doubt as to whether Distribution Coefficients are largely diffusion controlled after phenocrysts reach an optimum size is implied by Klusman's (1972) data. He shows that for small crystals of plagioclase, the Distribution coefficient for CaO does follow a perfect fractionation law, but this no longer is true after the crystals exceed a certain size.

A simple relationship suggested by Philpotts and Schnetzler (1969) for detection of Eu anomalies is utilised first in the discussion of Sr distribution for the Talisker flow. The assumption it makes, of a constant Distribution coefficient are not strictly true, but a calculation using a varying Distribution coefficient does not alter the predicted amounts of fractionated plagioclase by more than 1% (relative).

It is assumed that the major elements in the analyses will show groups with significant inter-element correlations. These groups, based on the dominant mineral assemblages of the rocks will be:

(A) SiO_2, Al_2O_3, Na_2O, K_2O: alkali feldspars.

(B) SiO_2, Al_2O_3, CaO: calcic plagioclases.

(C) CaO, MgO, FeO: clinopyroxenes + olivines.

(D) Total Fe, Ti, Mn: titanomagnetites

(E) CaO, P_2O_5: apatite.

There is, obviously, considerable overlap between the groups. Yet the groups do serve as a guide to the distribution of trace elements within the mineral assemblage. The correlations within the first two groups and group (D) tend to be preserved throughout the sequence examined, as these are the minerals that dominate the groundmass.

Correlation of trace elements with major elements in these groups will suggest in which minerals the trace elements are most abundant. The trace elements are listed below with a rough guide as to which elements they substitute for, and in which minerals they should be expected.

The ionic radii quoted are from the recent compilation by Whittaker and Muntus (1970); these are given for the co-ordination number of the site in the minerals in which they are usually assumed to be.

The distribution of the trace elements is best shown by the histograms (Figs. 1.6-3.6) upon which are superimposed frequency polygons for the range of compositions examined in the present thesis. The distribution of the elements is rarely normal, most are skewed and obviously represent several different populations within the discrete groups classified on the basis of major elements.

Ba^{2+} (7 fold: 1.47Å; 8 fold: 1.50Å) is usually concentrated in the residual liquids of the series examined; it is associated with the K sites in the alkali feldspars, but the concentrations show a large coefficient of variation due to both the poor precision of the analytical method and the variable amounts present in the plagioclases. The Distribution Coefficient is less than 1 in plagioclases until compositions close to An_{20} are reached, where it exceeds 1. There are exceptions to this, however, and the andesine phenocrysts of the composite dykes in SW Greenland exceed this value, possibly due to the large amount of Or present in solid solution. Ba ranges from 100 to 300 ppm in the hawaiites, 1000-1400 in the mugearites and 1300-1600 in the

Fig. 1.6

Histograms for the distribution of major and trace elements in hawaiites from data given by Baxter, (1973) for Mauritius, Upton and Wadsworth (1972) for Reunion, McBirney et al. (1969) for the Galapagos, Cox et al. (1969) for Aden.

Frequency polygons are superimposed on the histograms to show the distribution in hawaiites of the present study.

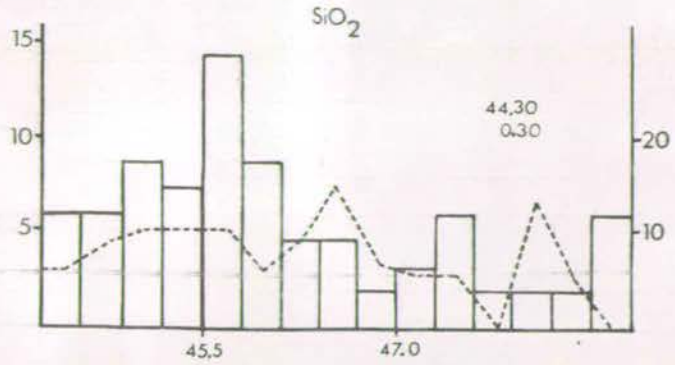

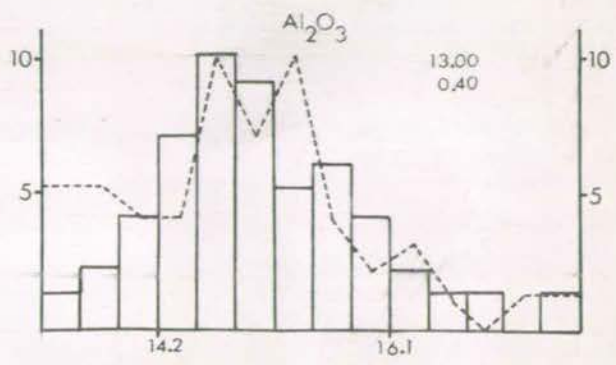

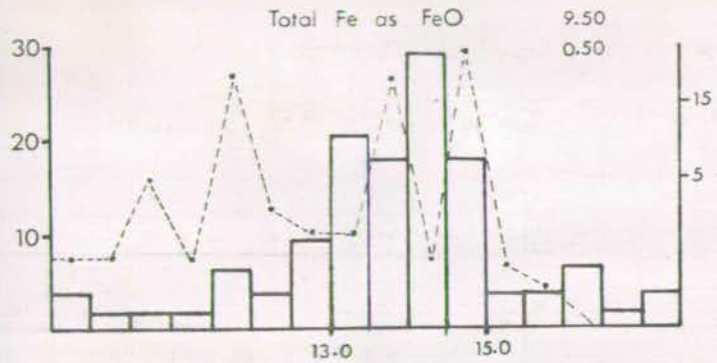

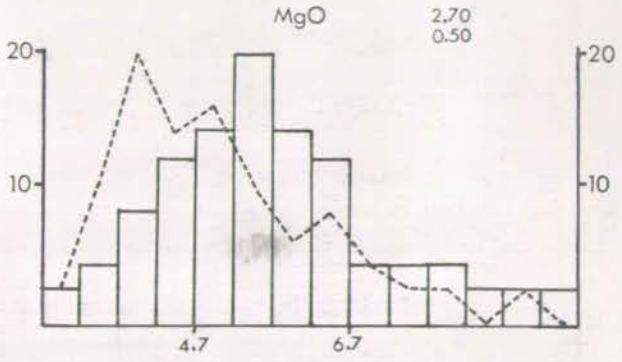

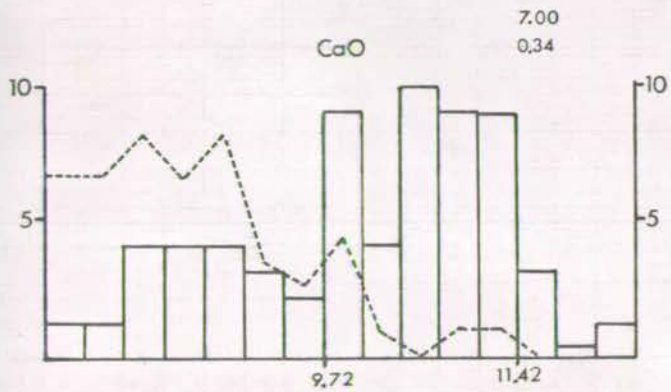

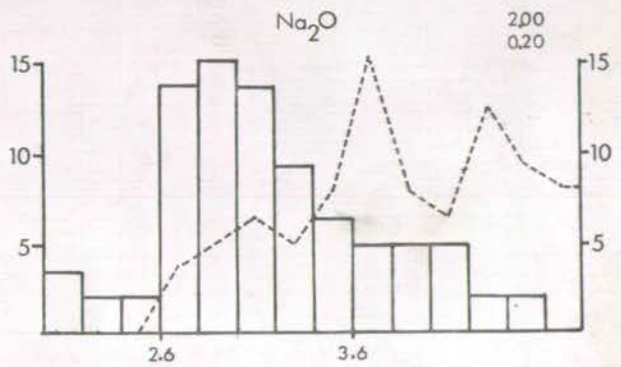

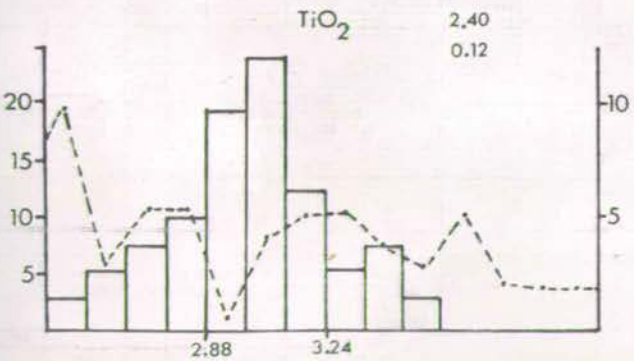

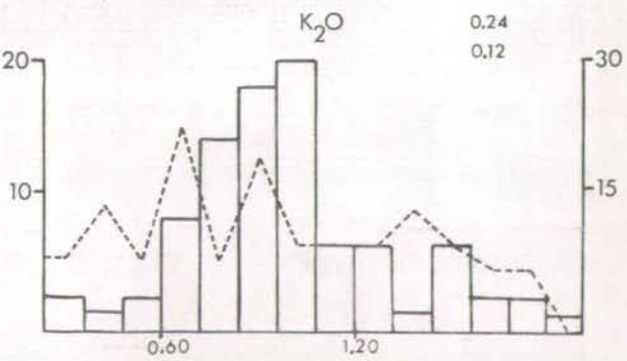

UPPER NUMBER INDICATES LOWER BOUND
LOWER NUMBER INDICATES INTERVAL

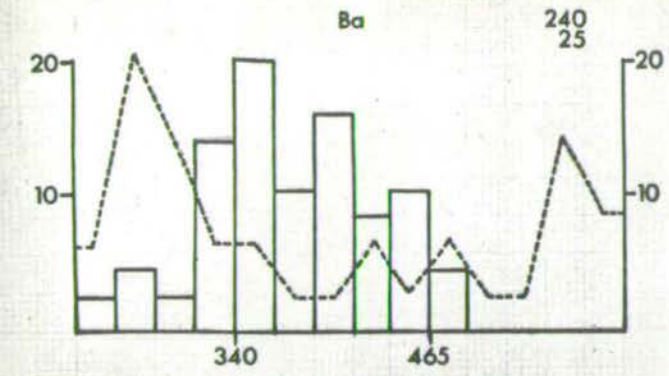
Ba
240
25
20
10
20
10
340
465

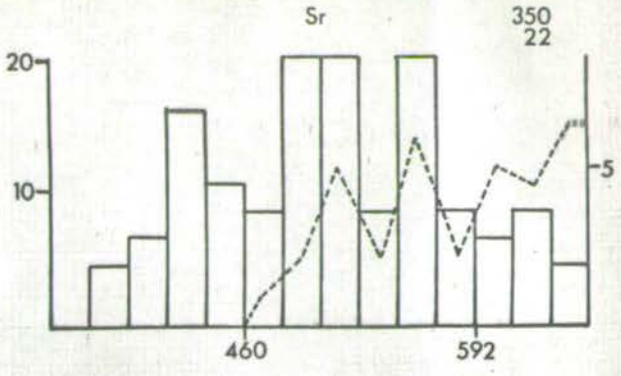
Sr
350
22
20
10
5
460
592

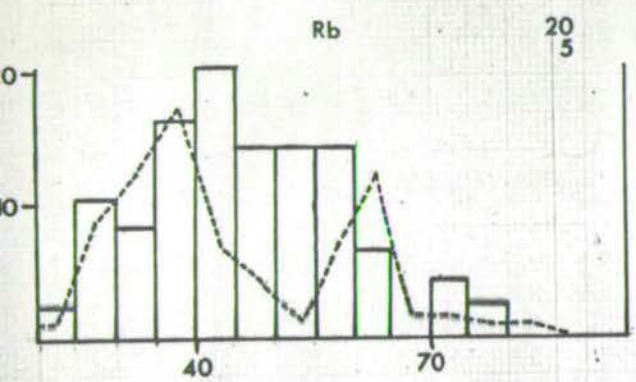
Rb
20
5
40
70

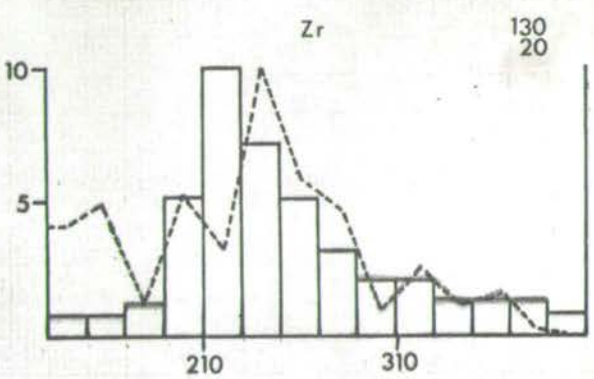
Zr
130
20
10
5
210
310

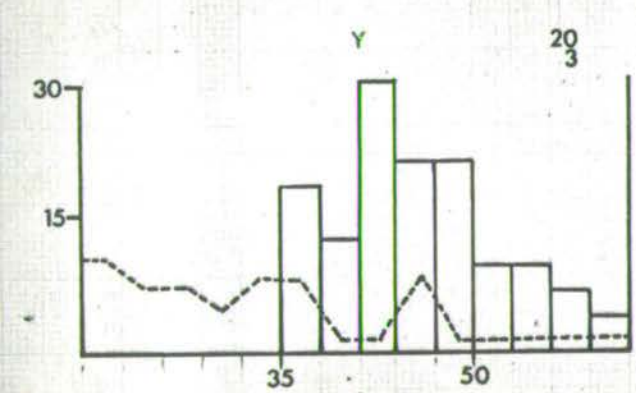
Y
20
3
30
15
35
50

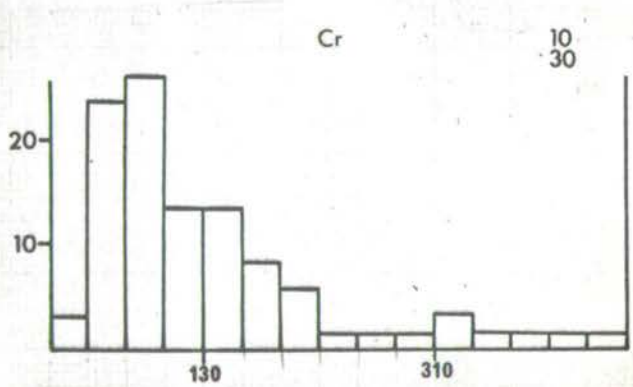
Cr
10
30
20
10
130
310

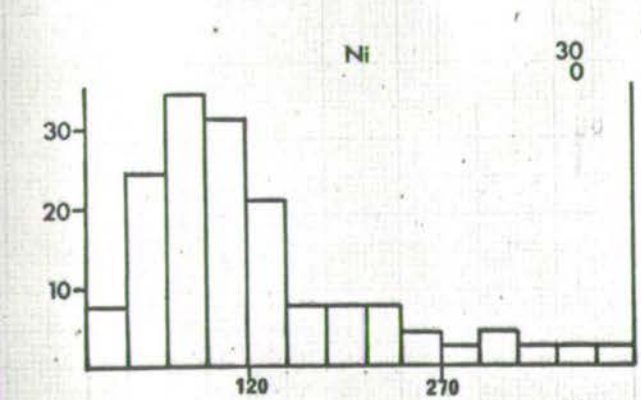
Ni
30
0
30
20
10
120
270

Fig. 2.6

Histograms for the distribution of major and trace elements in mugearites. Data from sources listed in Fig. 1.6.

Frequency polygons show distribution of elements in the mugearites studied.

Upper number in histograms indicates Lower Bound; lower number indicates the class interval.

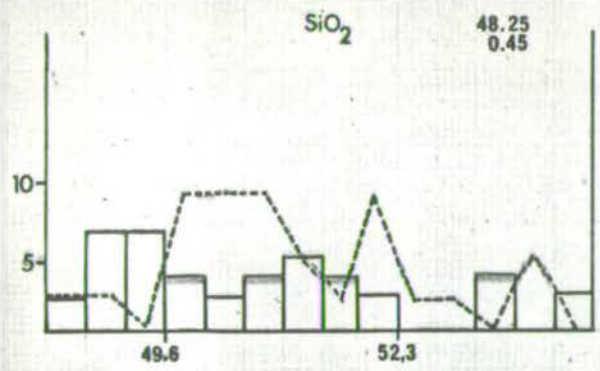
SiO_2
48.25
0.45
10
5
49.6
52.3

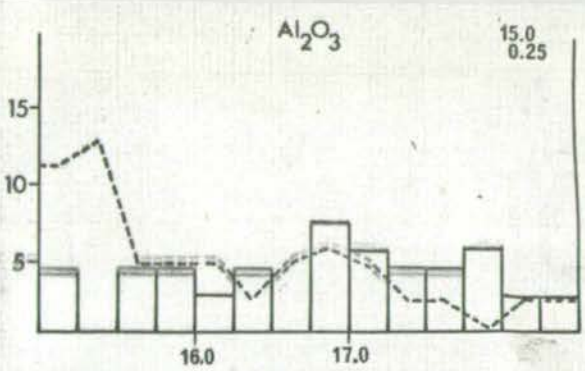
Al_2O_3
15.0
0.25
15
10
5
16.0
17.0

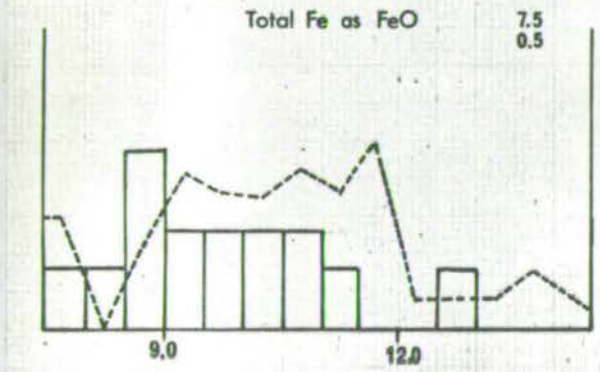
Total Fe as FeO
7.5
0.5
9.0
12.0

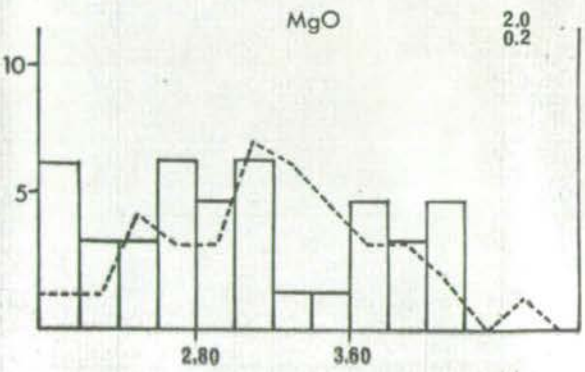
MgO
2.0
0.2
10
5
2.80
3.60

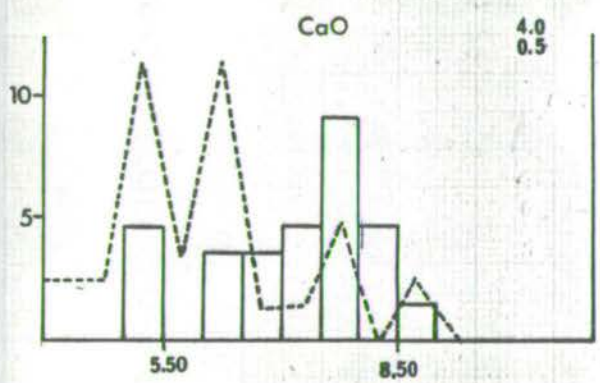
CaO
4.0
0.5
10
5
5.50
8.50

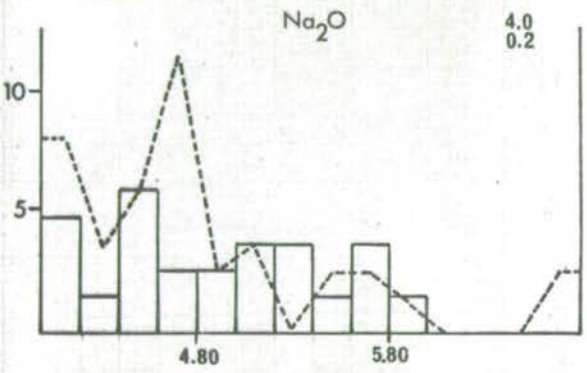
Na_2O
4.0
0.2
10
5
4.80
5.80

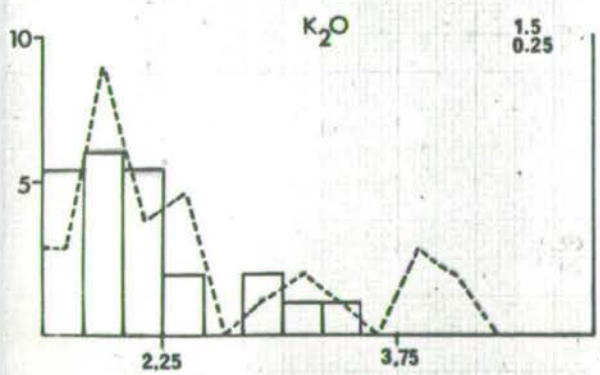
K_2O
1.5
0.25
10
5
2.25
3.75

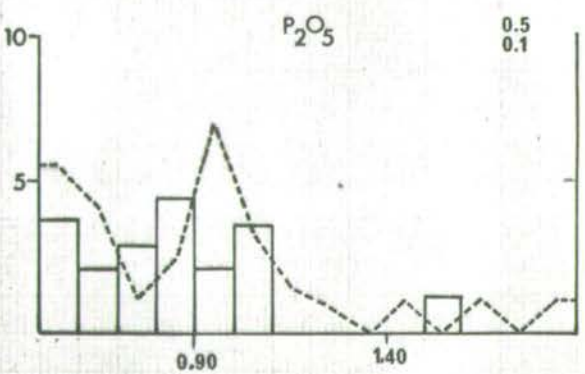
P_2O_5
0.5
0.1
10
5
0.90
1.40

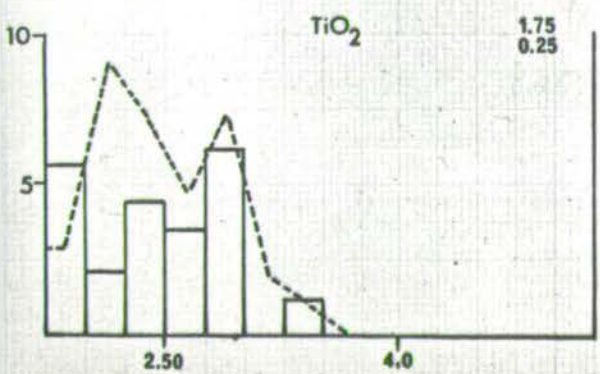
TiO_2
1.75
0.25
10
5
2.50
4.0

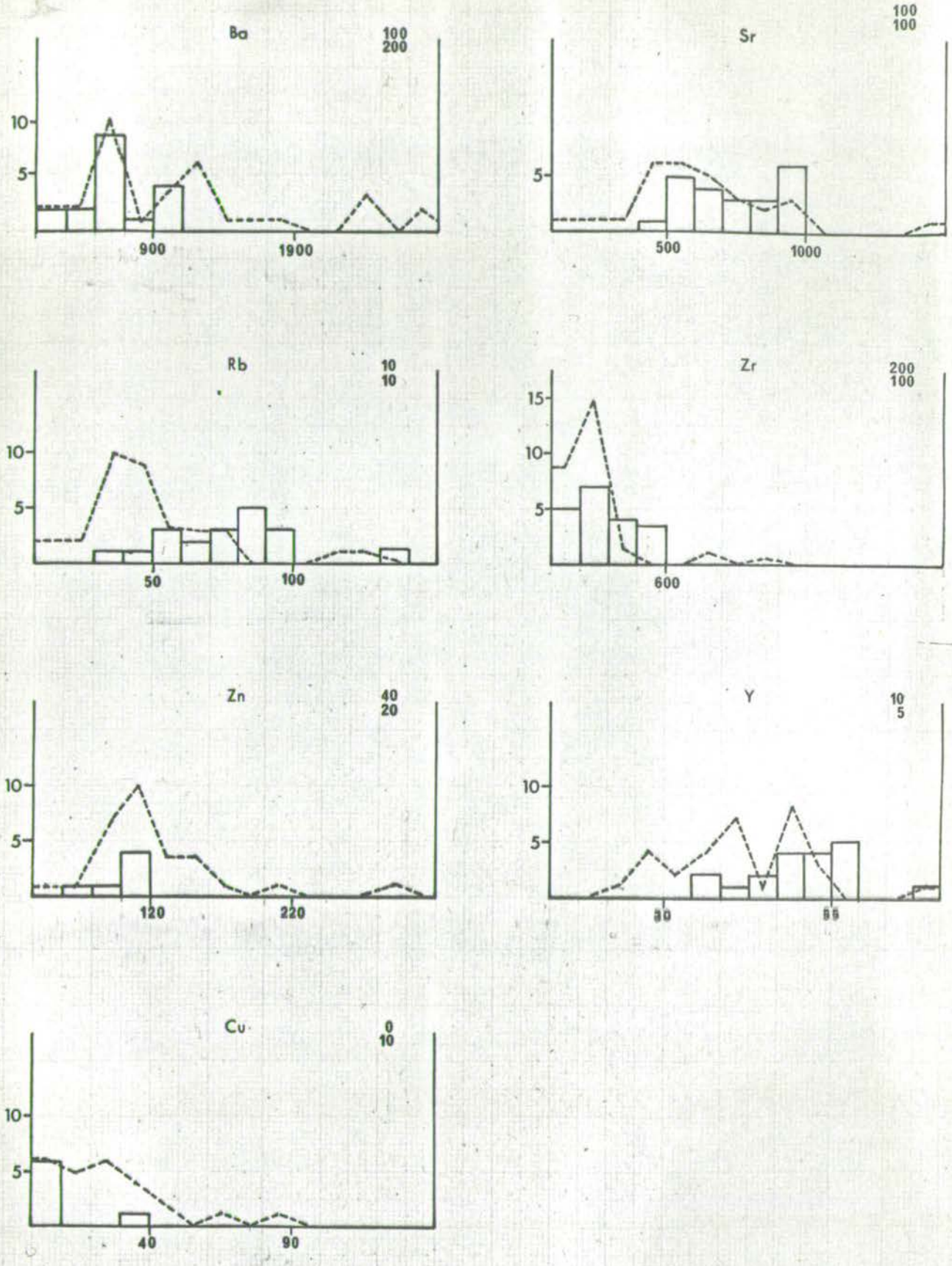
Ba
100
200
10
5
900
1900
Sr
100
100
5
500
1000
Rb
10
10
10
5
50
100
Zr
200
100
15
10
5
600
Zn
40
20
10
5
120
220
Y
10
5
10
5
30
Cu
0
10
10
5
40
90

Fig. 3.6

Histograms for the distribution of major and trace elements in benmoreites. Data from Baxter (1973) and Upton and Wadsworth (1972).

Frequency polygons show the distribution of elements in the benmoreites studied.

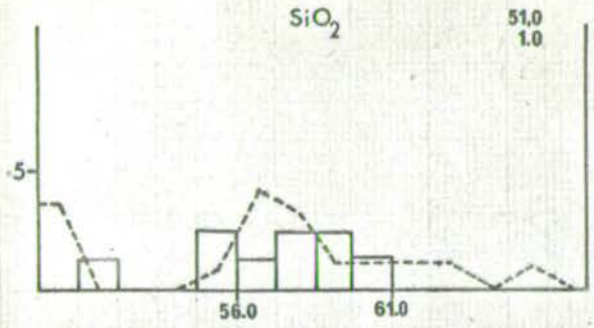
SiO_2
51.0
1.0
5
56.0
61.0

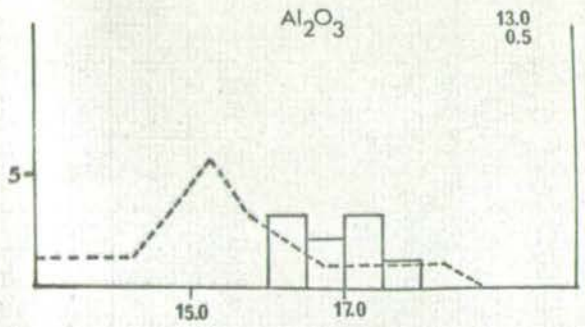
Al_2O_3
13.0
0.5
5
15.0
17.0

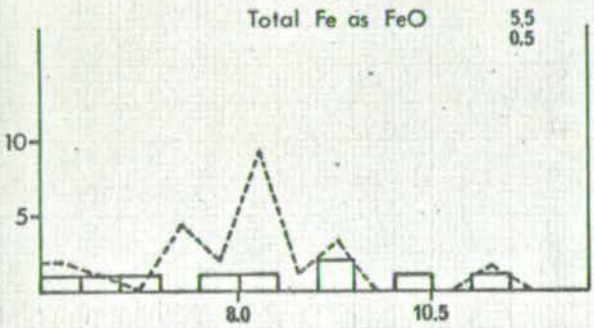
Total Fe as FeO
5.5
0.5
10
5
8.0
10.5

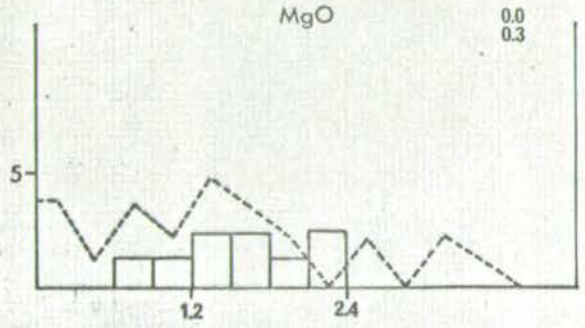
MgO
0.0
0.3
5
1.2
2.4

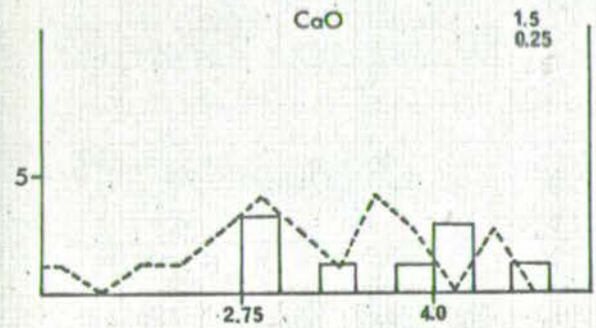
CaO
1.5
0.25
5
2.75
4.0

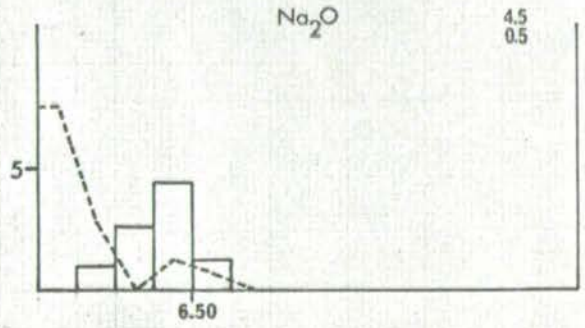
Na_2O
4.5
0.5
5
6.50

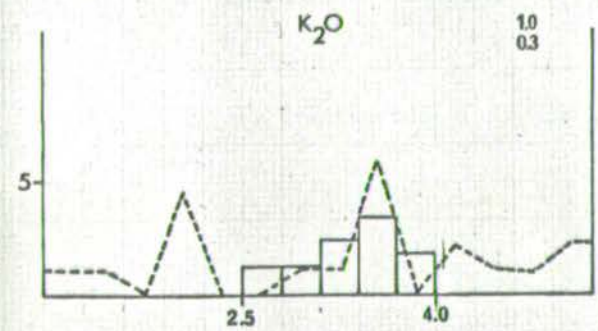
K_2O
1.0
0.3
5
2.5
4.0

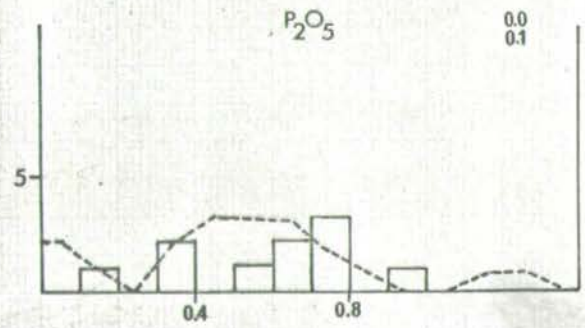
P_2O_5
0.0
0.1
5
0.4
0.8

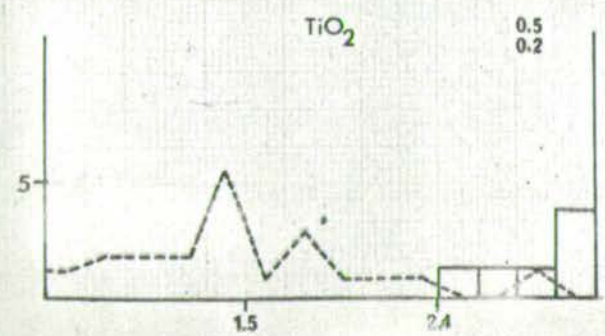
TiO_2
0.5
0.2
5
1.5
2.4

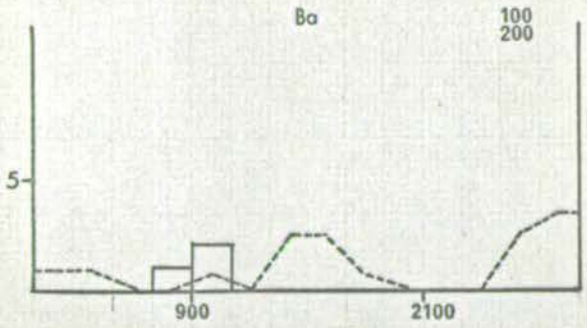
Ba
100
200
5
900
2100

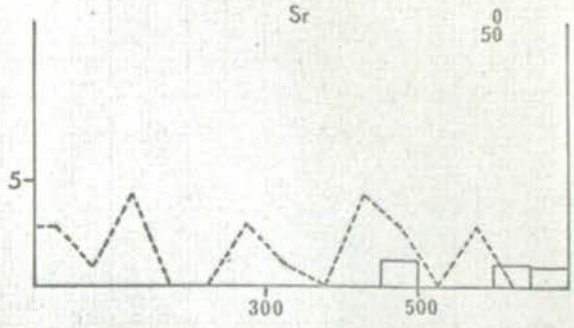
Sr
0
50
5
300
500

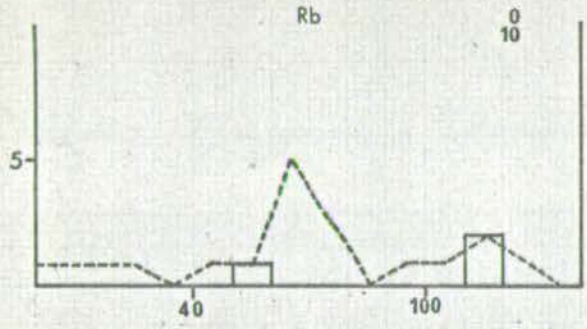
Rb
0
10
5
40
100

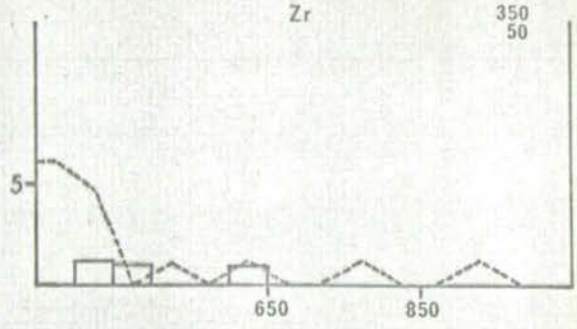
Zr
350
50
5
650
850

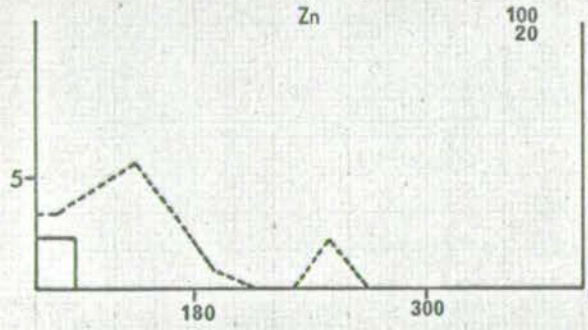
Zn
100
20
5
180
300

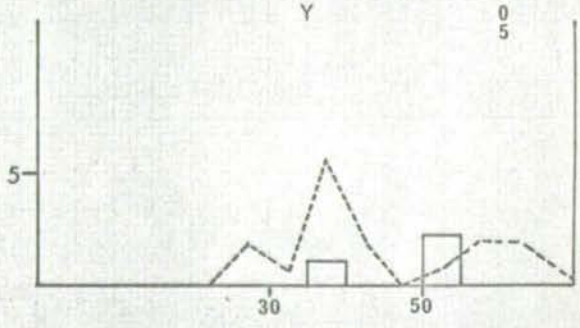
Y
0
5
5
30
50

TABLE 2.6

Distribution Coefficients (phenocryst/groundmass) for plagioclases listed in Table 1.4

		1	2	3	4	5	6
Talisker	23	260	96	.37	520	1132	2.18
"	21	256	35	.14	447	1147	2.57
"	19	286	56	.20	522	1155	2.21
"	17	281	6	.02	479	1100	2.30
"	15	297	65	.22	462	1097	2.37
"	13	270	87	.32	569	1130	1.99
"	11	270	140	.52	590	1115	1.89
Drum na Criche	7	966	342	.35	606	1454	2.40
Roineval	18	743	328	.44	693	1864	2.69
Dasses	13	560	370	.66	475	640	1.35
"	14	610	450	.74	610	795	1.30
"	15	2200	2080	.95	605	672	1.11
Greenock	17	440	160	.36	647	953	1.47
"	15	570	225	.39	590	985	1.67
"	13	440	180	.41	625	1010	1.62
"	11	620	91	.15	523	984	1.88
"	9	520	380	.73	592	822	1.39
"	7	590	360	.61	550	807	1.47
"	5	515	260	.50	637	940	1.48
SW Greenland	10	1309	1942	1.48	764	2222	2.91

Column 1 : Ba in groundmass
" 2 : " " phenocryst
" 3 : D_{Ba}
" 4 : Sr in groundmass
" 5 : " " phenocryst
" 6 : D_{Sr}

Fig 4.6 Distribution of Y plotted against Thornton Tuttle Index(D.I.).Position of the average hawaiite is given by the filled circle, that of the average mugearite by a filled triangle,and the average benmoreite by a square

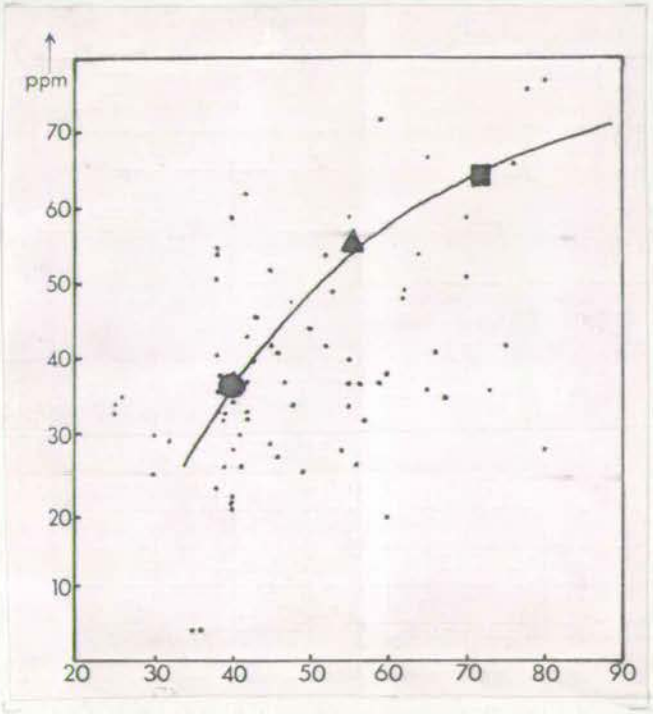

benmoreites.

Sr^{2+} (7 fold: 1.29Å; 8 fold: 1.33Å) is almost exclusively fractionated by plagioclase in the present suite of rocks. Jensen's (1973) Fig. 12 emphasizes the exponential fashion in which the Distribution Coefficient increases with a decrease in An content of the plagioclases, although data on plagioclases in the Greenland composite dykes does not follow this regular pattern (Cf. Table 1.4). Data from Heir (1962) and Corlett and Ribbe (1967) are consistent with this pattern, as are the data presented in this study with the exception of the Greenland dykes.

Hawaiites have a range of 500-600 ppm, mugearites 590-650 ppm and benmoreites, 430-500. The steady increase, from values in alkali-olivine basalts of ca. 370-390 through hawaiites and mugearites with a decrease in the benmoreites implies minor fractionation by plagioclase until the liquids reach this stage of evolution.

Rb^{1+} (7 fold: 1.64; 8 fold: 1.68) is typically low in the calcic plagioclases, with Distribution Coefficients less than unity. The hawaiites in the composite bodies contain up to 60 ppm, but show a considerable range, from a minimum of 3 ppm. Mugearites contain a maximum of 130, with a minimum of <1 ppm; the benmoreites contain an average of 88 ppm but show a considerable range, from a minimum of 8 ppm up to 126 ppm. The great variability partially obscures a progressive enrichment in residual liquids in passing from alkali-olivine basalts through hawaiites and mugearites to benmoreites.

Rb typically shows a close association with potassium; the typical rise in Rb content of plagioclase as the anorthite

content diminishes is not well shown by the plagioclase separates (Table 1.4).

A steady decrease in the K/Rb ratio is often used as an index of differentiation (Gast, 1968a, 1968b; Shaw, 1968), but single flows can show K/Rb ratios varying from 1600 to 640 (Watkins et al., 1970). Preferential fractionation of Rb by amphiboles will obviously also lead to a reversal of the trend (Hart and Aldrich, 1967).

Zr^{4+} (6 fold: 0.80) rises very slowly from levels of 160-200 ppm in the hawaiites through 350-400 in the mugearites to 400-600 in the benmoreites, indicative that it is partly concentrated in the residual liquids but possibly being removed in the titanomagnetites which can contain 260-380 ppm (Walker, 1969). MacDonald (1968) noted an overall increase throughout the series of peralkaline rocks examined, and that Zr was preferentially incorporated within amphiboles, particularly riebeckite-arfvedsonites or aegirines. It is frequently associated in sulphides but these are present only in minute amounts throughout the rock series studied. The high values in plagioclases (Table 1.4) are thought to be due primarily to inclusions of Zircon.

Zn^{2+} (4 fold: 0.68; 5 fold: 0.76) averages 60-80 in the hawaiites, 100 to 150 in the mugearites and is highly variable in the benmoreites analyzed (50-250). The sequence suggests concentration in residual liquids, possibly being removed by titanomagnetites in the more evolved rocks, and slowly declining; this is similar to the trend found by MacDonald (1968) for the Hviddal dyke. He suggested concentration in residual liquids and entrance into Fe-rich minerals only in the late stages of crystallization.

Y^{3+} (6 fold: 0.98; 8 fold: 1.10) is usually concentrated in the residual liquids, rising from 30-35 ppm in the hawaiites, 50-60 ppm in the mugearites, but showing little increase in the benmoreites (60-65). It is thought (Taylor, 1965) to be concentrated in titanomagnetites, and is certainly concentrated in apatites; the latter occur as phenocrysts only in the Greenland composite dykes, but there is no indication that fractionation of apatite has altered a trend of concentration in the residual liquids. The slope of the trend, if visualized in a scatter diagram plotted against some index of fractionation such as the Differentiation Index (Thornton and Tuttle, 1960) may be affected by titanomagnetite fractionation, but the data are inconclusive (Fig. 4.6).

Nb^{4+} (6 fold: 0.77); Nb^{5+} (6 fold: 0.72) was not analyzed for in all suites or in all rocks of a given suite; analytical precision is affected by overlap with satellite peaks of other elements (notably Y) so that the results should be treated with caution. The contents are quite low throughout the series, except in the suite of rocks from the composite flow at Greenock. Hawaiites tend to average 30-40 ppm, mugearites, 50-60, benmoreites 88 (1 analysis). The suite at Greenock, however, shows levels considerably above this: hawaiites have 60-70 ppm, mugearites, 100-110. The hawaiite flow on the Piton des Neiges is still higher, with 80-110 ppm. Huckenholz (1965) found levels of Nb in the alkaline volcanics of the Eifel that are similar to those levels in the Greenock composite body: alkaline olivine basalts (65), hawaiites (69) mugearites (86), trachytes (95). Most of the Nb is apparently

in the titanomagnetites possibly substituting for Ti^{4+}. Huckenholz (1965) found 500-600 ppm in titanomagnetites of hawaiites and mugearites. Preliminary microprobe analyses done on titanomagnetites in the suites studied failed to detect any; only in the ilmenites from the Bras Rouge Sill was it possible to detect amounts above the background. The level of detection was estimated to be 600-650 ppm of Nb; so in view of Huckenholz's data, the failure is not unexpected.

Ni^{2+} (6 fold: 0.77) was not analyzed for in all suites because of sample contamination by the methods of preparation; selected samples, thought to be representative of their respective compositions were prepared by different methods. The trend shows a gradual decrease from hawaiites (20-29 ppm), mugearites (3-9 ppm) to benmoreites (3) suggesting that it is constantly being removed by fractionating phases. The content of Ni in olivines correlates positively with Mg content (Simkin and Smith, 1970) rising to levels of over 1000 ppm in forsteritic olivine. Microprobe analyses of olivines in the Talisker hawaiites (Fo_{50-55}) give contents of 160-200 ppm. Ni in the associated titanomagnetites appears to be at levels of 800-1000 ppm. Fractionation of both phases, in amounts of only several percent seems sufficient to explain the decrease noted.

Th^{4+} (6 fold: 1.08; 8 fold: 1.12) showed a high coefficient of variation (Table 4.6): it was not analyzed for in all suites due primarily to this variation which appears to result both from lack of analytical precision and variance within rock suites. There is no coherent trend throughout

the suites studied. The element is not specifically included within any one mineral; the data are included merely to give a geochemical outline of the contents present.

Ga^{3+} (6 fold: 0.70) was analyzed for in only a few samples. It is known (Taylor, 1965) to vary little during fractionation, and seems to be mainly concentrated in two minerals: plagioclases (15–24 ppm) and Fe-Ti oxides (45–80 ppm) (Taylor, 1965). Since plagioclase is the predominant fractionating phase in the series it should be effective in removing Ga, but little change was noted in the levels found in the different compositional groups: hawaiites (16–18 ppm), mugearites (20–21), benmoreite (19).

La^{3+} the precision of the analytical method was not good for the range (generally less than 50 ppm) in concentrations usually present (Cf. Schilling and Winchester, 1969) in hawaiites and mugearites. The results, however, are similar to those obtained by Schilling and Winchester. There is considerable overlap in the ranges shown; thus alkali-olivine basalts contain 26–37 ppm, hawaiites, 18 to 52 ppm, mugearites have 48 to 53, and benmoreite, 60 ppm.

Schilling and Winchester (1969) noted that rare earth patterns in the alkali-olivine basalts, hawaiites, mugearites and trachytes suggested derivation of hawaiites and mugearites from alkali-olivine basalts by means of crystal fractionation, but that the origin of the trachyte possibly involved another mechanism.

$\underline{Ce^{3+}}$ (8 fold: 1.22Å) the analyses of Ce also showed poor precision. Again, comparison with Schilling and Winchester's data suggests that the levels are reasonable; their data shows that Ce contents are typically 2-3 times the level of La. Variability of content is considerable, ranging from 26 ppm to 115 ppm in the hawaiites with an average of 50 ppm to an average of 93 in the mugearites and a range of 62 to 166 ppm. The only benmoreite analyzed for Cerium contained 115 ppm.

$\underline{Cu^{2+}}$ (4 fold: 0.70Å) Cu is usually present in sulphide phases, but these were detected only in polished sections of the mugearite at Drum na Criche and in the alkali-olivine basalt of Talisker. Analytical precision is poor (coefficient of variation averaged 78%).

Cu averages 164 ppm in the alkali basalts, 38 ppm in the hawaiites, 20 ppm in the mugearites and 12 ppm in the benmoreites. This suggests that it is continually being removed by a phase or phases and not being concentrated in the residual liquids. Walker (1969) reports contents of Cu in the opaque minerals as ranging from 425 to 525 ppm; its content in plagioclase, clinopyroxene, olivine and orthopyroxene does not appear related to its distribution in the whole rock. Provided there is no co-precipitation of sulphide minerals, the content in the silicate minerals remains steady throughout a rock series (Walker, 1969).

Taylor (1965) suggested that the ratio Cu^{2+}/Cu^{1+} should be a sensitive indicator of the degree of oxidation of the magma. It has been assumed in this study that Cu is in the form Cu^{2+}, in the absence of sulphides (containing Cu^{1+}).

Pb^{2+} (4 fold: 1.02Å; 8 fold: 1.37Å) is reported for a few samples; the low levels found (<20 ppm) are of the same order of magnitude as reported for hawaiites and mugearites from N. Skye by Moorbath and Welke (1969). They suggested that the Pb isotope ratios implied contamination by the granitic country rocks of the mugearites, possibly during prolonged residence in high level magma chambers. Analytical precision at such low levels is poor using XRF techniques.

V^{3+} (6 fold: 0.72Å) is also reported in a few instances, but the line (Lα) used in X-ray fluorescence is not reliable when the total content of Rb and Sr exceeds 500 ppm. Upton and Wadsworth (1972) report an average of 314 ppm for hawaiites of the Differentiated Series of Réunion, 73 ppm for the mugearites and 17 ppm for the benmoreites. Taylor (1965) noted the preference of V for magnetite as opposed to ilmenite and pyroxenes instead of olivines. The steady depletion in passing from hawaiites through mugearites to benmoreites of the Réunion rocks implies constant removal by magnetite and clinopyroxene.

The individual suites are discussed below, primarily to emphasize accordance or discordance with the associations noted above.

Talisker

Introduction. The major and trace element chemistry with the exception of Sr is nearly identical in the matrices of the hawaiites comprising the two units. Both units are similar in composition to the hawaiite in the Greenock composite flow, but with phenocrysts considerably less (25%)

Fig. 5.6.

Distribution of major oxides showing the greatest variability in the Taliesker composite flow.

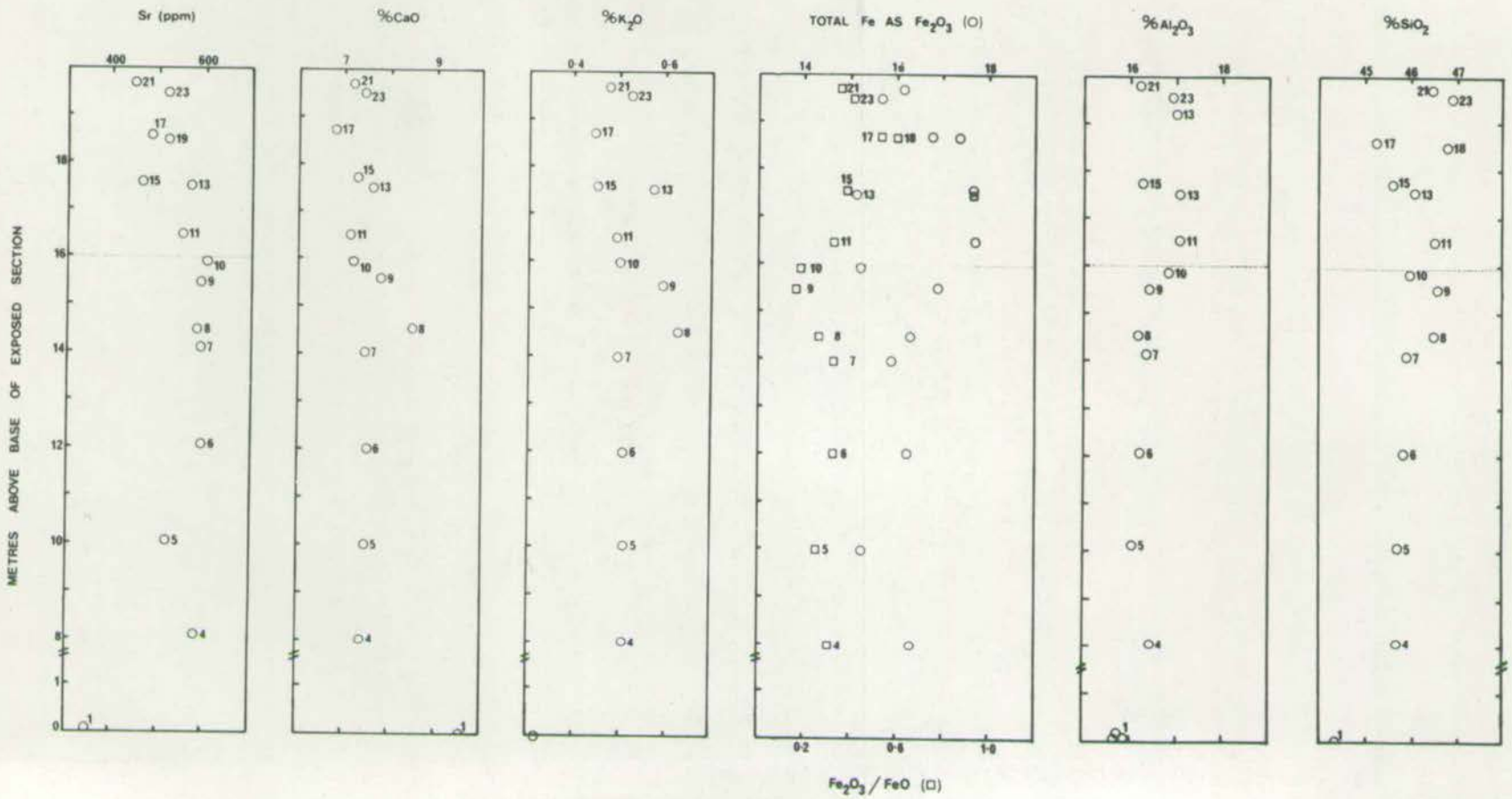
Sr (ppm)
400
500
%CaO
7
9
%K2O
0·4
0·6
TOTAL Fe AS Fe2O3 (O)
14
16
18
%Al2O3
16
18
%SiO2
45
46
47
METRES ABOVE BASE OF EXPOSED SECTION
0
1
8
10
12
14
16
18
Fe2O3 / FeO (□)
0·2
0·6
1·0

anorthitic. Both are less evolved than the hawaiites of Drum na Criche and Roineval (Fig. 1.5).

Element Distribution

There is little vertical or lateral variation within the three sections for all major oxides and trace elements (Table 1A, Appendix A, Fig. 5.6). The elements plotted in Fig. 5.6 emphasize the variability of elements in a zone approximately 1 m. above the junction of the two units.

The ratio Fe_2O_3/FeO has been used as a rough guide to the distribution of cooling isotherms within a single flow (Watkins et al., 1970). The maximum variability of this ratio coincides with that of the other elements and suggests that this region (ca. 9-10 m. above the base) represents the zone of maximum oxygen fugacity described by Sato and Wright (1966) and the region of slowest cooling. Application of Jaeger's (1968) curves and equations with the boundary conditions of 1150°C as the extrusion temperature and a thickness of 12 m. indicates temperatures of ca. 800-900°C in this region at the end of several months. No difference in mineral distribution or composition in specimens within this zone as compared with those outside it was noted.

There is a pronounced Sr depletion (15%) in the groundmass of the upper hawaiite as compared with the nearly aphyric hawaiite below. Plagioclase is the predominant phenocryst phase, varying from 17-22% in volume; the Sr Distribution Coefficients calculated for phenocrysts at various levels in the upper unit are given in Table 2.6. These show considerable variation; it is possible that the variation is not solely due to analytical error but is a true reflection

of compositional differences. Microprobe data do not support this hypothesis inasfar as major elements are concerned.

It can be shown (Philpotts and Schnetzler, 1969) that the amount of plagioclase fractionated (assuming perfect fractional crystallization) may be estimated by:

$$Sr = (1 - X)^{D_{Sr}} = 0.85$$

Where D_{Sr} is the Distribution Coefficient and 0.85 represents the amount of Sr remaining after a depletion of 15%. Solving for X gives the amount of plagioclase (6%) necessary before such a depletion can be detected. A combination of equilibrium and fractional crystallization would necessitate lesser (ca. 4%-5%) amounts. An estimate of the bulk D_{Sr} was made assuming a composition of An_{52}, with outer margins zoned to An_{34}. Only an estimate of the volume of this outer portion was made, using Griscom's (1960) curves for estimating the bulk composition of zoned crystals from the area of the zones of varying composition. This gave an estimated 92% of An_{52}, <2% An_{60} and 6-7% with an average composition of An_{40}. The D_{Sr} based on these proportions and calculated from Jensen's (1973) Fig. 12 differs slightly from the average D_{Sr} (2.3 as opposed to 2.25) of the separated plagioclase phenocrysts. Use of either the maximum (2.6) or minimum (1.9) D_{Sr} changes the amount fractionated by only 2%.

These results suggest that there has been accumulation of plagioclase phenocrysts within the hawaiite of the upper unit.

The low correlation coefficient of K_2O with Rb (0.427) and Ba with Rb (0.362) is surprising in view of their well known association, but it seems to be a result of the low

and quite variable content of Rb. This is again apparent in the significant correlation of Ba (0.892) and K_2O (0.742) with height (at the 99.9% confidence level). Rb shows little correlation (0.236) with height.

The positive correlation of Ba with K (0.671) and Na (0.873) and the negative correlation with CaO (-0.798) suggests that it is concentrated in the interstitial alkali feldspar and possibly analcime, as expected. Sr shows a similar significant correlation with both Na (0.744) and K (0.785) and a negative correlation with CaO (-0.828). It is consistent, however, with the progressive increase in Sr of plagioclases up to a composition of An_{23} as noted earlier.

Y shows a negative correlation with Fe_2O_3 (-0.786), but a positive one with FeO (o.577) possibly indicative that it is concentrated in the titanomagnetites. It does not show a significant correlation with P_2O_5 (0.199) suggesting that either it is preferentially incorporated in titanomagnetite as opposed to apatite, or the possible variable distribution of the accessory apatite.

The correlation of Mn with FeO (0.839) and TiO_2 (0.656) suggests, as expected, concentration in the titanomagnetites.

The correlation coefficients between the major elements conform generally to the groups of predominant mineral assemblages noted in the introductory section.

Drum na Criche

Introduction. The lower mugearite shows minor amounts (0.1, 1.2%) of normative qz and Ne (5, 6) although it should be noted that the analyses showing ne is quoted from Yoder and Tilley (1962). The mugearites show more variation in content

of alkali and silica than those of Roineval or the composite flow at Greenock. The difference in the two analyses of hawaiite show a similar, parallel trend, almost at right angles to the trends shown in Fig. 1.5. by the other composite bodies, as noted in the brief section on Classification. There is no indication in the phenocryst aseemblage that the ratios of the phases are significantly different than those of other composite bodies, and so might be responsible for this unique trend. The implication of the trend is that of greater variability in the mugearites within the unit, but not necessarily that it represents fractionation of phases other than those in the composite flows of Roineval and Greenock.

Element Distribution

Rb and Ba both increase strikingly over the contents present in the hawaiite. Ba averages 1242 ppm, Rb 40 ppm versus 966 (Ba) and 22(Rb) in the hawaiite. Sr (667 ppm) increases less rapidly (606 ppm).

Zr, Zn and Nb all show pronounced increases relative to the associated hawaiite; this concentration in the residual liquid is not unexpected as there is no evidence of phenocryst phases carrying these elements being extensively fractionated. Titanomagnetite can contain up to several hundred ppm of Nb and Zn, but it is present as phenocrysts in amounts of only 1-2%.

Ni shows a decrease from ca. 20 ppm in hawaiite to less than 9 ppm in the mugearite; it is presumed to be a result of olivine and titanomagnetite fractionation.

K_2O shows a significant correlation with Rb (0.955) and Ba (0.836); this should be true as the groundmass feldspar

is largely potassic oligoclase, as noted by Muir and Tilley (1961). It is reflected in the low correlation coefficient between K_2O and Sr (0.163).

Zn shows a significant positive correlation with FeO, as is expected on the basis of the analyses of groundmass titanomagnetites which contain up to 600 ppm of Zn.

Neither Na_2O nor CaO show a significant correlation with Sr (0.801) at the 98% confidence level, which is similar to the relation found at Talisker, although there is a more significant correlation than between K_2O and Sr.

Roineval

Introduction. In contrast to the mugearite of Drum na Criche, the mugearites contain neither ne or qz, but are all ol + hy normative. They show less variation in total alkalis and silica than Drum na Criche (Fig. 1.5).

Element Distribution

The average content of Sr is higher (699 ppm as opposed to 667 ppm) in the mugearites of Roineval, especially if the one high value (930 ppm) in the Drum na Criche mugearite is excluded (579 ppm average). The higher level of Sr is also true of the hawaiites: 693 ppm for Roineval, 606 for Drum na Criche, but the difference here is within the error of analytical precision. The high content of Sr is also reflected in the plagioclase phenocrysts (Table 1.4).

The plagioclase phenocryst separates from Roineval as well as Drum na Criche and Talisker were analyzed for La, Ce and Nd by XRF; the levels (50-100 ppm) were not consistent with the results given by Philpotts and Schnetzler (1970) and Schnetzler and Philpotts (1969) for plagioclases of

similar compositions.

The content of the other trace elements is very similar for both Drum na Criche and Roineval.

The Midland Valley of Scotland

North Berwick

Introduction. Even after adjustment of the Fe^{3+}/Fe^{2+} ratios, the more evolved flows show ca. 5% normative qz; the presence of normative corundum suggests selective removal of the alkalis; as does the high Fe_2O_3:FeO ratio (ca. 51) as compared with that (<1.3) of relatively recent and presumably little altered benmoreites from Réunion. (Analyses 4-7; Table 1D).

Both the overlying hawaiite (Analyses 1, 2, Table 1D) and the underlying alkali-olivine basalt (8) show evidence of alteration in thin section and this is partially reflected in the Fe_2O_3/FeO ratios of the analyses, and the presence of normative corundum in (2).

Element Distribution

The average content of Ba in the hawaiite (804 ppm) is significantly higher than the hawaiites of the Talisker composite flow, but analogous to that of Drum na Criche (966 ppm) and slightly higher than that of Roineval (743 ppm). Sr shows a similar relationship: high (644 ppm) when compared with Talisker (532 ppm), but similar to that of Drum na Criche (606 ppm) and Roineval (693 ppm).

The average content of Rb (48 ppm) is, again, high compared with that of Talisker (15 ppm), and also Drum na Criche (22 ppm) and Roineval (20 ppm).

The content of Zr and Y are similar to those of the hawaiites in the North Skye composite flows (ca. 225 ppm and

40 ppm respectively) but Zr shows a wide range in values; 119 to 592 ppm, which covers the range showed by the other hawaiites.

The benmoreites, although extensively altered, show contents of Ba (1466 ppm) covered by the range found for the benmoreites analyzed on N. Skye (21-24, Table 1C): 1300 to 6400 ppm. The level of Sr is also similar; 450 ppm (N. Berwick) and 385 (N. Skye). Rb is higher (114 ppm) than in the N. Skye benmoreite (50 ppm); as is Zr (481 vs. 263 ppm) and Y (63 vs. 23 ppm).

The extensive alteration naturally makes such comparisons suspect, and delineation of the content of various trace elements in the province is hampered by lack of published data for the East Lothian volcanics. The levels are within the range of analyses compiled for the histograms (Figs. 1.6-3.6) from the data on similar compositions in Mauritius (Baxter, 1973), Upton and Wadsworth (1972) and Strong (1970).

The Royal Park, Edinburgh

Introduction

Both St. Leonard's Sill and the Dasses are altered, locally quite extensively. Clarke (1956) and Rutledge (1952) believed the feldspars to have been "albitized" or replaced by analcime. This is reflected in the Differentiation Indices (D.I.) which vary from those of hawaiite to those of benmoreite, yet the petrography of the rocks suggests that the central facies of both St. Leonard's Sill and the Dasses are alkali-olivine basalts (12,15,18,19 Table 1D) and the outer facies hawaiite and benmoreite, respectively (11,14,16,17).

TABLE 4.6

Average trace element content of the composite bodies with the co-efficient of variation(v) in brackets; when missing only one analysis was made.

		Ba		Sr		Rb		Zr		Zn		Y		Cu	Nb	Ni	La	Ce	Pb	Ga
Tuliskar	L	257	(8.1)	577	(4.8)	14	(13.9)	221	(2.8)	63	(17)	39	(24.4)	33 (39.7)	38(11.8)	28(23.2)				
" groundmass	U	272	(6.9)	468	(5.4)	12	(22.4)	264	(21.3)	70	(16.1)	19	(49.9)	37 (27.8)	27(56.5)					
Druim na Criche	L	1242	(9.0)	666	(26.4)	40	(16.3)	365	(12.2)	118	(20.3)	51	(32.6)	19 (58.3)	57(12.4)	6 (70.7)				
"	U	966	-	606	-	22	-	312	-	110	-	25	-	5 (?)	30					
Roineval	L	1228	(3.9)	699	(8.5)	33	(6.7)	317	(2.9)	100	(7.5)	54	(6.9)	32 (18.0)	63(15.7)	8 (6.7)	40(28.8)	87(6.3)		
"	U	743	-	693	-	20	-	203	-	91	-	38	-		36	23				
Greenock	L	558	(23.3)	530	(25.4)	49	(34.0)	294	(10.1)	115	(16.7)	31	(42.9)	19 (82.1)	107(5.7)	8(15.2)	34(35.7)	65(5.4)	16(40)	19(14.9)
	U	531	(12.1)	505	(9.7)	42	(7.1)	275	(9.5)	108	(11.1)	31	(13.3)	15(110.7)	83(13.5)	6(45.7)	28(24.2)	55(35.7)		
Rasses - central		718	(10.2)	752	(11.1)	44	(4.5)	220	(8.2)	105	(53.3)	33	(12.1)	33 (6.1)		27(15.2)	21(23.8)	56(43.6)		
" marginal		123	-	332	-	16	-	297	-	67	-	52	-			20	46	115		
St.Leonard's Hill - centre		550	-	562	-	20	-	205	-	40	-	33	-	33						
" margin		160	-	130	-	8	-	335	-	345	-	48	-	18						
Greenland hawaiites		1613	(42.2)	826	(46.7)	29	(29.9)	196	(18.7)	163	(10.4)	27	(58.1)	37		4				
" mugearites		2160	(47.6)	723	(72.3)	96	(36.3)	262	(21.2)	129	(28.1)	37	(47.1)	36(54.7)	32(109)					
" benmoreites		1611	(110.3)	265	(147.2)	52	(69.1)	426	(63.7)	147	(39.2)	45	(61.2)		110(79.1)	3.4(73.6)				
Reunion - alkali-basalts		317	(11.1)	590	(6.3)	17	(29.4)	147	(3.4)	65	(4.6)	28	(3.6)	71 (38.2)		18(10.9)	18 (25)	36(5.6)	11	14
" hawaiites		453	(14.8)	614	(2.5)	37	(11.9)	230	(19.1)	80	(5.5)	39	(12.8)	40 (47.6)		13(16.4)	15	40(27.4)	10(70.5)	17(8.3)
" mugearites		534	(19.4)	338	(30.7)	60	(14.0)	338	(5.4)	100	(3.5)	50	(10.0)	14 (47.2)		14(7.1)	40			

Fig. 6.6.

Distribution of major elements and Sr with height in the Greenock composite flow. Filled circles represent whole rock analyses, open circles, the groundmass analyses.

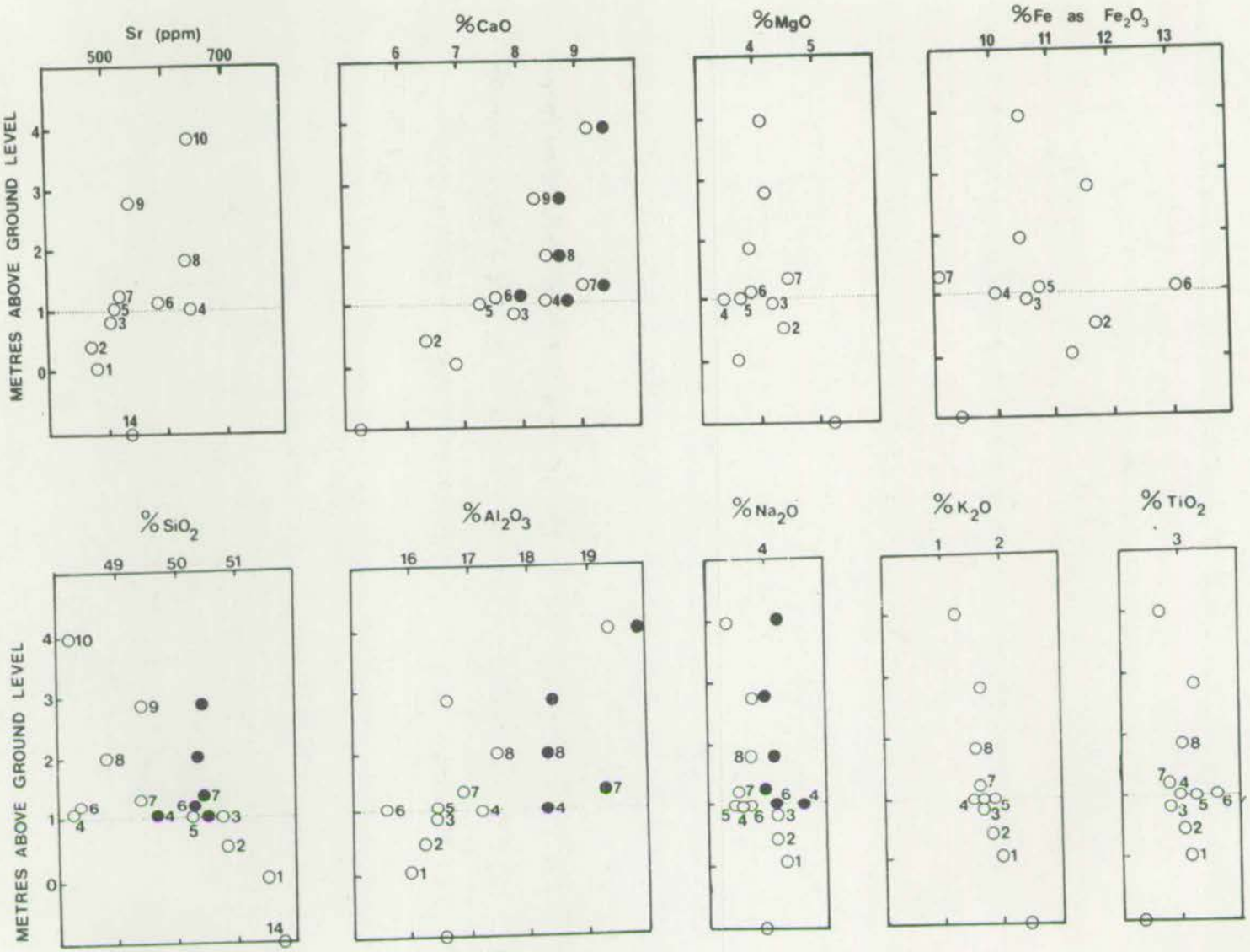
Sr (ppm)
500
700
%CaO
6
7
8
9
%MgO
4
5
%Fe as Fe_2O_3
10
11
12
13
METRES ABOVE GROUND LEVEL
0
1
2
3
4
%SiO_2
49
50
51
%Al_2O_3
16
17
18
19
%Na_2O
%K_2O
%TiO_2

The composite sill of the Dasses shows a gradational compositional change from the outer hawaiite (11,14) or mugearite (13) to the inner alkali-olivine basalt (15) or hawaiite (12). This gradation may, in part, be the result of the alteration noted above and in the section on Petrography.

St. Leonard's Sill, in contrast, shows a distinct compositional change from the highly altered benmoreite (17) to a hawaiite (16,18) central facies which is relatively unaltered. The transition zone between the two facies is 80-90 cm wide, and may be represented by Day's analysis (16) which is intermediate in composition between the samples analyzed from the outer and inner facies respectively (17,18).

Element Distribution

Almost all the elements show a high coefficient of variation (Table 4.6), particularly Ba and Sr, in both facies of the Dasses. The groundmass separates analyses (Table 4.6) show less, except for Sr, which shows a wide range (560-2200 ppm).

The significant points of Table 4.6 are the decrease in content of Rb in the outer facies of the Dasses (16 ppm) from the levels of the inner facies (44 ppm). The changes between the two facies of St. Leonard's Sill are even more abrupt with decreases in Ba (550 to 160 ppm), Sr (562 to 130 ppm) and Rb (20 to 8 ppm) suggestive of alkali feldspar fractionation. Zr increases (205 to 335 ppm) as does Zn (40 to 345 ppm) and Y (33 to 48 ppm). The least squares models, assuming crystal fractionation to be operative, do not suggest a simple sequence, deriving the benmoreite from the alkali-olivine basalt by crystal fractionation alone.

The composite flow near Greenock

Introduction. Fig. 1.5 showed that both units of the composite flow lie parallel to the trend shown by most other composite bodies in the alkalis versus silica diagram. The hawaiites are shown to be intermediate in composition between those of Talisker and those of Roineval and Drum na Criche.

The rocks are ol + hy normative, except for one rock showing qz (6,7) and two showing ne (4,16,17) in the norms.

Element Distribution

There is no significant correlation between height above the base of the flow and any chemical variable (Table C, Appendix D); if, however, the extreme values in the data are excluded (i.e., those analyses at the junction of the two units) then there is (Table D) a significant positive correlation between height and Al_2O_3 and a significant negative correlation between height and SiO_2, Na_2O, K_2O (Fig. 6.6). There is depletion of Sr in the hawaiite as noted in the porphyritic unit at Talisker; the mugearite shows a decrease of some 23% in the level of Sr, which is suggestive of plagioclase fractionation. The Distribution coefficient for Sr between plagioclase and groundmass shows a range of 1.62 to 1.47 (Table 2.6). The simple relationship used earlier in estimating the amount of plagioclase fractionated from the Talisker flow shows that 15-16% of plagioclase would have to fractionate before the observed Sr distribution would result. This is very nearly the amount present (15-20%) in the upper 2 m. of the hawaiite; the lower metre shows amounts varying from 7-33%, probably as a result of post-extrusive settling

in the flow. Evidence of some settling of both phenocrysts and groundmass minerals is present in the plots of Fig. 7.6, especially of Fe and Ti.

The progressive decrease in the amount of groundmass and interstitial alkali feldspar (plus analcime?) already noted in Petrography, are shown by the positive and negative correlations with height of Al_2O_3 and SiO_2, Na_2O, K_2O respectively. Correlation of the trace elements with the dominant mineral groups outlined in the introduction is not clearly defined. The usual association of Ba and Rb with the alkali feldspar-rich mugearite is present. Sr, however, shows a positive correlation with CaO possibly reflecting the decreasing amount of Sr-poor alkali feldspar with height. Fig. 6.6 very clearly shows the sympathetic variation with the CaO in the groundmass.

There are no other obvious associations of trace elements with the dominant mineral groups.

Craigmarloch Wood

Introduction. There are minor differences between Kennedy's (1932) analyses (19, 21; Table 1D) of the two units and the ones (20,22) made for this study; the most notable differences lie in the SiO_2 (48 vs. 53.7) and Fe_2O_3 (12.16 vs. 9.89) for the mugearite; the analyses of the benmoreite are but slightly different.

The mugearites reflect these differences, one (19) being ne normative, the other (20) qz normative. As seems to be typical of the benmoreites examined in this study, both analyses are qz normative (21: 9.8; 22: 7.7).

TABLE 6.6

Calculated groundmass analyses of the porphyritic rocks from the central portions of the composite dykes in SW Greenland. Analysis numbers are those of the whole rocks given in Table 1G, Appendix A.

	7	8	20	21	22
SiO_2	49.7	49.0	51.9	51.3	50.0
Al_2O_3	14.8	14.9	16.5	16.0	15.8
Fe_2O_3	3.5	4.2	2.3	3.0	3.6
FeO	7.4	6.8	7.1	6.4	8.3
MgO	3.3	3.5	3.8	3.4	3.5
CaO	6.1	6.2	6.8	7.6	8.5
Na_2O	3.9	3.8	4.8	4.4	4.3
K_2O	4.1	3.8	2.1	2.2	1.9
H_2O	2.2	2.5	1.5	1.3	1.0
TiO_2	2.7	2.7	2.2	2.4	2.3
P_2O_5	1.7	1.9	1.1	1.4	1.5
MnO	0.2	0.2	0.2	0.2	0.2
TOTAL	99.6	99.5	100.3	99.6	100.9

Analysis 7 recalculated by removing 4% plagioclase of An_{30} and 1% of alkali feldspar: $An_{15}Ab_{55}Or_{30}$

" 8 recalclated by removing 10% plagioclase (An_{40})

" 20 " " 16% " (An_{48})

" 21 " " 19% " "

" 22 " " 26% " "

Element Distribution

The content of all trace elements in the mugearite is similar to those in the mugearite of the composite flow at Greenock. There is the typical increase of Ba, Rb, Zr, Zn and Y over these levels in the benmoreite, with a decrease in Sr. The presence of 7-10% plagioclase phenocrysts in the benmoreite suggests that Sr would be depleted by just this amount assuming an average Sr Distribution Coefficient (Jensen 1973) for plagioclases of An_{35-30}.

The content of trace elements in the benmoreite shows some similarity to the levels found in the benmoreite at North Berwick (Fig. 3.6). There seems to be a high degree of variability in the content of Ba, but the other elements show relatively minor variation. This also seems to be true of the benmoreites at Am Bile (21-24) and Vidigill Burn (13). But not the benmoreite facies of St. Leonard's Sill.

South-west Greenland

Introduction. It was noted earlier (viz. Petrography) that the composite BFD dykes are characterized by more evolved marginal facies, which may be benmoreite (1-3; 10, 11, 14 Table 1G) or mugearitic (18-20; 27,28) in composition. Individual dykes may show a gradation from benmoreite margins (5) to mugearite (6) within the outer facies alone.

The more basic central facies have groundmass compositions that are hawaiitic (22) or mugearitic (13,8) in bulk; calculated groundmass compositions are mugearitic (Table 6.6).

The compositional fluctuation noted in Bridgwater and Harry's analyses (1968, pp.124-6), and in the present study appear to be a function of fluctuations in the amount of

included plagioclase phenocrysts and not fluctuations in the groundmass composition (Table 6.6).

The norms calculated for the rocks indicate the nearly saturated nature of most of the compositions involved. This is depicted graphically in Fig. 1.5 where the compositional field straddles the division (marked "Gardar") between the fields of saturated and undersaturated compositions.

Bridgwater and Harry (1968, p.136) noted that the differentiation trends shown by the composite dykes are similar to that of the Isortoq giant dyke, a syeno-gabbro intrusion. Comparison of the trend shown by this dyke in a plot of $\Sigma Fe/\Sigma Fe + Mg$ vs. Ca with the composite dykes showed depletion in CaO and was interpreted as possibly indicating the earlier fractionation of plagioclase during the early evolution of the suite.

Bridgwater and Harry (1968, p.136) interpreted the variable K/Na ratios found in "...comparable samples taken from different traverses across a single dyke." as indicative of a process other than crystal fractionation.

Dr. D. Bridgwater has kindly sent the powders from which the analyses quoted in Bridgwater and Harry (1968, pp.124-126) were made; these have been reanalyzed for trace elements and Fe_2O_3, which were not reported in the original analyses.

Element Distribution

The bulk analyses of central facies quoted in Table 1G (Appendix A) contain up to 45% plagioclase phenocrysts; the groundmass of specimen 86052 (21) was analyzed separately for trace elements, and the major elements calculated after removal

of 35% plagioclase of An_{45} (Table 6.6). Comparison of trace element contents in the two analyses showed that the Sr, Ba and Rb contents, enhanced by ca. 35% plagioclase phenocrysts in the bulk rock analyses, could be estimated in the groundmass analyses by subtraction of 34% Sr, 42% Ba and 10% Rb. Adjustments in the levels of these specific trace elements for bulk rock analyses of the central facies are necessary before comparing them with the marginal facies. This has been done (Table 6.6) in the dyke suites for which hand specimens were available, and estimated for the suites in which only thin sections were available.

On the basis of Distribution Coefficients derived from analyzed phenocrysts and matrix in the dyke represented by analyses 18-22, the decrease in Sr and Ba in the outer facies is produced by fractionation of 6-7% plagioclase (An_{45}), emphasizing the cumulate enriched nature of the central facies which contains 20-40% plagioclase phenocrysts.

The minor amounts ($\leq$5%) of other phases seem to be in the correct relative proportions, judged by least squares models used to derive the composition of the marginal facies from that of the central facies. Fractionation of these phases has apparently affected the content of Zr, Zn, Y and Rb, which show an increase in the marginal facies of mugearitic composition, but not at the rate predicted by assuming a crystal fractionation model. In the more evolved marginal facies of benmoreite composition there is a sharp decrease in the content of Ba, Sr, Rb suggesting the fractionation of ca. 4-5% of alkali feldspar, based again on a crystal fractionation model using the analyses of alkali feldspars

Figure 7.6(overleaf).Distribution of trace elements from the margin to the centre of selected composite dykes in SW Greenland. The symbols utilized for the different dykes are given below:

● Analyses 1-4, Table 1G
▲ " 5-8 " "
■ " 11-13 " "
△ " 14-16 " "
○ " 18-22 " "

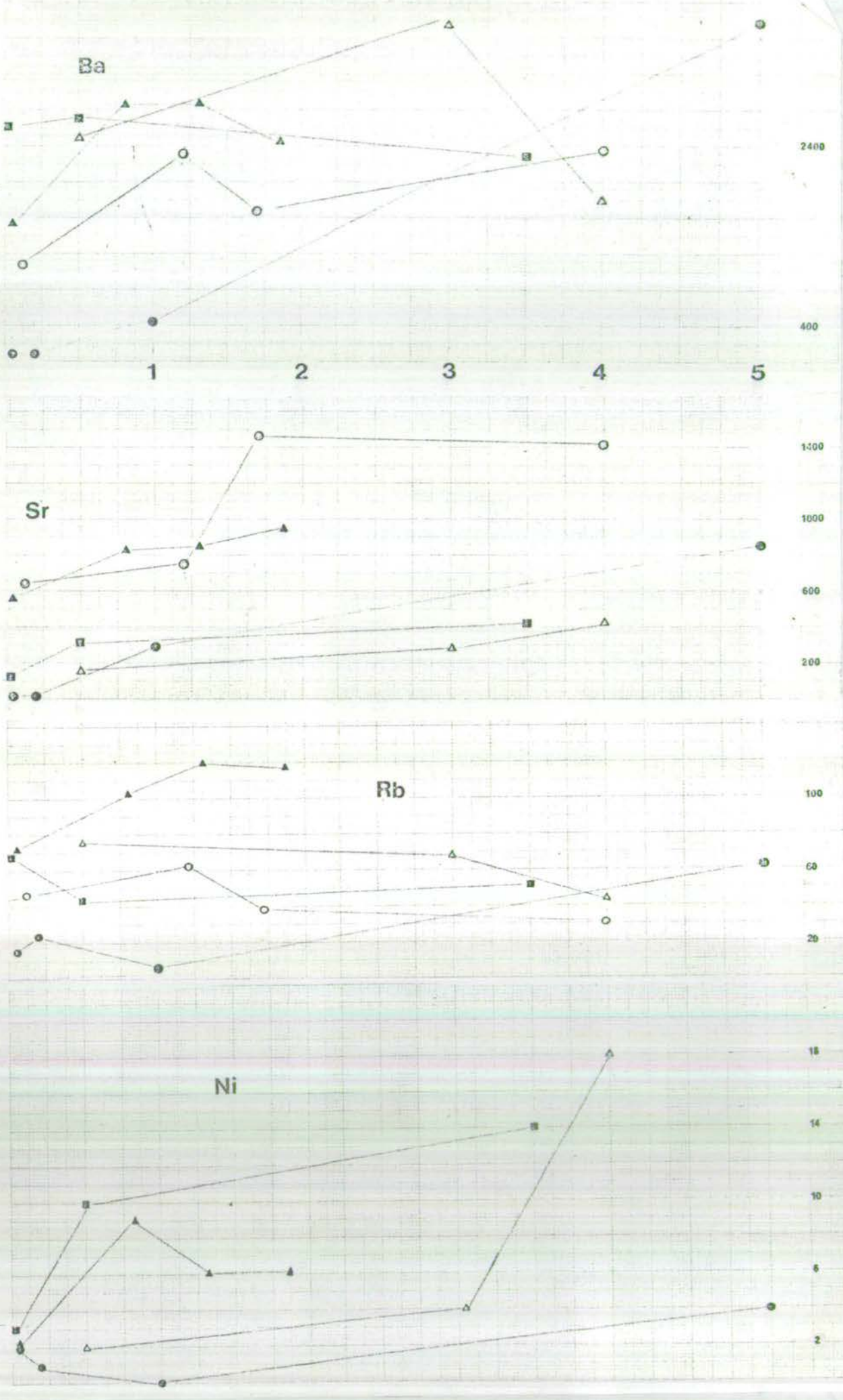
Ba
2400
400
1
2
3
4
5
Sr
1400
1000
600
200
Rb
100
20
Ni
14
10
6
2

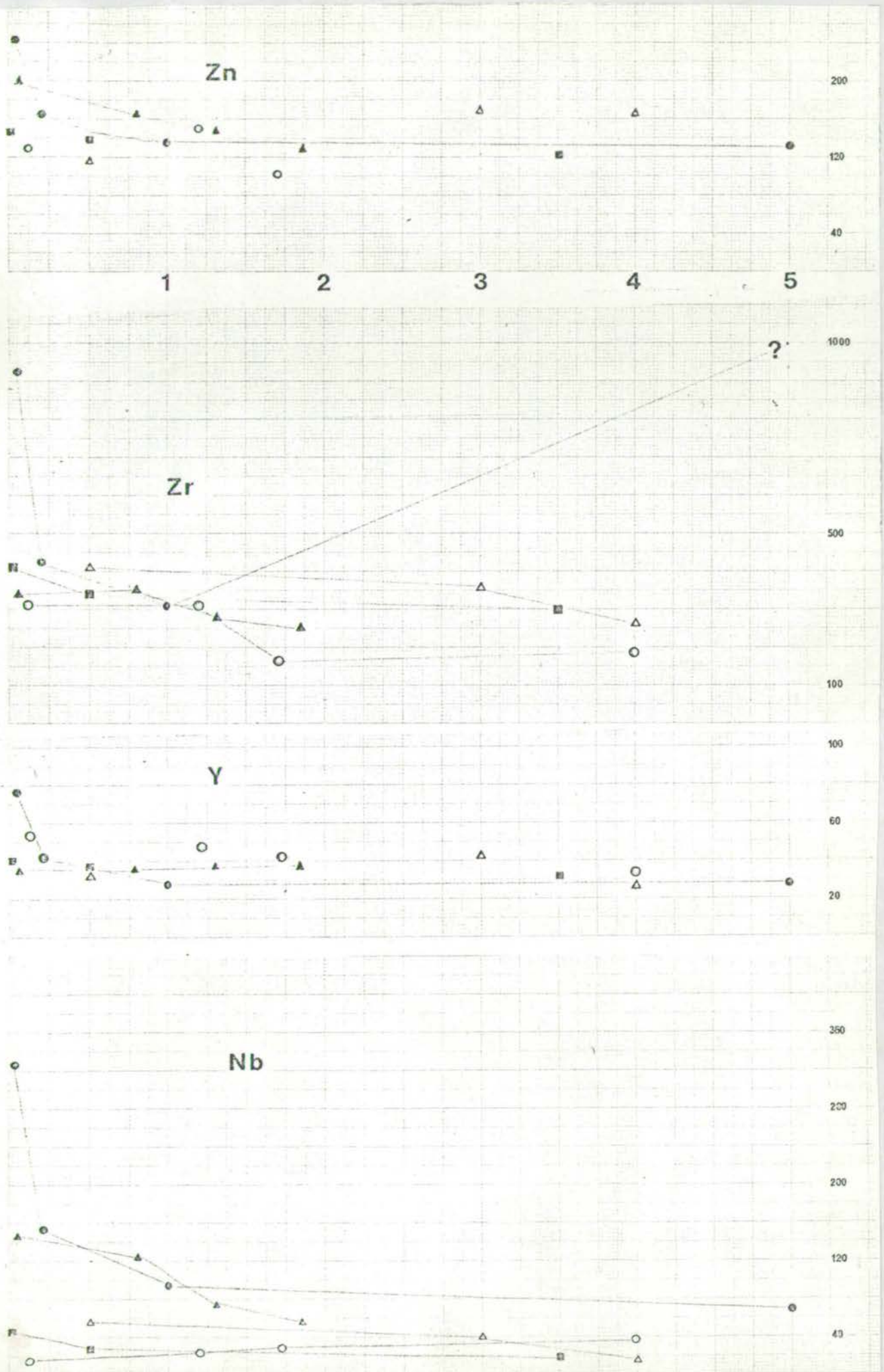
Zn
200
120
40
1
2
3
4
5
?
1000
Zr
500
100
100
Y
60
20
350
Nb
200
200
120
40

from Tugtutoq. These relations are summarized in Fig. 7.6.

The high content of Ba in the feldspars has been noted in the chapter on Mineralogy; this is true also of the rocks. The hawaiites show a considerable range, 592 to 3757 ppm; mugearites contain an average of 1970 ppm and benmoreites, 1611 ppm, although the range (71 to 3793 ppm) is far greater than for the mugearites.

The other striking geochemical feature of the rocks is the high content of Zr (cf. Analysis 4, Table 1G). Examination of the thin section loaned by Dr. Bridgwater did not have abundant zircons.

MacDonald (1968) reported high values for the peralkaline acid rocks (5240-300 ppm); Taylor (1965) notes that there is a general increase in the late magmatic or pegmatitic stages of alkaline rocks. The results for the one sample are suspect, especially since a similar high level is not present in the other rocks of the dyke suite.

The distribution of the other trace elements is noted in the frequency polygons of Fig. 7.6.

Réunion

Bras Rouge Sill

Introduction. On the basis of petrographic evidence, liquid compositions are assumed to be represented by analyses 1-6 (Table 1H). Upton and Wadsworth (1967) considered that their analysis of late stage leucocratic sheets in the middle part of the sill also approximated a liquid composition; there is, thus, a liquid compositional range from hawaiite to benmoreite. Analyses of the rocks in the central portion of

the sill (7-12) are considerably more basic (alkali-olivine basalt) and, on petrographic evidence, appear to be accumulitic. It is thought that in situ fractional crystallization of the last, basaltic, magma to be injected into the sill resulted in: (a) segregation of an alkalic residue, and (b) a residual, more basic series represented by the hawaiites (5,6) and at least partly accumulitic rocks (7-12); Upton and Wadsworth (1967). The compositional sequence was believed to be derived by successive tapping of a compositionally zoned magma chamber.

The main points noted by Upton and Wadsworth (1967) were:

(A) The mugearitic margins do not correspond to a weighted average composition of the sill.

(B) There is a complete gradation in composition and grain size from the mugearitic lower chilled zone to the most basic rocks in the central portion of the sill.

Normative qz is present in all but 3 of the analyses. The plot of total alkalis versus silica (Fig. 1.5) spans the entire field of compositions covered by the other composite bodies studied. The differentiation trend parallels the axis along which most of the other bodies lie, but with a greater variation normal to it. The trend in other similar series (cf. Upton and Wadsworth, 1972) is considered a result of crystal fractionation. The possibility that a differentiation trend at right angles to this might be due to some other mechanism, such as volatile transfer, was raised when discussing Drum na Criche. Upton and Wadsworth (1967), however,

Fig. 8.6.

Distribution of K_2O, Na_2O and CaO with height in the Bras Rouge Sill.

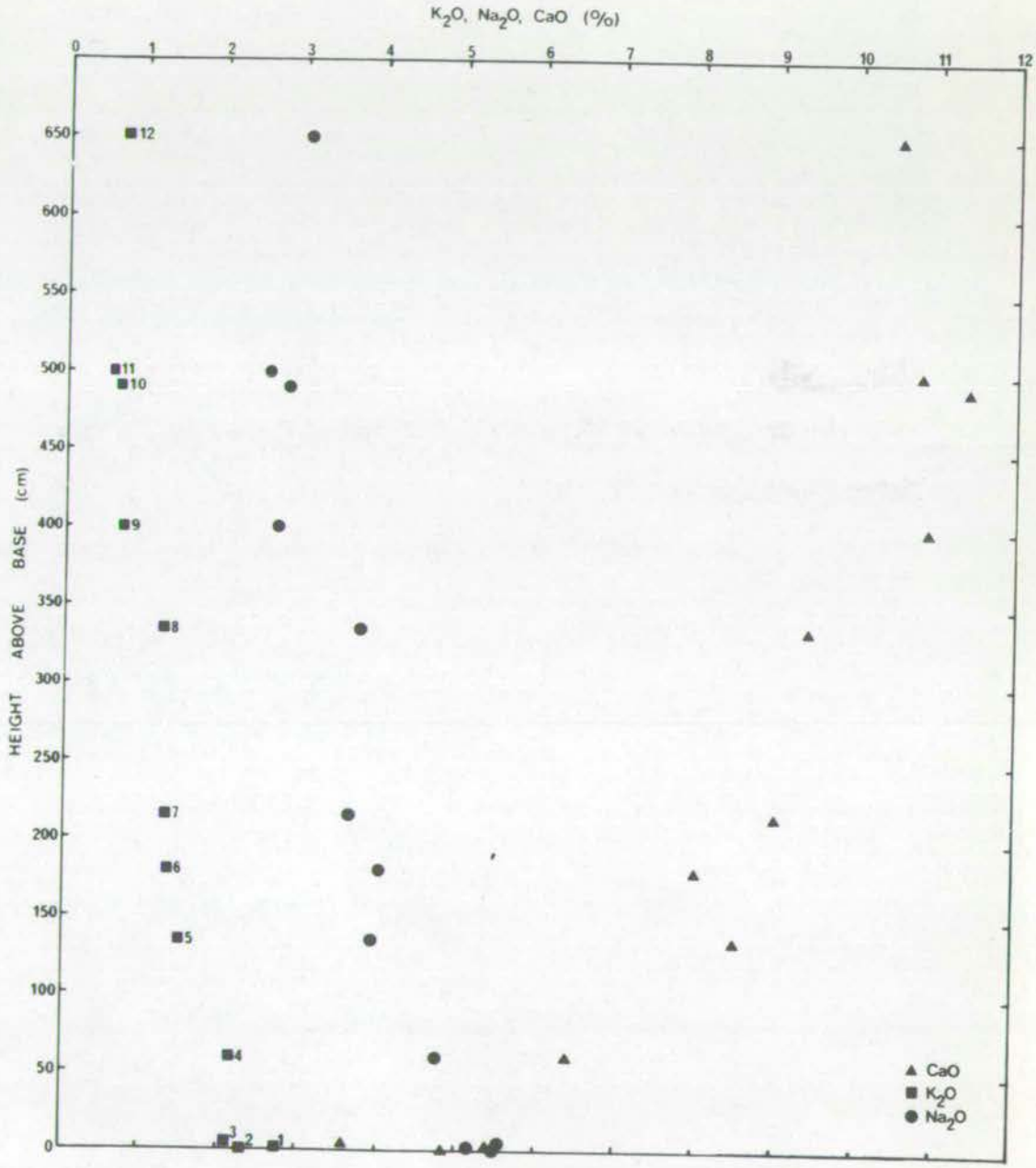
K_2O, Na_2O, CaO (%)
0 1 2 3 4 5 6 7 8 9 10 11 12
HEIGHT ABOVE BASE (cm)
650 600 550 500 450 400 350 300 250 200 150 100 50 0
12
11
10
9
8
7
6
5
4
3
2
1
CaO
K_2O
Na_2O

Fig. 9.6.

Distribution of TiO_2 and MgO with height in the Bras Rouge Sill.

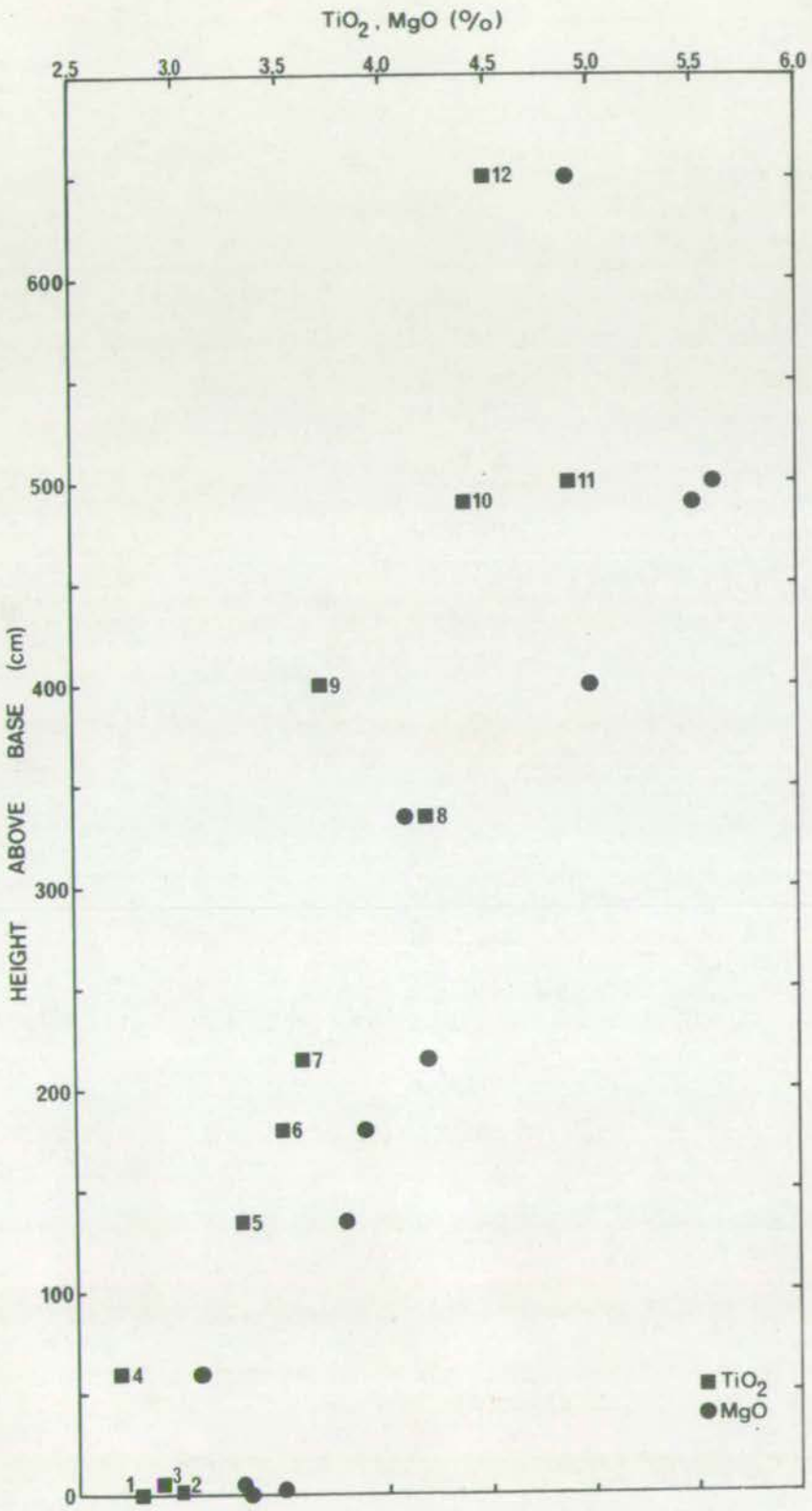
TiO2 , MgO (%)
2.5
3.0
3.5
4.0
4.5
5.0
5.5
6.0
HEIGHT ABOVE BASE (cm)
0
100
200
300
400
500
600
12
11
10
9
8
7
6
5
4
3
2
1
TiO2
MgO

Fig. 10.6.

Distribution of Zr (x 0.1) and Y with height in the Bras Rouge Sill.

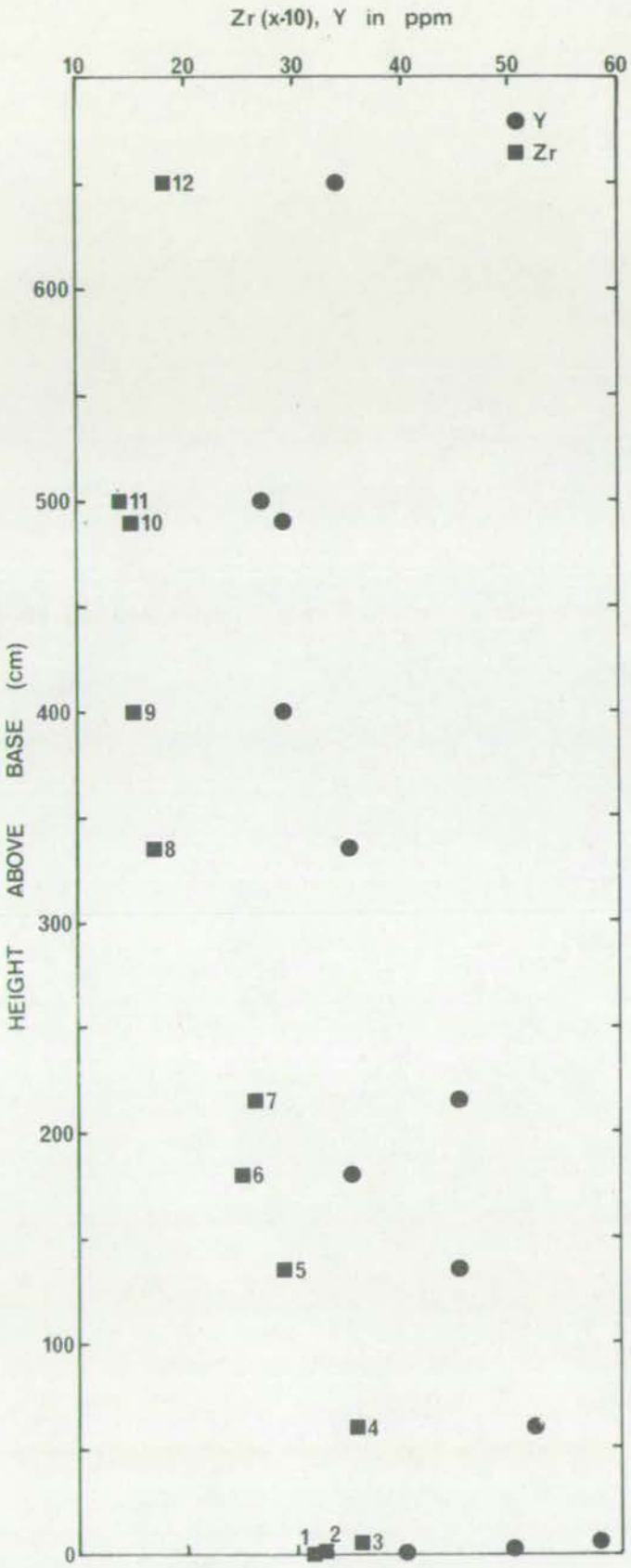
Zr (x10), Y in ppm
10
20
30
40
50
60
Y
Zr
12
11
10
9
8
7
6
5
4
3
2
1
0
100
200
300
400
500
600
HEIGHT ABOVE BASE (cm)

interpreted the sequence of compositions present in the sill as a result of crystal fractionation.

Element Distribution

The decrease in alkalis with a commensurate increase in CaO towards the centre of the sill is shown in Fig. 8.6; this is accompanied by an equally steady increase in TiO_2 and MgO (Fig. 9.6) and decrease in Zr and Y (Fig. 10.6). These trends are true for both liquids and accumulitic rocks; they show no deflection in passing from one into the other.

Ba does not show a significant correlation with K_2O (Table E, Appendix D), or indeed with any element except for a negative correlation with Fe_2O_3 (-0.896).

Sr shows a negative correlation with Rb (-0.837), Na (-0.921) and K_2O (-0.868), but a positive correlation with CaO (0.922). This is dissimilar to patterns noted for Drum na Criche and Roineval which suggested that Sr might be concentrated in the less calcic feldspars; here the opposite is implied.

Rb shows a negative correlation with total Fe and MgO (-0.899 and -0.887) and a positive correlation with Na (0.918) and at a lower confidence level, with K_2O (0.767), and SiO_2 (0.911). This is the behaviour predicted on the assumption that Rb is associated with the alkali feldspars, which diminish in amount with height above the base, as shown by the negative correlation that Rb has with height (-0,798); Ba also shows a negative correlation with height, but at a lower confidence level (-0.570; 90% confidence level).

Y, Zr, and Zn all show a negative correlation with height above the base of the sill (-0.871, -0.889, -0.782)

i.e. they are increasingly concentrated in the more evolved liquids (cf. Fig. 10.6); their positive correlation with SiO_2 (0.930, 0.930, 0.873), Na_2O (0.938, 0.918, 0.886) and K_2O (0.852, 0.871, 0.904) would be as predicted.

Cu shows variable concentrations in the more evolved mugearites (10-20 ppm) but increases steadily (30-55 ppm) in the hawaiites where chalcopyrite and pyrite are present as discrete grains and reaches a maximum in the accumulitic rocks (90 ppm).

Ni shows an almost constant level throughout both the presumed liquid compositions (<10 to 15 ppm) and in the rocks thought to be accumulitic (13 to 20 ppm).

The analytical precision for Th is poor, especially at the levels reported here (<10 ppm); it is not known what level is present throughout the Differentiated Series. The range reported here is from 2 ppm in the more evolved mugearitic rocks to between <1 and 4 ppm in the accumulitic rocks.

Pb shows very low levels in the mugearites and hawaiites (<1 ppm) but much higher levels (8-16 ppm) in the hawaiites and accumulitic rocks. Data from Oversby (1972) gives somewhat lower contents (ca. 2-4 ppm) for the Differentiated Series, but is based on a far more precise analytical technique.

Ga shows little change in either the hawaiite (18 ppm) or accumulitic rock (16 ppm).

V is present in amounts (140-215 ppm) higher than those reported by Upton and Wadsworth (1972) (40-190 ppm) for mugearites of the Differentiated Series. The hawaiite (analysis 6; Table 1H) shows a content (240 ppm) within the range (150-

440 ppm) reported by Upton and Wadsworth (1972) for the Differentiated Series.

Cr is present throughout the series at low levels (<5 ppm), analogous to the levels found by Upton and Wadsworth (1972) for hawaiites and mugearites of the Differentiated Series.

The relation of the average trace element content for the hawaiites, and mugearites is summarized in the histograms of Figs. 1.6 and 2.6, as compared with rocks of similar major element composition.

Hawaiite Flow, Piton des Neiges

The youngest flow from the volcano varies in composition as defined by the Differentiation Index from a mugearite (13) to hawaiite (14-16); it is mildly undersaturated, with 0.5% ne in the norms of two of the hawaiites.

The average content of Ba (583) is slightly less than (650 ppm) the average of 3 compositionally similar rocks reported by Upton and Wadsworth (1972) from the Differentiated Series (Analyses 9-11, Table 3).

Sr (647 ppm) is also slightly less than the value for the same 3 rocks (680 ppm). Rb is higher (60 ppm versus 40 ppm). Zr is higher (372 versus 303 ppm) as is Zn (102 versus 93) but within the analytical precision of the method used. Y shows a considerable difference present at almost half the level in the samples of Upton and Wadsworth (24 versus 40 ppm).

Nb is not reported by Upton and Wadsworth (1972); the high content (95 ppm) in the flow is similar to that found in the mugearites (103 ppm) in the composite flow of Greenock.

La (90 ppm) and Ce (160 ppm) are reported only from the nearly aphyric mugearite. They are considerably higher than the levels found in the flow at Greenock (33 and 63 ppm) for La and Ce.

It was originally thought that analysis of the flow might provide evidence for the existence of zoned magma chambers; this it does not do. The minor variations shown in major and trace elements are ascribed to the differences usually found in analyses of a single flow (cf. Watkins et al., 1970).

CHAPTER 7

PETROGENESIS

Introduction

Petrographic and field evidence of texturally and compositionally distinct units within a single flow, or eruptive event, was interpreted by Kennedy (1931) as evidence of pre-extrusive differentiation into at least two units, presumably coexisting within a single magma chamber. Lack of a brecciated zone or chilled surface between the two units implied that they were erupted sequentially, within a short period of time (several hours by analogy with observed lava flows). In cross-section the units were asymmetrically distributed, but there is no evidence that either unit is more voluminous than the other. Kennedy also noted that the composite flow was the uppermost flow in the sequence of flows examined.

MacDonald (1967) examined in detail the composition of a single hawaiite flow; the data suggested that the composition of the magma became progressively more basic as the eruption progressed. In contrast to the composite flow earlier described by Kennedy (1931) in which the "...main mass of each of the two members is always very uniform", the single flow showed a gradational compositional change, with no sign of any discontinuity. MacDonald believed that crystal fractionation could not produce a gradational series of liquids, and adopted the mechanism suggested earlier by Hamilton (1956) to explain the overall variation in the Clyde Plateau lavas. Hamilton had postulated that selective melting of a gabbroic layer or body, with continuous removal of the

Fig. 1.7.

Block diagram after Bridgwater and Harry (1968; Plate 3) showing their interpretation of the relations between the compositions present in the composite dykes of SW Greenland.

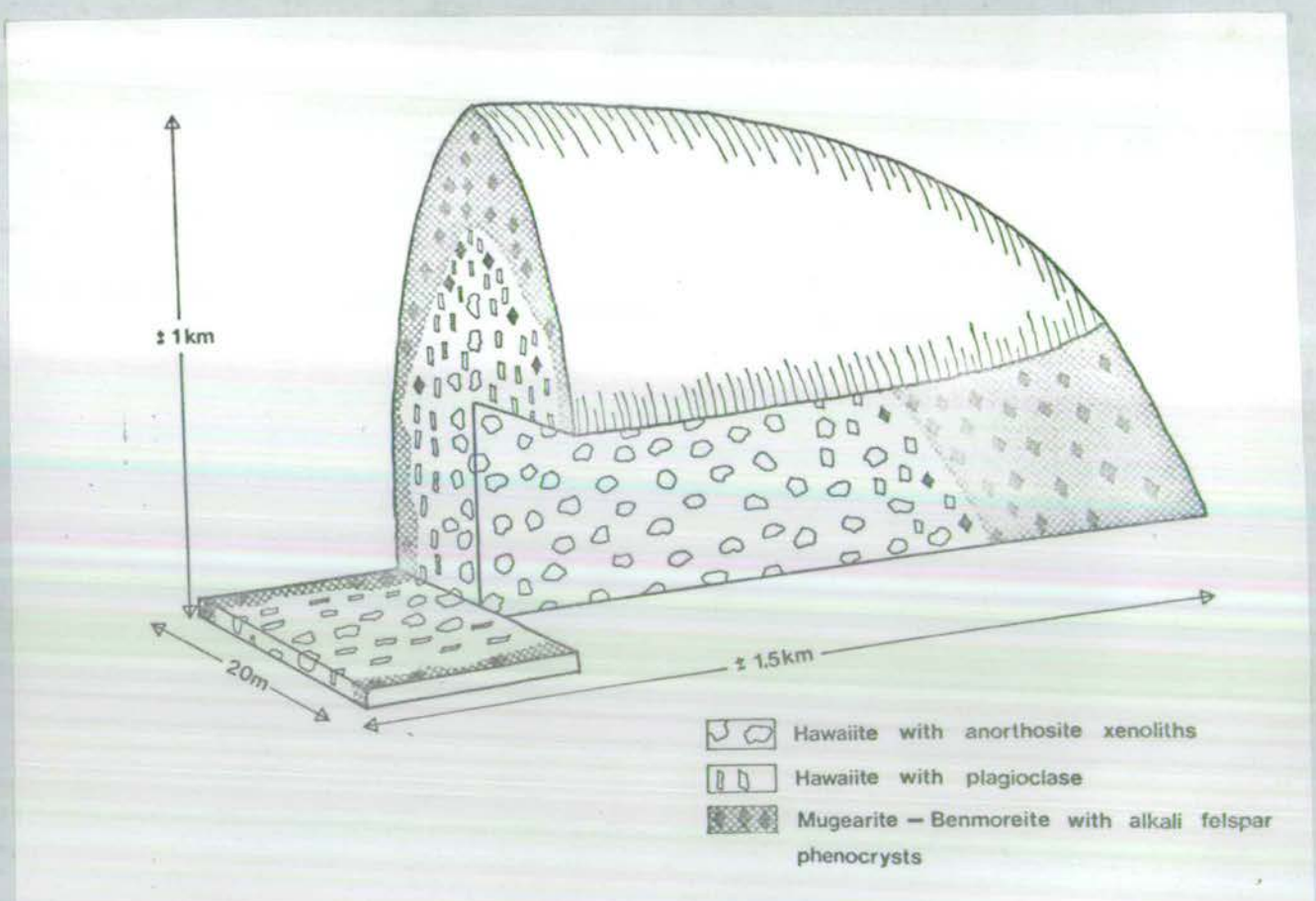

Fig. 2.7.

Block diagram after Upton and Wadsworth (1967; Fig. 5) showing the progressive influx of magma from a compositionally zoned magma chamber. Sequence of events is shown from 1 to 3.

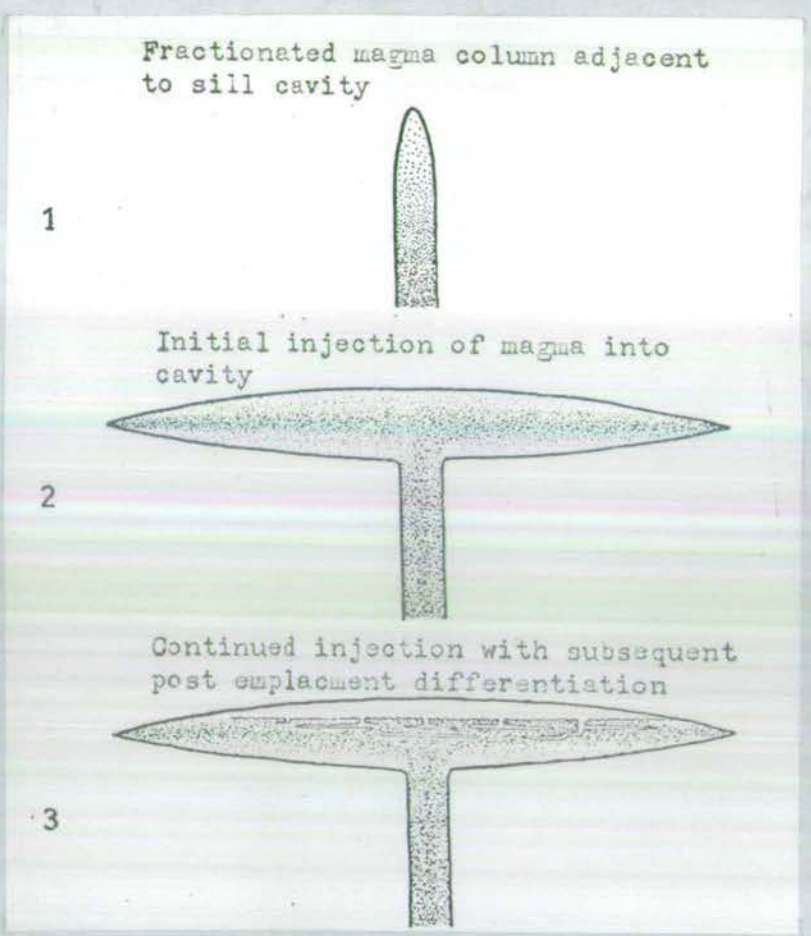

liquid would give progressively more basic magmas.

Upton and Wadsworth (1967) suggested that the gradational compositional variation found in the Bras Rouge Sill resulted from the serial tapping of progressively more basic magmas from a differentiated column of magma. The model postulated was one in which the original basaltic magma, by means of crystal fractionation, became compositionally zoned from mugearite at the top to a basalt in the lowest portions. Post-emplacement, i.e. *in situ* differentiation of the latest basaltic magma fraction produced accumulitic rocks and an alkalic residuum which injected partially solidified portions of the sill.

Baker (1968) interpreted the variation in composition and areal distribution of dykes on St. Helena as resulting from the injection of magmas contained in a single, compositionally zoned magma chamber.

Bridgwater and Harry (1968) when explaining the composite dykes of SW Greenland, envisaged magma chambers similar in form and compositional zoning to the model devised by Upton and Wadsworth in explaining the compositional nature of the Bras Rouge Sill. The composite dykes were thought to represent planar sections through these magma chambers at various erosional levels.

Bridgwater and Harry minimized crystal fractionation as a mechanism because:

(A) a series of magmas from a chamber differentiated by fractional crystallization must always follow the same sequence from least differentiated to most differentiated. Field evidence suggested the reverse was true of the Greenland

composite dykes.

(B) in conjunction with (A), the variation of K/Na does not show the increase typical of the trend found as differentiation proceeded from gabbro to syenite throughout the province, presumably a result of crystal fractionation. In contrast, K/Na ratios were variable and showed no consistent trend.

Although Bridgwater and Harry (1968, p. 136) believed the compositional trends observed in the composite dykes resulted from the interaction of crystal fractionation and a diffusion of alkalis, they did not consider crystal fractionation to be the main mechanism by which the trends were generated (p. 148). Effects not attributable directly to crystal fractionation were attributed to "liquid fractionation", a mechanism which included alkali diffusion. The details of such a mechanism had been set forth by Hamilton (1965) based partly on experimental work (Morey and Hesselgesser (1951); Orville, (1963)) and the earlier suggestions of Kennedy (1955) that alkalis and sulphides would diffuse upwards in the presence of water. Later experimental work with more complex natural systems than Orville's feldspar series did not support such a mechanism in geologically realistic times (Burnham, 1967) or as to the ratios of the elements actually diffusing (Luth and Tuttle, 1969).

The association of specific plagioclase and liquid compositions was believed to be a function of their relative densities (i.e. plagioclases found their appropriate level in a compositionally zoned chamber by flotation or sinking).

Recent hawaiite flows with phenocryst-rich upper and more nearly aphyric lower sections have been noted from the

1910 Mt. Etna flow (Kennedy, 1931) and from the Galapagos (McBirney et al., 1969) but in both instances there is no concomitant compositional change.

Although composite lava flows with compositionally as well as texturally distinct units are uncommon, composite ash-flows appear to be quite typical of certain caldera sequences (Cf. Lipman et al., 1966; Lipman, 1967) in southern Nevada and Japan. They are analogous to the composite flows described in this study in having phenocryst-rich quartz-latite upper units with nearly aphyric rhyolite lower units. The compositional gradation shows no abrupt changes; Lipman et al., (1966) suggested that the sequence erupted from a single, zoned magma chamber, derived by fractional crystallization of the observed phenocryst phases (plagioclase + clinopyroxene + alkali feldspar + biotite).

Compositional gradations without the obvious accompanying textural differences may be common within individual flows (Schminke, 1969) although detailed sampling of single flows is not often undertaken. The rapid compositional change in magmas erupted from single centres implies the existence of compositionally zoned chambers (cf. Murata and Richter, 1966; Jakobsson et al., 1973).

In summary, then, both field and chemical data support the hypothesis of compositionally zoned magma chambers. The mechanism usually held responsible is that of crystal fractionation, although other processes may also have been operative. The sequential tapping of such chambers manifests itself in the compositional gradation present in single flows, sometimes, but not invariably accompanied by variations

in the amount of phenocrysts present.

Models involving crystal fractionation alone are most easily tested, for the effect of alkali diffusion or liquid fractionation are difficult to predict quantitatively. In the next sections the possible density and viscosity differences between members of the composite flows are examined; this is followed by a review of melting data for the relevant compositions. Finally, utilizing the data provided in earlier chapters and the physical constraints imposed by the intensive properties discussed in the next few sections, a series of least-squares extract calculation models tests the extent to which fractional crystallization alone is responsible for the observed phenomenon.

Derived physical parameters of the lavas.

In all of the composite bodies studied, plagioclase is the predominant phenocryst phase, often present in proportions to the other phases that suggest preferential concentration. Two hypotheses to account for this are usually cited:
(A) Flotation of the plagioclases from less evolved, more dense magmas. (Gorbatschev, 1961; Tilley et al., 1967; Bridgwater and Harry, 1968).
(B) Difference in the settling rates of plagioclase relative to the other phenocryst phases (Cox and Bell, 1972).

The measurement of liquid densities at or near the liquidus temperatures of the compositions present in the composite bodies (ca. 1200-1150°C) is difficult. Relatively minor differences (± 1-2%) between measured values of density and values calculated by the simple relationship given below

were noted by Bottinga and Weill (1970)

$$\rho = \sum_i X_i M_i / X_i \bar{V}_i$$

where the density, ρ, is given by the mole fraction (X_i) of each oxide (i) of formula weight M_i divided by the mole fraction X_i of each oxide times the partial molar volume ($\bar{V}_i$). The calculated densities (Table 1.7) are more influenced by variations in the amount of water than by any other single component. It is not known to what extent the amounts of water measured in the rocks reflect the amounts present in the magma itself; the amounts given in the analyses (Appendix A) usually exceed the theoretical limit of saturation (Hamilton et al., 1964) or the average for recently erupted alkali-rich basalts (Moore, 1970). The analyses report only H_2O^+ (i.e. H_2O above 110°C); it is the opinion that H_2O^- represents water contents higher than that normally present in magmas (Moore, 1970; Swanson and Fabbi, 1973).

The density calculations utilize the amount of H_2O^+ reported in Appendix A; where this value exceeds that (0.9% H_2O) given by Moore (1970), the density will probably lie between that calculated as hydrous and anhydrous magmas. Figures 4.7 (Talisker) and 5.7 (Greenock) illustrate the variation in calculated densities for two flows sampled in detail.

Plagioclase densities were calculated from the unit-cell data of Table 5C (Appendix C), the analyses of Appendix C and the thermal expansion data for a calcic labradorite (An_{62}) given by Stewart et al. (1966) according to the relationship:

$$\rho = C \Sigma A/V$$

Fig. 3.7.

Observed and calculated distribution of phenocrysts in the upper (porphyritic) unit of the Talisker composite flow. Curves (b) and (c) are based on curves given in Grey and Crain (1969) Fig.2 and making the simplifying assumptions of: (a) initially homogeneous phenocryst distribution after emplacement, and (b) the phenocrysts are of the same size and their settling velocity is independent of height above the lower boundary of the porphyritic unit.

The curves are:

a = observed phenocryst distribution

b = mean settling velocity of 0.6×10^{-5} cm/sec.

c = mean settling velocity of 0.3×10^{-5} cm/sec.

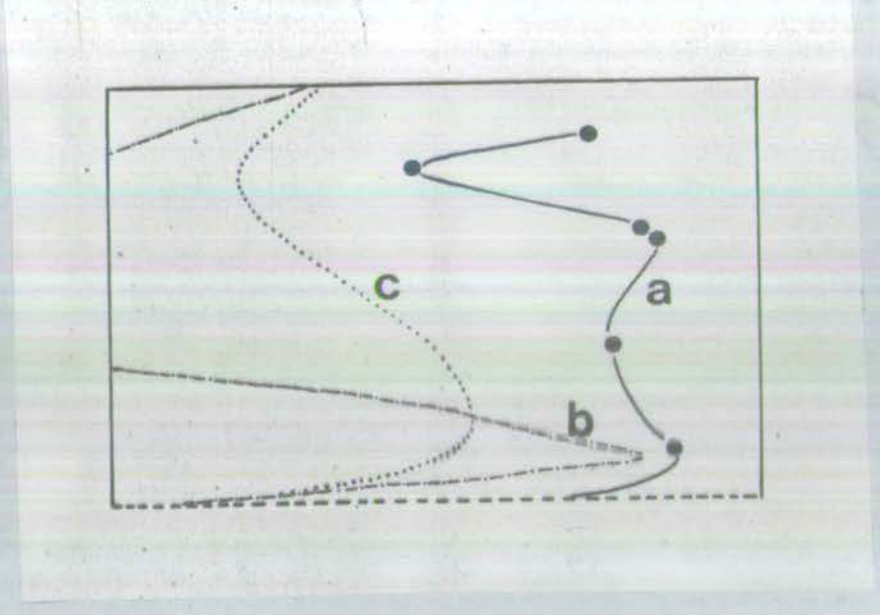

Fig. 4.7.

Calculated densities for the Talisker composite flow near the liquidus temperatures given by Tilley et al., 1965; 1967, and Thompson, 1972.

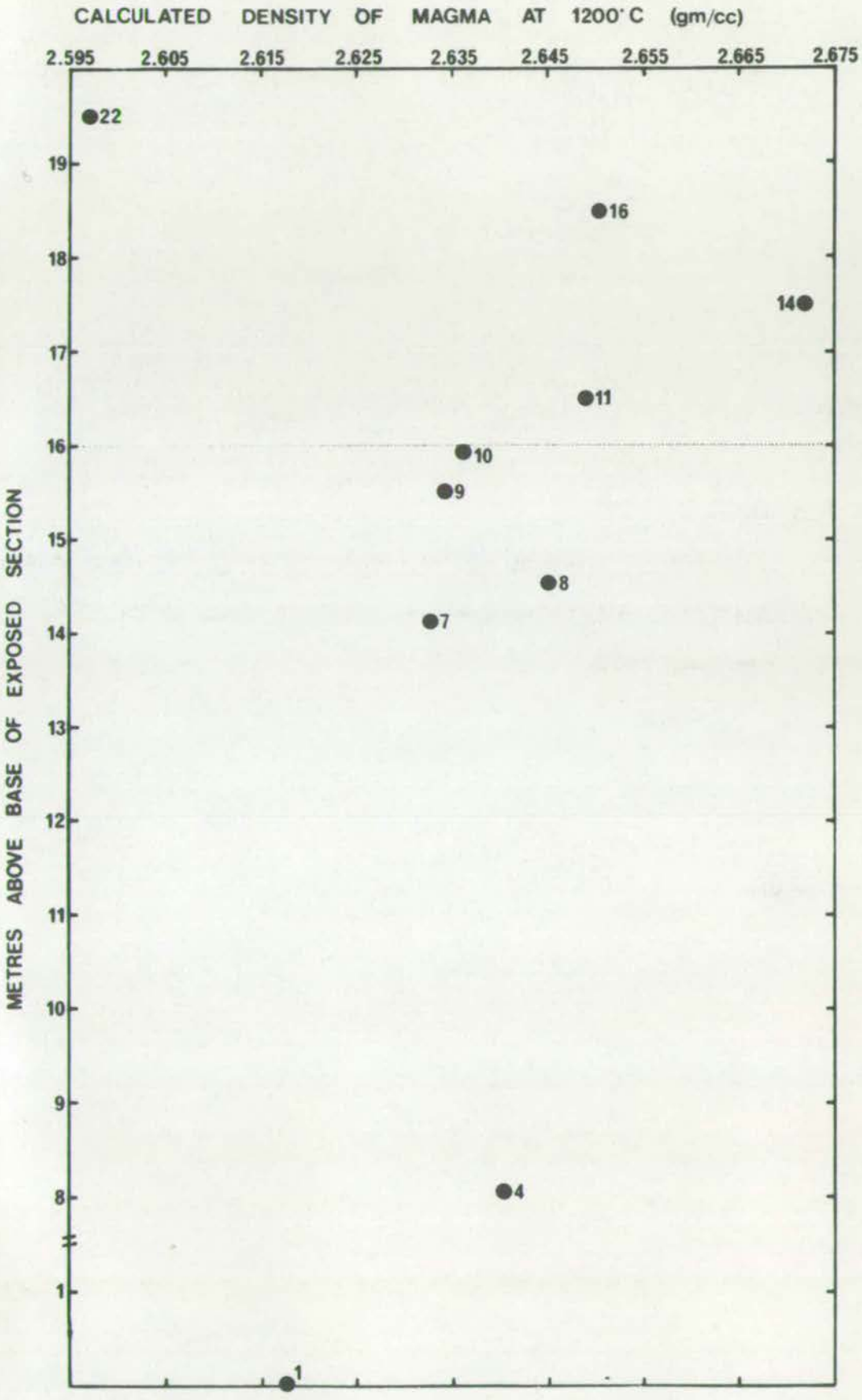
CALCULATED DENSITY OF MAGMA AT 1200° C (gm/cc)
2.595
2.605
2.615
2.625
2.635
2.645
2.655
2.665
2.675
METRES ABOVE BASE OF EXPOSED SECTION
19
18
17
16
15
14
13
12
11
10
9
8
1
22
16
14
11
10
9
8
7
4
1

Fig. 5.7.

Calculated densities for the Greenock composite flow, assuming the liquidus temperatures to be similar to those of N. Skye hawaiites and mugearites given by Tilley et al., 1965, 1967; Thompson, 1972.

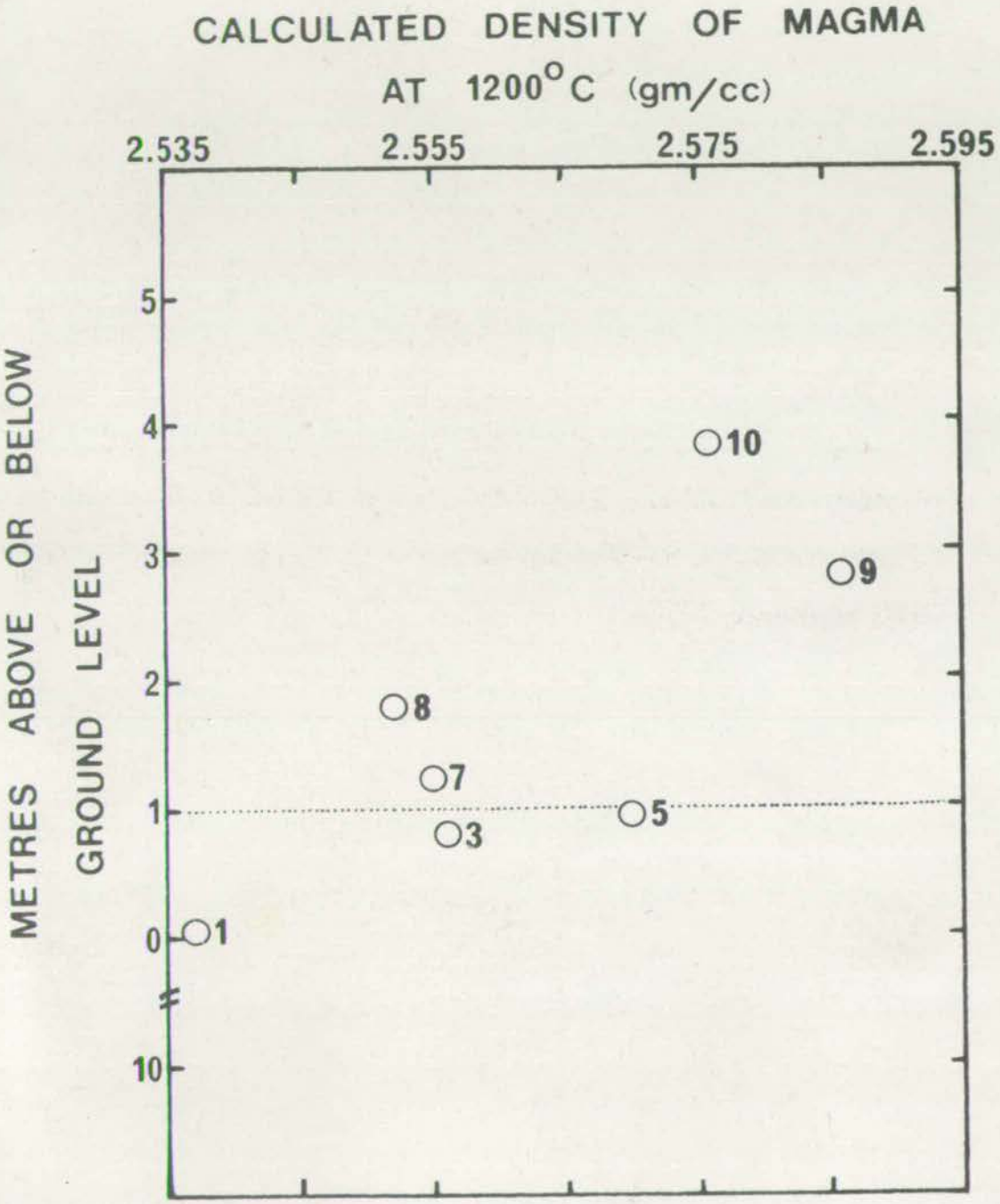
CALCULATED DENSITY OF MAGMA
AT 1200°C (gm/cc)
2.535
2.555
2.575
2.595
METRES ABOVE OR BELOW
GROUND LEVEL
5
4
3
2
1
0
10
10
9
8
7
5
3
1

KEY TO TABLE 1.7

Column A : Analysis Number and relevant Table Number in Appendix A.

Column B : Calculated Density

Column C : Calculated Density for anhydrous magma

Column D : Calculated Density for magma with Fe as FeO

Column E : " " " " at 1 kb.

Column F : " " " " " 2 kb.

Column G : " " " " " 5 kb.

Column I : Rock type

The first row for every specimen gives the calculated density at 1200°C; the second row gives the calculated density at 1150°C.

TABLE 1.7

Calculated Densities of Magmas
At or Near Liquidus Temperatures

	A	B	C	D	E	F	G	H	I
1	1A	2.617	2.751	2.638	2.635	2.642	2.655	2.668	AKB
	"	2.626	2.776	2.648	2.644	2.650	2.664	2.676	
4	"		2.635	2.653	2.622	2.629	2.642	2.655	H
	"		2.643	2.661	2.630	2.636	2.649	2.662	
7	"		2.630	2.648	2.618	2.624	2.637	2.650	"
			2.638	2.657	2.625	2.631	2.644	2.657	
8	"	2.643	2.733	2.655	2.625	2.631	2.644	2.657	"
		2.650	2.756	2.663	2.632	2.639	2.652	2.664	
9	"	2.632		2.641	2.622	2.628	2.642	2.654	"
		2.640		2.649	2.630	2.636	2.649	2.662	
10	"	2.638		2.647	2.631	2.637	2.650	2.663	"
		2.646		2.655	2.639	2.645	2.658	2.671	
11	"	2.648	2.666	2.666	2.633	2.639	2.653	2.666	"
		2.656	2.674	2.674	2.641	2.647	2.660	2.673	
13	"	2.616		2.644	2.586	2.592	2.605	2.617	"
		2.624		2.652	2.593	2.599	2.612	2.624	
15	"	2.662		2.672	2.656	2.662	2.676	2.639	"
		2.670		2.680	2.663	2.669	2.683	2.696	
16	"	2.652		2.672	2.637	2.643	2.651	2.670	"
		2.660		2.680	2.645	2.651	2.664	2.677	
22	"	2.578	2.672	2.597	2.566	2.572	2.585	2.597	"
		2.586	2.694	2.605	2.574	2.579	2.592	2.604	
3	1B	2.473	2.611	2.496	2.509	2.514	2.527	2.539	M
		2.481	2.630	2.503	2.515	2.521	2.533	2.545	

	A	B	C	D	E	F	G	H	I
7	1B	2.575	2.670	2.586	2.568	2.574	2.587	2.599	H
		2.581	2.690	2.593	2.575	2.581	2.594	2.606	
12	1B	2.566	2.690	2.587	2.580	2.586	2.599	2.611	H
		2.574	2.712	2.596	2.587	2.593	2.606	2.618	
23	1C	2.419		2.443	2.410	2.415	2.427	2.437	B
		2.426		2.450	2.417	2.422	2.433	2.444	
4	1D	2.381		2.390	2.418	2.423	2.434	2.445	B
		2.389		2.398	2.424	2.430	2.441	2.452	
5	"	2.545		2.557	2.601	2.607	2.621	2.633	B
		2.554		2.566	2.609	2.615	2.629	2.641	
17	"		2.380	2.388	2.455	2.461	2.473	2.484	B
			2.388	2.396	2.461	2.467	2.479	2.490	
18	"		2.313	2.320	2.593	2.599	2.613	2.626	H
			2.326	2.333	2.608	2.608	2.622	2.634	
19	"		2.469	2.485	2.529	2.535	2.547	2.559	H
			2.478	2.495	2.537	2.543	2.555	2.567	
1	1E	2.537	2.609	2.546	2.515	2.521	2.533	2.545	M
		2.544	2.630	2.554	2.522	2.528	2.540	2.552	
3	"	2.556		2.567	2.524	2.529	2.543	2.553	H
		2.563		2.575	2.531	2.537	2.549	2.561	
6	"	2.570		2.583	2.540	2.546	2.558	2.570	H
		2.576		2.590	2.547	2.553	2.565	2.577	
10	"	2.555		2.567	2.547	2.553	2.565	2.577	
		2.563		2.574	2.554	2.560	2.573	2.584	
12	"	2.552		2.564	2.538	2.544	2.557	2.568	H
		2.559		2.571	2.545	2.551	2.564	2.575	
15	"	2.586	2.656	2.603	2.553	2.559	2.572	2.584	H
		2.593	2.678	2.610	2.561	2.566	2.579	2.591	

	A	B	C	D	E	F	G	H	I
17	1E		2.530	2.542	2.543	2.549	2.562	2.574	H
			2.538	2.550	2.551	2.556	2.569	2.581	
1	1H		2.402	2.430	2.467	2.473	2.485	2.496	H
			2.410	2.439	2.474	2.480	2.492	2.503	
2	"	2.443	2.584	2.467	2.484	2.489	2.501	2.513	H
		2.452	2.606	2.475	2.491	2.496	2.508	2.520	
6	"		2.543	2.582	2.530	2.536	2.548	2.560	H
			2.550	2.589	2.537	2.542	2.555	2.566	
7	"		2.569	2.611	2.559	2.565	2.578	2.590	H
			2.577	2.619	2.566	2.572	2.584	2.596	
8	"		2.595	2.619	2.595	2.601	2.614	2.626	H
			2.602	2.627	2.602	2.608	2.621	2.633	
11	"		2.673	2.738	2.650	2.656	2.670	2.683	AKB
			2.680	2.746	2.656	2.663	2.676	2.689	
13	"	2.585		2.594	2.509	2.515	2.527	2.538	H
		2.591		2.601	2.516	2.522	2.534	2.545	

TABLE 2.7

Calculated viscosities ca. 1200°C and settling rates for phenocrysts of observed size range in hawaiites and mugearites

Mineral	Radius (cm)	Density of mineral	Magma type	Density (gm/cc.)	Viscosity (poises)	Settling rates for observed phenocrysts (cm/sec.$\times 10^{-3}$)
Plagioclase	0.8	2.65-2.67	H	2.578-2.662	2000-3000	6.41 - 0.04
"	"	" "	M	2.473-2.537	8000-2 x 10^4	3.08 - 0.079
Olivine	0.03	3.4 - 3.5	H	2.578-2.662	2000-3000	0.008 - 0.003
"	"	" "	M	2.473-2.537	8000-2 x 10^4	0.02 - 0.009
Titanomagnetite	0.03	5.2 - 5.4	H	2.578-2.662	2000-3000	0.26 - 0.16
"	"	" "	M	2.473-2.537	8000-2 x 10^4	0.03 - < 0.01

The higher settling rates in hawaiites for the phases suggests that concentration of the plagioclases in the hawaiites is either mechanical, or the density and/or viscosity of the mugearites in the compositionally zoned column is significantly decreased by a higher volatile content.

The higher settling rates for the phases in the hawaiites suggests that either:

(a) concentration in the hawaiites is a mechanical effect (cf. Komar, 1972); or

(b) increased volatile content in the compositionally zoned chamber near the top has decreased the viscosity below that calculated, and this has been lost during eruption.

where A = molecular weights of the individual elements, V is the volume in $Å^3$ and C is a constant usually given as 1.6620 (Henry et al., 1960). The difference between measured and calculated densities for the phenocrysts are usually less than 10%.

The viscosities of the magmas can be estimated by two different methods:

(A) Utilizing the chemical data in a fashion similar to that used in calculating the densities (Bottinga and Weill, 1972; Shaw, 1972) by the so-called Arrhenius mixture relationship

$$\ln \bar{\eta} = \sum_{i=1}^{n} X_i \ln \eta_i$$

where $\bar{\eta}$ is the viscosity in poises of the mixture and η_i is the characteristic viscosity contribution of component i of mole fraction X_i. A simplification made by relating viscosity to composition with the index R = O/(Si + Al + P), or the ratio of non-bridging oxygens to network-forming cations (Scarfe, 1973) gives comparable results.

(B) making assumptions about the rate of cooling in the composite body and the initial distribution of phenocrysts within the porphyritic unit.

The first method has given results within ± 2% of measured values for basalts and andesites (Bottinga and Weill, 1972; Shaw, 1972). The simplifying assumption that there is a unique temperature-viscosity relation that is a function of composition may be satisfied within a temperature range of 1700-1200°C. Extrapolation to temperatures below this may seriously underestimate the viscosity. Shaw's (1972) data

suggest that below 1200°C the viscosity rises rapidly, as the rheological nature of the magma changes (Shaw, 1969). Extrapolation of Shaw's data to temperatures of ca. 1100°C gives viscosities of 2000-3000 poises. Dr. G.P.L. Walker (pers. comm., 1969) estimated the viscosity of a recently erupted hawaiite flow on Mt. Etna as close to 3000 poises, so that the extrapolation of data on Shaw's diagram is probably correct to within an order of magnitude.

The density and viscosity data in Tables 1.7 and 2.7 have been utilized in Stoke's equation for the settling velocity of a sphere:

$$V = 2gr^2(\Delta\rho)/9\eta$$

where g = acceleration due to gravity, assumed here to be 980 cm./sec.^{2}

r = radius of the sphere

$\Delta\rho$ = density difference between magma and fractionating phase

η = viscosity in poises.

The correction to settling velocities for shapes other than spheres may be made with the data of McNown and Malaika (1950) as -7 to -10% for the calculated velocities. Table 2.7 presents data for mineral settling velocities, using the measured diameters of phenocrysts.

Viscosities estimated by the second method for the composite flows at Talisker and Greenock represent post-extrusive, maximum viscosities obtaining in the flows. If it is assumed that the distribution of phenocrysts in the upper porphyritic unit was homogeneous, then the present distribution (Fig. 3.7) is similar to the curves given by

Grey and Crain (1969) for low setting velocities. Their equations have been used to calculate the curves in Fig. 3.7, and are shown with the measured phenocryst distribution. Although the viscosities obtained by this second method are too high to model accurately the conditions prevailing in a subsurface magma chamber, they do allow some assessment of post-extrusive phenocryst movement. Locally, as at Roineval, it was noted that the underlying mugearite had a considerable volume (15%) of phenocrysts. It may be that the flow was thicker here than in the other exposures at Talisker and Drum na Criche. At Greenock, it seems probable that the scarce, more calcic phenocrysts present sank from the overlying porphyritic unit after extrusion.

Melting experiments

Data from melting experiments on alkali-olivine basalts, hawaiites, mugearites and benmoreites from N. Skye have been presented by Tilley et al. (1965; 1967), Thompson (1972) and Thompson et al. (1972). These data are summarized in Table 3.7. Thompson's (1972) and Thompson et al.'s (1972) data show a significant difference both in the appearance of phases and liquidus temperatures. Thompson (1972) attributes this to a difference in experimental technique. The experimental charges of Tilley et al. (1965,1967) showed evidence of intense reduction, reducing of the oxygen fugacities and resulting in a general reduction of liquidi temperatures as well as a reversal of the appearance of clinopyroxene and olivine. The fusion temperature of magnetite was not noted in Tilley et al.'s data; Thompson (1972) and

TABLE 3.7

Rock Type[1]	Fusion temperatures (°C) of major phases	Reference[2]
AKB	Ol(1265), Pl(1180), Cpx(1175)	1
"	Ol(1332), Pl(1194), Cpx(1168), Mt(ca.1115)	3
"	Ol(1315), Pl(1194), Cpx(1160), Mt(ca.1120)	3
"	Ol(1267), Pl(1194), Cpx(1160), Mt(ca.1135)	3
"	Ol,Pl(1201), Cpx(1138) Mt(ca.1135)	3
" "	Pl(1201), Ol(1188), Cpx(1138), Mt(ca.1170)	3
"	Pl(1196), Ol(1184), Cpx(1136), Mt(ca.1150)	3
H	Plag(1245), Cpx(1180), Ol(1115)	2
H(groundmass of above)	Plag(1180), Cpx(1160), Ol(1115)	2
H	Plag(1170), Cpx(1165), Ol(1160)	2
H	Plag(1165), Cpx(1150), Ol(1130)	2
H	Plag(1130), Cpx,Ol(1090)	1
H	Pl(1193), Ol(1168), Cpx(1128), Mt(ca.1193)	3
H	Pl(1184), Ol(1152), Cpx(1119), Mt(>1120)	3
H	Pl(1168), Ol(1139), Cpx(1092), Mt(>1220)	3
M	Pl(1130), Cpx,Ol(1090)	1
M	Pl(1180), Ol(1130), Cpx(1088), Mt(>1220)	3
M	Pl(1171), Ol,Cpx(1104), Mt(ca.1210)	3
M	Pl(1140), Ol,Cpx(1103), Mt(>1165)	3
B	Pl(1110), Cpx(1100), Ol(1090)	1
B	Cpx(1090), Pl(1060), Ol(1055)	2
B	Pl(1131), Cpx(1092), Ol(1073), Mt(>1165)	3

1. AKB = alkali-olivine basalt; H = hawaiite; M = mugearite; B = benmoreite.

2. 1 is Tilley et al., 1965; 2 is Tilley et al., 1967; 3 is Thompson et al., 1972.

Thompson et al. (1972) note the approximate appearance of magnetite, acknowledging that the fo_2 is not necessarily the equilibrium one for the compositions concerned. In view of the lack of control of the oxygen fugacities for Tilley et al.'s (1965, 1967) data, the following brief general summary uses only the data of Thompson (1972) and Thompson et al. (1972).

(A) alkali-olivine basalts have silicate liquidi temperatures ranging from 1267 to 1194°C with olivine followed by plagioclase (ca. 1190°), clinopyroxene (1175 to 1138°).

(B) hawaiites have silicate liquidi temperatures of 1193° to 1168° with plagioclase or plagioclase + magnetite followed by olivine (1168° to 1139°) and clinopyroxene (1128°-1092°).

(C) mugearites have silicate liquidi temperatures of 1180° to 1140° with plagioclase followed by olivine or olivine + clinopyroxene (1130° to 1090°)

(D) benmoreite has a silicate liquidus temperature of 1131° (plagioclase) followed by clinopyroxene (1092°) and olivine (1073°).

Thompson (1972) noted that as the suite of lavas becomes iron enriched, then:

(A) the magnetite phase field appears to expand, suggesting that fo_2 fell less rapidly than in a closed system.

(B) the delayed appearance of a Ca-rich clinopyroxene may result from fractionation of a clinopyroxene at high pressures.

(C) the difference in fusion temperatures of plagioclase and olivine in anhydrous melts believed on petrological evidence to precipitate together (with magnetite), could be reconciled with the natural system if the magma contained an appreciable P_{H_2O}.

The projection of intermediate members of the alkali-olivine basalt-trachyte suite into the simplified basalt tetrahedra systems of Yoder and Tilley (1962), Coombs (1963) or O'Hara (1968) as an aide in depicting the evolution of liquids is not justified since the liquids are not in equilibrium solely with Ol + Plag + Cpx + Opx but with magnetite as well. They should not be considered as liquids of low variancy but as liquids lying in zones ("piercing zones") that are the loci of liquids parental to more evolved compositions.

Fractional Crystallization models

Of the several mechanisms suggested in the introductory section, that of fractional crystallization is the most easily tested. The general model first tested is one of a magma chamber, compositionally zoned, narrow enough to inhibit convectional mixing, although this may occur within the individual, compositionally similar layers. The technique utilized in this study, that of linear regression or least squares models, treats all the data in a systematic fashion. Discussions of the petrological uses of this type of analyses are given by Greenwood, 1967; Bryan et al., 1969; Wright and Doherty, 1970; Grey, 1973 and Reid et al., 1973.

The basic assumption made is that the rock analyses approximate a liquid composition which may be represented by a linear combination of the constituent minerals. Evaluation of the quantitative difference between two liquid compositions, assumed to be genetically related, in terms of the observed and probable phases fractionated relies on the data presented

in mineralogy for the phenocryst assemblages; no constraints on the models are placed by the ratios in which these phases occur within the individual units.

The computer program used is the one described by Wright and Doherty (1970) modified by D.J. Humphries for use with the facilities available at the Edinburgh Regional Computing Centre. The data input is the weight percent of oxides for the possible parent-daughter liquid compositions, as well as the observed phenocryst phases. Additional phases, observed in compositionally similar suites are added one by one, to give an optimal solution. Conversely, if one of the observed phenocryst phases contributed nothing to the optimal solution, it is discarded. The solution arrived at gives the amounts of the daughter composition plus the amounts of the fractionating phases necessary to best approximate the parent composition. The perfect solution to this series of linear equations describing liquid and mineral compositions would result in no difference between this ideal combination of daughter and phenocryst phases and the possible parent composition; the difference between the ideal and observed model is given as the residual sum of squares of the differences between the oxides in the two models. It is this, the sum of squares of the residuals, that is the usual criterion by which the validity of the model is judged.

Even when all the fractionating phases in the model have been analyzed, evaluation of the model by the optimization criterion of a minima in the residuals is difficult. A significant part of the discrepancies in the various models may be attributed to:

(A) the degree of analytical precision, as well as the variability, particularly of the trace elements, in the rocks taken as representing the parent-daughter pairs.

(B) Fractionation systems that are open rather than closed.

(C) The probability that both of the compositions believed to be genetically related has undergone further modification since the initial fractionation event.

Although fractional crystallization models do successfully explain the compositional association of the composite bodies, they do not exclude the presence of other processes such as volatile transfer. What is implied is that it is the main mechanism responsible for the generation of such bodies. The derivation of individual composite bodies are discussed below; derivation of compositionally analogous individual flows is discussed last, with a review of other possible fractionation schemes and mechanisms.

North Skye

All three composite flows have the phenocryst assemblage plagioclase + olivine + titanomagnetite, although, as noted in Mineralogy, the composition of the individual phases is different. The composite flow at Talisker is unique in that it contains scarce hercynite and andesine phenocrysts as well as showing no compositional difference between the matrices of the two units, whereas both Drum na Criche and Roineval have mugearitic lower units.

Talisker

Although there is little compositional difference between the two units, SiO_2, Al_2O_3, CaO, and Na_2O showed

more variation in the upper unit; there was a relative (to the lower unit) depletion in Sr, which could be explained by ca. 5% fractional crystallization of plagioclase.

If it is assumed that the immediate parental liquid for the hawaiite is an alkali-olivine basalt, fractionation of the observed phenocryst assemblage plagioclase (An_{52}) + olivine (Fo_{55}) + titanomagnetite should yield hawaiite, as observed in compositionally analogous suites (cf. Zielinski and Frey (1970), Hughes and Brown (1972)), and assumed to be a low pressure fractionation event. No combination of these phases does, in fact yield hawaiite of the observed composition (Table 4.7).

The presence of hercynite and andesine phenocrysts is suggestive of at least one other step in a fractionation sequence from alkali-olivine basalt to hawaiite. Analogous assemblages in compositionally similar suites elsewhere (Binns et al., 1970; Wilkinson and Binns, 1969) have been interpreted as cognate xenocrysts from higher pressure fractionation events. It has been shown (Coombs and Wilkinson, 1969; Zielinski and Frey, 1970) that low pressure fractional crystallization can produce differentiates of hawaiite from alkali-olivine basalt, but the presence of lherzolite xenoliths and possible cognate xenocrysts has led many workers to emphasize the importance of high pressure fractionation events leading to the same sequence of compositions (Binns et al., 1970; Thompson, 1973; Wright, 1968).

Binns et al. (1970) suggested on the basis of limited experimental data that the liquidus or near liquidus plagioclases for alkali basaltic compositions would become more sodic at higher pressures, an effect possibly enhanced by

TABLE 4.7

Bracketed numbers refer to analyses used and relevant Table numbers

Model	Compositions involved		Parent and amount	Composition and amount of fractionating phases					Residuals
				Plag	Cpx	Magnetite	Ol	other	
Talisker 1	AKB	H	AKB	An52	(1;1.3)	(4;1.2)	(2;1.4)	hercynite	
			1.407	-	0.331	-	-	.0766	7.336
2	AKB	H	AKB	An55	Al-cpx[1]	(4;1.2)	(2;1.4)		
			4.3394	1.409	1.408	0.4433	0.1322		0.739
um na Criche	H	M	H	An49	(1;1.3)	(8;1.2)	-		
			1.8462	0.5294	0.1733	0.1435			0.722
oineval	H	M	H	An55	(1;1.3)	(8;1.2)	(4;1.4)		
			1.563	0.3826	0.0492	0.04203	0.08892		0.361
Dasses	AKB	H	AKB	An51	(9;1.3)	(8;1.2)			
			1.8954	0.3400	0.3810	0.1744			0.623
St.Leonard's	AKB	central facies	AKB	An51	(8;1.3)	(8;1.2)			
			1.4833	0.2513	0.1455	0.0865			0.395
Greenock flow	H	M	1.2416	An63	(10;1.3)	(8;1.2)			
			1.2416	0.1045	0.0874	0.0497	-		0.367
Greenland dyke	H	M	H	An45	(13;1.3)	(8;1.2)	Fa 52	apatite	
			2.6503	1.0734	0.2258	0.0813	0.1972	0.0726	1.107
Reunion 1	H (5,3;1H)	M	H	An45	(14;1.3)	(12;1.2)			
			2.0755	0.5291	0.3968	0.1496			1.047
2	AKB (9,8;1H)	H	AKB	An78	(14;1.3)	(12;1.2)			
				0.2190	0.1630	0.0994			2.108
General Fractional Crystallization Models									
Midland Valley	AKB	H	AKB	An63	Al-cpx[1]		(7;1.4)		
			1.127	0.003	0.1019	-	0.02502		2.29817
	H	M	H	An55	(9;1.3)	(8;1.2)			
			2.520	0.7697	0.5852	0.1651			2.536
North Skye	M	B	M	An44	(4;1.3)	(8;1.2)	Fa 52	apatite	
			1.732	0.4969	0.0329	0.0909	0.0892	0.0222	0.787

[1]Aluminous clinopyroxine megacryst (Binns et al., 1970; Analysis 1 (WA9); Table 4)

TABLE 4.7 (contd.)

	Ba		Sr		Rb		Zr		Zn		Y	
	obs.	cal.	obs.	cal.	obs.	cal.	obs.	cal.	obs.	cal.	obs.	cal.
Talisker 1	156	142	390	442	6	9	176	137	84	81	35	31
2	156	72	390	490	6	3	176	84	84	74	35	17
Drum na Criche	966	813	606	571	22	28	312	271	100	82	25	35
Roineval	743	633	693	740	20	22	283	212	91	71	38	35
Greenock	608	507	546	478	44	48	289	269	114	111	26	23
Greenland Dyke	1309	1193	764	1143	48	25	297	260	193	92	33	35
Reunion 1	449	342	599	429	45	34	289	199	80	61	45	31
2	292	379	612	570	24	21	152	115	60	51	29	24
					General Models							
Midland Valley 1	848	752	666	591	52	46	207	184	119	106	37	33
2	General model based on T.C.Day's (1930) analyses.											
North Skye	1252	1185	594	650	44	37	366	350	111	78	57	37

The Dasses and St.Leonard's Sill use a parental composition similar to an alkali olivine basalt thought by Clark (1956) to be parental to the lavas of Arthur's Seat.

Data used for Ba, Sr, Rb, are from separated feldspars (N.Skye, Greenock, Greenland), others use data from Cotlett and Ribbe (1967). Data for ZR, Zn, Y, are based on Walker's (1969) data for mineral separates of the Palisades Sill and are intended as very rough guides.

the entry of the anorthite component to enter clinopyroxene as Ca-Tschermak's molecule. Experimental data is also scarce on the composition of spinel appearing in basaltic compositions at high pressures; Binns et al. (1970) suggest that for spinel to be preserved undersaturation (with respect to silica) is necessary. If an aluminous clinopyroxene is an additional liquidus phase, thus enriching the residual liquid in silica, a level of undersaturation equivalent to that of a basanitic liquid is necessary (ca. 10% normative ne) or else the spinel would react with the liquid to yield aluminous orthopyroxene or enrichment of $Mg_2Si_2O_6$ - $MgAl_2O_6$ in subcalcic clinopyroxene.

Inclusion of an aluminous clinopyroxene (Binns et al., 1970 Analysis No. 1 (WA9)) significantly reduces the residuals (Table 4.7).

Several reasons for the discrepancies are advanced; it seems probable that the sequence of liquids generated in passing from alkali-olivine basalt to hawaiite were generated by polybaric fractionation in a system that was very probably open rather than closed. It seems reasonable to suggest that all of the phases participating in the sequence have not been observed in this one composite flow, but that by utilizing data from other, compositionally analogous flows, a more complete sequence may be adduced.

The plagioclase utilized in the model (An_{55}) is only slightly more calcic than the phenocrysts observed (An_{52}). The latter commonly show evidence of resorption, commonly, but not invariably, with subsequent growth on the ovoid cores.

Hawaiites in the Drum na Criche and Roineval composite flows include plagioclases that are slightly less calcic in composition but typically lacking the distinctive ovoid form. These (Talisker) phenocrysts could represent a sequence of higher pressure fractionation events, resorbed and jacketed by more calcic plagioclase rims in a lower pressure environment, and finally rimmed by more sodic plagioclase in the present low T.P. environment. This hypothesis would still necessitate the fractionation of at least equally large amounts of a very calcic bytownite, which is, again, not observed.

Wilkinson and Binns (1969) have suggested that at least some hawaiites originate in the upper mantle, on the basis of their interpretation of the origin of the phenocrysts found in hawaiites near Kyogle, N.S.W. Aoki (1969) interpreted the presence of similar assemblages of andesine, aluminous clinopyroxene, spinels, orthopyroxene and kaersutite as cognate xenocrysts that crystallized from an alkali-olivine basalt at depths of 30-60 km.

Thompson (1972) on the basis of the ubiquitous compositional gap between basalts and hawaiites suggested that most hawaiites originate at upper mantle depths, and not in high level, sub-volcanic magma chambers.

The model suggested for the flow at Talisker involves fractionation of an aluminous clinopyroxene, spinel and andesine, at depths of 30-60 km. The absence of aluminous clinopyroxenes, but presence of spinel and andesine implies that the latter two phases fractionated at higher levels. Polybaric fractionation of both the hawaiite and alkali-olivine basalt during their ascent could explain the residuals in the least squares models.

Drum na Criche

Although no clinopyroxene occurs as phenocrysts, a satisfactory model necessitates its fractionation (Table 4.7); conversely, olivine, although present as scarce microphenocrysts, is not utilized as a fractionating phase in the model. Assuming that the groundmass clinopyroxene in the Talisker flow approximates a composition on a clinopyroxene compositional trend analogous to that followed in the hawaiites of Drum na Criche, this has been used to model the possible fractionating clinopyroxene.

The residuals for the different oxides are well within the estimated analytical error. Since apatite was not observed as a phenocryst phase, one possible indicator that the parent:daughter ratio is a reasonable estimate is the insignificant difference between the calculated and observed P_2O_5. It should be noted, however, that the analytical precision of P_2O_5 determinations at this level is approximately $\pm$ 12% (relative) and that apatite has been observed as phenocrysts in compositionally analogous sequences (Coombs and Wilkinson, 1969).

The content of trace elements show discrepancies in Ba and Sr which are opposite in sign and lie outside the estimated analytical error, but are not outside the standard deviation (expressed as a percentage of the mean: 15.7% for Ba; 45.7% for Sr) for the mugearites. It is interesting that Nb does not appear to be fractionated by the magnetite; Huckenholz (1965) found that titanomagnetites in hawaiites from the Eifel district contain 350-600 ppm of Nb. Qualitative microprobe scans of titanomagnetites and ilmenites

from the composite bodies detected Nb only in ilmenite, with the level of detection estimated to be 650-600 ppm.

The contents of Zr and Zn in the titanomagnetites are averages reported by Walker (1969) for analyzed magnetites in the Palisades Sill, and are intended as rough guides only.

Roineval

The optimal solution (Table 4.7) is only attainable by fractionation of clinopyroxene, as at Drum na Criche; the same pyroxene composition is used, making the assumption that governed its choice in the Drum na Criche model. The optimal solution also utilizes olivine in contrast to the model used for Drum na Criche. The residuals lie within the precision of the analytical method. Although the difference in P_2O_5 is within these bounds, it could be indicative that the parent:daughter ratio is not correct, or that apatite was a fractionating phase, although it was not observed as such.

The most significant discrepancy in the trace elements lies in the higher calculated content of Sr, which is not accounted for by either the lack of analytical precision or variation in the mugearites.

Royal Park, Edinburgh

Data presented in previous chapters suggested that the Dasses and St. Leonard's Sill might have different origins, since:

(A) The Dasses showed little compositional or petrographic difference between the two units, whereas St. Leonard's Sill showed a basic, possibly accumulitic, core with a more evolved, nearly aphyric margin.

(B) The aluminous clinopyroxene phenocrysts of St. Leonard's Sill are compositionally distinct from those of the Dasses; their higher content of Ca-Tschermak's molecule implies crystallization at greater depth.

The model considered is one in which the serial tapping of a subadjacent magma column, with slight compositional and textural gradations would result in the successive influx of magmas that were increasingly basic. Oertel (1952) noted that the marginal facies (of a slightly more evolved composition) was later introduced by the more basic central facies.

The fractionation of phases observed in the Dasses from an alkali-olivine basalt similar in composition to that postulated by Clark (1956) as parental to the series of lavas he observed in the Royal Park shows relatively little difference, except in Na_2O and K_2O (Table 4.7) from the central facies of the Dasses.

The junction between the facies of St. Leonard's Sill is gradational over ca. 50 cm. Phenocryst content diminished steadily outwards from the central, accumulitic and more basic facies to a nearly aphyric, more evolved benmoreite facies. The disparity between analyses of the central facies (18, 19; Table 1D) implied that a compositional gradient existed as well. These data were interpreted as either <u>in situ</u> differentiation of a basaltic magma of the same composition as that involved in the evolution of the Dasses, or the rapid injection of magma from a compositionally zoned adjacent chamber. The gradual compositional and textural transition between the two units suggests the former model (Table 4.7).

The composite flow at Greenock

Fractionation of the observed phenocryst phases alone results in a model that shows minor differences between the observed and calculated compositions (Table 4.7).

The sequence of flows at Craigmarloch Wood represents part of the sequence that accords with the evidence for compositionally zoned magma chambers, but the porphyritic unit here is the more evolved. It is also the last of the two units to be emplaced. Field evidence implies a greater interval of time between the emplacement of the two units, than that between the emplacement of the units of the composite flows. Several possible explanations are advanced to explain this:

(A) increasing viscosity in the benmoreite due to periodic rupture of the chamber cupola with consequent escape of volatiles. This is not likely in view of the field evidence which suggests that the benmoreite had a low viscosity.

(B) nearly simultaneous eruption and emplacement of magmas from adjacent chambers. More likely than (A) in view of the time lag between emplacement of the two units and possible misinterpretation of poor exposures of the precise relation.

Neither explanation is wholly satisfactory.

S.W. Greenland

A crystal fractionation model (Table 4.7) satisfactorily explains the derivation of the marginal facies (Analysis 18;1G)

from the central facies (22; 1G) utilizing the phenocryst assemblages analyzed in this suite of samples (19-22) from one dyke. Analyses of olivines and titanomagnetites, which are present as pseudomorphed phenocrysts were taken from the analyses of these minerals in the hawaiite of the Roineval composite flow. Apatite is assumed to be stoichiometric. These compositions are believed to be reasonable extrapolations; in any case, neither apatite, magnetitenor ilmenite fractionate in large amounts, and different compositions would produce only small deviations in the residuals. The approximation to the olivine composition is more doubtful; it was shown in Mineralogy that the olivines present in hawaiites show a wide range in composition.

Derivation of the more evolved facies (1,2; 1G) is feasible by crystal fractionation, but the discrepancy in observed and calculated trace elements is greater.

Extrapolation of this mechanism to explain the genesis of other composite dykes in the Gardar province may not be warranted on the basis of its success in explaining the genesis of one dyke. The dyke suite is, however, believed to be representative of the composite dykes of the province as represented by the analyses of Bridgwater and Harry (1968) and the present study.

There is some justification for believing that volatile transport, as exemplified by the work of Luth and Tuttle (1969) and Morey and Hesselgesser (1951) may have been operative. The difference (residuals) between the calculated and observed compositions is highest for Na_2O and K_2O; Na_2O being over-estimated and K_2O underestimated.

There is some doubt that the analyses represent very accurately the compositions of the liquids themselves. MacDonald (1968), in discussing the compositionally more evolved peralkaline dykes, considered that at least three mechanisms could realistically be considered to have modified the composition of these rocks.

(A) Preferential loss of a vapor phase

(B) Alkali loss in a fluid phase during magmatic crystallization or post-magmatic devitrification.

(C) Alkali-ion exchange in the presence of temperature gradients.

Bridgwater and Harry (1968) and Bridgwater (1967) questioned the importance of crystal fractionation as the process responsible for the trend in the Gardar dykes as a whole, primarily because the distribution of alkalis cannot be explained satisfactorily by this mechanism. In this instance it is argued that if the analyses do represent the unmodified liquid composition then crystal fractionation alone is sufficient to explain the differentiation trend.

The K_2O/Na_2O ratio may have been altered by volatile transport; the discrepancy between the observed and calculated contents is the opposite to that observed by Murata and Richter (1966) for the alkali enriched zone beneath the crust of the Kilavea lava lake.

Bras Rouge Sill

Upton and Wadsworth (1967) postulated that progressively more basic zones in a differentiated column of magma were

tapped and injected into the cavity now filled by the sill (Fig. 2.7).

The compositionally zoned magma column was believed to be narrow enough to inhibit convective mixing of the magma. The parental magma was thought to be basaltic.

Petrographic evidence suggested that the most basic rocks in the sill were, at least in part, accumulitic. There is a stepwise progression from the mugearitic margins to the most evolved liquid of hawaiite composition (i.e. from Analysis 3 to 5, Table 1H) and from this composition (5) to (8) and from (8) to (9). The difference between calculated and observed compositions becomes progressively greater (Table 5.7), suggesting that the compositions represented by analyses are not those of liquids, but, as the petrographic evidence suggests, are accumulitic rocks.

The association of hawaiite and mugearite flows that is commonly observed can also be ascribed to fractionation models similar to those proposed for the association for analogous compositions in the composite flows (Table 4.7). It suggests the existence, in certain stages of volcanic development, of compositionally zoned chambers that usually lose only part of the column, either because the gas pressure is insufficient in most instances to provide the energy for the emptying of the whole chamber, or because the increased content of phenocrysts in the lower parts of the chamber provide too viscous a liquid (cf. Komar, 1972).

Summary

Fractionation of the observed phenocryst phases alone appears adequate to explain the differentiation trends present in the Greenock composite flow only. It is necessary to postulate the fractionation of a clinopyroxene to generate the observed trends in the composite flows of Drum na Criche and Roineval, although clinopyroxene was not observed as a phenocryst phase.

Derivation of the composite flow at Talisker from a basaltic parent necessitates the fractionation of an aluminous clinopyroxene which was not observed in the composite flow. The contribution to the trend made by the observed, high pressure phenocrysts, appears to have been minimal.

The suite of composite flows studied are thought to represent part of a sequence in the generation of such bodies; the steps envisaged are:

(A) no compositional difference between the two units, which show only a textural difference generated by the settling of plagioclase phenocrysts into a liquid of increasing density, from magmas of similar composition but lower density due to the concentration of volatiles near the roof of the chamber.

(B) a distinct compositional and textural difference between the two units. The textural difference is generated by the simple mechanism proposed for (A); with the fractionation of plagioclase ± olivine +Cpx + magnetite, a compositional gradient develops in the magma chamber. The most evolved compositional unit observed in a composite flow unit is a mugearite,

but the association in composite intrusions of benmoreite, mugearite and alkali-olivine basalt suggests that such compositionally zoned magma chambers exist.

The variability of alkalis and silica observed in the mugearite and hawaiite of Drum na Criche (Fig. 1.5) are not explicable in terms of the fractionation of observed phenocrysts. It is possible that volatile transport does affect the composition of the liquids with prolonged residence time in the magma chamber.

The sequence of steps is seen as a function of residence time in a single chamber. The range in plagioclase phenocryst composition seen in the hawaiites of the composite flows as well as the range in composition of the host rock themselves may represent the sequence of compositions generated at various depths.

Two different modes of evolution are suggested for the intrusions of the Royal Park, Edinburgh.

The Dasses is best explained by the successive tapping of a compositionally zoned magma chamber. This is in accordance with the structural evidence presented by Oertel (1952) for two distinct pulses of magma. The compositional gradient in the column was apparently slight.

St. Leonard's Sill appears to represent the <u>in situ</u> differentiation of a similar basaltic parent to give a central core of basic accumulitic rocks with an envelope of

increasingly evolved compositions, the most extreme being a nearly aphyric benmoreite.

The sequence of compositions found in the composite dykes of S.W. Greenland can be derived by fractionation of the observed phenocryst phases. The rare occurrence of a chilled contact between the central and marginal facies suggests that some dykes represent the influx of liquids serially tapped from subadjacent, compositionally zoned magma chambers. The schematic model (Fig. 1.7) of Bridgwater and Harry (1968) implying that the dykes represent planar sections through such chambers is equally plausible for the majority of dykes, which display no chilled contact between facies or apophyses of the central facies in the marginal ones.

The compositional range present in the plagioclases, whether they are termed phenocrysts or cognate xenocrysts, suggests that at least several generations of phenocrysts are present. These represent at least part of the assemblage fractionated from the immediate parental liquids during their ascent. It is possible that the other phases reported by Bridgwater and Harry (1968) as megacrysts (olivine, clinopyroxene, Fe-Ti oxides) represent assemblages fractionated at higher pressures as well. In this respect they are analogous with the Talisker hawaiites which contain plagioclases not in equilibrium with their present host rock, and which may have fractionated at higher pressures. In this latter instance, however, the spinel and andesine phenocrysts give some indication of what the fractionation assemblage was.

Upton and Wadsworth (1967) explained the genesis of the Bras Rouge Sill by fractionation of the observed phenocryst

phases from a basaltic parent, resulting in a compositionally zoned magma chamber. Fractionation of the analyzed phases from hawaiite gives a reasonable approximation to the marginal mugearites. Part of the discrepancies in this simple model, as in those for the intrusions of the Royal Park, are due to the post-emplacement modification of the rocks representing the original sequence of liquids present in the parental magma chamber. The feldspars present in the marginal facies indicate that the liquids were precipitating two feldspars; fractionation of an alkali feldspar is not, however, of importance in the least squares models.

The presence of bytownite phenocrysts in the hawaiite flow of Piton des Neiges as well as in the mugearitic margins of the sill suggests that the wide range of plagioclase phenocrysts found in other hawaiites is present in the Réunion hawaiites as well.

Fractional crystallization models appear adequate to explain the differentiation trends found in composite bodies. The success of such models in deriving a series of lavas of similar composition has been shown by Zielinski and Frey (1970) for the Gough Island lavas. Derivation of individual flows, such as the sequence at North Berwick, seldom attains the low residuals found when deriving the units of a composite flow. This is especially true of that part of the sequence deriving an alkali-olivine basalt from hawaiite; it is true to a lesser extent in the steps from hawaiite to mugearite and mugearite to benmoreite. This does not imply the lack

of a genetic link; it lies rather in the possibility that hawaiites are derived from alkali-olivine basalts at a wider range of pressures than the other intermediate members of the alkali-olivine basalt-trachyte suite.

The ratios of parental to daughter liquids are difficult to estimate unless one element can be shown to be continuously concentrated in the residual liquids. Anderson and Greenland (1969) and Greenland (1970) have shown that in systems that approach the ideal "closed" system model, the ratio of P_2O_5 in the original liquid to that in the derived liquid is an effective index of differentiation, if apatite is not being fractionated. The models for the composite flows show differences between observed and calculated P_2O_5 that implies the ratio of parent:daughter liquids is nearly correct; this criterion fails, of course, for the Greenland composite dykes where apatite is being fractionated.

The discrepancies shown in the distribution of trace elements for the various models are believed to be a result of several factors:

(A) a high coefficient of variation for most trace elements resulting from the variable distribution within the flow (cf. Watkins et al., 1970) and lack of analytical precision (cf. Table A.2, Appendix A).

(B) assumption that fractionation occurs within a closed rather than open system.

Two approaches to the distribution of trace elements between the liquid and the minerals fractionated have been utilized in this study:

(A) use of published trace element contents for the minerals being fractionated and

(B) utilizing the Distribution Coefficients published by Berlin and Henderson (1968); Gast (1968); Griffin and Murthy (1969); Huckenholz (1965a); Iiyama (1968); Jensen (1973); Korringa and Noble (1971); Masuda and Kushiro (1970); Philpotts and Schnetzler (1968, 1970, 1972); Schilling and Winchester (1967, 1969) and Schnetzler and Philpotts (1968, 1969).

While the content of trace elements in minerals is variable, Jensen (1973) shows that the Distribution Coefficient varies with the composition of the mineral in a systematic fashion; this seems to be true for plagioclases, clinopyroxenes, olivine and to a lesser extent, amphiboles. Where possible, then, method (B) has been used. Method (A) was utilized primarily in dealing with the titanomagnetites.

The models are naive in that they assume fractional crystallization and not a combination of both equilibrium and fractional crystallization. The simple relationship used by Philpotts and Schnetzler (1968) to explain Eu anomalies and utilized here to estimate the extent of plagioclase fractionation is not strictly correct although it gives a useful approximation. Klusman's (1972) data suggest that after phenocrysts reach a certain limiting size, diffusion is important in controlling the distribution of certain elements. Similarly, the variability in the values given

for the Distribution Coefficient are interpreted by Albarede and Bottinga (1972) as both an imbalance between the rate of crystal growth and trace element diffusion in both lava and crystals.

Comparison of the trace element geochemistry of hawaiites, mugearites and benmoreites from several different provinces emphasizes the multimodal nature of the populations classified as single groups.

Whether this variance implies a heterogeneous source region for the parental magmas or varying degrees of partial melting in the source region followed by polybaric fractionation is difficult to say. It is probable that the hawaiites undergo variable amounts of polybaric fractionation at widely varying ascent rates since they show a variety of polybaric phenocryst assemblages. The variability in the geochemistry of the mugearites and benmoreites is seen both as a result of derivation from a heterogeneous population of hawaiites at high levels in the crust and continued fractionation of plagioclase + alkali feldspar + olivine + augite + FeTi oxides.

ACKNOWLEDGEMENTS

I wish to thank Professor F.H. Stewart for the use of laboratory and computing facilities at the Grant Institute of Geology.

I am very grateful to my supervisor, Dr. B.G.J. Upton for suggesting the problem and discussion of the work, and certainly for his patience.

M.J. Saunders, G.R. Angell and all of the staff at the Grant Institute were always helpful and it is a pleasure to acknowledge their support in the analysis and preparation of the samples and illustrations.

I also wish to thank my wife Aila for her patience during the preparation of the work.

BIBLIOGRAPHY

BIBLIOGRAPHY

ABBOTT, M.J. 1969. Petrology of the Nandewar volcano, N.S.W., Australia. Contr. Mineral. and Petrol. 20, 115-134.

ALBAREDE, F. and BOTTINGA, Y. 1972. Kinetic disequilibrium in trace element partitioning between phenocrysts and host lavas. Geochim. Cosmochim. Acta. 36, 141-156.

ALBEE, A.L., and CHODOS, A.A. 1970. Semiquantitative electron microprobe determination of Fe^{2+}/Fe^{3+} and Mn^{2+}/Mn^{3+} in oxides and silicates and its application to petrologic problems. Amer. Mineral. 55, 491-501.

ANDERSON, A.T. 1968. The oxygen fugacity of alkaline basalt and related magmas, Tristian da Cunha. Am. J. Sci. 266, 704-27.

ANDERSON, A.T. and GREENLAND, L.P. 1969. Phosphorus fractionation diagram as a quantitative indicator of crystallization differentiation of basaltic liquids. Geochim. Cosmochim. Acta. 33, 493-505.

ANDERSON, A.T. and GOTTFRIED, D. 1971. Contrasting behavior of P, Ti and Nb in a differentiated high-alumina olivine tholeite and a calc-alkaline andesitic suite. Bull. Geol. Soc. Am. 82, 1929-42.

ANDERSON, A.T. and WRIGHT, T.L. 1972. Phenocrysts and glass inclusions and their bearing on oxidation and mixing of basaltic magmas, Kilauea volcano, Hawaii. Amer. Mineral., 57, 188-216.

ANDERSON, F.W. and DUNHAM, K.C. 1966. The geology of northern Skye. Memoirs Geol. Surv. Scotland. H.M.S.O.

AOKI, K-I. 1964. Clinopyroxenes from Alkaline rocks of Japan. Am. Mineral.,49, 1199-1223.

_____ 1966. Phenocrystic spineliferous titanomagnetites from trachyandesites, Iki Island, Japan. Am. Mineral., 51, 1799-1805.

_____ 1970a. Petrology of magnetite-bearing ultramafic and mafic inclusions from Iki Island, Japan. J. Japan Assoc. Min. Pet. Econ. Geol., 64, 107-122.

_____ 1970b. Andesine megacrysts in alkali basalts from Japan. Contr. Mineral. and Petrol., 25, 284-288.

BAIRD, A.K. and WELDAY, E.E. 1969. Precision and accuracy of silicate analyses by X-ray fluorescence. Advances in X-ray Analysis, Vol. 12, Plenum Press, N.Y. 114-127.

BAKER, I. 1968. Compositional variation of minor intrusions and the form of a volcano magma chamber. Q. Jl. geol. Soc. Lond., 124, 67-79.

BAMBAUER, H.U., CORLETT, M., EBERHARD, E. and VISWANATHAN, K. 1967. Diagrams for the Determination of Plagioclases using X-ray Powder Methods. Schweiz. Min. Petr. Mitt., 47/1, 333-349.

_____ EBERHARD, E., and VISWANATHAN, K. 1967. The lattice constants and related parameters of "Plagioclase (low)". Schweiz. Min. Petr. Mitt., 47/1, 351-64.

BARBERI, F., BIZOUARD, H. and VARET, J. 1971. Nature of the clinopyroxene and iron enrichment in alkalic and transitional basaltic magmas. Contr. Mineral. and Petrol., 33, 93-107.

BARNETT, V.D. 1972. Fitting Straight Lines - the linear functional relationship with replicated observations. Applied Statistics, 21, 135-144.

BENCE, A.E. 1966. The differentiation history of the earth by Rb-Sr isotopic relationships. Unpublished Ph.D. thesis, Mass. Inst. Technology.

BENNETT, J.A.E. 1945. Some occurrences of leucite in East Lothian. Trans. Edinb. geol. Soc., 14, 34-52.

BERLIN, R. and HENDERSON, C.M.B. 1968. A reinterpretation of Sr and Ca fractionation trends in plagioclases from basic rocks. Earth and Planet. Sci. Let., 4, 79-83.

BINNS, R.A., DUGGAN, M.B. and WILKINSON, J.F.G. 1970. High pressure megacrysts in alkaline lavas from north-eastern New South Wales. Am. J. Sci., 269, 132-168.

BLAKE, D.H., ELWELL, R.W.D., GIBSON, I.L., SKELHORN, R.R. and WALKER, G.P.L. 1965. Some relationships resulting from the intimate association of acid and basic magmas. Q. Jl. geol. Soc. Lond., 121, 31-49.

BOTTINGA, Y. and WEILL, D.F. 1970. Densities of liquid silicate systems calculated from partial molar volumes of oxide components. Am. J. Sci., 269, 169-182.

BOTTINGA, Y. and WEILL, D.F. 1972. The viscosity of magmatic silicate liquids: a model for calculation. Am. J. Sci., 272, 438-475.

BRIDGWATER, D. 1967. Feldspathic inclusions in the Gardar igneous rocks of South Greenland and their relevance to the formation of major anorthosites in the Canadian Shield. Can. J. Earth Sci., 4, 995-1014.

_____ and HARRY, W.T. 1968. Anorthosite xenoliths and plagioclase megacrysts in Precambrian intrusions of South Greenland. Medd. Grøn., Vol. 185, No. 2.

BRYAN, W.B. 1970. Mineralogy of a mugearite from Clarion Island, Mexico. Ann. Rep. Geophys. Lab. Carneg. Inst. Yearbook 68, 190-194.

_____, FINGER, L.W. and CHAYES, F. 1969. Estimating proportions in petrographic mixing equations by least-squares approximation. Science, 163, 926.

BURNHAM, C.W., 1967. Hydrothermal fluids at the magmatic stage. In: Geochemistry of Hydrothermal Ore Deposits; editor, H. L. Barnes. Holt, Rinehart & Winston, Inc.

BUSSIÈRE, P. 1959. Etude Géologique de l'ile de la Réunion. Serv. Geol., Tananarive, Madagascar.

CARMICHAEL, I.S.E. 1963. The crystallization of feldspar in volcanic acid liquids. Q. Jl. geol. Soc. Lond., 119, 95-131.

_____ 1967. The iron-titanium oxides of salic volcanic rocks and their associated ferromagnesian silicates. Contr. Mineral. and Petrol., 14, 36-64.

CHAYES, F. 1963. Relative abundance of intermediate members of the oceanic basalt-trachyte association. J. Geophys. Res., 68, 1519-34.

_____ 1964. Variance-covariance relations in some published Harker diagrams of volcanic suites. J. Petrology, 5, 219-237.

_____ 1965. Classification in a ternary diagram by means of discriminant functions. Amer. Mineral., 50, 1618-33.

_____ 1966. Alkaline and subalkaline basalts. Am. J. Sci., 264, 128-45.

CLARKE, D.B., 1970. Tertiary basalts of Baffin Bay: possible primary magma from the mantle. Contr. Mineral. and Petrol. 25, 203-224.

CLARK, R.H. 1956. A petrological study of the Arthur's Seat volcano. Trans. R. Soc. Edinb., 63, 37-70.

CLARK, S.P., SCHAIRER, J.F., and DE NEUFVILLE, J. 1962. Phase relations in the system Ca Mg Si_2O_6 - $CaAl_2SiO_6$-SiO_2 at low and high pressure. Ann. Rep. Geophys. Lab. Carneg. Inst. Yearbook 61, 59-68.

CLOUGH, C.T., BARROW, G., CRAMPTON, C.B., MAUFE, H.B., BAILEY, E.B. and ANDERSON, E.M. 1910. The Geology of East Lothian. 2nd edition. Mem. Geol. Surv. U.K.

COOLEY, W.W. and LOHNES, P.R. 1971. Multivariate Data Analysis. John Wiley & Sons, Inc., New York.

COOMBS, D.S. 1963. Trends and affinities of basaltic magmas and pyroxenes as illustrated on the diopside-olivine-silica diagram. Spec. Pap. miner. Soc. Am. 1, 227-250.

_____ and WILKINSON, J.F.G. 1969. Lineages and fractionation trends in undersaturated volcanic rocks from the East Otago Volcanic Province (New Zealand) and related rocks. J. Petrology 10, 440-501.

CORLETT, M. and RIBBE, P. 1967. Electron probe microanalysis of minor elements in plagioclase feldspars. Schweiz. Min. Petr. Mitt., 47/1, 317-32.

COX, K.G. and BELL, J.D. 1972. A crystal fractionation model for the basaltic rocks of the New Georgia Group, British Solomon Islands. Contr. Mineral. and Petrol., 37, 1-13.

COX, K.G., GASS, I.G. and MALLICK, D.I.J. 1969. The evolution of the volcanoes of Aden and Little Aden, South Arabia. Q. J. Geol. Soc. Lond., 124, 283-308.

DAY, T.C. 1930. Chemical analyses of thirteen igneous rocks of East Lothian. Trans. Edinb. geol. Soc., 12, 263-6.

DEER, W.A., HOWIE, R.A. and ZUSSMAN, J. 1962. Rock forming minerals. 5 Vols., John Wiley & Sons, N.Y. and London.

DREVER, H.I. 1969. I.A.V.C.E.I. Symposium on Volcanoes and their roots. Supplementary notes for Itinerary IV. Oxford mimeograph.

EMSLIE, R.F. and LINDSLEY, D.H. 1969. Experiments bearing on the origin of anorthosite inclusions. Carneg. Inst., Yearbook 67, 108-112.

FRANCIS, E.H. 1967. Review of Carboniferous-Permian Volcanicity in Scotland. Geol. Rdsch., 57, 219-46.

FRISCH, T. and WRIGHT, J.B., 1971. Chemical composition of high pressure megacrysts from Nigerian Cenozoic lavas. Neves Jb. Mineral. Monatsch., 7, 289-304.

FUDALI, R.F. 1965. Oxygen fugacities of basaltic and andesitic magmas. Geochim. Cosmochim. Acta., 29, 1063-75.

GAST, P.W. 1968. Trace element fractionation and the origin of tholeiitic and alkaline magma types. Geochim. Cosmochim. Acta, 32, 1057-86.

_____ 1968. Upper mantle chemistry and evolution of the Earth's Crust. From: History of the Earth's Crust. R. Phinney, ed., Princeton University Press.

GEORGE, T.N. 1960. The Stratigraphical evolution of the Midland Valley. Trans. geol. Soc. Glasg., 24, 32-107.

GIBB, F.G.F. 1968. Flow differentiation in the Xenolithic Ultrabasic dykes of the Cuillins and the Strathaird Peninsula, Isle of Skye, Scotland. J. Petrology, 9, 411-43.

GIBSON, I.L. and WALKER, G.P.L. 1963. Some composite rhyolite/basalt lavas and related composite dykes in eastern Iceland. Proc. Geol. Assoc. Lond., 74, 301-18.

GORBATSHEV, R. 1961. Dolerites of the Eskilstuna region. Sveriges geol. Unders., Årsbok 55, No. 4, Ser. C., No. 580.

GREEN, D.H. 1969. The origin of basaltic and nephelenitic magmas in the earth's mantle. Tectonophys. 7, 409-422.

_____ and RINGWOOD, A.E. 1967. The genesis of basaltic magmas. Contr. Mineral. and Petrol. 15, 103-190.

GREENLAND, L.P. 1970. An equation for trace element distribution during magmatic crystallization. Am. Mineral. Vol. 55, 455-65.

GREY, N.H. 1973. Estimation of parameters in Petrologic Materials Balance Equations. Math. Geol., 5, 225-236.

_____ and CRAIN, I.K. 1969. Crystal Settling in sills: A model for suspension settling. Canad. Jour. Earth Sci., 6, 1211-16.

GRIFFIN, W.L. and MURTHY, V.R., 1969. Distribution of K, Rb, Sr and Ba in some minerals relevant to basalt genesis. Geochim. Cosmochim. Acta, 33, 1389-1414.

GRISCOM, A. 1960. The bulk composition of a zoned crystal. Amer. Mineral. 45, 1309-12.

GROVER, J.E. and ORVILLE, P.M. 1969. The Partitioning of cations between coexisting single- and multisite phases with application to the assemblages orthopyroxene-clinopyroxene and orthopyroxene-olivine. Geochim. Cosmochim. Acta, 33, 205-226.

HAMILTON, D.L., BURNHAM, C.W. and OSBORN, E.F. 1964. The solubility of water and effects of oxygen fugacity and water content on the crystallization in mafic magmas. J. Petrology, 5, 21-39.

HAMILTON, J. 1956. Mineralogy of basalts from the Western Kilpatrick Hills and its bearing on the petrogenesis of Scottish Carboniferous olivine basalts. Trans. Edinb. geol. Soc., 16, 280-98.

HAMILTON, W. 1965. Diabase sheets of the Taylor Glacier Region, Victoria Land, Antarctica. U.S.G.S. Prof. Paper, 456-B.

HAMM, H.-M. and VIETEN, K. 1971. Zur berechnung der Kristallchemischen formel und des Fe^{3+}-gehaltes von klinopyroxenen aus elektronen-strahl-mikroanalysen. Neues Jb. Mineral. Monatsh., 7, 310-314.

HARKER, A. 1904. The Tertiary Igneous rocks of Skye. Geol. Surv. U.K. Memoirs.

HARNIK, A.B. 1969. Strukturelle Zustände in den Anorthoklasen der Rhombenporphyre des Oslogebietes. Schweiz. Min. Petr. Mitt., 49, 509-67.

HART, S.R. and ALDRICH, L.T. 1967. Fractionation of K/Rb by amphiboles; implications regarding composition. Science, 155, 325-327.

HATCH, F.H. and WELLS, A.K. and WELLS, M.K. 1961. Petrology of the igneous rocks (12th ed.) London, Thomas Murby and Co.,

HEIR, K.S. 1962. Trace elements in feldspars. A review. Norsk. Geol. Tidsskr. A2/2, 415-54.

HENRY, N.F.M., LIPSON, H. and WOOSTER, W.W. 1960. The interpretation of X-ray diffraction photographs. MacMillan & Co. Ltd., London. 2nd edition.

HESS, P.C. 1970. Polymer model of silicate melts. Geochim. Cosmochim. Acta, 35, 289-306.

HUGHES, D.J. and BROWN, G.C. 1972. Basalts from Madeira: A Petrochemical contribution to the genesis of oceanic alkali rock series. Contr. Mineral. and Petrol., 37, 91-109.

HUCKENHOLZ, H.G. 1965. Die Verteilung des Niobs in den gesteinen und mineralen der Alkalibasalt-Assoziation der Hocheifel. Geochim. Cosmochim. Acta, 29, 807-820.

_____ 1965b. Der petrogenetische Werdegang der klinopyroxene in den tertiaren Vulkaniten der Hocheifel. I. Der Klinopyroxene der Alkaliolivin-basalt-Trachyt-Assoziation. Beitr. Mineral. u. Petrog., 11, 138-195.

IDDINGS, J.P. 1913. Igneous rocks, Vol. 2. John Wiley & Sons, N.Y.

IIYAMA, J.T. 1968. Étude expérimentale de la distribution d'éléments en traces entre deux feldspaths. Feldspath potassique et plagioclase coexistants. I. Distribution de Rb, Cs, Sr et Ba à 600°C. Bull. Soc. fr. Minéral. Cristallogr. 91, 130-140.

INGAMELLS, C.O., ENGELS, J.C. and SWITZER, P. 1972. Effect of laboratory sampling error in geochemistry and geochronology. 24th Int. Geol. Congress, Section 10, 405-415.

JAEGER, J.C. 1968. Cooling and solidification of igneous rocks. In: Hess, H.H. and Poldervaart, A. (eds.) Basalts, Vol. 2, 503-36.

JAKOBSSON, S.P., PEDERSEN, A.K., RÖNSBO, J.G. and LARSEN, L.M. 1973. Petrology of mugearite-hawaiite: early extrusives in the 1973 Heimaey eruption, Iceland. Lithos, 6, 203-14.

JAMIESON, B.G. 1970. Differentiation of ascending basic magma. (In) Mechanism of Igenous Intrusion, N. Rast, ed. 165-176.

JASMUND, K. and SECK, H.A. 1972. Partition of elements in coexisting feldspars as determined by experiment and in trachytic rocks. 24th Int. Geol. Congress, Section 10, 78-84.

JENKINS, R. and de VRIES, J.L., 1967. Practical X-ray Spectrometry. Philips Technical Library, Eindhoven.

JENSEN, B.B. 1973. Patterns of trace element partitioning. Geochim. Cosmochim. Acta, 37, 2227-42.

JONES, M.P. and BEAVEN, C.H.J. 1971. Sampling of non-Gaussian mineralogical distributions. Trans. Instn. Min. Metall. (Sect. B: Appl. earth sci.), 80, 316-323.

KASTNER, M. 1971. Authigenic Feldspars in carbonate rocks. Am. Mineral., 56, 1403-1442.

KEIL, K., FODOR, R.V. and BUNCH, T.E. 1972. Contributions to the Mineral Chemistry of Hawaiian Rocks. II. Feldspars and interstitial material in rocks from Haleakala and West Maui volcanoes, Maui, Hawaii. Contr. Mineral. and Petrol., 37, 253-276.

KENNEDY, W.Q. 1931. On Composite lava flows. Geol. Mag., 68, 166-81.

_____ 1933. Composite auto-intrusion in a carboniferous lava flow in: Summary of Progress of the Geological Survey of Great Britain and the Museum of Practical Geology for the Year 1932. Part II. H.M.S.O. 83-93.

KING, B.C. 1965. The nature of basic igneous rocks and their relations with associated acid rocks. Part V. Sci. Progr., 53, 117-25.

KLUSMAN, R.W. 1972. Calcium fractionation in zoned plagioclase from the Tobacco Root batholith, southwestern Montana. Chem. Geol., 90, 45-56.

KOMER, P.D. 1972. Mechanical Interactions of Phenocrysts and Flow Differentiation of Igneous Dikes and Sills. Bull. Geol. Soc. Am., 83, 973-988.

KORRINGA, M.K. and NOBLE, D.C. 1971. Distribution of Sr and Ba between natural feldspar and igneous melt. Earth Planet. Sci. Let. 11, 147-151.

KRUMBEIN, W.C. and GRAYBILL, F.A. 1965. An Introduction to Statistical Models in Geology. N.Y.: McGraw-Hill.

KUNO, H. 1950. Composite lava flows and dykes found in North Izu, Japan. Jour. Geol. Soc. Japan., 56, No. 655.

KUSHIRO, I. 1962. Clinopyroxene solid solutions. Part I. The $CaAl_2SiO_6$ component. Jap. J. Geol. Geogr., 33, 213-20.

LACROIX, A. 1936. Le volcan actif de l'ile de la Réunion et ses produits. Gauthier Villars, Paris.

LANG, A.R. 1972. Pressure and temperature gradients in ascending fluids and magmas. Nature (Physical Science), 238, 98-100.

LE BAS, M.J. 1962. The role of aluminium in igneous clinopyroxenes with relation to their parentage. Am. J. Sci., 260, 267-88.

LEEMAN, W.P. and RODGERS, J.J.W. 1970. Late Cenozoic alkali-olivine basalts of the Basin-Range Province, U.S.A. Contrib. Mineral. and Petrol., 25, 1-24.

LIPMAN, P.W. 1967. Mineral and chemical variations within an ash-flow sheet from Aso Caldera, Southwestern Japan. Contrib. Mineral. Petrol. 16, 300-27.

LIPMAN, P.W., CHRISTIANSEN, R.L. and O'CONNOR, J.T. 1966. A compositionally zoned ash-flow sheet in southern Nevada. U.S.G.S. Prof. Paper. 324F, 47pp.

LOVERING, J.F. and WIDDOWSON, J.R. 1968. The Petrological environment of magnesian ilmenites. Earth and Planetary Science Letters, 4, 310-314.

LUTH, W.C. and TUTTLE, O.F. 1969. The hydrous vapour phase in equilibrium with granite and granite magmas, in Igneous and Metamorphic Geology, eds. Larsen, L., Manson, V. and Prinz, M. Geol. Soc. Am. Mem. 115, 513-548.

MACDONALD, G.A. 1960. Dissimilarity of continental and oceanic rock types. J. Petrology, 1, 172-77.

MACDONALD, G.A. and KATSURA, T. 1964. Chemical composition of Hawaiian lavas. J. Petrology, 5, 82-133.

MACDONALD, G.A., POWERS, H.A. and KATSURA, T. 1973. Interlaboratory comparison of some chemical analyses of Hawaiian volcanic rocks. Bull. Volc., 36, 127-139.

MACDONALD, J.G. 1965. The Petrology of the Clyde Plateau lavas of the Campsie and Kilpatrick Hills. Univ. Glasgow Ph.D. thesis (unpubl.).

_____ 1967. Variations within a Scottish Lower Carboniferous lava flow. Scott. J. Geol., 3, 34-45.

MACDONALD, R. 1968. Petrological studies of some peralkaline acid rocks from the Gardar Province, South Greenland. Unpub. Ph.D. thesis, University of Edinburgh.

_____ 1969. The Petrology of alkaline dykes from the Tugtutôq area, South Greenland. Medd. Dansk. Geolog. For., 19, No. 3, 257-282.

MACGREGOR, A.G. 1928. The classification of Scottish Carboniferous olivine-basalts and mugearites. Trans. geol. Soc. Glasg., 18, 324-60.

_____ 1936. The composite sill of St. Leonard's Craig and Heriot Mount, Edinburgh. Trans. Edinb. geol. Soc. 13, 317-31.

_____ 1948. Problems of Carboniferous-Permian volcanicity in Scotland. Q. Jl. geol. Soc. Lond. 104, 133-153.

MANSON, V., 1967. Geochemistry of basaltic rocks: major elements, in Basalts: the Poldervaart treatise on rocks of basaltic composition, eds. Hess, H.H. and Poldervaart, A., New York: Interscience, 215-269.

MASUDA, A. 1966. Lanthanides in basalts of Japan with three distinct types. Geochemical Journal, Vol. 1, 11-26.

MASUDA, A. and KUSHIRO, I. 1970. Experimental determination of partition coefficients of ten rare earth elements and barium between clinopyroxene and liquid in a synthetic silicate system of 20 kilobar pressure. Contrib. Mineral. and Petrol., 26, 42-49.

MATHEZ, E.A. 1973. Refinement of the Kudo-Weill Plagioclase Thermometer and its application to basaltic rocks. Contr. Mineral. and Petrol., 41, 61-72.

MCBIRNEY, A.R., WILLIAMS, H. and AOKI, K. 1969. Geology and petrology of the Galápagos Islands. Geol. Soc. Amer. Memoir. 118.

MCNOWN, J.S. and MALAIKA, Jamil. 1950. Effects of particle shape on settling velocity at low Reynolds numbers. Am. Geophys. Union Trans., 31, 74-82.

MEDFORD, G.A. 1973. Calcium diffusion in a mugearite melt. Canad. Jour. Earth Sci., 10, 394-402.

MERCY, E.L.P. 1965. Caledonian Igneous Activity. In The Geology of Scotland (ed. G.Y. Craig). Oliver and Boyd, Edinburgh and London.

MOORBATH, S. and WELKE, H. 1969. Lead isotope studies on igneous rocks from the Isle of Skye, Northwest Scotland. Earth. Planet. Sci. Let., 5, 217-30.

MOORE, J.G. 1970. Water content of basalt erupted on the Ocean floor. Contrib. Mineral. and Petrol., 28, 272-79.

MOREY, G.W. and HESSELGESSER, J.M., 1951. The solubility of some minerals in superheated steam at high pressure. Econ. Geol. 46, 821-835.

MUIR, I.D. and SMITH, J.V. 1956. Crystallisation of Feldspars in Larvikites. Z. Kristallogr. 107, 182-195.

MUIR, I.D. and TILLEY, C.E. 1961. Mugearites and their place in alkali igneous rock series. J. Geol. 69, 186-203.

MUKHERJEE, A. 1967. Role of fractional crystallization in the descent: basalt → trachyte. Contrib. Mineral. and Petrol., 16, 139-148.

MURATA, K.G. and RICHTER, D.H. 1966. Chemistry of the lavas of the 1959-60 eruption of Kilauea volcano, Hawaii. U.S.G.S. Prof. paper. 537A.

NORRISH, K. and CHAPPELL, B.W. 1967. X-ray fluorescence spectrography. From: Physical Methods in determinative mineralogy (J. Zussman ed.) Academic Press, London and New York, 161-214.

OERTEL, G. 1952. A structural investigation of the porphyritic basalts of Arthur's Seat, Edinburgh. Trans. Edinb. geol. Soc. 14, 360-78.

O'HARA, M.J. 1968. The bearing of phase equilibria studies in synthetic and natural systems on the origin and evolution of basic and ultrabasic rocks. Earth-Sci. Rev. 4, 69-133.

_____ 1970. Upper mantle composition inferred from laboratory experiments and observation of volcanic products. Phys. Earth Planet. Interiors. 3, 236-245.

ORVILLE, P.M. 1963. Alkali ion exchange between vapor and feldspar phases. Am. J. Sci., 261, 201-37.

OVERSBY, V.M. 1972. Genetic relations among the volcanic rocks of Réunion: chemical and lead isotopic evidence. Geochim. Cosmochim. Acta, 36, 1167-1179.

PANTONY, D.A., 1972 Statistical and Practical Considerations of limits of detection in X-ray spectrometry. The Analyst, 97, 497-518.

PRÉVOT, M. and MERCOIL, J. 1973. Crystallization trend of titanomagnetites in an alkali basalt from Saint-Clément (Massif Central, France). Mineral Mag., 39, 474-81

PHILPOTTS, A.R. 1971. Density, surface tension and viscosity of the immiscible phase in a basic alkaline magma. Lithos, 3, 309-17.

PHILPOTTS, J.A. and SCHNETZLER, C.C. 1968. Europium anomalies and the genesis of basalt. Chem. Geol., 3, 5-13.

_____ and _____ 1970. Phenocryst-matrix partition coefficients for K, Rb, Sr and Ba, with applications to anorthosite and basalt genesis. Geochim. Cosmochim. Acta, 34, 307-22.

_____ and _____ 1972. Large trace cation partitioning in igneous processes. 24th Int. Geol. Congress. Section 10, 51-59.

PRESNALL, D.C. 1969. The geometrical analysis of partial fusion. Am. J. Sci. 267, 1178-1194.

PRINZ, M., 1967. Geochemistry of basaltic rocks: trace elements, in Basalts: the Poldervaart treatise on rocks of basaltic composition, eds. Hess, H.H. and Poldervaart, A., New York: Interscience, 271-323.

RAMDOHR, P. 1969. The Ore Minerals and their intergrowths. Pergammon Press.

REID, M.J., GANCARZ, A.J. and ALBEE, A.L. 1973. Constrained least squares analysis of petrologic problems with an application to lunar sample 12040. Earth Planet. Sci. Let. 17, 433-445.

RITTMAN, A. 1971. The probable origin of high alumina basalts. Bull. Volc., 34, 414-420.

ROSE, H.J., ADLER, I. and FLANAGAN, F.J. 1963. X-ray fluorescence analysis of the light elements in rock and minerals. Appl. Spectrosc., 17 81-85.

RUTLEDGE, H. 1952. A petrological note on a composite sill, The Dasses, Arthur's Seat. Trans. Edinb. geol. Soc. 14, 379-88.

SAMUELSSON, L. 1971. The relationship between Permian dikes of dolerite and rhomb porphyry along the Swedish Skagerak Coast. Sveriges Geol. Unders., Ser. C. No. 663, Arsb. 65, No. 9.

SATO, M. and WRIGHT, T.L. 1966. Oxygen Fugacities directly measured in magmatic gases. Science, 153, 1103-5.

SCARFE, C.M. 1973. Viscosity of Basic Magmas of Varying Pressure. Nature, 241, 101-102.

SCHARBERT, H.G. 1966. The alkali feldspars from micro-syenitic dykes of southern Greenland. Min. Mag. 35, 903-19.

SCHILLING, J.G. and WINCHESTER, J.W. 1967. Rare-earth fractionation and magmatic processes in Mantles of the Earth and Terrestrial Planets. ed. Runcorn, S.K., New York. Interscience, 267-283.

SCHILLING, J.G. and WINCHESTER, J.W. 1969. Rare-earth contribution to the origin of Hawaiian Lavas. Contr. Mineral. and Petrol. 23, 27-37.

SCHMINKE, H-U. 1969. Ignimbrite sequence on Gran Canaria. Bull. Volc., 33, 1199-1219.

SCHNETZLER, C.C. and PHILPOTTS, J.A. 1968. Partition coefficients of rare earth elements and barium between igneous matrix material and rock forming mineral phenocrysts. From: Origin and Distribution of the Elements, ed. L.H. Ahrens, Pergamon Press.

_____ and _____ 1969. Partition coefficients of rare earth elements between igneous matrix material and rock forming mineral phenocrysts - II. Geochim. Cosmochim. Acta, 34, 331-340.

SHAPIRO, L. and BRANNOCK, W.W. 1962. Rapid analysis of silicate, carbonate and phosphate rocks. U.S. Geol. Surv. Bull. 1144-A.

SHAW, D.M. 1968. A review of K/Rb fractionation trends by covariance analysis. Geochim. Cosmochim. Acta, 32, 573-602.

_____ 1970. Trace element fractionation during anatexis. Geochim. Cosmochim. Acta, 34, 237-243.

_____ 1969-72. Chapter 11. "Evaluation of Data" in Handbook of Geochemistry. ed. K.H. Wedepohl. Springer. Verlag, Germany.

SHAW, H.R. 1965. Comments on viscosity, crystal settling, and convection in granitic magmas. Am. J. Sci. 263, 120-52.

_____ 1969. Rheology of Basalt in the Melting Range. J. Petrology, 10, 510-35.

SIMKIN, T. and SMITH, J.V. 1970. Minor element distribution in olivine. J. Geol. 78, 304-25.

SIPPEL, R.F., SPENCER, A.B. 1970. Cathodoluminescence properties of lunar rocks. Science, 167, 677-679.

SHIMAZU, Y. and URABE, T. 1967. Development of the earth's mantle and behavior of minor elements. Geochem. Jour. 1, 71-94.

SMITH, A.L. and CARMICHAEL, I.S.E. 1969. Quaternary trachybasalts from Southeastern California. Am. Mineral., 54, 909-23.

SMITH,J.V. and MacKENZIE,W.S.,1958.The Alkali Feldspars.IV. The cooling history of high temperature sodium rich feldspars.Am.Mineral.,43,872-889.

SMITH, J.V. and MUIR, I.D. 1958. The reaction sequence in larvikite feldspars. Z. Kristallogr. 110, 11-20.

STEPHENSON, D. 1972. Alkali clinopyroxenes from nepheline syenites of the South Qôroq centre, South Greenland. Lithos, 5, 187-201.

STEWART, D.B. and ROSEBOOM, E.H. 1962. Lower temperature terminations of the three phase region Plagioclase-Alkali feldspar-Liquid. J. Petrology, 3, 280-315.

STEWART, D.B., WALKER, G.W., WRIGHT, T.L., FAHEY, J.J. 1966. Physical properties of calcic labradorite from Lake County, Oregon. Amer. Mineral., 51, 177-197.

STEWART, J.W. 1964. The earlier Gardar igneous rocks of the Ilimaussaq area, South Greenland. Ph.D. thesis (unpubl.) University of Durham.

SWANSON, D.A. and FABBI, B.P. 1973. Loss of volatiles during fountaining and flowage of basaltic lava at Kilavea Volcano, Hawaii. U.S.G.S. Jour. Res., 1, 649-658.

SWEATMAN, T.R. and LONG, J.V.P. 1969. Quantitative electron-probe microanalysis of rock-forming minerals. J. Petrology, 10, 332-79.

TAYLOR, S.R. 1965. The application of trace element data to problems in petrology. Phys. Chem. Earth, 6, Chapter 2, 133-213.

THOMPSON, R.N. 1972a. Evidence for a chemical discontinuity near the basalt-"andesite" transition in many anorogenic volcanic suites. Nature, 236, 106-110.

_____ 1972b. The 1 atmosphere melting patterns of some basaltic volcanic series. Am. J. Sci., 272, 901-932.

THOMPSON, R.N., ESSON, J., and DUNHAM, A.C. 1972. Major element chemical variation in the Eocene lavas of the Isle of Skye, Scotland. J. Petrology, 13, 219-53.

THORNTON, C.P. and TUTTLE, O.F. 1960. Chemistry of igneous rocks. I. Differentiation Index. Am. J. Sci., 258, 664-84.

TILLEY, C.E. 1950. Some aspects of magmatic evolution. Q. Jl. Geol. Soc. Lond., 106, 37-61.

TILLEY, C.E. and MUIR, I.D. 1964. Intermediate members of the oceanic basalt-trachyte association. Geol. För. Stock. Forh., 85, 436-44.

TILLEY, C.E., YODER, H.S.Jr., and SCHAIRER, J.F. 1965. Melting relations of volcanic tholeiite and alkali rock series. Ann. Rep. Geophys. Lab. Carneg. Inst. Yearbook 64, 69-82.

_____, _____ and _____ 1967. Melting relations of volcanic rock series. Ann. Rep. Geophys. Lab. Carneg. Inst. Yearbook 65, 260-9.

TOMKEIEFF, S.I. 1937. Petrochemistry of the Scottish Carboniferous - Permian Igneous rocks. Bull. Volc. 1, Ser. 11, 59-87.

TURNER, F.J. and VERHOOGEN, J. 1960. Igneous and metamorphic petrology. New York: McGraw-Hill.

TYRRELL, G.W. 1912. The Petrology of the Kilpatrick Hills, Dunbartonshire, with notes on the Scottish Carboniferous basalts. Trans. Geol. Soc. Glasgow. 14, 219-57.

UCHIMIZU, M. 1966. Geology and Petrology of alkali rocks from Dōgo, Oki Islands. J. Fac. Sci. Univ. Tokyo, 16, 85-159.

UPTON, B.G.J. 1960. The alkaline igneous complex of Kûngnât Fjeld, South Greenland. Medd. Grøn. Vol. 123, No. 4.

_____ 1962. Geology of Tugtutôq and neighbouring islands, South Greenland. Pt. I. Medd. Grøn. Vol. 169, No.8.

_____ 1964. The geology of Tugtutôq and neighbouring islands, South Greenland. Pt.III. Olivine gabbros, syeno-gabbros and anorthosites. Medd. Grøn. Vol. 169, No. 3, 1-47.

_____ (ed.) 1969. Carboniferous volcanic rocks of the Midland Valley of Scotland, field excursion guide. Symposium on Volcanoes and their Roots, Int. Ass. Volc. Chem. Earth's Interior.

_____ 1971. Melting experiments on chilled gabbros and syenogabbros. Carneg. Inst. Washington Yearbook 69, 112-118.

UPTON, B.G.J. and WADSWORTH, W.J. 1966. The basalts of Reunion Island, Indian Ocean. Bull. Volc., 29, 7-24.

_____ and _____ 1967. A complex Basalt-Mugearite sill in Piton des Neiges Volcano, Reunion. Amer. Mineral., 52, 1475-92.

_____ and _____ 1970. Intra-volcanic intrusions of Reunion. in. Mechanism of Igneous Intrusion, N. Rast, ed. 141-156.

_____ and _____ 1972. Aspects of magmatic evolution on Reunion Island. Phil. Trans. Roy. Soc. London, Ser. A, 271, 101-130.

URUNO, K. 1963. Optical study of the ordering degree of plagioclases. Tohoku Univ. Sci. Rept., 3rd Ser. 8, 171-200.

WAGER, L.R. 1956. A chemical definition of fractionation stages as a basis for comparison of Hawaiian, Hebridean and other basic lavas. Geochim et Cosmochim. Acta, 9, 217-248.

WALKER, K.R. 1969. The Palisades Sill, New Jersey: A re-investigation. Geol. Soc. Amer., Sp. Paper 111.

WALTON, B.J. 1965. Sanerutian appinitic rocks and Gardar diatremes north of Narssarssuaq, South Greenland. Medd. Grøon Bd. 179, No. 9.

WASHINGTON, H.S., AUROUSSEAU, M. and KEYES, M. 1926. The lavas of Etna. Am. J. Sci. XII, 371-408.

WATKINS, N.D., GUNN, B.M. and COY-YLL, R. 1970. Major and trace element variations during the initial cooling of an Icelandic lava. Am. J. Sci. 268, 24-49.

WATT, W.S. 1968. Petrology and Geology of the Precambrian Gardar dykes on Qaersuarssuk, South Greenland. Greenland Geol. Surv. Rep. 14.

WELLS, A.K. 1954. Mugearites and oligoclase-basalts. Geol. Mag. 93, 14-16.

WILKINSON, J.F.G. 1965. Titanomagnetites from a differentiation sequence, analcime-olivine theralite to analcime-tintuaite. Mineral. Mag., 34, 528-41.

WILKINSON, J.F.G. and BINNS, R.A. 1969. Hawaiite of high pressure origin from northeastern New South Wales. Nature, 222, 553-5.

WRIGHT, J.B. 1968. Oligoclase-andesine phenocrysts and related inclusions in basalts from part of the Nigerian Cenozoic province. Mineral. Mag. 36, No. 283, 1024-31.

WRIGHT, T.L. and DOHERTY, P.C. 1970. A linear programming, and least squares method for solving petrologic mixing problems. Bull. Geol. Soc. Amer. 81, 1995-2008.

WRIGHT, T.L. and FISKE, R.S. 1971. Origin of the differentiated and hybrid lavas of Kilauea Volcano, Hawaii. J. Petrology, 12, No. 1, 1-65.

YODER, H.S. Jr. 1969a. Experimental studies bearing on the origin of anorthosite. From: Origin of Anorthosite and Related Rocks. ed. Y. Isachsen. New York State Museum and Science Service Me. 18.

_____ 1969b. Calcalkaline Andesites: experimental data bearing on the origin of their assumed characteristics. From: Proceedings of the Andesite Conference (A.R. McBirney, ed.) Oregon Dept. Mineral Ind. Bull. 65, 77-89.

_____ 1973. Contemporaneous basaltic and rhyolitic magmas. Am. Mineral, 58, 153-171.

YODER, H.S.,Jr. and TILLEY, C.E. 1962. The origin of basalt magmas: an experimental study of natural and synthetic systems. J. Petrology 3, 342-532.

WILSON, A.D. 1958. A new method for the determination of ferrous iron in rocks and minerals. Bull. geol. Surv. Gt. Br., 9, 56-58.

ZIELINSKI, R.A. and FREY, F.A. 1970. Gough Island: Evaluation of fractional crystallization model. Contr. Mineral. and Petrol., 29, 242-254.

APPENDIX A

CHEMICAL ANALYSES

(N.B. Fe_2O_3:FeO ratios are adjusted to 0.26, if necessary before calculation of the CIPW normative minerals.)

AKB: alkali-olivine basalt

H: Hawaiite

PH: porphyritic hawaiite

M: Mugearite

B: Benmoreite

APPENDIX A

1.A. Sample preparation

Specimens of 300-400 g weight were trimmed of weathered surfaces, washed and scrubbed with a stiff bristle brush under running tap water, then rinsed in deionised water and dried.

The dried specimens were split with a hydraulic splitter ("Cutrock") into chips less than 3 cm. across; these (after discarding any weathered surfaces) were crushed to $\leq$ 50 mesh (B.S.) in the Manchester Rollers. The sample was then crushed in the "Columboy" Tema for 30-40 seconds. Samples prepared in this manner were contaminated with Ni and Cr (D.F. Strong, pers. comm. 1969). Samples analyzed for these elements were prepared in the Agate tema, available later, after grinding for 10-12 minutes.

The sample was then sieved through silk bolting (-120 mesh B.S.) held in a plastic cylinder. The remaining few grammes were ground by hand in an agate mortar and pestle and added to the sample.

The ground samples were stored in glass bottles until analyzed; 10-20 g of the sample to be analyzed were dried overnight in small glass jars. A series of checks on weight loss of the samples suggested that 4 hours was sufficient to remove hygroscopic moisture.

2.A. Analysis.

X-ray Spectrometry. Trace and major elements, with the exception of FeO, Na_2O and H_2O were determined by X-ray

fluorescence analysis, using a Phillips PW 1212 twenty-four channel automatic or PW 1540 single channel spectrometers with the settings given in Jenkins and DeVries(1967)

Trace elements were determined using the dried sample powders, calculating the ratios of peak to background and reading concentrations from calibration curves assumed to be linear. The calibration curves were constructed from the best (visual) fit of 10-12 international standards and 3 departmental standards. The ratios of peak to background counts were calculated from counts corrected for instrumental drift by means of computer programs written in IMP by D.H. Doff, J.D. Appleton and R. Cheeney.

The major elements were determined by a modification of the method used by Rose et al., (1963). Addition of the sample to lithium tetraborate ($Li_2B_4O_7$) and lanthanum oxide (La_2O_3) in the ratio 1:1:8 removes matrix effects by means of the dilutant (lithium tetraborate) and heavy absorber. Calibration curves are essentially linear for the compositions studied. The calibration curves were based on the same 10-12 international and 3 departmental standards used for the trace elements. Correction of the counts for instrumental drift, calculation of the regression line and calculation of the sample chemistry was done by means of a computer program written by J.D. Appleton after a program of D.H. Doff.

The accuracy and precision of the X-ray fluorescence analyses are presented in Table A.1.

3.A. Wet Chemical Methods.

FeO was determined using Wilson's (1955) method; cold HF is added to approximately 0.5 g of sample with an excess of ammonium vanadate in PTFE crucibles. The crucibles are left covered for 5 days, stirred daily to ensure complete attack by the acid and then placed carefully by means of platinum tipped clamps into plastic beakers containing boric acid plus sulphuric acid to adjust the pH. The crucibles are stirred with a plastic mixer to ensure that the mixture is homogeneous. Titration of the excess vanadate with ferrous ammonium sulfate, using sodium diphenylamine sulphonate as an indicator, is then done. The precision is given in Table A.2.

Na_2O was determined using an EEL flame photometer by the method of M.J. Saunders of this department. The steps are outlined below.

The sample in platinum crucibles is dissolved in concentrated nitric and hydrofluoric acid. Addition of 1:1 sulphuric acid to this, and evaporation to dryness is repeated several times to remove excess HF.

Dilute sulphuric acid is added, then deionised water, to ensure that all sodium enters the solution. Any insoluble residue ($CaSO_4$ largely) is filtered off or allowed to settle; the resulting solution is analysed in the flame photometer with a double Na filter to minimise interference from any remaining calcium in solution. The precision is given in Table A.2.

$\underline{H_2O^+}$ was determined gravimetrically by a modified version of the method described by Shapiro and Brannock (1962). Fusion of 1 g of sample with 3 g of a flux (2:1 mixture of lead oxide and lead chromate) in a test tube evolved water which was collected on dried, pre-weighed filter paper near the end of a stoppered test tube. An estimate of the precision is given in Table A.2.

TABLE A.1

Estimated Precision of XRF Analyses

where $\bar{x}$ = sample (Analysis 3, Table 1 A) mean based on 12 determinations

V = Percent (std. deviation/mean), i.e. the coefficient of variation

Columns 3, 4, 5 and 6 are estimates of V given in the following Ph.D theses (unpublished), Edinburgh University, using the same analytical methods and instruments.

Appleton, J.D., 1970.	The petrology of the potassium-rich lavas of the Roccamorfina Volcano, Italy.
Baxter, A.N., 1973.	Magmatic evolution of Mauritius, Western Indian Ocean.
Gandi, M.K., 1973.	The petrology and geochemistry of the lower old red sandstone lavas of the Sidlaw hills, Perthshire.
Strong, D.F., 1970.	Petrology of the lavas of Grande Comore.

Major oxides (wt. %)	$\bar{x}$	V	3	4	5	6
SiO_2	44.6	0.21	0.32	0.55	0.4	0.27
Al_2O_3	15.9	2.1	1.09	1.02	2.25	0.60
Fe as Fe_2O_3	14.77	2.9	0.93	1.76	2.38	1.18
MgO	8.5	3.2	1.85	1.96	4.46	1.09
CaO	9.6	1.5	0.26	0.54	1.87	0.53
K_2O	0.33	3.0	0.49	0.4	1.92	0.76
TiO_2	2.34	4.3	3.4	1.94	4.67	1.14
P_2O_5	0.4	2.3	1.11	3.8	6.9	4.65
MnO	0.19	1.1		3.8		
Trace elements (ppm)						
Ba	135	3.7	1.7	6	3.6	6
Sr	370	3.2	1.3	3	6.3	2
Rb	3	35.0		7		20
Zr	158	4.4	2.5	2	5.6	5
Zn	78	6.1			4.1	5
Y	34	11.8	6.9	6	14.5	
Cu	95	13.7			34.5	8
Nb	17	23.5				
La	26	46.1				
Ce	34	35.3				

TABLE A.2

Estimates of wet chemistry precision

	$\bar{x}$	n	v	4	5
FeO	9.64	11	2.6	1.19	1.01
"	1.73	5	2.3		
Na_2O	4.91	10	0.93	0.9	0.44
H_2O	1.86	7	4.9	5.65	5.53

where $\bar{x}$ = mean of samples analyzed

n = number of determinations

v = Percent (std. deviation/mean), i.e. the coefficient of variation

4 = v from Baxter, A.N., 1973 (op.cit. Table A.2)

5 = " " Appleton, J.D., 1970 " "

KEY TO ANALYSES OF TABLE 1 A

Analysis Number	Location	Distance above (A) or below (B) junction of two units in metres	Rock Type
1.	Near "Dun"; first exposure of rock below composite flow. Ledge 2 - 3 metres thick.	-	AkB
2.	East of Loch Dubh. First exposure of rock below composite flow. 10 - 12m. below specimen of (14) below.	-	AkB
3.	Same as (1); basal metre of ledge.	-	AkB
4.	Small knob west of "Dun". Aphyric	8.5(B)	H
5.	" " " " " "	6.5(B)	H
6.	" " " " " "	4.5(B)	H
7.	" " " " " " Groundmass of slightly porphyritic rock.	2.5(B)	H
8.	"Dun" hill. Lowest aphyric rock exposed.	5.0(B)	H
9.	"Dun" hill - aphyric	4.0(B)	H
10.	Small knob west of "Dun" - aphyric	0.10(B)	H
11.	" " " " " "	0.10-0.15(A)	H
12.	"Dun" hill	1.5(A)	PH
13.	" " ; groundmass of (12)	1.5(A)	PH
14.	East of Loch Dubh	≃2.0(A)	PH
15.	" " " " ; groundmass of (14)	≃2.0(A)	PH
16.	" " " "	≃2.5(A)	PH
17.	" " " " ; groundmass of (16)	≃2.5(A)	PH
18.	"Dun" hill	≃2.5(A)	PH
19.	" " ; groundmass of (18)	≃2.5(A)	PH
20.	East of Loch Dubh	≃3.5(A)	PH
21.	" " " "	≃3.75(A)	PH
22.	"Dun" hill	3.7(A)	PH
23.	" " ; groundmass of (22)	3.7(A)	PH
24.	" " ; analysis from Tilley et al., 1967. Basal part of composite flow	-	H
25.	820m. N.E. of Loch Sguirr Mhoir, north of Talisker	-	H

TABLE 1A

Analyses of composite flow near Talisker, North Skye

Analysis No.	1	2	3	4	5	6	7	8	9	10	11	12	13	14	15	16	17
Field No.	T-6	T-16	T-AA	T-11B	T-11A	T-10	FL-6G	T-5	T-4	FL-3	FL-4	T-3	T-3G	T-15	T-13G	T-14	T-14G
SiO_2	44.6	44.8	44.2	46.2	45.9	45.8	45.8	46.5	46.5	46.9	46.5	47.3	46.0	45.9	45.6	46.0	45.2
Al_2O_3	15.9	15.8	15.6	16.3	16.1	16.2	16.3	16.2	16.4	16.8	17.0	18.9	17.0	16.7	16.2	17.8	15.8
Fe_2O_3	4.26	2.35	4.12	3.64	3.04	3.77	3.71	3.09	1.84	2.20	3.69	5.78	5.29	3.93	4.10	5.05	6.23
FeO	9.20	10.49	9.58	11.68	12.10	11.50	11.22	11.92	12.06	12.81	11.49	6.19	8.90	10.24	11.27	9.41	9.82
MgO	8.5	8.5	8.6	4.9	5.5	5.3	5.0	5.2	5.0	4.9	5.2	4.1	4.9	5.4	4.9	4.9	4.7
CaO	9.6	9.8	9.7	7.4	7.4	7.5	7.8	7.8	7.8	7.2	7.1	8.1	7.7	8.0	7.3	7.4	6.8
Na_2O	2.78	2.58	2.71	4.10	4.60	4.30	4.50	4.14	4.24	4.30	4.30	4.75	4.60	4.34	4.15	4.46	4.30
K_2O	0.33	0.44	0.32	0.51	0.55	0.51	0.49	0.63	0.59	0.50	0.49	0.54	0.57	0.49	0.45	0.53	0.44
H_2O^+	1.76	2.06	1.86	1.25	0.78	1.12	1.15	1.18	1.23	1.18	1.08	1.11	1.32	1.52	1.49	1.89	1.94
TiO_2	2.34	2.31	2.43	3.20	3.07	3.24	3.30	3.31	3.28	3.09	3.55	2.42	2.87	2.95	3.72	3.02	3.91
P_2O_5	0.4	0.3	0.3	0.4	0.3	0.4	0.4	0.5	0.4	0.4	0.37	0.33	0.39	0.3	0.4	0.4	0.4
MnO	0.19	0.20	0.19	0.20	0.20	0.20	0.20	0.21	0.20	0.20	0.20	0.16	0.18	0.19	0.20	0.19	0.20
Total	99.7	99.7	99.7	99.8	99.6	99.8	99.5	100.3	100.0	100.5	100.8	99.8	99.9	99.9	99.8	99.8	99.7
TRACE ELEMENTS IN PPM																	
Ba	156	120	135	230	290	260	270	249	230	260	270	200	270	241	297	220	281
Sr	390	540?	370	577	520	597	590	580	590	605	555	622	469	623	462	568	479
Rb	6	12	3	16	12	13	17	12	13	15	16	12	17	14	15	10	3
Zr	176	160	158	250	225	255	255	242	240	230	70	194	266	220	258	232	250
Zn	84	75	78	72	60	63	58	72-75	76	43	61	61	64	63	74	62	63
Y	35	33	34	37	33	36	33	55	54	34	32	43	22	51	23	59	20
Cu	101	102	95	51	50	30	37	15	30	24	32	27	27	37	39	27	29
Nb	26	-	17	-	34	-	-	43	38	-	-	29	-	-	22	-	11
La	37	-	26	-	-	-	-	-	-	-	-	38	-	18	-	22	-
Ce	8	-	34	-	-	-	-	-	-	-	-	29	-	40	-	48	-
Ni	-	-	-	29	-	20	20	-	-	36	28	31	-	-	-	-	-
Th	4	3	2	-	-	-	-	3	n.d.	-	-	n.d.	-	<5	-	<5	-
Pb	<1	-	<5	-	-	-	-	n.d.	-	-	-	<5	-	<5	-	<5	-
Ga	17	-	-	-	-	-	-	-	-	-	-	-	-	-	-	-	-
CIPW NORMATIVE MINERALS																	
Qz	0.0	0.0	0.0	0.0	0.0	0.0	0.0	0.0	0.0	0.0	0.0	0.0	0.0	0.0	0.0	0.0	0.0
Or	2.0	2.7	1.9	3.1	3.3	3.1	2.9	3.6	3.5	3.0	2.9	3.3	3.4	2.9	2.7	3.2	2.7
Ab	23.9	22.3	23.5	35.1	30.6	32.6	33.4	32.5	32.2	36.9	33.9	36.6	34.2	31.8	34.4	34.8	35.8
An	30.3	30.8	30.1	24.8	22.0	23.7	23.3	24.0	24.3	25.4	25.5	29.2	24.5	25.1	24.6	27.3	23.0
Ne	0.0	0.0	0.0	0.1	4.8	2.3	2.9	1.5	2.3	0.0	1.2	2.3	2.9	3.0	0.6	1.8	0.7
Di	12.7	13.7	13.8	8.2	10.9	9.6	9.7	10.2	10.3	6.9	6.0	7.6	9.3	10.5	8.0	5.8	7.4
Hy	1.8	1.2	1.00	0.0	0.0	0.0	0.0	0.0	0.0	0.0	0.0	0.0	0.0	0.0	0.0	0.0	0.0
Ol	17.6	20.2	18.1	16.2	17.3	16.1	15.0	16.5	17.3	16.1	17.7	7.0	11.3	14.4	15.9	13.1	15.9
Mt	6.3	4.0	6.1	5.4	4.5	5.5	5.5	4.5	2.7	4.8	5.3	8.5	7.8	5.8	5.9	7.4	6.1
Il	4.5	4.5	4.7	6.2	5.9	6.2	6.4	6.3	6.3	6.0	6.7	4.7	5.5	5.7	7.1	5.8	7.6
Ap	0.9	0.8	0.7	0.9	0.7	0.9	0.9	1.0	1.1	0.9	0.9	0.8	0.9	0.8	0.9	0.9	0.9
OR)	3.5	4.8	3.5	4.9	5.9	5.1	4.9	5.9	5.9	4.6	4.6	4.7	5.5	4.9	4.4	4.8	4.3
AB)	42.6	40.0	42.3	55.7	54.8	54.9	56.0	54.1	53.7	56.5	54.5	53.1	55.0	53.1	55.7	53.3	58.3
AN)	53.9	55.2	54.4	39.4	39.3	40.0	39.0	40.0	40.5	39.0	40.9	42.3	39.5	42.0	39.9	41.9	37.4
D.I.	25.9	24.9	25.4	38.2	38.7	38.0	39.2	37.5	38.1	39.9	37.9	42.2	40.5	37.7	37.7	39.7	39.1

TABLE 1A (contd.)

Analysis No.	18	19	20	21	22	23	24	25
Field No.	T-2	T-2G	T-13	T-12G	T-1	T-1G		
SiO_2	47.6		47.9	46.4	47.6	46.8	45.73	46.46
Al_2O_3	18.6		17.8	16.2	18.2	16.9	16.30	16.05
Fe_2O_3	4.84		2.58	3.92	9.07	4.17	3.87	4.57
FeO	8.12		9.56	11.01	3.60	10.03	11.45	10.45
MgO	4.5		5.1	5.5	4.2	5.1	5.25	4.45
CaO	8.2		7.0	7.2	8.1	7.5	7.42	6.88
Na_2O	4.55		5.00	4.00	4.85	4.25	4.33	5.26
K_2O	0.50		0.48	0.47	0.54	0.52	0.59	0.79
H_2O^+	0.94		2.27	1.18	1.29	1.68	0.97	0.88
TiO_2	2.54		2.55	3.34	2.46	3.21	3.36	3.94
P_2O_5	0.4		0.3	0.4	0.3	0.3	0.33	0.43
MnO	0.17		0.16	0.20	0.17	0.22	0.20	0.19
Total	100.9		100.6	99.8	100.5	100.7	100.28	100.50
			TRACE ELEMENTS IN PPM					
Ba	234	286	231	256	246	260	-	-
Sr	665	522	520	477	605	520	-	-
Rb	9	11	8	18	12	8	-	-
Zr	210	262	-	282	209	265	-	-
Zn	57	74	53	78	58	67	-	-
Y	51	29	52	26	50	24	-	-
Cu	54	53	47	-	35	37	-	-
Nb	30	16	-	40	-	46	-	-
La	-	-	16	-	20	-	-	-
Ce	22	-	29	-	54	-	-	-
Ni	30	-	24	-	25	37	-	-
Th	<5	-	<5	-	-	-	-	-
Pb	<5	-	<5	-	<5	-	-	-
Ga	13	-	18	-	14	-	-	-
			CIPW NORMATIVE MINERALS					
Qz	0.0		0.0	0.0	0.0	0.0	0.0	0.0
Or	3.0		2.9	2.8	3.2	3.0	3.34	5.00
Ab	35.9		36.6	34.3	39.2	33.6	31.76	33.64
An	28.8		25.1	25.2	26.5	25.3	23.35	17.51
Ne	1.4		3.4	0.0	1.2	1.1	2.66	5.99
Di	7.5		7.0	6.9	9.3	7.8	9.65	11.66
Hy	0.0		0.0	3.9	0.0	0.0	0.0	0.0
Ol	10.6		15.6	14.0	4.4	16.5	15.45	10.75
Mt	7.0		3.8	5.5	5.1	6.0	5.57	6.61
Il	4.8		4.9	6.4	4.7	6.0	6.38	7.45
Ap	1.0		0.6	0.9	0.8	0.7	0.67	1.01
OR)	4.4		4.5	4.5	4.7	4.9	5.6	8.9
AB)	53.0		56.7	55.0	56.9	54.3	54.4	60.0
AN)	42.6		38.8	40.5	38.5	40.8	40.0	31.1
D.I.	40.3		42.9	37.1	43.6	37.7	37.8	44.6

KEY TO ANALYSES OF TABLE 1 B

Analysis Number	Location	Rock type	Distance above base (cm)
1.	Drum na Criche; knob lying to east of series below	M	-
2.	Drum na Criche; centre knob	M	100
3.	Drum na Criche; centre knob	M	200
4.	Drum na Criche; centre knob. Collected 1 m to the west of above series, close to patch of freshly hammered rock	M	170
5.	Drum na Criche. Quoted from Yoder and Tilley (1962), pg. 418, Table 24	M	-
6.	Drum na Criche. Collected from exposure lying to north of the series noted above	PH	-
7.	Drum na Criche. Groundmass of Number 6	PH	-
8.	Drum na Criche. Groundmass analysis. Quoted from Yoder and Tilley, (1962). Table 24.	PH	-
9.	Base of Roineval, at roadcut near Carbost road turnoff. Includes normative minerals: 0.7 Q, 4.5 Perov.; 14.9 HM.	volcanic ash	-
10.	Dyke exposed at same locality as (9)	TB	-
11.	Meadale Burn base of Roineval, Sluiceway below road crossing the streambed	H	-
12.	Exposure about 5 metres below (11)	H	-
13.	Exposure 700 m south of (11) but close to same level	H	-
14.	Roadmetal quarry near (13), base of Roineval	H	-
15.	Roineval. Lower unit of composite flow, base of main massif, midway along prominent north facing scarp, and 20 m west of a small valley leading towards the summit	M	0
16.	Roineval. Same locality as (15)	M	42
17.	Roineval. Same locality as (15). 28-30 cm below junction with porphyritic unit	M	52

TABLE 1B

Analysis of the composite flows of Drumna Criche and Roineval with additional analyses of single flows at Roineval and Ben Horneval, North Skye.

Analysis No.	1	2	3	4	5	6	7	8	9	10	11	12	13	14
Field No.	DC-1	DC-4	DC-5	DC-7		DC-3	DC-3C		Cr-3A	CR-3D	MB-1	MB-3	MB-4	MB-5
SiO_2	50.2	52.5	49.9	51.4	49.68	50.4	49.6	49.35	47.8	47.3	47.3	47.7	45.9	47.4
Al_2O_3	16.1	15.6	18.3	17.0	16.99	19.6	16.7	17.36	16.6	17.8	16.5	16.3	16.9	16.4
Fe_2O_3	4.01	6.50	4.54	4.81	3.45	2.90	3.26	4.09	14.45	4.08	2.43	4.35	5.21	5.68
FeO	9.10	5.42	5.82	6.20	8.99	5.93	9.26	7.56	0.09	5.87	12.10	8.86	9.76	8.09
MgO	3.0	2.7	2.8	3.1	2.79	3.1	3.3	3.45	3.1	6.7	4.5	4.8	4.3	4.1
CaO	5.2	5.1	7.9	5.7	5.46	8.1	7.4	7.35	4.4	14.0	6.8	8.0	6.7	6.8
Na_2O	5.20	4.85	4.36	4.80	5.78	4.10	4.00	4.52	6.12	1.71	4.25	4.15	4.44	4.59
K_2O	1.98	2.36	1.10	2.10	1.90	0.97	1.31	1.30	1.49	0.08	1.21	1.01	1.02	1.21
H_2O^+	1.39	1.50	1.25	1.56	1.77	1.27	1.33	0.96	2.74	1.49	1.20	1.42	1.47	1.92
TiO_2	1.99	2.02	2.78	2.43	2.13	2.15	3.23	2.88	2.89	0.88	2.99	3.50	3.46	2.92
P_2O_5	1.30	1.07	0.42	0.84	0.48	0.38	0.57	0.36	0.20	0.12	0.35	0.52	0.49	0.5
MnO	0.20	0.21	0.17	0.24	0.27	0.20	0.20	0.22	0.20	0.20	0.20	0.20	0.22	0.20
Total	99.67	99.83	99.86	100.18	100.03	99.13	100.1	100.12	100.1	100.2	99.74	100.81	99.92	99.9
						TRACE ELEMENTS (PPM)								
Ba	1350	1281	1085	1252	-	738	966	-	406	77	824	640	534	634
Sr	930	578	565	594	-	872	606	-	686	120	630	676	557	569
Rb	38	45	31	44	-	20	22	-	28	6	45	23	26	20
Zr	345	410	340	366	-	165	312	-	250	35	242	280	307	315
Zn	145	100	114	111	-	70	100	-	73	38	82	52	78	59
Y	59	55	52	37	-	33	25	-	22	21	62	59	50	56
Cu	30	7	25	12	-	5	-	-	52	105	32	68	-	14
Nb	-	65	51	56	-	28	30	-	-	-	35	-	65	52
Ni	9	-	-	3	-	-	-	-	-	-	19	-	-	-
La	-	-	48	47	-	-	-	-	-	-	-	21	-	-
Ce	-	-	-	82	-	-	-	-	-	-	-	50	-	-
Th	-	-	6	<5	-	-	-	-	-	-	-	-	-	-
Pb	-	-	7	9	-	-	-	-	-	-	-	-	-	-
Ga	-	-	-	-	-	-	-	-	-	-	-	-	-	-
						CIPW NORMATIVE MINERALS								
Qz	0.0	0.0	1.2	0.1	0.0	0.7	0.0	0.0	0.0	0.6	0.0	0.0	0.0	0.0
Or	11.9	14.2	6.6	12.6	11.1	5.9	7.8	7.8	9.1	0.5	7.3	6.0	6.1	7.3
Ab	43.1	41.7	37.6	41.2	38.9	35.5	34.2	38.3	51.6	14.7	33.2	35.3	35.5	38.7
An	15.9	14.1	27.6	18.9	14.5	32.9	24.0	23.1	11.8	41.0	22.7	23.0	23.8	21.2
Ne	0.0	0.0	0.0	0.0	5.6	0.0	0.0	0.0	0.92	0.0	1.8	0.0	1.2	0.5
Di	1.4	3.8	7.7	3.4	6.5	4.6	7.8	9.1	0.0	23.0	7.5	11.0	5.6	7.9
Hy	6.4	13.1	6.1	10.1	0.0	11.1	13.5	2.0	0.0	12.3	0.0	0.9	0.0	0.0
Ol	8.3	2.3	0.0	0.0	10.7	0.0	0.3	6.0	5.5	0.0	17.4	9.5	12.2	9.1
Mt	5.9	4.4	6.7	7.1	5.0	4.3	4.8	6.0	0.0	6.0	3.6	6.3	7.7	8.4
Il	3.9	3.9	5.4	4.7	4.1	4.2	6.2	5.5	0.6	1.7	5.8	6.7	6.7	5.7
Ap	3.1	2.6	1.0	2.0	1.3	0.9	1.4	0.8	0.5	0.3	0.8	1.2	1.2	1.2
OR	16.8	20.3	9.2	17.3	17.2	7.9	11.9	11.3	12.5	0.9	11.5	9.3	9.4	10.8
AB	60.8	59.6	52.3	56.7	60.3	47.8	51.8	55.3	71.2	26.1	52.6	54.9	54.3	57.6
AN	22.5	20.1	38.5	26.0	22.5	44.4	36.3	33.4	16.3	73.1	36.0	35.8	36.3	31.6
D.I.	55.0	55.9	45.5	53.9	55.6	42.0	42.1	46.1	61.5	15.7	42.2	41.3	42.9	46.5

1 B (continued)

Analysis Number	Location	Rock type	Distance above base (cm)
18.	Roineval. Top of massif. Groundmass analysis only	PH	1600-1800
19.	Ben Horneval. Western slope, due east of Dunvegan. Middle of 2 m high cliff; first break in slope	AKB	
20.	Ben Horneval. Same location as above. second break in slope, middle of outcrop	H	
21.	Ben Horneval. Same location as above. Flow just below small knob, several hundred metres to the south of the trig station on Ben Horneval	H	
22.	Ben Horneval. Same location as above. Flow exposed in knob at top. Lies just above (21)	PH	

TABLE 1B (contd.)

Analysis No.	15	16	17	18	19	20	21	22
Field No.	R-1	R-2	R-3	R-5G	BH-1	BH-2	BH-3	BH-5
SiO_2	50.3	49.9	50.4	48.7	45.3	46.7	45.2	50.9
Al_2O_3	15.5	15.5	15.7	17.3	16.1	16.6	17.0	16.0
Fe_2O_3	5.90	5.22	4.77	2.39	4.32	3.90	3.31	3.10
FeO	6.75	7.09	7.01	9.72	9.61	9.20	10.28	9.16
MgO	3.8	3.4	4.2	3.9	7.7	5.0	6.5	4.3
CaO	6.4	6.2	6.2	7.9	9.3	6.9	8.6	7.8
Na_2O	4.69	4.51	4.65	4.25	2.78	4.34	3.74	3.93
K_2O	1.82	1.92	1.80	1.12	0.34	0.60	0.34	1.35
H_2O^+	1.28	1.91	1.23	1.25	1.91	2.51	1.35	0.86
TiO_2	2.85	2.83	2.79	3.00	2.65	3.45	2.74	1.90
P_2O_5	0.61	0.65	0.68	0.49	0.3	0.6	0.3	0.4
MnO	0.27	0.25	0.26	0.17	0.18	0.20	0.18	0.17
Total	100.1	99.8	99.9	100.1	100.4	99.4	99.5	99.9
				TRACE ELEMENTS (PPM)				
Ba	1255	1190	1239	743	109	207	147	912
Sr	719	650	727	693	562	930	729	505
Rb	33	32	35	20	4	2	4	16
Zr	313	320	317	283	193	277	196	166
Zn	104	102	94	91	95	70	76	88
Y	53	57	52	38	26	35	36	30
Cu	44	11	40	-	122	52	13	35
Nb	-	56	70	36	28	44	33	22
Ni	8	-	7	23	-	34	-	36
La	39	29	52	-	22	<20	12	88
Ce	92	87	82	-	39	40	45	26
Th	-	-	<6	-	<5	<5	<5	<5
Pb	-	-	-	-	<5	9	<5	<5
Ga	-	-	-	-	17	-	-	19
				CIPW NORMATIVE MINERALS				
Qz	0.0	0.0	0.0	0.0	0.0	0.0	0.0	0.0
Or	10.9	11.7	10.8	6.7	2.0	3.7	2.1	8.1
Ab	40.3	39.2	40.0	36.1	23.7	38.2	28.5	33.6
An	16.1	16.8	16.9	25.1	30.5	24.9	29.2	22.2
Ne	0.0	0.0	0.0	0.2	0.0	0.0	2.0	0.0
Di	9.9	8.7	7.9	9.3	10.8	7.1	10.2	12.2
Hy	1.9	4.6	4.8	0.0	9.8	0.8	0.0	11.1
Ol	9.1	7.5	7.5	12.3	9.6	13.6	17.3	3.8
Mt	5.0	4.5	5.0	3.5	6.3	5.9	4.9	4.5
Il	5.5	5.5	5.4	5.8	6.4	5.2	5.3	3.7
Ap	1.5	1.6	1.6	1.2	1.0	0.7	0.7	0.8
OR	16.2	17.2	16.0	9.9	3.6	5.5	3.5	12.6
AB	59.9	58.0	59.0	53.2	42.1	57.2	47.7	52.7
AN	23.9	24.8	25.0	36.9	54.3	37.3	48.8	34.7
D.I.	51.1	50.9	50.8	43.0	25.7	41.8	32.4	41.7

KEY TO ANALYSES OF TABLE 1 C

Analysis Number	Location
1.	Analyses 1 - 5 are from a single 1.5m. wide dyke on the eastern shore of the small inlet below the composite flow at the "Dun". The inlet is part of Fiskavaig Bay; the dykes are to the west of the rocky promontory Sgurr nan Uan.
2.	0.60 metres from the N.E. side (contact) of dyke.
3.	0.95 metres from contact.
4.	0.84 metres from contact.
5.	Anorthosite from contact rock.
6.	Central portion of a dyke exposed nearby, approximately 1.0 - 1.2 metres wide.
7.	Central portion of dyke to S.W. of dyke in analysis (6); 1.2m. wide.
8.	Ullinish Point, dyke mapped as mugearite on the North Skye sheet. It is 2.84 metres from the western contact of the dyke (3 metres wide). Dyke marked as X^{m} on map.
9.	Same dyke as (8); 1:00 metre from western contact.
10.	Smaller, phenocryst free dyke (30 - 50cm. wide), possibly an apophyses of the larger dyke.
11.	A small (30 - 35cm. wide) dyke immediately to the west of the large "mugearite" dyke. Contact sample.
12.	Next dyke to west, 35 - 40cm. wide. Contact sample.
13.	Vidigill Burn: 13 is the central benmoreite.
14.	Marginal "basaltic" part of (13).
15.	Isolated flow of hawaiite exposed in a road cut by the fifth passing place going north, from the sharp bend where the road goes over the Summardale River.
16.	Analysis of phenocryst free margins of a plagioclase-phyric dyke exposed in prominent knob on the north bank of the Summardale River, below (15).
17.	Analyses 17 and 18 are of dyke rocks exposed at Ardtreck Point, which lies almost due east of the localities collected at Ullinish Point , and N.N.E. of

of Fiskavaig Bay. The dykes were exposed on the shore below the "Dun". Centre of a 1.5 metre wide dyke striking north, nearly vertical, on north side of inlet.

18. Same dyke, within 10cm. of eastern contact.
19. Preshal More; collected from the lowest tier of columnar joints, above platy volcanics.
20. Same massif as above, several metres to left.
21. Analysis of benmoreite flow near Tortador by J.H.Scoon; Muir and Tilley (1961).
22. Analysis of benmoreite dyke near Portree (Am Bile) by J.H.Scoon; Tilley et al. (1967).
23. Analysis of Am Bile dyke; approximately 60cm. from southern contact.
24. Analysis of Am Bile dyke; approximately 1.5cm. from southern contact.
25. Analyses 25 - 28 are of isolated hawaiite flows near the base of Preshal More. Analysis 25 is the flow directly below the first columnar joints, or the third break in slope above the road leading to Talisker.
26. Flow at second break in slope above road.
27. Flow at first break in slope above road.
28. Flow from small knob on the western side of the massif, same level as (27).
29. Analyses 29 - 31 are of isolated flows at Fiskavaig Bay, as described for analyses 1 - 5. Analysis 29 is of a massive flow above the dyke of analyses 1 - 5.
30. Flow just below (29).
31. Platy flow in small cliff near the dyke of analysis 7.
32. Dike exposed in stream cut east of Balmeanach on the east shore of Loch Caroy. Possibly the dyke marked as U on the North Skye sheet.
33. Gabbro dyke (marked as U^{A}) across road, to south of (32).
34. Olivine rich dyke from the pier at Dunvegan. Marked as "picrite" on North Skye sheet.
35. Isolated hawaiite flow collected near Tortador, at end of Loch Beagoon the north side of the Loch.

TABLE 1C

Single Flows and Dykes from localities in the vicinity of the composite flows on North Skye

Analysis No.	1	2	3	4	5	6	7	8	9	10	11	12	13	14	15	16	17	18	19	20	21	22	23	24	25	26	27	28	29	30	31	32	33	34	35
Field No.	FA-1	FA-2	FA-3	FA-5	FA-OB	FA-8	FA-9	UD-6	UD-7	UD-8	UD-2	UD-4	Vid.B 10A	Vid.B 10B	SH-8	SH-9	ARD-3	ARD-4	FM-2	FM-3			AB-2	AB-3	FM-1	FM-4	FM-5	FM-6	FA-6	FA-7	FA-10	SB-2	SB-3	D-1	TORT-1
SiO_2	46.7	48.2	47.4	47.7	49.3	47.1	50.3	46.7	45.8	46.9	47.6	46.6	59.1	50.0	46.2	46.5	46.9	46.6	48.2	48.6	58.64	56.71	57.4	56.8	45.4	51.9	47.8	46.6	46.4	46.9	49.5	49.9	43.8	47.4	47.7
Al_2O_3	16.2	16.1	16.1	16.1	28.0	15.4	14.4	16.9	16.7	14.3	16.3	14.9	16.1	16.1	16.4	16.0	16.4	16.5	15.4	14.4	16.38	15.11	15.1	14.6	15.5	17.2	16.4	16.4	16.3	15.2	15.8	14.7	15.0	14.5	16.7
Fe_2O_3	4.09	3.82	3.06	3.18	0.87	8.36	4.90	4.38	4.65	5.36	3.46	4.05	5.66	4.71	5.06	7.32	4.20	4.20	1.47	1.94	3.05	5.18	4.84	4.48	6.73	6.35	5.19	5.94	5.98	2.68	2.36	1.65	4.36	4.06	4.10
FeO	9.21	8.58	9.30	9.35	1.33	8.14	6.77	9.81	10.80	8.43	8.11	7.95	2.08	6.61	6.16	7.82	7.20	7.20	9.82	9.01	4.91	3.67	4.10	4.52	9.96	3.63	8.65	8.36	9.34	11.35	10.08	9.82	10.04	8.24	9.45
MgO	6.0	6.2	7.2	7.7	1.4	5.2	6.9	4.4	5.1	7.8	7.3	7.6	1.4	3.7	3.5	4.5	7.9	7.7	9.0	9.0	1.06	1.45	1.7	2.0	5.7	4.0	4.4	4.6	5.3	7.5	5.5	6.0	9.2	8.4	4.2
CaO	8.6	10.1	9.6	9.7	13.6	6.7	10.8	7.7	7.6	12.2	12.7	13.1	3.1	7.4	6.5	7.0	12.1	12.4	12.7	13.1	2.90	3.61	4.3	3.9	7.8	6.0	6.8	6.8	6.9	9.6	8.1	9.8	8.0	13.2	7.6
Na_2O	2.92	2.93	3.10	3.08	3.19	3.79	2.60	3.86	3.48	2.28	2.17	2.20	6.49	3.96	4.10	4.14	2.22	2.30	1.74	1.71	6.07	5.01	4.88	5.06	3.21	4.64	4.63	4.03	4.20	2.86	4.52	2.89	3.10	1.94	4.36
K_2O	0.76	0.48	0.50	0.56	0.18	1.22	0.61	0.98	1.01	0.12	0.08	0.24	3.67	2.04	1.28	0.85	0.12	0.26	0.10	0.08	3.49	3.54	3.27	3.61	0.88	2.37	1.15	1.07	0.43	0.53	0.47	0.83	0.29	0.08	0.96
H_2O^+	1.66	1.34	1.30	1.26	1.76	1.22	1.10	1.85	1.78	1.35	0.86	1.79	1.22	2.86	2.60	2.51	2.01	1.79	0.61	1.31	0.55	1.14	1.32	1.54	1.82	1.91	1.81	2.05	1.67	1.15	1.34	0.59	4.05	0.93	1.78
TiO_2	2.97	1.42	1.19	1.35	0.10	3.06	1.12	2.55	2.65	1.10	0.99	1.03	0.99	1.66	2.89	3.19	0.90	0.70	0.86	0.89	0.89	1.80	1.93	1.85	2.61	2.14	3.03	3.20	3.36	1.21	1.33	0.85	2.19	0.84	3.50
P_2O_5	0.4	0.2	0.2	0.2	0.1	0.4	0.3	0.4	0.3	0.1	0.1	0.1	0.5	0.5	0.6	0.5	0.1	0.2	0.1	0.1	0.66	0.49	0.9	0.7	0.4	0.6	0.4	0.6	0.5	0.2	0.3	0.2	0.2	0.1	0.4
MnO	0.20	0.19	0.20	0.20	0.04	0.18	0.20	0.19	0.20	0.20	0.20	0.20	0.17	0.17	0.19	0.23	0.20	0.20	0.19	0.19	0.18	0.26	0.27	0.27	0.24	0.17	0.21	0.19	0.21	0.20	0.20	0.20	0.20	0.23	0.20
T	99.7	99.5	99.2	100.3	99.9	99.8	100.1	99.7	100.1	100.1	99.9	100.3	100.4	99.7	95.5	100.6	99.7	100.1	100.2	100.3	99.90	100.35	100.0	99.3	100.3	100.8	100.5	99.8	100.6	99.5	99.7	97.4	100.4	99.9	100.8
TRACE ELEMENTS (PPM)																																			
Ba	372	358	330	357	141	887	445	626	593	28	6	-	1888	1186	657	446	16	40	50	83	1300	6400	4225	4580	515	1260	590	543	158	340	136	395	149	21	431
Sr	757	299	331	341	717	488	375	665	679	95	115	-	580	676	679	615	114	120	111	106	-		445	325	565	825	580	538	684	310	647	254	648	100	569
Rb	17	12	9	13	5	71	13	22	23	45	4	-	62,72	28	28	17	2	2	5;0	4	-	-	50	51	18	45	30	27	6	7	5	26	7	<1	23
Zr	100	84	100	66	27	131	115	140	136	48	41	-	531	211	299	309	37	80	95	40	-	-	265	260	122	315	228	326	244	100	232	111	168	38	242
Zn	65	73	85	75	n.d.	92	80	65	70	77	70	-	101	104	64	62	57	68	74	55	-	-	150	142	75	95	44	49	62	20	66	81	65	73	68
Y	30	31	41	18	n.d.	18	23	22	26	15	17	-	57	30	53	63	16	35	38	24	-	-	-	-	23	98;21	42	46	21	33	21	28	29	16	55
Cu	77	90	-	118	25	62	124	17	19	189	177	-	26	84	50	58	143	-	-	118	-	-	11	14	8	21	22	43	22	92	24	105	80	164	56
Ni	-	-	-	-	-	-	-	-	-	-	-	-	-	37	7	7	-	-	-	-	-	-	-	-	-	-	-	-	-	-	-	-	-	-	-	-
La	-	-	-	-	-	-	-	-	-	-	-	-	60	32	53	22	-	-	-	-	-	-	-	-	-	-	-	-	-	-	-	-	-	-	<5
Ce	-	-	-	-	-	-	-	-	-	-	-	-	115	80	47	33	-	-	-	-	-	-	-	-	-	-	-	-	-	-	-	-	-	-	28
Ga	-	-	-	-	-	-	-	-	-	-	-	-	16	19	13	9	-	-	-	-	-	-	-	-	-	-	-	-	-	-	-	-	-	-	-
CIPW NORMATIVE MINERALS																																			
Qz	0.0	0.0	0.0	0.0	0.0	0.0	0.4	0.0	0.0	0.0	0.0	0.0	0.0	0.0	0.0	0.0	0.0	0.0	0.0	0.0	2.16	6.90	8.3	5.2	0.0	0.2	0.0	0.0	0.0	0.0	0.0	0.0	0.0	0.0	0.0
Or	4.6	2.9	3.0	3.3	1.1	7.3	3.8	5.9	6.1	0.7	0.5	1.45	21.9	12.5	8.1	5.1	0.7	1.6	0.6	0.5	20.94	20.57	19.6	21.8	5.3	14.1	6.9	6.5	2.6	3.2	2.8	5.1	1.8	0.5	5.7
Ab	25.2	25.2	26.8	26.3	27.5	32.6	22.3	33.0	30.0	19.5	18.5	19.0	55.4	34.7	37.3	35.7	19.1	19.8	14.8	14.6	51.35	42.44	41.8	43.8	27.6	39.7	38.3	34.9	35.9	24.6	37.3	25.5	26.9	16.6	36.6
An	29.4	29.9	29.2	28.6	62.6	21.7	26.2	26.4	27.4	28.8	34.7	30.6	4.0	20.9	24.3	23.0	35.0	34.6	34.0	31.8	6.95	6.95	9.8	6.6	25.7	19.3	20.8	24.0	24.6	27.6	21.9	25.9	27.1	30.8	23.4
Ne	0.0	0.0	0.0	0.0	0.0	0.0	0.0	0.2	0.0	0.0	0.0	0.0	0.0	0.0	0.0	0.0	0.0	0.0	0.0	0.0	0.0	1.88(Cs)	0.0	0.0	0.0	0.0	0.7	0.0	0.0	0.0	0.9	0.0	0.2	0.0	0.3
Di	9.5	15.8	14.9	15.4	4.3	8.0	21.6	8.6	7.3	25.8	23.1	28.3	7.2	11.7	5.0	7.3	20.5	21.8	23.1	26.8	2.85	5.62	4.7	6.9	8.7	5.3	8.4	5.3	5.4	16.2	14.2	19.3	10.5	28.0	9.9
Hy	15.6	13.1	4.0	2.7	1.5	4.8	18.6	0.0	0.6	10.0	10.4	3.3	0.8	3.7	9.9	1.5	9.8	4.6	13.6	16.1	6.56	1.00	2.9	3.9	4.1	7.6	0.0	7.9	7.8	3.3	0.0	17.4	0.0	10.4	0.0
Ol	3.0	4.2	14.8	16.0	1.3	13.2	0.0	15.0	17.5	5.0	5.6	9.1	4.6	7.9	0.0	14.4	6.6	9.7	9.8	5.4	0.0	0.0	0.0	0.0	16.7	0.0	10.3	5.0	7.3	18.4	16.1	2.2	22.3	5.8	10.5
Mt	6.1	5.6	4.5	4.7	1.3	5.5	4.4	5.2	5.4	7.9	5.1	6.0	3.2	4.3	7.9	5.3	6.2	6.2	2.1	2.8	4.41	7.42	7.1	6.6	5.9	6.1	7.6	8.8	8.8	4.0	3.5	2.5	6.6	5.9	6.0
Il	5.8	2.7	2.3	2.6	0.2	5.9	2.2	5.0	5.1	2.1	1.9	2.0	1.9	3.3	5.9	6.2	1.7	1.4	1.6	1.7	1.67	3.50	3.7	3.6	5.0	4.1	5.8	6.2	6.5	2.3	2.6	1.7	4.3	1.7	6.7
Ap	0.9	0.6	0.5	0.4	0.3	0.9	0.7	0.9	0.8	0.2	0.2	0.3	1.1	1.1	1.5	1.3	0.3	0.3	0.3	0.2	1.68	1.34	2.2	1.7	1.0	1.4	1.1	1.5	1.2	0.5	0.8	0.5	0.4	0.3	1.0
OR	7.7	5.0	5.1	5.7	1.2	11.9	7.3	9.1	9.6	1.5	0.9	2.8	26.9	18.3	11.7	8.0	1.3	2.8	1.2	1.0	26.4	29.4	27.5	30.2	9.0	19.4	10.4	9.9	4.1	5.8	4.6	9.1	3.2	1.0	8.7
AB	42.6	43.5	45.4	45.1	30.2	52.9	42.6	50.5	47.3	39.8	34.5	37.2	68.1	50.9	53.5	56.0	34.8	35.4	29.9	31.2	64.8	60.7	58.8	60.6	47.1	54.3	58.1	53.4	56.9	44.5	60.2	45.2	48.3	34.6	55.7
AN	49.7	51.5	49.4	49.1	68.6	35.2	50.1	40.4	43.1	58.7	64.6	60.0	5.0	30.7	34.8	36.0	63.9	61.8	68.9	67.8	8.8	9.9	13.7	9.2	43.9	26.4	31.5	36.7	39.0	49.8	35.3	49.8	48.5	64.4	35.6
D.I.	29.8	28.1	29.8	29.7	28.6	40.0	26.5	39.1	36.1	20.3	19.0	20.4	77.2	47.1	45.5	41.0	19.8	21.4	15.4	15.1	74.45	69.9	69.7	70.7	32.8	54.0	46.0	41.4	38.5	27.8	41,0	30.6	28.9	17.1	42.6

KEY TO ANALYSES OF TABLE 1 D

Analysis Number	Location	Rock type
1.	Uppermost flow at North Berwick Pier; 1 metre above cliff base and contact with underlying benmoreite	H
2.	Uppermost flow; 0.5 metres from contact with underlying benmoreite. Contains 2.9 % titanite in CIPW Norm	H
3	Uppermost Flow (T.C. Day, 1930)	
4.	Middle flow; 1.5 metres above lower surface and contact with underlying alkali-olivine basalt. Contains 2.8 % in CIPW Norm	B
5.	Middle flow; central part of the flow. Contains 2.0 % titanite in the CIPW Norm	B
6.	Middle flow; Major oxide analysis by T.C. Day (1930). Trace elements are from a separate sample collected near flow top	B
7.	Mugearite-Trachyte of Muir and Tilley (1961). Specimen from Gongelton Mains, East Lothian	B
8.	Basal flow; 0.4 metres above base of cliff on east side of point, near contact with underlying tuff layer	AKB
9	Basal Flow (T.C. Day, 1930)	
10.	Dasses' Basalt I; from lower sill-like portion, southern craig. Quoted from Rutledge, 1952; Analyst: W.H. Herdsman	H
11.	Dasses' Basalt II; southern end of middle craig, 3.1 m above base. Quoted from Rutledge, 1952. Analyst: W.H. Herdsman	AKB
12.	Dasses' Basalt II; north end of southern craig. 3.7 m above base. Quoted from Rutledge, 1952. Analyst: T.C. Day	AKB
13.	Dasses' Basalt I; 30 m from northern end of north craig. Highest exposed section	
14.	Dasses' Basalt II; top of middle craig	AKB
15.	Dasses' Basalt II; 2.5 m above base in northern craig includes 17 ppm Ga	AKB
16.	St.Leonard's Sill; central porphyritic facies, from Locality D, Figure Quoted from Rutledge, 1952. Analyst: T.C. Day	AKB
17.	St.Leonard's Sill; non porphyritic facies. Locality D. Figure Contains 3.1 % Q in CIPW Norm	B

TABLE 1D

Analyses of lavas at North Berwick and the composite sills of The Royal Park, Edinburgh

Analysis No.	1	2	3	4	5	6	7	8	9	10	11	12	13	14	15
Field No.	B-3	NB-4		NB-2	NB-3			NB-1					D-1.68		D-2.68
SiO_2	46.1	46.1	45.62	56.6	56.9	56.29	55.73	44.5	45.10	48.09	46.24	46.02	51.0	47.9	46.6
Al_2O_3	15.5	17.0	18.17	18.1	17.7	16.82	17.05	15.4	15.04	20.26	17.89	16.84	19.5	17.4	17.5
Fe_2O_3	9.50	9.93	1.28	10.16	9.90	6.11	9.92	8.65	8.85	1.62	3.01	3.17	2.54	4.85	3.50
FeO	3.34	1.90	8.30	0.20	0.32	0.59	0.33	3.52	4.62	6.06	6.42	6.50	4.65	6.01	5.08
MgO	5.8	7.1	6.48	0.9	1.9	3.22	0.56	8.4	6.68	2.98	6.24	6.31	3.9	5.4	4.9
CaO	8.6	6.2	9.43	2.6	2.1	2.67	2.83	9.1	8.71	5.62	6.48	8.39	5.5	6.5	12.3
Na_2O	3.30	2.95	4.22	4.50	4.72	5.35	5.16	2.75	3.78	3.08	3.63	3.61	5.69	4.33	3.21
K_2O	2.09	1.83	1.43	4.02	3.53	3.93	4.17	1.05	1.04	1.06	1.69	1.39	0.80	2.05	1.77
H_2O^+	2.25	3.23	1.54	1.00	0.96	2.30	0.87	3.29	1.76	4.68	5.18	4.56	3.62	2.10	1.65
H_2O^-	-	-	0.47	-	-	-	0.84	-	1.31	0.92	0.83	0.53	-	-	-
TiO_2	3.42	3.50	2.09	1.44	1.37	1.27	1.41	2.63	2.66	1.64	1.70	2.15	2.09	2.10	1.90
P_2O_5	0.9	1.0	0.71	0.5	0.5	0.77	0.40	0.5	0.56	0.97	0.44	0.40	0.9	0.4	0.4
MnO	0.17	0.19	0.35	0.18	0.18	0.09	0.13	0.21	0.45	0.06	0.09	0.22	0.07	0.27	0.17
CO_2	-	-	0.0	-	-	0.30	0.62	-	0.0	2.73	-	0.40	-	-	-
Total	100.9	100.9	100.09	100.2	100.1	99.71	100.18	100.0	100.60	99.77	99.84	100.49	100.2	99.9	99.1
						TRACE ELEMENTS (PPM)									
						NB-5									
Ba	848	760	-	1660	1360	1378	1600	625	-	-	-	-	123	790	645
Sr	666	622	-	490	430	430	-	614	-	-	-	-	332	667	836
Rb	52	44	-	126	99	118	-	28	-	-	-	-	16	46	42
Zr	207	252	-	400	420	622	-	170	-	-	-	-	297	238	201
Zn	119	592	-	50	245	118	-	116	-	-	-	-	67	161	49
Y	37	41	-	65	65	59	-	25	-	-	-	-	52	37	29
Cu	8	24	-	10	20	4	-	24	-	-	-	-	-	31	35
Nb	-	-	-	-	-	88	-	31	-	-	-	-	-	-	-
La	30	-	-	-	-	-	-	-	-	-	-	-	46	15	26
Ce	-	-	-	-	-	-	-	-	-	-	-	-	115	73	39
Ni	28	-	-	-	-	-	-	-	-	-	-	-	20	30	23
						CIPW NORMATIVE MINERALS									
Qz	-	1.8	-	5.2	5.6	-	1.1	-	-	17.6	-	-	-	-	-
Or	12.6	11.1	8.6	24.0	21.0	23.8	25.1	6.4	6.3	6.7	10.6	8.6	4.9	12.5	10.7
Ab	24.3	25.5	17.9	38.5	40.3	46.5	44.7	22.8	24.5	27.7	31.9	28.7	49.8	30.1	14.2
An	21.5	24.8	26.9	9.8	7.2	6.5	7.5	27.5	21.5	4.6	29.3	26.9	22.1	22.6	28.9
Ne	2.2	-	10.0	-	-	-	-	0.7	4.5	-	0.5	1.8	-	4.1	7.4
C	-	1.3	-	2.9	3.5	1.5	1.3	-	-	13.2	-	-	1.5	-	-
Di	12.8	-	13.1	-	-	-	-	12.8	15.6	-	1.5	9.2	-	6.4	25.3
Hy	1.2	15.8	-	12.1	14.8	14.1	11.3	-	-	15.5	-	-	6.0	-	-
Ol	13.0	7.9	15.8	-	-	-	-	18.9	16.0	-	17.8	14.8	6.6	15.2	5.7
Mt	4.9	4.4	1.9	3.6	3.8	2.6	3.9	4.6	5.1	2.5	3.7	3.8	2.9	4.0	3.1
Il	6.6	6.8	4.1	2.8	2.6	2.5	2.7	5.2	5.2	3.3	3.4	4.3	4.1	4.1	3.7
Ap	2.2	2.4	1.9	1.2	1.2	1.9	1.0	1.2	1.4	2.4	1.1	1.0	2.2	1.0	1.0
Cc	-	-	-	-	-	0.7	1.4	-	-	6.6	-	1.0	-	-	-
OR	21.6	18.1	16.1	33.2	30.7	31.0	32.5	11.3	12.0	17.2	14.8	13.4	6.4	19.2	19.9
AB	41.6	41.5	33.5	53.3	58.8	60.5	57.8	40.2	46.8	71.0	44.4	44.7	64.8	46.2	26.4
AN	36.8	40.4	50.4	13.5	10.5	8.5	9.7	48.5	41.2	1.2	40.8	41.9	28.8	34.6	53.7
D.I.	39.1	38.4	36.5	67.7	66.9	70.3	70.9	29.9	35.3	52.0	43.0	39.1	54.7	46.7	32.3

Analysis Number	Location	Rock type
18.	St.Leonard's Sill; porphyritic facies. Locality D, Figure	AKB
19.	Craigmarloch Wood. Upper "andesine mugearite" of Kennedy, 1932. Analyst: B.E.Dixon	M
20.	Same rock type collected at same locality. New analysis	M
21.	Craigmarloch Wood. Interior of flow unit; "Trachyandesite" of Kennedy, 1932. Analyst: B.E.Dixon	B
22.	Same rock type collected at same locality	B

TABLE 1D (contd.)

Analysis No.	16	17	18	19	20	21	22
Field No.		STLS-2	STLS-3		KW-1		KW-2
SiO_2	48.43	55.0	44.1	48.04	53.7	63.89	62.1
Al_2O_3	15.84	17.0	15.1	14.93	15.3	14.33	15.3
Fe_2O_3	3.65	8.02	2.13	12.16	9.89	4.75	6.41
FeO	6.89	0.90	9.10	2.33	1.87	1.14	0.88
MgO	5.09	3.0	8.2	3.45	3.2	1.30	1.40
CaO	7.21	3.7	7.0	6.81	5.5	1.98	2.3
Na_2O	4.65	5.10	5.00	4.74	4.85	5.85	6.20
K_2O	2.02	0.45	0.67	1.94	1.65	3.68	2.56
H_2O^+	2.39	2.60	5.91	1.00	1.10	0.79	1.00
H_2O^-	0.37	-	-	0.95	-	0.52	-
TiO_2	2.56	1.35	2.00	3.50	2.22	1.24	0.98
P_2O_5	0.52	0.7	0.5	0.55	1.1	0.59	0.31
MnO	0.21	0.20	0.20	0.14	0.18	0.21	0.19
CO_2	0.16	2.0	-	-	-	-	-
Total	100.0	99.7	99.9	100.54	99.7	100.27	99.4
			TRACE ELEMENTS (PPM)				
Ba	-	160	550	-	565	-	710
Sr	-	130	562	-	460	-	385
Rb	-	8	20	-	27	-	54
Zr	-	335	205	-	324	-	425
Zn	-	345	40	-	290	-	530
Y	-	48	33	-	49	-	66
Cu	-	18	33	-	20	-	14
Nb	-	-	-	-	-	-	-
La	-	-	-	-	-	-	-
Ce	-	-	-	-	-	-	-
Ni	-	-	-	-	-	-	-
			CIPW NORMATIVE MINERALS				
Qz	-	14.9	-	-	2.1	9.8	7.7
Or	12.3	2.7	4.2	11.6	9.8	22.0	15.4
Ab	31.5	44.3	25.7	33.4	41.2	50.0	53.3
An	16.8	1.2	17.9	13.9	15.2	2.1	6.6
Ne	4.9	-	10.5	4.0	-	-	-
C	-	7.9	-	-	-	-	-
Di	12.6	-	12.6	13.9	4.2	3.4	2.7
Hy	-	17.1	-	-	16.4	6.9	9.6
Ol	11.4	-	20.6	9.6	-	-	-
Mt	3.9	3.0	3.3	5.6	4.3	2.1	2.6
Il	5.0	2.6	4.0	6.7	4.2	2.4	1.9
Ap	1.3	1.7	1.3	1.3	2.6	1.4	0.8
Cc	0.4	4.7	-	-	-	-	-
OR	20.3	5.6	8.8	19.7	14.8	29.7	20.5
AB	52.0	91.9	53.8	56.7	62.2	67.5	70.8
AN	27.7	2.5	37.4	23.6	23.0	2.8	8.7
D.I.	48.7	61.9	40.4	49.0	53.1	81.8	76.4

KEY TO ANALYSES IN TABLE 1 E

Analysis Number	Location	Rock type	Height above base (cm)
1.	Lowest exposure on cliff face. Whole rock	M	0
2.	Above (1) but to the right by 3 metres. Whole rock	M	10
3.	Above (2) nearly aphyric. Whole rock	M	80
4.	Above (3) by 10 cm. Whole rock	M	90
5.	Groundmass of (4)	M	90
6.	To right of (4) by 50 cm. Junction of two units. Whole rock	M	95
7.	Groundmass of (6)	M	95
8.	Above (6) by 10-12 cm. Above junction of two units by 5 cm. Whole rock	PH	105-110
9.	Groundmass of (8)	PH	105-110
10.	Same level as (6), but to right by 30 cm. Whole rock	PH	95
11.	Groundmass of (10)	PH	95
12.	10-20 cm above (10) but 6 metres to right of it. Whole rock	PH	105-115
13.	Groundmass of (12)	PH	105-115
14.	1 m above (12). Whole rock		210
15.	Groundmass of (14)		
16.	Highest exposed outcrop in cliff. 100-150 m ESE of (14) 1.0 to 1.5 m above (14). Whole rock	PH	310-360
17.	Groundmass of (16)		
18.	Analysis of lower unit in composite flow. Quoted from Kennedy (1931)	M	?
19.	Analysis of upper unit in composite flow. Quoted from Kennedy (1931)	PH	?
20.	Flow below composite flow. Exposure 500-600 m WNW	M	-

TABLE 1E

The composite flow to the south of Greenock, near Loch Thom, Western Scotland

Analysis No.	1	2	3	4	5	6	7	8	9	10	11	12	13	14	15
Field No.	LT-1	LT-2	LT-3	LT-4	LT-4G	LT-5	LT-5G	LT-6	LT-6G	LT-7	LT-7G	LT-8	LT-8G	LT-9	LT-9G
SiO_2	51.5	50.9	50.7	49.7	48.3	50.5	50.3	50.3	49.3	50.5	49.4	50.4	48.8	50.5	49.4
Al_2O_3	15.9	16.2	16.4	18.2	17.1	17.2	16.4	16.4	15.5	19.2	16.8	18.2	17.4	18.3	16.6
Fe_2O_3	9.34	9.71	7.50	8.00	9.45	9.31	9.85	9.43	10.10	6.01	3.62	7.66	4.72	8.01	3.51
FeO	1.74	1.74	1.77	1.79	2.40	1.89	2.02	1.92	2.30	1.81	6.29	1.85	7.14	2.00	8.13
MgO	3.7	4.5	4.2	3.5	3.5	3.7	3.7	3.6	3.9	3.6	4.5	3.8	3.8	3.5	4.1
CaO	6.9	6.4	7.9	8.8	8.5	7.6	7.3	8.0	7.6	9.4	9.1	8.6	8.5	8.7	8.3
Na_2O	4.31	4.13	4.15	4.53	3.55	3.63	3.51	4.10	3.70	3.92	3.51	3.96	3.75	3.63	3.75
K_2O	1.95	1.80	1.67	1.49	1.52	1.83	1.84	1.91	1.73	1.65	1.60	1.65	1.51	1.61	1.62
H_2O^+	1.03	1.64	0.9	0.94	1.39	0.92	0.97	0.76	0.97	1.02	1.27	0.93	1.17	0.84	0.98
TiO_2	3.16	3.07	2.80	2.61	3.00	3.02	3.23	3.05	3.58	2.33	2.91	2.64	3.04	2.65	3.21
P_2O_5	0.6	0.6	0.5	0.5	0.4	0.3	0.6	0.6	0.5	0.6	0.6	0.5	0.5	0.4	0.4
MnO	0.31	0.20	0.18	0.20	0.39	0.18	0.19	0.15	0.19	0.22	0.28	0.18	0.23	0.16	0.19
Total	99.9	100.1	99.9	100.2	99.5	99.5	99.9	100.2	99.4	100.1	99.9	100.4	100.3	100.3	99.7
							TRACE ELEMENTS IN PPM								
Ba	624	460	613	533	516	571	531	538	529	464	620	510	475	513	608
Sr	488	478	509	645	637	605	515	628	592	674	523	652	638	672	546
Rb	60	47	52	37	42	45	49	42	43	36	45	34	37	37	44
Zr	315	303	308	248	247	295	315	271	285	234	278	248	252	245	289
Zn	111	135	116	96	108	110	125	93	93	77	99	112	122	89	114
Y	25	27	29	42	26	46	32	41	37	37	28	40	36	38	26
Cu	6	<5	33	32	4	29	3	40	40	39	39	11	9	34(?)	7
Nb	110	111	100	-	92	-	88	-	-	-	64	-	-	-	83
La	41	20	41	-	-	28	-	31	-	-	-	33	-	-	-
Ce	61	65	68	58	-	43	-	46	-	-	-	84	-	-	-
Ni	7	10	8	8	<5	6	5	6	3	7	7	7	7	6	<5
Pb	17	19	22	7	-	13	-	8	-	14	-	17	-	13	-
Ga	-	17	-	21	-	20	-	18	-	16	-	-	-	15	-
							CIPW NORMATIVE MINERALS								
Qz	0.0	0.0	0.0	0.0	0.0	1.2	0.7	0.0	0.0	0.0	0.0	0.0	0.0	0.0	0.0
Or	11.8	10.6	10.0	8.9	9.2	11.0	11.4	11.4	10.4	8.1	9.6	9.8	9.2	9.5	9.7
Ab	37.3	35.5	35.4	34.8	30.6	31.4	30.0	34.9	31.9	33.7	30.1	33.7	30.8	30.8	32.0
An	18.8	21.0	24.2	25.2	26.9	23.5	23.6	21.0	21.1	31.3	25.7	27.5	28.0	29.1	23.8
Ne	0.0	0.0	0.0	2.2	0.0	0.0	0.0	0.0	0.0	0.0	0.0	0.0	0.0	0.0	0.0
Di	10.6	6.2	10.0	12.8	9.3	9.1	7.9	12.5	11.4	10.2	13.0	9.8	9.7	10.0	12.1
Hy	9.7	14.5	5.2	0.0	7.9	12.5	14.7	2.9	11.3	2.8	7.0	4.5	9.5	9.7	5.2
Ol	1.5	1.2	5.2	4.9	4.7	0.0	0.0	6.0	1.3	5.4	3.7	4.6	2.0	0.9	5.8
Mt	3.0	4.0	3.6	5.0	4.5	4.1	4.3	4.1	4.5	2.9	3.8	3.8	3.7	3.9	4.2
Il	6.1	5.8	5.4	5.0	5.9	5.9	0.1	5.8	6.9	4.5	5.6	5.2	5.9	5.0	6.1
Ap	1.2	1.4	1.2	1.1	1.0	1.4	1.3	1.4	1.3	1.2	1.5	1.1	1.2	1.0	1.0
Or	17.4	15.8	14.3	12.9	13.7	16.8	17.5	16.9	15.6	11.1	14.7	13.8	13.5	13.7	14.7
Ab	54.9	52.9	51.0	50.5	46.0	47.6	46.2	51.9	50.6	46.1	46.1	47.5	45.3	44.4	48.9
An	27.7	31.3	34.7	36.6	40.3	35.6	36.3	31.2	33.9	42.9	39.3	38.7	41.2	41.9	36.4
D.I.	49.1	46.1	45.4	45.8	39.8	43.6	42.1	46.3	41.3	41.8	39.7	43.6	40.0	40.3	41.6

TABLE 1E (Contd.)

Analysis No.	16	17	18	19	20
Field No.	LT-10	LT-10G			LT-14
SiO_2	48.0	48.1	48.40	47.71	53.8
Al_2O_3	19.9	19.3	16.66	18.09	16.6
Fe_2O_3	6.00	6.20	8.54	8.57	7.45
FeO	2.76	3.05	2.85	2.61	1.62
MgO	3.6	4.0	4.85	4.45	3.5
CaO	9.4	9.2	7.44	8.52	5.3
Na_2O	4.13	3.80	3.42	3.58	4.70
K_2O	1.90	1.25	1.76	1.68	2.43
H_2O^+	1.65	1.60	1.19	1.12	1.30
TiO_2	2.24	2.69	3.06	2.52	2.34
P_2O_5	0.3	0.4	0.49	0.41	0.7
MnO	0.16	0.16	-	-	0.19
Total	100.0	99.8	99.90	100.26	99.9
	TRACE ELEMENTS IN PPM				
Ba	437	444	-	-	660
Sr	713	647	-	-	540
Rb	34	39	-	-	74
Zr	195	240	-	-	345
Zn	89	97	-	-	216
Y	30	23	-	-	40
Cu	44-45	4	-	-	<1
Nb	-	89	-	-	-
La	18	-	-	-	-
Ce	46	-	-	-	-
Ni	11	12	-	-	<5
Pb	-	-	-	-	-
Ga	16	-	-	-	-
	CIPW NORMATIVE MINERALS				
Qz	0.0	0.0	0.0	0.0	0.3
Or	11.4	7.5	10.8	10.1	14.6
Ab	24.1	31.4	30.0	28.7	40.3
An	30.6	32.6	25.8	28.8	17.3
Ne	6.2	0.7	0.0	1.2	0.0
Di	11.8	8.8	7.4	9.4	3.9
Hy	0.0	0.0	11.0	0.0	14.3
Ol	7.5	9.4	3.9	12.2	0.0
Mt	3.2	3.5	3.9	3.8	3.1
Il	4.3	5.2	6.0	4.9	4.6
Ap	0.8	1.0	1.2	1.0	1.7
Or	17.2	10.5	16.2	15.0	20.4
Ab	36.5	43.9	45.0	42.5	55.0
An	46.3	45.6	38.7	42.7	24.6
D.I.	41.7	39.6	40.8	40.0	54.9

KEY TO ANALYSES OF TABLE 1 G

Analysis Number	Location (All location numbers refer to Figure in the text)	Distance from contact (cm)
1.	Locality 1. Dyke cutting southern giant gabbro east coast of Tugtutôq	5
2.	Same as (1)	20
3.	Same as (1)	100
4.	Same as (1)	500
5.	Locality 2. 11 m wide dyke on south coast of Tunugdliarfik	5
6.	Same as (5)	80
7.	Same as (5)	130
8.	Same as (5)	190
9.	Locality 3. Basic margin of larvikitic syeno-gabbro (Dyke 4 of Bridgwater and Harry, 1968)	0
10.	Locality 4. Chilled contact of Dyke 12 of Bridgwater and Harry, 1968	0
11.	Locality 5. Dyke 12 at the margin of the Ice cap	0
12.	Same as (11)	50
13.	Same as (11)	centre
14.	Locality 6. Dyke 12,3 km west of the mouth of Isortoq	50
15.	Same as (14)	300
16.	Same as (14)	400
17.	Locality 7. Recalculated analysis of central portion of Dyke 12. Graphical adjustment by removal of 31 % phenocrysts of plagioclase (An_{48})	650
18.	Locality 8. Dyke on Tugtutôq, NW of Sigsardluqtôq	10
19.	Same as (18). At first appearance of plagioclase megacrysts	120
20.	Same as (18). In central porphyritic facies	130
21.	Same as (18) " " " "	170
22.	Same as (18) " " " "	400

TABLE 1G

Analysis of composite dykes in South-west Greenland

Analysis No.	1	2	3	4	5	6	7	8	9	10	11	12	13	14	15
Field No.	80002	80003	80004	80005	42654	42655	42656	42658	25352	44898	61170	61171	61172	33011	33012
SiO_2	66.64	61.21	60.42	48.16	51.40	51.43	49.88	49.04	49.38	57.57	58.04	53.75	52.20	57.93	56.20
Al_2O_3	13.08	14.32	15.55	14.70	15.35	15.73	14.95	15.10	18.35	14.61	15.27	14.95	15.40	14.75	15.18
Fe_2O_3	3.33	2.88	2.74	6.86	2.16	3.26	3.59	4.24	2.15	1.53	2.86	3.29	3.20	3.66	6.25
FeO	4.36	5.47	5.06	5.14	7.13	6.59	7.46	6.90	7.56	7.49	5.69	6.92	7.55	4.89	3.00
MgO	0.20	0.30	0.86	3.56	2.43	2.44	3.20	3.39	5.86	1.33	1.06	2.18	2.51	0.82	1.60
CaO	1.50	2.86	3.04	7.08	5.19	5.03	6.12	6.29	8.40	3.35	3.61	5.46	6.07	3.56	4.32
Na_2O	7.70	8.08	8.59	4.66	6.24	4.53	3.99	3.80	3.54	4.54	4.86	4.79	4.48	3.87	4.18
K_2O	1.39	2.18	1.02	2.92	2.11	4.58	4.19	3.83	0.97	4.92	5.12	3.10	3.10	6.03	4.69
H_2O^+	0.70	0.82	1.04	1.26	2.11	2.12	2.19	2.38	1.50	1.50	1.20	1.51	1.54	2.05	1.59
H_2O^-										0.32					
TiO_2	0.71	0.95	1.28	2.99	2.20	2.35	2.69	2.68	1.11	1.50	1.42	2.06	2.25	1.37	1.66
P_2O_5	0.08	0.18	0.40	1.62	1.11	1.25	1.69	1.85	0.23	0.53	0.53	0.96	0.92	0.53	0.78
MnO	0.20	0.21	0.20	0.20	0.12	0.15	0.12	0.20	0.13	0.23	0.18	0.20	0.21	0.18	0.20
CO_2					2.20										
Total	99.89	99.46	100.20	99.25	99.75	99.46	100.07	99.90	99.68	99.42	99.84	99.17	99.43	99.64	99.65
TRACE ELEMENTS (PPM)															
Ba	71	72	460	3757	1542	2875	2889	2436	592	2711	2624	2700	2348	2539	3793
Sr	6	8	293	852	573	819	842	944	497	131	115	312	429	145	290
Rb	15	24	6	63	72	102	120	118	16	63	68	44	52	76	68
Zr	933	425	309	16620	336	350	287	255	146	391	405	338	298	407	358
Zn	242	166	136	130	199	162	154	130	74	152	148	139	121	117	168
Y	77	42	28	28	35	36	37	38	4	36	40	38	32	36	41
Cu	-	-	-	-	-	-	-	-	-	-	-	-	-	-	-
Nb	328	150	95	68	151	125	76	57	8	39	47	29	19	57	40
Ni	2	1	n.d.	4	2	9	6	6	61	4	3	10	14	2	4
CIPW NORMATIVE MATERIALS															
Qz	11.7	0.0	0.0	0.0	0.0	0.0	0.0	0.0	0.0	2.6	0.8	0.1	0.0	3.4	2.3
Or	8.3	13.1	6.1	17.6	12.8	27.8	25.3	23.2	5.9	29.8	30.7	18.8	18.7	36.5	28.3
Ab	60.0	62.4	73.3	31.6	54.0	33.8	31.7	32.9	30.7	39.4	41.7	41.5	38.7	33.6	36.1
An	0.0	0.0	0.9	10.8	4.7	9.3	10.7	13.1	32.1	5.1	4.8	10.4	13.0	5.2	9.0
Ne	0.0	0.0	0.0	4.7	0.0	3.0	1.5	0.0	0.0	0.0	0.0	0.0	0.0	0.0	0.0
Di	6.2	11.6	10.1	11.8	0.0	6.6	7.5	5.4	7.4	7.2	8.5	9.2	9.7	8.1	6.5
Hy	6.9	2.8	0.4	0.0	5.7	0.0	0.0	0.3	7.3	8.5	6.6	10.0	4.7	6.0	9.4
Ol	0.0	1.7	3.1	9.1	6.4	8.1	10.2	11.2	10.8	0.0	0.0	0.0	4.4	0.0	0.0
Mt	0.3	0.0	2.9	4.7	3.2	3.7	3.8	4.3	3.2	3.3	3.1	3.8	4.2	3.3	3.4
Il	1.4	1.8	2.5	5.8	4.3	4.6	5.2	5.2	2.2	2.9	2.7	4.0	4.4	2.7	3.2
Ap	0.2	0.4	1.0	3.9	[1]2.7	3.0	4.1	4.5	0.6	1.3	1.3	2.3	2.2	1.3	1.9
OR	12.2	17.4	7.6	29.3	17.9	39.2	37.4	33.5	8.6	40.1	39.8	26.6	26.6	48.5	38.6
AB	87.8	82.6	91.3	52.7	75.5	47.7	46.8	47.5	44.7	53.0	54.0	58.7	55.0	44.6	49.2
AN	0.0	0.0	1.1	1.8	6.6	13.1	15.8	19.0	46.7	6.9	6.2	14.7	18.4	6.9	12.2
D.I.	80.0	75.5	79.4	53.9	66.8	64.6	58.5	56.1	36.6	71.8	73.2	60.4	57.4	73.5	66.7

[1]Includes 1.1 C and 5.1 Calcite as normative minerals.

KEY TO ANALYSES OF TABLE 1 G
(continued)

Analysis Number	Location	Distance from contact (cm)
23.	Locality 8. Chilled margin of dyke, Tugtutoq	0
24.	" " " " "	10
25.	" " " " "	10
26.	Locality 9. Marginal zone; fine grained, no phenocrysts	-
27.	" " " .	-
28.	" " " ; Analysis 7 of Bridgwater and Harry (1968) with trace element analysis of whole rock	-
29.	Mugearitic dyke (MacDonald, 1968). Includes: 800 ppm Cl; 37 ppm Sc; 125 ppm La; 195 ppm Ce; 385 ppm Sr; 26 ppm Ga.	-
30.	Watt's (1968) least differentiated Gardar magma type.	-

TABLE 1G (contd.)

Analysis No.	16	17	18	19	20	21	22	23	24	25	26	27	28	29	30
Field No.	33013	44116	86049	86050	86051	86052	86054	86084	85985	85984	61165	61168	61109	40471	20632
SiO_2	50.44	52.18	53.00	52.0	52.2	51.4	49.7	55.7	50.9	63.7	50.3	50.6	52.41	49.2	44.60
Al_2O_3	15.51	13.54	15.1	15.3	17.7	17.2	17.0	15.8	17.3	13.9	14.1	14.2	15.14	15.40	16.46
Fe_2O_3	3.10	5.07	1.32	1.35	2.26	2.90	3.63	1.60	3.54	2.28	3.86	2.79	5.40	3.20	2.28
FeO	7.65	7.09	9.15	9.40	7.00	6.27	8.25	6.82	5.54	5.40	8.85	8.37	4.96	8.93	9.44
MgO	2.48	3.15	2.6	2.9	3.5	3.1	3.4	1.8	2.4	0.3	3.3	3.6	3.13	2.56	9.77
CaO	6.07	4.29	5.3	5.4	7.1	7.8	8.9	4.0	6.3	2.5	5.2	6.3	4.95	5.54	8.68
Na_2O	4.68	4.51	6.73	5.96	5.10	4.65	4.50	6.62	4.36	9.10	3.02	4.20	4.08	4.58	2.50
K_2O	2.36	4.16	1.54	2.35	2.07	1.98	1.91	1.97	3.34	0.05	3.98	2.00	3.92	3.60	0.85
H_2O^+	1.89	2.40	1.26	0.92	1.10	1.15	0.90	2.00	2.00	1.10	3.50	4.00	3.18	1.17	2.06
TiO_2	2.32	2.66	2.48	2.49	2.04	2.16	2.28	1.89	2.14	0.67	2.46	2.33	1.98	2.49	1.49
P_2O_5	0.85	0.98	1.0	1.2	1.0	1.2	1.5	0.7	1.1	0.1	1.0	1.1	0.79	1.24	0.32
MnO	0.21	0.17	0.19	0.20	0.19	0.20	0.20	0.13	0.15	0.20	0.21	0.20	0.19	0.19	0.16
Total	97.56	100.20	99.67	99.46	100.3	99.9	100.2	99.1	99.0	99.3	99.8	99.7	100.13	98.3	98.61
TRACE ELEMENTS (PPM)															
Ba	1803	-	1080	2309		1680	2393	929	1990	110	2209	1856	2309	2880	510
Sr	419	-	645	756		1474	1407	456	995	79	530	575	610	820	520
Rb	44	-	47	63		39	31	79	159	<1	269	40	97	70	15
Zr	261	-	308	305		162	191	351	175	774	244	251	245	-	110
Zn	165	-	130	155		109	-	123	-	-	187	179	126	-	62
Y	26	-	54	49		42	34	51	72	76	-	44	19	50	-
Cu	-	-	18	22		29	37	61	71	20	30	37	-	43	38
Nb	16	-	-	-		-	-	-	-	-	-	-	16	45	-
Ni	18	-	-	-		-	4	3	33	<1	-	17	12	-	172
CIPW NORMATIVE MINERALS															
Qz	0.0	0.0	0.0	0.0	0.0	0.0	0.0	0.0	0.0	5.0	0.6	0.6	0.0		
Or	14.6	25.1	9.2	14.1	12.3	11.8	11.4	12.0	20.3	0.3	24.4	12.3	24.4		
Ab	41.4	39.0	51.1	44.8	41.5	39.8	35.2	57.7	37.1	72.5	26.4	37.1	36.3		
An	15.0	4.5	6.7	8.2	19.4	20.4	20.7	7.8	18.3	0.0	13.8	14.6	12.0		
Ne	0.0	0.0	3.5	3.4	1.1	0.0	1.7	0.0	0.5	0.0	0.0	0.0	0.0		
Di	9.0	8.9	11.2	9.2	7.8	8.9	11.5	6.7	5.4	10.5	5.2	8.7	6.9		
Hy	3.1	0.3	0.0	0.0	0.0	2.3	0.0	2.6	0.0	4.1	17.5	15.0	9.9		
Ol	6.2	10.0	7.3	8.7	8.6	6.3	7.8	5.4	8.0	0.0	0.0	0.0	0.5		
Mt	4.1	4.6	3.7	3.9	3.0	3.5	3.8	2.4	3.5	0.8	4.8	4.2	4.0		
Il	4.6	5.2	4.8	4.8	3.9	4.2	4.4	3.7	4.2	1.3	4.9	4.6	4.0		
Ap	2.1	2.4	2.4	2.9	2.4	2.9	3.6	1.7	2.7	[2]0.2	2.5	2.7	2.0		
OR	20.6	36.6	13.7	21.0	16.8	16.4	16.9	15.5	26.8	10.4	37.8	19.2	33.6		
AB	58.3	56.9	76.3	66.8	56.7	55.3	52.3	74.5	49.0	99.6	40.9	58.0	50.0		
AN	21.1	6.5	10.0	12.2	26.5	28.3	30.8	10.0	24.2	0.0	21.3	22.8	16.4		
D.I.	56.0	64.1	63.8	62.3	54.9	51.6	48.3	69.7	57.9	77.8	51.4	50.0	60.7		

[2]Includes 5.2 Acmite as a normative mineral.

KEY TO ANALYSES OF TABLE 1 H

Analysis Number*	Location	Distance from contact (cm)
1.	Re 27. Lower chilled margin of sill	0
2.	Re 567 (inner). Lower chilled margin of sill	0-5
3.	Re 567 (outer). " " " " "	5-8
4.	Re 28	60
5.	Re 569	130-140
6.	Re 29	180
7.	Re 570	215
8.	Re 571	335
9.	Re 572	400
10.	Re 573	490
11.	Re 30A	500
12.	Re 574	650
13.	Re 619. Vesicular, nearly aphyric specimen. Nearest to vent	-
14.	Re 620. Porphyritic. Further along flow	
15.	Re 621. Porphyritic " " "	
16.	Re 622. Porphyritic. Nearest to terminus of flow	

* Two digit numbers in location column refer to analyses quoted by Upton and Wadsworth (1967). All others are analyses done for present study.

TABLE 1H

Analyses of the Composite Sill on the Bras Rouge, Piton des Neiges (1-12) and single flow on the Piton des Neiges (13-16)

Analysis No.	1	2	3	4	5	6	7	8	9	10	11	12	13	14	15	16
Field No.	Re27	Re5671	Re5670	Re28	Re569	Re29	Re570	Re571	Re572	Re573	Re30A	Re574	Re619	Re620	Re621	Re622
SiO_2	50.26	48.6	50.8	50.71	47.9	47.96	46.8	45.8	42.9	42.7	41.57	46.0	52.3	50.5	51.1	51.2
Al_2O_3	15.26	15.5	16.6	15.18	15.6	14.69	14.8	14.6	15.3	14.5	13.07	16.7	17.1	17.2	17.2	17.1
Fe_2O_3	5.55	5.97	5.22	5.86	5.98	6.63	7.16	4.78	8.71	9.46	9.86	7.13	2.00	2.21	2.04	2.00
FeO	4.74	5.63	5.67	4.44	6.22	5.20	5.94	8.34	5.09	6.58	6.93	6.29	8.06	8.50	8.50	8.02
MgO	3.34	3.5	3.3	3.06	3.8	3.93	4.2	4.1	5.0	5.5	5.64	4.9	3.3	3.8	3.6	3.9
CaO	4.84	5.4	3.6	6.42	8.5	7.99	9.0	9.4	10.9	11.4	10.82	10.5	7.0	7.9	7.7	8.1
Na_2O	5.49	5.16	5.55	4.73	3.93	4.01	3.63	3.75	2.70	2.83	2.58	3.05	4.60	4.35	4.55	4.55
K_2O	2.32	2.76	2.11	2.16	1.49	1.34	1.29	1.27	0.75	0.70	0.60	0.78	2.22	1.70	1.80	1.65
H_2O^+	2.54	2.12	2.32	1.59	1.25	1.32	1.41	1.50	1.64	1.18	1.35	1.16	0.21	0.25	0.22	0.25
TiO_2	2.80	3.00	2.89	2.67	3.33	3.49	3.61	4.21	3.74	4.41	4.93	4.52	2.44	2.73	2.75	2.57
P_2O_5	0.32	0.4	0.4	0.39	0.4	0.34	0.3	0.2	0.3	0.3	0.24	0.3	0.8	0.7	0.7	0.7
MnO	0.18	0.26	0.22	0.23	0.23	0.21	0.24	0.23	0.19	0.22	0.22	0.22	0.20	0.20	0.17	0.17
CO_2	2.14	1.9	1.5	2.31	1.8	2.23	1.9	1.8	1.8	0.8	1.78	-	-	-	-	-
Total	99.82	100.0	100.1	99.75	100.5	99.35	99.8	99.8	99.3	100.4	99.58	100.4	100.0	99.9	100.4	100.2
TRACE ELEMENTS (PPM)																
Ba	537	380	552	670	449	535	402	562	292	289	370	318	642	581	582	528
Sr	170	326	256	600	599	590	614	621	612	625	535	646	575	647	621	745
Rb	55	47	71	65	45	37	39	31	24	18	10	31	85	44	59	52
Zr	315	325	358	355	289	250	262	170	152	150	140	181	399	367	350	370
Zn	95	107	98	100	80	80	92	75	60	70	65	75	114	100	99	93
Y	40	50	58	52	45	35	45	35	29	29	27	34	27	23	23	23
Cu	10	20	14	10	38	30		55	35	-	90	51	-	-	-	-
Cr	<5			<5			<5				<5					
Nb	-	-	-	-	-	-	-	-	-	-	-	-	112	98	81	89
La	-	-	40	-	-	-	-	15	-	21	-	14	90	-	-	-
Ce	-	-	-	-	-	-	48	-	31	34	-	38	160	-	-	-
Ni	<10	15	12	<10	13	10	13	14	16	20	20	15	-	-	-	-
Th	-	2	2	-	1	-	4	<1	2	<1	-	6	-	-	-	-
Pb	-	<1	<1	-	<1	-	16	16	8	11	-	<1	-	-	-	-
Ga	-	-	-	-	18	-	-	16	-	-	-	14	-	-	-	-
V	215	-	-	140	-	240	-	-	-	-	405	-	-	-	-	-
CIPW NORMATIVE MINERALS																
Qz	1.0	-	2.3	4.2	2.5	4.7	3.5	-	2.2	-	2.2	0.8	-	-	-	-
Or	13.7	16.6	12.7	12.8	8.9	7.9	7.7	7.6	4.6	4.2	3.6	4.6	13.0	10.1	10.6	9.8
Ab	46.5	44.5	48.0	40.0	33.5	33.9	31.1	32.2	23.5	24.1	21.8	25.7	38.9	36.9	37.6	37.6
An	8.1	11.2	5.9	13.8	20.7	18.1	20.5	19.6	28.1	24.9	22.3	29.5	19.6	22.4	21.3	21.3
C	0.7	-	3.1	-	-	-	-	-	-	-	-	-	-	-	-	-
Ne	-	-	-	-	-	-	-	-	-	-	-	-	-	-	0.5	0.5
Di	-	1.0	-	0.7	6.1	4.0	8.2	12.1	10.7	19.4	14.4	15.9	8.0	10.2	10.3	11.9
Hy	8.3	0.3	10.2	7.3	8.1	7.9	6.8	7.0	7.9	2.5	7.3	4.8	3.7	0.1	-	-
Ol	-	6.5	-	-	-	-	-	1.8	-	1.6	-	-	7.3	10.3	10.0	9.5
Mt	7.5	8.8	7.7	7.1	8.7	5.9	9.6	7.0	6.4	9.2	7.9	7.9	2.9	3.2	3.0	2.9
Hem	0.4	-	-	1.0	-	2.6	0.6	-	4.6	3.2	4.4	1.7	-	-	-	-
Il	5.3	5.8	5.6	5.1	6.4	6.6	6.9	8.1	7.3	8.4	9.3	8.6	4.6	5.2	5.2	4.9
Ap	0.9	1.0	1.0	0.9	1.0	0.8	0.7	0.5	0.7	0.7	0.5	0.7	2.0	1.6	1.7	1.7
Cc	4.9	4.4	3.5	5.3	4.1	5.1	4.4	4.2	4.2	1.8	4.0	-	-	-	-	-
Py	0.1	-	-	0.1	-	0.8	-	-	-	-	0.4	-	-	-	-	-
OR	20.1	23.0	19.1	19.2	14.1	13.2	13.0	12.8	8.2	7.9	7.4	7.3	18.2	14.5	15.3	14.2
AB	68.0	61.5	72.1	60.1	53.1	56.6	52.4	54.2	42.0	45.3	45.8	43.1	54.4	53.3	54.1	54.7
AN	11.9	15.5	8.8	20.7	32.8	30.2	34.6	33.0	49.8	46.8	46.8	49.6	27.4	32.2	30.6	31.1
D.I.	61.2	61.1	63.0	57.0	44.9	46.5	42.3	39.8	30.3	28.3	27.6	31.1	51.9	47.0	48.7	47.8

APPENDIX B

Modal analyses of rocks whose analyses are presented in Appendix A.

MODAL ANALYSES OF ROCKS IN TABLE 1A

ANALYSIS NUMBER	PHENOCRYSTS (%) PLAG[1]	OL	TITANO-MAGNETITE	cpx	GROUND MASS Feldspar	cpx	Ol	ores	apatite	chlorite biotite	amphibole	Rock type
1	1.2	15.1	2.1	-	+	+	+	+	-	+	-	AkB
2	0.9	17.1	1.9	-	+	+	+	+	-	+	-	AkB
3	1.5	20.1	0.9	-	+	+	+	+	-	+	-	AkB
4	<0.5	<0.5	<0.5	-	+	+	+	+	+	+	-	H
5	<0.5	-	-	-	+	+	+	+	+	+	+	H
6	<0.5	<0.5	<0.5	-	+	+	+	+	+	+	-	H
7	1.3	<0.5	<0.5	-	+	+	+	+	+	+	-	H
8	<0.5	<0.5	<0.5	-	+	+	+	+	+	+	+	H
9	<0.5	<0.5	<0.5	-	+	+	+	+	+	+	-	H
10	<0.5	<0.5	<0.5	-	+	+	+	+	+	+	-	H
11	2.1	<0.5	<0.5		+	+	+	+	+	+	+	H
12	24.2	0.9	0.8	-	+	+	+	+	+	+	-	H
13	groundmass analysis of 12											
14	21.3	0.6	0.9	-	+	+	+	+	+	+	+	H
15	groundmass analysis of 14											
16	23.8	0.7	0.8	-	+	+	+	+	+	+	+	H
17	groundmass analysis of 16											
18	20.4; 4.2	<0.5	<0.5	-	+	+	+	+	+	+	+	H
19	groundmass analysis of 18											
20	9.3; 5.1	<0.5	<0.5	-	+	+	+	+	+	+	+	H
21	groundmass analysis of 20											
22	15.6; 5.2	0.9	0.9	-	+	+	+	+	+	+	+	H
23	groundmass analysis of 22											
24)												
25)	analysis quoted from Tilley et al, 1965, 1967											

1 The first of two numbers indicates the macrophenocryst content, the second is microphenocryst content.

MODAL ANALYSES OF ROCKS IN TABLE 1B

ANALYSIS NUMBER	PHENOCRYSTS (%) PLAG	OL	MAGNETITE	cpx	GROUNDMASS Feldspar	cpx	Ol	ores	apatite	chlorite biotite	amphib.	Rock type
1	0.8	<0.5	<0.5	-	+	+	+	+	+	+	+	M
2	0.6	<0.5	<0.5	-	+	+	+	+	+	+	+	M
3	0.8	<0.5	<0.5	-	+	+	+	+	+	+	+	M
4	0.6	<0.5	<0.5	-	+	+	+	+	+	+	+	M
5	analysis quoted from Yoder and Tilley, 1962											M
6	24.3	0.8	0.6	-	+	+	+	+	+	+	+	H
7	groundmass of analysis 6											H
8	analysis quoted from Yoder and Tilley, 1962											H
9	-	-	-	-	+	?	?	+	-	+	-	volcanic ash
10	3.1	1.3	1.1	0.9	+	+	+	+	-	+	-	B
11	1.1	0.8	<0.5	-	+	+	+	+	-	+	-	H
12	0.9	0.8	<0.5	-	+	+	+	+	+	+	-	H
13	1.3	0.9	<0.5	-	+	+	+	+	+	+	-	H
14	0.8	0.7	<0.5	-	+	+	+	+	+	+	-	H
15	0.7	<0.5	<0.5	-	+	+	+	+	+	+	+	M
16	0.9	<0.5	<0.5	-	+	+	+	+	+	+	+	M
17	1.0	<0.5	<0.5	-	+	+	+	+	+	+	+	M
18(1)	27.1	1.2	0.7	-	+	+	+	+	+	+	+	M
19	1.6	15.6	1.1	-	+	+	+	+	+	+	+	AkB
20	4.6	1.3	1.1	-	+	+	+	+	+	+	-	H
21	3.2	0.9	1.3	-	+	+	+	+	+	+	-	H
22	10.1	1.3	1.6	-	+	+	+	+	+	+	-	H

(1) Mode is given for whole rock.

MODAL ANALYSES OF THE ROCKS IN TABLE 1C

ANALYSIS NUMBER	PHENOCRYSTS (%) PLAG	OL	cpx	MAGNETITE	GROUND MASS Feldspar	Ol	cpx	opaque	apatite	chlorite biotite	Rock type
1	10.1	6.5	-	3.2	+	+	+	+	-	+	AkB
2	12.6	3.4	-	2.1	+	+	+	+	-	+	AkB
3	8.2	7.9	-	1.8	+	+	+	+	-	+	AkB
4	10.1	12.9	-	2.1	+	+	+	+	+	+	AkB
5	98.0	0.5	-	0.5	-	-	-	-	-	-	Anorthasite
6	3.5	2.1	-	1.2	+	+	+	+	+	+	H
7	10.1	12.1	-	2.1	+	+	+	+	-	+	AkB
8	15.3	1.1	-	1.3	+	+	+	+	+	+	H
9	19.2	0.8	-	2.1	+	+	+	+	+	+	H
10	2.2	0.7	-	1.1	+	+	+	+	+	+	AkB
11	3.2	4.9	2.1	2.1	+	+	+	+	-	+	TB
12	10.1	3.4	1.1	3.4	+	+	+	+	-	+	TB
13	23.0	-	-	2.1	+	+	-	+	+	+	B
14	9.2	2.1	-	1.3	+	+	+	+	+	+	H
15	5.1	1.1	-	2.1	+	+	+	+	+	+	H
16	2.1	0.7	-	1.2	+	+	+	+	+	+	H
17	3.1	6.5	-	2.6	+	+	+	+	+	+	AkB
18	5.7	10.1	-	3.5	+	+	+	+	+	+	AkB
19	1.1	0.9	-	0.7	+	+	+	+	-	+	AkB
20	1.3	0.7	-	0.9	+	+	+	+	-	+	AkB
21	Analysis quoted from Muir and Tilley (1961)										B
22	Analysis quoted from Tilley et al, (1967)										B
23	6.3	2.1	-	0.5							B
24	-------- course grained --------				+	+	+	+	tr.	+	B
25	2.3	1.2	-	0.7	+	+	+	+	-	+	H
26	5.1	-	-	0.9	+	+	+	+	+	+	M
27	3.5	2.1	-	1.1	+	+	+	+	+	+	H
28	4.2	0.9	-	1.3	+	+	+	+	+	+	H
29	6.8	1.2	-	0.9	+	+	+	+	+	+	H
30	3.2	8.1	-	1.8	+	+	+	+	+	+	AkB
31	4.6	0.6	-	1.2	+	+	+	+	+	+	H
32	--- coarse grained gabbro ------				+	+	+	+	-	+	Gabbro
33	"	"	"		+	+	+	+	-	+	Gabbro
34	"	"	"		+	+	+	+	-	+	Gabbro
35	6.5	0.8	-	1.3	+	+	+	+	+	+	H

MODAL ANALYSES OF ROCKS IN TABLE 1D

ANALYSIS NUMBER	PHENOCRYSTS (%) PLAG	OL	MAGNETITE	cpx	GROUNDMASS Feldspar	cpx	Ol	ores	apatite	chlorite biotite	Rock type
1	17.8	2.1	0.8	-	+	+	+	+	+	+	H
2	20.1	1.8	0.9	-	+	+	+	+	+	+	H
3 - T.C. Day analysis											
4 ~~3~~	1.1	-	-	-	+	+	?	+	+	+	B
5 ~~4~~	0.8	-	-	-	+	+	?	+	+	+	B
6 ~~5~~	analysis quoted from T.C. Day (1930)										B
7 ~~6~~	analysis quoted from Muir and Tilley (1961)										B
8 ~~7~~	19.1	7.2	0.7	9.2	+	+	+	+	+	+	AkB
9 ~~8~~	analysis quoted from Rutledge, 1952										H
10 T.C. Day analysis 11 ~~9~~	"	"	"	"	"						AkB
12 ~~10~~	"	"	"	"	"						AkB
13 ~~11~~	26.2	1.9	0.9	-	+	+	?	+	+	+	H
14 ~~12~~	27.8	1.2	2.1	1.9	+	+	+	+	+	+	AkB
15 ~~13~~	25.9	0.9	0.7	2.1	+	+	+	+	+	+	AkB
16 ~~14~~	analysis quoted from Rutledge, 1952										AkB
17 ~~15~~	<0.5	-	-	-	+	+	+	+	+	+	B
18 ~~16~~	18.1	1.2	0.9	4.8	+	+	+	+	+	+	AkB
19 ~~17~~	analysis quoted from Kennedy, 1932										M
20 ~~18~~	0.9	0.7	0.6	-	+	+	+	+	+	+	M
21 ~~19~~	analysis quoted from Kennedy, 1932										B
22 ~~20~~	12.1	-	-	3.1	+	+	-	+	+	+	B

MODAL ANALYSES OF ROCKS IN TABLE 1E

ANALYSIS NUMBER	PHENOCRYSTS (%) PLAG[1]	OL	TITANO-MAGNETITE	cpx	GROUND MASS Feldspar	cpx	01	ores	apatite	chlorite biotite	Rock type
1	<1	-	<1	<1	66.5	11.1	9.2	8.3	1.8	3.1	M
2	<1	-	<1	<1	+	+	+	+	+	+	M
3	<1	-	<1	<1	+	+	+	+	+	+	M
4	15.6; 16.8	-	<1	<1	+	+	+	+	+	+	M
5	groundmass analysis of 4										
6	2.9; 4.8				+	+	+	+	+	+	H
7	groundmass analysis of 6										
8	6.2; 13.5	-	<1	<1	+	+	+	+	+	+	H
9	groundmass analysis of 8										
10	9.3; 11.6	-	<1	<1	+	+	+	+	+	+	H
11	groundmass analysis of 10										
12	4.3; 17.5	-	<1	<1	+	+	+	+	+	+	H
13	groundmass analysis of 12										
14	8.9; 6.7	-	<1	<1	+	+	+	+	+	+	H
15	groundmass analysis of 14				65.3	12.6	7.8	10.8	1.4	2.1	H
16	10.1; 4.8	-	<1	<1	+	+	+	+	+	+	H
17	groundmass analysis of 16										
18)	analysis from Kennedy (1931) no modal data given										
19)											
20	6.2	-	<1	<1	+	+	+	+	+	+	M

1 First number gives macrophenocrysts, second gives microphenocrysts

MODAL ANALYSES OF THE ROCKS IN TABLE 1G

ANALYSIS NUMBER	PHENOCRYSTS (%) PLAG	ALK.FLD.	cpx	OL(PSD)	Fe-Tioxide	Apatite	GROUNDMASS Feldspar	cpx	opaque	apatite	chlorite biotite	Rock type
1	analyses quoted from Bridgwater and Harry (1968)											B
2	"	"	"	"	"	"						B
3	"	"	"	"	"	"						B
4	"	"	"	"	"	"						H
5	-	1.3	-	-	1.6	-	+	+	+	+	+	B
6	0.9	1.9	-	-	1.1	0.6	+	+	+	+	+	B
7	4.1	1.1	<1.0	-	1.1	-	+	+	+	+	+	M
8	10.1	-	-	-	2.1	-	+	+	+	+	+	M
9	analyses quoted from Bridgwater and Harry (1968)											H
10	"	"	"	"	"	"						B
11	"	"	"	"	"	"						B
12	"	"	"	"	"	"						M
13	"	"	"	"	"	"						M
14	"	"	"	"	"	"						B
15	"	"	"	"	"	"						B
16	"	"	"	"	"	"						M
17	"	"	"	"	"	"						M
18	1.2	2.1	0.9	-	1.1	0.5	+	+	+	+	+	M
19	0.8	1.1	tr.	-	-	-	+	+	+	+	+	M
20	16.1	1.1(?)	-	-	0.7	0.6	+	+	+	+	+	M
21	19.1	-	-	-	1.1	0.8	+	+	+	+	+	M
22	26.2	-	-	tr.(?)	1.1	0.5	+	+	+	+	+	H
23	-	1.1	-	-	tr.	-	+	?	+	?	+	B
24	-	4.2	-	-	1.1	-	+	?	+	+	+	M
25	-	2.1	-	-	0.7	-	+	?	+	+	+	B
26	analyses quoted from Bridgwater and Harry (1968)											M
27	"	"	"	"	"	"						M
28	"	"	"	"	"	"						M
29(1)	-	-	-	-	-	tr.	60.6	9.7	7.1	1.9	20.7	M
30	analyses quoted from Watt (1968)											

(1) Analysis quoted from MacDonald, 1968.

MODAL ANALYSES OF ROCKS IN TABLE 1H

ANALYSIS NUMBER	Feldspar	cpx	ore	chlorite + biotite	amphibale	quartz	cakite	olivine pseudom	
1	4.5	0.7	0.7	-	tr.	-	-	-	)
2	5.6	0.8	1.2	-	-	-	-	-	) phenocrysts
3	12.1	1.5	1.4	-	-	-	-	-	)
4	67.3	1.3	8.4	16.2		0.5	6.2	-	
5	62.3	5.1	13.1	14.1	-	0.5	4.9	-	
6	59.3	6.5	12.9	13.2	1.6	0.7	5.8	tr.	
7	56.1	12.1	15.9	11.2	0.5	-	4.2	-	
8	55.9	17.1	14.2	10.2	-	0.3	2.3	-	
9	57.1	17.9	11.1	10.6	-	-	3.3	-	
10	48.9	24.2	13.1	9.3	-	0.2	4.3	-	
11	52.0	22.0	12.4	3.4	-	-	5.0	5.1	
12	53.1	25.3	15.8	2.1	-	-	3.7	- (olivine)	
13	2.0	0.5	1.3					1.9	)
14	21.2	2.0	0.6					2.1	) phenocrysts
15	19.7	0.5	0.6					1.6	)
16	16.9	1.0	0.5						

APPENDIX C

MINERAL ANALYSES

(Bracketed numbers in the Analyses Keys refer to the rock sample analysis and relevant Table number in Appendix A.)

KEY TO ANALYSES OF TABLE 1.1 (FELDSPARS)

North Skye composite flows

1. Phenocryst centre. Talisker T-13 (20; 1A).
2. " margin. " " " "
3. " outer rim " " " "
4. " discontimuous outer rim. " " " "
5. " ;Group B. Talisker PL-4 (11; 1A).
6. " Bulk analysis of separate. " " " " XRF analysis.
7. " " " " " T-14 (16; 1A) XRF analysis.
8. Groundmass feldspar. T-13 (20; 1A).
9. " " " " "
10. Analcite. T-13 (20; 1A).
11. Microphenocryst centre. T-4 (9; 1A).
12. Groundmass feldspar. T-4 (9; 1A).
13. Microphenocryst in alkali olivine basalt. T-AA (3; 1A).
14. Microphenocryst. Drum na Criche hawaiite. (6; 1B).
15. Phenocryst centre. "
16. " " "
17. " " "
18. Phenocryst margin. "
19. " " "
20. Groundmass feldspar. "
21. " " "
22. Phenocryst centre. Roineval hawaiite. (18; 1B).
23. " margin. "
24. Groundmass feldspar. "
25. Roineval phenocryst, bulk separate. XRF analysis.
26. Drum na Criche " " " "

TABLE 1.1

FELDSPAR ANALYSES

		1	2	3	4	5	6	7
SiO_2		55.86	52.77	56.28	59.71	59.90	56.17	56.93
Al_2O_3		26.87	29.33	27.89	24.79	24.99	27.16	27.45
Fe_2O_3		0.35	0.47	-	0.46	0.02	1.18	0.71
CaO		9.74	12.40	9.14	7.02	6.72	9.68	10.12
Na_2O		6.12	4.48	6.14	7.25	7.62	5.76	5.10
K_2O		0.22	0.16	0.43	0.56	0.76	0.31	0.20
BaO		-	-	-	-	-	-	-
Total		99.05[1]	99.52	99.88	99.79	100.01	100.40[3]	100.51[4]
		ATOMIC RATIOS ON THE BASIS OF 32 OXYGENS						
	Si	10.155	9.620	10.125	10.694	10.730	10.116	10.172
Z	Al	5.765	6.289	5.913	5.233	5.230	5.776	5.780
	Fe	0.044	0.066	-	0.062	0.001	0.160	0.095
	Ca	1.900	2.422	1.761	1.347	1.289	1.826	1.937
XY	Na	2.120	1.578	2.140	2.518	2.626	2.008	1.767
	K	0.044	0.044	0.099	0.128	0.972	0.071	0.046
		END MEMBERS (MOL PERCENT)						
AB		46.8	39.0	53.5	63.1	64.4	51.4	47.1
AN		52.2	59.9	44.0	33.7	31.4	46.8	51.7
OR		1.0	1.1	2.5	3.2	4.2	1.8	1.2
Z		15.986[2]	15.975	16.038	15.989	15.961	16.052	16.047
XY		4.064	4.044	4.000	3.993	4.078	3.905	3.750

1. Includes TiO_2 = 0.16
2. Includes Ti+4 = 0.222
3. Includes TiO_2 = 0.02; P_2O_5 = 0.12, MgO = 0.01.
   Trace elements (ppm): Ba = 87; Sr = 1130; Rb = 4; Zr = 170.
4. Includes TiO_2 = 0.01; P_2O_5 = 0.09; MgO = 0.04. Trace elements (ppm): Ba = 6; Sr = 1100; Rb = 2; Zr = 152.

TABLE 1.1 (Contd.)

		8	9	10	11	12	13	14
SiO_2		55.88	66.60	51.58	54.06	55.86	49.75	57.70
Al_2O_3		27.49	20.78	24.71	28.25	26.97	31.17	26.55
Fe_2O_3		0.02	-	0.13	0.71	0.67	0.76	0.59
CaO		9.44	0.93	1.25	11.86	10.63	14.65	8.95
Na_2O		6.20	8.39	7.56	4.69	5.48	3.12	6.10
K_2O		0.25	3.85	0.05	0.22	0.30	0.16	0.60
BaO		-	-	-	-	-	-	-
Total		99.27	100.55	85.32[5]	99.79	99.91	99.61	100.49
		ATOMIC RATIOS ON THE BASIS OF 32 OXYGENS						
	Si	10.121	11.741		9.814	10.097	9.135	10.354
Z	Al	5.868	4.317		6.045	5.745	6.745	5.569
	Fe	0.004	-		0.097	0.090	0.104	0.064
	Ca	1.832	0.176		2.308	2.060	2.881	1.698
XY	Na	2.177	2.868		1.650	1.919	1.111	2.085
	K	0.058	0.866		0.051	0.069	0.036	0.129
		END MEMBERS (MOL PERCENT)						
AB		53.5	73.4		41.2	47.4	27.6	53.3
AN		45.1	4.5		57.6	50.9	71.5	43.4
OR		1.4	22.1		1.3	1.7	0.9	3.3
Z		15.993	16.058		15.956	15.932	15.984	15.987
XY		4.067	3.910		4.009	4.048	4.028	3.912

5. Analcite; specimen current unsteady. H_2O contents (from Deer, Howie, Zussman, vol. 4, p.343) range from 7.66 to 9.32. The remaining 5-6% is probably Na_2O and K_2O that volatolized during the analysis.

TABLE 1.1 (Contd.)

		15	16	17	18	19	20
SiO_2		57.53	57.40	54.37	56.54	56.94	56.24
Al_2O_3		26.56	26.50	28.49	27.56	27.52	27.34
Fe_2O_3		0.59	0.48	0.52	0.53	0.48	0.76
CaO		8.93	10.09	10.76	10.26	10.13	10.08
Na_2O		6.07	5.56	5.33	5.44	5.57	5.55
K_2O		0.60	0.33	0.26	0.40	0.34	0.43
BaO		-	-	-	-	-	-
Total		100.28	100.37	99.73	100.72	100.97	100.40
		ATOMIC RATIOS ON THE BASIS OF 32 OXYGENS					
	Si	10.327	10.278	9.866	10.127	10.158	10.118
Z	Al	5.590	5.596	6.068	5.790	5.771	5.815
	Fe	0.064	0.065	0.065	0.064	0.042	0.086
	Ca	1.715	1.937	2.084	1.958	1.930	1.934
XY	Na	2.093	1.931	1.855	1.872	1.909	1.924
	K	0.129	0.086	0.043	0.086	0.064	0.064
		END MEMBERS (MOL PERCENT)					
AB		53.2	48.8	52.3	47.8	48.9	49.3
AN		43.6	49.0	46.6	50.0	49.5	49.1
OR		3.2	2.2	1.1	2.2	1.6	1.6
Z		15.981	15.939	15.999	16.024	15.971	16.019
XY		3.937	3.954	3.982	3.916	3.903	3.922

TABLE 1.1 (Contd.)

		21	22	23	24	25	26
SiO_2		55.58	54.65	55.43	56.21	54.68	54.41
Al_2O_3		27.33	27.84	27.52	27.31	27.26	27.35
Fe_2O_3		0.94	0.52	0.52	0.60	1.33	0.96
CaO		9.57	10.60	10.15	9.77	10.59	10.53
Na_2O		5.89	5.49	5.63	5.31	5.45	5.90
K_2O		0.42	0.29	0.34	0.35	0.36	0.46
BaO		-	0.16	0.19	0.20	0.03	0.03
Total		99.73	99.40	99.61	99.58	99.63	99.55
		ATOMIC RATIOS ON THE BASIS OF 32 OXYGENS					
	Si	10.081	9.938	10.041	10.155	9.911	9.898
Z	Al	5.820	5.967	5.876	5.815	5.926	5.864
	Fe	0.108	0.071	0.071	0.071	0.181	0.131
	Ca	1.852	2.065	1.970	1.891	2.016	2.045
XY	Na	2.070	1.936	1.977	1.860	1.879	2.208
	K	0.087	0.067	0.079	0.081	0.083	0.107
		END MEMBERS (MOL PERCENT)					
AB		51.8	47.6	49.1	48.5	47.2	50.6
AN		46.2	50.8	48.9	49.3	50.7	46.9
OR		2.2	1.6	2.0	2.2	2.1	2.5
Z		16.009	15.976	15.988	16.041	16.013	15.893
XY		4.009	4.068	4.026	3.832	3.978	4.360

KEY TO ANALYSES OF TABLE 2.1 (FELDSPARS)

Greenock Composite Flow

1. Phenocryst centre. (8; 1E).
2. Microphenocryst. "
3. Phenocryst centre. (16; 1E).
4. " border. "
5. " centre. (12; 1E).
6. " border. "
7. Groundmass feldspar. "
8. Phenocryst bulk separate (12; 1E). XRF analysis.
9. " " " (16; 1E). "
10. Phenocryst centre. (8; 1D).
11. " margin "
12. " centre.

TABLE 2.1

FELDSPAR ANALYSES

		1	2	3	4	5	6
SiO_2		48.67	48.98	48.72	49.09	50.51	53.59
Al_2O_3		32.15	32.31	32.59	32.30	30.70	28.01
Fe_2O_3		0.66	0.56	0.65	0.74	0.73	0.75
CaO		15.50	15.57	15.75	15.48	14.12	11.94
Na_2O		2.58	2.48	2.36	2.59	3.51	4.59
K_2O		0.10	0.11	0.09	0.16	0.16	0.32
BaO		-	-	-	-	-	-
Total		99.66	100.03	100.15	100.37	99.90[1]	99.19
		ATOMIC RATIOS ON THE BASIS OF 32 OXYGENS					
	Si	8.965	8.963	8.908	8.960	9.235	9.810
Z	Al	6.950	6.968	7.023	6.949	6.611[2]	6.034
	Fe	0.088	0.077	0.089	0.102	0.110	0.088
	Ca	3.065	3.053	3.086	3.027	2.767	2.334
XY	Na	0.841	0.880	0.837	0.917	1.252[3]	1.629
	K	0.022	0.026	0.021	0.037	0.044	0.066
		END MEMBERS (MOL PERCENT)					
AB		23.0	22.2	21.2	23.0	30.8	40.5
AN		76.4	77.1	78.2	76.0	68.1	57.9
OR		0.6	0.7	0.6	1.0	1.1	1.6
Z		16.002	16.008	16.020	16.011	15.967	15.932
XY		3.994	3.959	3.944	3.981	4.096	4.029

1. Includes MgO = 0.10; TiO_2 = 0.06.
2. Includes Ti^{+4} = 0.011.
3. Includes Mg^{+2} = 0.033.

TABLE 2.1 (contd.)

		7	8	9	10	11	12
SiO_2		54.62	52.35	50.04	51.65	51.11	56.28
Al_2O_3		27.83	28.56	30.79	29.55	30.28	27.45
Fe_2O_3		0.98	0.98	0.80	0.44	0.49	0.25
CaO		11.21	13.39	14.92	13.53	13.28	9.68
Na_2O		4.94	9.81	2.50	4.09	3.91	5.20
K_2O		0.36	0.57	0.41	0.49	0.39	0.65
BaO		-	-	-	-	-	-
Total		99.94	99.66	99.46	99.75	99.45	99.51
		ATOMIC RATIOS ON THE BASIS OF 32 OXYGENS					
	Si	9.936	9.590	9.189	9.455	9.369	10.164
Z	Al	5.946	6.166	6.670	6.375	6.542	5.842
	Fe	0.131	0.135	0.111	0.061	0.068	0.034
	Ca	2.175	2.628	2.938	2.654	2.608	1.873
XY	Na	1.727	1.350	0.891	1.452	1.390	1.821
	K	0.065	0.133	0.096	0.114	0.091	0.150
		ENE MEMBERS (MOL PERCENT)					
AB		43.5	32.8	22.7	34.4	34.0	47.5
AN		54.8	63.9	74.9	62.9	63.8	48.7
OR		1.6	3.2	2.4	2.7	2.2	3.9
Z		16.013	15.890	15.979	15.891	15.979	16.040
XY		3.967	4.111	3.925	4.220	4.089	3.844

KEY TO ANALYSES OF TABLE 3.1 (FELDSPARS)

Greenland Composite Dykes.

1. Phenocryst centre. (24; 1G).
2. " " "
3. " " "
4.
5.
6. Phenocryst margin. (24; 1G).
7. " centre. "
8. " margin "
9. Phenocryst from GGU No. 85990. No analysis of rock; termed as microsyenite
10. " " "
11. " " "
12.-18. Traverses across phenocrysts of anorthoclase in GGU 85990.
19.-22. Traverses across anorthoclase phenocrysts from another microsyenite (GGU 50153) of which there is no analysis.

TABLE 3.1

FELDSPAR ANALYSES

		1	2	3	4	5	6
SiO_2		56.52	56.10	56.43	55.62	55.10	55.09
Al_2O_3		27.53	27.46	27.58	28.03	28.34	27.24
Fe_2O_3		0.46	0.41	0.45	0.39	0.57	0.55
CaO		9.35	8.70	9.08	9.21	9.79	10.33
Na_2O		5.42	5.59	5.57	5.67	5.53	5.50
K_2O		1.04	1.02	1.06	0.98	0.46	0.77
BaO					-	-	0.14
Total		100.33	99.48	100.17	100.10	100.05	99.61
		ATOMIC RATIOS ON THE BASIS OF 32 OXYGENS					
	Si	10.152	10.153	10.149	10.026	9.931	10.022
Z	Al	5.828	5.857	5.846	5.955	6.026	5.840
	Fe	0.062	0.056	0.061	0.053	0.077	0.075
	Ca	1.799	1.726	1.750	1.779	1.893	2.013
XY	Na	1.887	1.962	1.942	1.982	1.935	1.940
	K	0.238	0.235	0.243	0.225	0.106	0.179
		END MEMBERS (MOL PERCENT)					
	AB	48.1	50.0	49.4	49.7	49.2	46.8
	AN	45.8	44.0	44.5	44.6	48.1	48.6
	OR	6.1	6.0	6.2	5.7	2.7	4.3
	Z	16.042	16.066	16.056	16.034	16.034	15.937
	XY	3.924	3.923	3.935	4.023	3.979	4.142

TABLE 3.1 (contd.)

		7	8	9	10	11
SiO_2		56.85	56.38	62.80	63.43	63.00
Al_2O_3		26.07	26.70	22.29	22.03	21.70
Fe_2O_3		0.61	0.46	-	-	-
CaO		9.32	9.67	3.96	4.11	3.38
Na_2O		5.54	5.47	6.25	6.12	6.30
K_2O		0.95	0.81	3.96	3.69	4.38
BaO		0.04	0.14			
Total		99.39	99.64	99.30	99.40	99.40
		ATOMIC RATIOS ON THE BASIS OF 32 OXYGENS				
Z	Si	10.310	10.226	11.297	11.371	11.429
	Al	5.572	5.690	4.726	4.655	4.595
	Fe	0.083	0.043			
XY	Ca	1.811	1.875	0.763	0.789	0.651
	Na	1.948	1.918	2.197	2.127	2.195
	K	0.220	0.174	0.909	0.844	1.004
		END MEMBERS (MOL PERCENT)				
	AB	48.9	47.26	56.8	56.6	57.0
	AN	45.5	48.34	19.7	21.0	16.9
	OR	5.5	4.38	23.5	22.4	26.1
	Z	15.965	15.959	16.023	16.026	16.024
	XY	3.982	3.967	3.869	3.760	3.850

TABLE 3.1 (Contd.)

		12	13	14	15	16	17
SiO_2		61.63	62.35	62.29	62.26	61.83	61.71
Al_2O_3		22.14	21.57	21.52	21.61	21.56	21.97
Fe_2O_3		-	-	-	-	-	-
CaO		3.39	2.35	3.27	2.86	2.99	3.01
Na_2O		6.33	6.00	6.55	6.45	5.75	6.55
K_2O		4.99	5.91	4.82	4.92	4.98	4.70
BaO		0.35	0.66	-	-	-	-
Total		98.84	98.85	98.49	98.14	97.14	97.97
		ATOMIC RATIOS ON THE BASIS OF 32 OXYGENS					
Z	Si	11.251	11.433	11.322	11.341	11.405	11.308
	Al	4.742	4.630	4.643	4.674	4.655	4.712
	Fe						
XY	Ca	0.658	0.449	0.641	0.553	0.587	0.583
	Na	2.239	2.106	2.321	2.325	2.039	2.312
	K	1.163	1.360	1.127	1.151	1.152	1.101
		END MEMBERS (MOL PERCENT)					
	AN	16.20	11.46	15.67	13.72	15.53	14.58
	AB	55.14	53.79	56.76	57.70	53.97	57.85
	OR	28.64	34.73	27.56	28.56	30.49	27.55
	Z	15.993	16.063	15.965	16.015	16.060	16.020
	XY	4.060	3.915	4.089	4.029	3.778	3.996

TABLE 3.1 (contd.)

		18	19	20	21	22
SiO_2		63.20	64.86	66.99	65.95	67.15
Al_2O_3		18.45	20.79	19.82	19.47	19.05
Fe_2O_3		-	0.20	0.22	0.17	0.21
CaO		3.07	2.66	0.99	0.71	0.68
Na_2O		0.30	7.46	8.47	6.75	7.13
K_2O		14.86	4.23	4.11	6.11	5.71
BaO		-	0.205	0.062	0.072	0.09
Total		99.92	100.40	100.66	99.24	100.03
		ATOMIC RATIOS ON THE BASIS OF 32 OXYGENS				
	Si	11.758	11.588	11.853	11.873	11.971
Z	Al	4.027	4.366	4.102	4.131	4.003
	Fe			0.021	0.023	0.028
	Ca	0.604	0.504	0.180	0.137	0.130
XY	Na	0.089	2.576	2.891	2.356	2.465
	K	3.535	0.966	0.914	1.403	1.299
		END MEMBERS (MOL PERCENT)				
	AN	14.28	63.7	4.51	60.4	63.3
	AB	2.10	12.5	72.54	3.5	3.3
	OR	83.60	23.8	22.93	36.0	33.4
	Z	15.785	15.954	15.977	16.027	16.002
	XY	4.228	4.046	3.985	3.901	3.894

KEY TO ANALYSES OF TABLE 4.1 (FELDSPARS)

Bras Rouge Sill, Reunion.

1-10. Traverse across a single zoned feldspar in Re 574. (12; 1H). Analyses 1, 9, 10 represent the margins.

11. Phenocryst margin; (12; 1H).

12. " centre. "

13. Microphenocryst. (3; 1H).

14. " "

15. " "

TABLE 4.1.

FELDSPAR ANALYSES

		1	2	3	4	5	6
SiO_2		60.61	55.58	55.04	53.64	54.07	53.83
Al_2O_3		24.28	26.87	27.40	28.72	29.70	29.82
Fe_2O_3		0.32	0.43	0.43	0.55	0.62	0.54
CaO		5.69	9.24	10.23	11.30	11.41	11.59
Na_2O		8.19	6.03	5.71	4.20	4.09	3.82
K_2O		0.65	0.30	0.28	0.19	0.17	0.19
BaO		-	-	-	-	-	-
Total		99.75	98.45	99.09	98.61	100.04	99.79
		ATOMIC RATIOS ON THE BASIS OF 32 OXYGENS					
	Si	10.845	10.168	10.023	9.884	9.757	9.727
Z	Al	5.099	5.804	5.865	6.133	6.295	6.325
	Fe	0.043	0.044	0.043	0.065	0.065	0.065
	Ca	1.086	1.804	1.991	2.186	2.203	2.239
XY	Na	2.840	2.134	2.013	1.457	1.411	1.326
	K	0.129	0.066	0.175	0.046	0.021	0.043
		END MEMBERS (MOL PERCENT)					
	AB	70.0	53.3	48.2	39.5	38.8	36.8
	AN	26.8	45.1	47.6	59.3	60.6	62.1
	OR	3.2	1.6	4.2	1.3	0.6	1.2
	Z	15.987	16.016	15.931	16.082	16.117	16.117
	XY	4.055	4.004	4.179	3.689	3.635	3.608

TABLE 4.1 (contd.)

		7	8	9	10	11	12
SiO_2		53.42	52.11	65.01	65.62	61.53	58.49
Al_2O_3		29.98	29.35	20.83	19.37	24.03	26.40
Fe_2O_3		0.62	0.60	0.26	0.57	0.28	0.29
CaO		11.20	12.70	2.25	0.13	5.35	7.81
Na_2O		4.06	4.24	8.50	8.29	8.17	5.97
K_2O		0.17	0.16	2.30	5.07	1.04	0.34
BaO		-	-	-	-	0.10	0.11
Total		99.46	99.15	99.15	99.06	100.49	99.41
		ATOMIC RATIOS ON THE BASIS OF 32 OXYGENS					
	Si	9.702	9.569	11.630	11.966	10.923	10.487
Z	Al	6.395	6.328	4.364	3.922	5.035	5.583
	Fe	0.065	0.066	0.021	0.065	.043	.043
	Ca	2.171	2.491	0.429	0.021	1.013	1.498
XY	Na	1.418	1.565	2.945	2.914	2.816	2.069
	K	0.021	0.022	0.515	1.161	0.235	0.086
		END MEMBERS (MOL PERCENT)					
AB		39.3	38.4	75.7	71.1	69.3	56.6
AN		60.1	61.1	11.0	0.6	24.9	41.0
OR		0.6	0.5	13.2	28.3	5.8	2.4
Z		16.162	15.953	16.015	15.953	16.001	16.113
XY		3.610	4.078	3.889	4.096	4.064	3.653

KEY TO ANALYSES OF TABLE 1.2
MAGNETITES, ILMENITE, HERCYNITE

1. Microphenocryst (Talisker 13; 20, 1A).
2. Groundmass titanomagnetite; same rock as (1).
3. " " " " " "
4. Microphenocryst (Talisker 15; 14, 1A).
5. " " " " "
6. " " " " "
7. Phenocryst margin, Roineval. (18; 1B)
8. " centre, " " "
9. Microphenocryst, " " "
10. Phenocryst centre, Greenland composite dyke (GGU 85990; no rock analysis).
11. Margin of (10).
12. Groundmass titanomagnetite, Reunion 574 (12, 1H).
13. Hercynite phenocryst; centre (20; 1A).
14. " inclusion in phenocryst (20; 1A).
15. " " centre (20; 1A).
16. Megacryst in basanite (Binns et al. 1970; Analysis 2 Table 8).
17. Spineliferous titanomagnetite outer border to (13).
18. " " centre of border.
19. " " closest to hercynite.

TABLE 1.2

MAGNETITE ANALYSES

	1	2	3	4	5	6
SiO_2	0.23	0.07	0.13	0.66	0.10	0.10
Al_2O_3	1.03	1.24	1.45	1.52	0.95	0.93
FeO	64.32	65.27	66.67	62.30	64.88	63.55
MgO	2.30	2.24	2.00	2.53	2.27	2.57
CaO	0.06	0.18	0.07	0.10	0.06	0.10
TiO_2	26.17	27.19	27.07	25.99	26.18	26.28
MnO	0.52	0.71	0.80	1.05	0.90	0.66
Total	94.64	96.96[1]	98.56[2]	94.15	95.33	94.29
	RECALCULATED ANALYSES					
	Ilmenite basis					
Fe_2O_3	30.22	30.24	31.36	28.85	30.63	29.57
FeO	37.12	38.05	38.45	36.34	37.32	36.94
Total	97.66	99.98	100.6	97.04	98.4	97.25
	Ulvospinel basis					
Fe_2O_3	12.63	12.29	13.49	10.87	13.26	12.20
FeO	52.95	54.14	54.53	52.52	52.81	52.51
Total	95.90	98.12	98.81	95.24	96.52	95.45
Mol % Ulvöspinel	75.7	76.8	75.7	75.2	75.0	76.0

1. Includes Cr_2O_3: 0.06
2. Includes ZnO: 0.07

TABLE 1.2 (contd.)

	7	8	9	10	11	12
SiO_2	0.10	0.10	0.18	0.14	0.14	0.15
Al_2O_3	1.69	1.56	1.74	1.96	2.90	1.34
FeO	65.92	66.86	66.79	63.57	65.42	64.16
MgO	2.15	2.04	2.61	2.03	2.20	1.65
CaO	0.0	0.0	0.04	0.01	0.01	0.08
TiO_2	25.32	25.54	25.41	28.47	24.77	23.65
MnO	0.40	0.35	0.70	0.60	0.60	0.70
Total	95.59	96.45	97.47	96.78	96.04	91.73
	RECALCULATED ANALYSES					
	Ilmenite basis					
Fe_2O_3	31.96	32.58	32.56	28.12	31.97	31.78
FeO	37.14	38.12	37.49	38.25	36.65	35.56
Total	98.77	100.29	100.73	99.58	99.24	94.91
	Ulvospinel basis					
Fe_2O_3	15.44	14.21	15.87	9.46	16.06	16.13
FeO	52.02	54.07	52.45	55.01	51.00	49.55
Total	97.13	97.87	98.97	97.68	97.68	93.25
Mol % Ulvöspinel	72.2	74.8	71.2	80.8	70.7	70.8

TABLE 1.2 (contd.)

	13	14	15	16	17	18	19
SiO_2	0.15		0.18	0.17	0.16	0.11	0.20
Al_2O_3	51.88	52.46	49.91	59.48	9.32	9.17	30.31
ΣFe as FeO	35.09	32.83	33.17	15.72	64.05	65.95	49.07
Fe_2O_3	-	-	-	6.69	-	-	-
MgO	11.23	12.94	12.78	17.21	4.05	3.03	6.80
CaO			0.04	0.01	0.04	0.06	0.07
TiO_2	1.72	1.34	1.66	0.76	19.81	17.39	10.45
MnO				0.12	0.13	0.45	0.54
Cr_2O_3	0.29		0.28	0.02	0.55	0.55	
Total	100.33	99.57	98.15[1]	100.38[2]	98.10	96.64[3]	97.43
	NUMBER OF IONS ON THE BASIS OF 32 OXYGENS						
Si	0.034	0.034	0.042	0.035	0.048	0.028	0.053
Al	13.874	13.92	13.615	14.639	3.285	3.348	9.416
Fe^{3+}	-	-	-	1.051	-	-	-
Fe^{2+}	6.658	6.181	6.421	2.745	16.02	17.083	10.816
Mg	3.798	4.342	4.409	5.354	1.805	1.399	2.672
Ca	-	-	0.010	0.003	0.013	0.020	0.020
Ti	0.293	0.227	0.289	0.119	4.455	4.05	2.071
Cr	0.052	0.050	0.051	0.002	0.13	0.135	0.135
Mn	-	-	-	0.021	0.033	0.118	0.121

1. contains 0.14 ZnO
2. contains 0.12 ZnO, 0.08 NiO
3. contains 0.49 V_2O_3

KEY TO ANALYSES OF TABLE 1.3 (CLINOPYROXENES)

1.Groundmass pyroxene fromm Talisker porphyritic hawaiite; (Talisker 13;Analysis 20,Table 1A,Appendix A)

2. " " " " "

3.Groundmass clinopyroxene,Kyogle hawaiite.(Wilkinson and Binns,1969)

4.Groundmass clinopyroxene from mugearite,Drum na Criche. (Muir and Tilley,1961)

5.Phenocryst from alkali olivine basalt;North Berwick. (Analysis 8,Table 1D)

6.Corroded phenocryst from same flow as (5).

7.Outer rim of phenocryst from the central facies of St. Leonard's Sill.(Anaysis 14,18;Table 1D)

8.Interior of same phenocryst.

9.Phenocryst from central facies of the Dasses Sill (Analysis 12,Table 1D)

10.Phenocryst from upper porphyritic unit of the Greenock composite flow.(Analysis 16,Table 1E)

11. " " " " " " "
" " " 8 " "

12.Outer rim of phenocryst from central facies of Greenland composite dyke.(no rock analysis;GGU no.85992)

13.Center of phenocryst,same rock.

14.Groundmass clinopyroxene from the Bras Rouge Sill; (Re 574;Analysis 12,Table 1H)Centre of crystal.

15.Margin of same crystal.

16.Phenocryst in hawaiite flow,Piton des Neiges.(13,Table 1H)

TABLE 1.3.

Clinopyroxene Analyses

	1	2	3	4	5	6
SiO_2	48.82	49.76	50.45	52.23	46.59	47.73
Al_2O_3	3.32	3.19	3.51	6.64	7.84	6.21
ΣFe as FeO	10.71	10.26	9.02	9.64	8.35	8.85
Fe_2O_3	1.57	1.68	2.96	0.59	1.47	1.40
FeO	9.28	8.73	6.33	9.10	7.01	7.57
MgO	12.27	12.24	13.31	9.55	12.79	13.43
CaO	21.44	21.59	20.37	18.17	21.57	21.64
Na_2O	0.63	0.69	1.07	2.00	0.57	0.54
TiO_2	2.56	2.20	2.16	0.78	2.66	2.23
MnO	0.23	0.29	0.21	0.33	0.21	0.20
Total	100.12	100.37	100.37	99.58	100.71	100.95
	NUMBER OF IONS ON THE BASIS OF 6 OXYGENS					
Si	1.844	1.868	1.868	1.936	1.734	1.774
Al	0.148	0.132	0.132	0.064	0.266	0.226
Ti	0.008	-	-	-	-	-
Al^{3+}	-	.009	.022	.225	.078	.047
Fe^{3+}	.045	.049	.082	.018	.041	.038
Fe^{2+}	.293	.273	.196	.280	.217	.234
Mg	.691	.685	.731	.531	.709	.744
Ca	.868	.869	.808	.722	.860	.862
Na	.046	.050	.077	.142	.041	.039
Ti	.065	.062	.060	.022	.074	.063
Mn	.007	.009	.007	.009	.007	.006
K	-	-	.004	.027	-	-
Mg	36.3	36.4	40.2	34.0	38.8	39.5
ΣFe(+Mn)	18.1	17.4	15.6	19.7	14.1	14.7
Ca	45.6	46.2	44.2	46.3	47.1	45.8
Z	2.000	2.000	2.000	2.000	2.000	2.000
X+Y+W	2.015	2.006	1.987	1.976	2.027	2.033

TABLE 1.3 (Contd.)

	7	8	9	10	11	12
SiO_2	49.01	47.71	50.27	49.40	50.85	50.64
Al_2O_3	7.18	7.33	3.34	4.49	3.85	1.62
ΣFe as FeO	7.25	7.28	10.27	8.51	8.49	12.25
Fe_2O_3	1.27	1.29	1.16	0.97	1.13	6.91
FeO	6.10	6.10	9.21	7.64	7.46	5.97
MgO	12.41	13.11	13.03	14.07	14.51	11.53
CaO	21.74	21.61	21.24	21.14	20.64	20.28
Na_2O	0.51	0.51	0.46	0.36	0.43	2.65
TiO_2	2.12	2.15	1.31	1.96	1.35	1.01
MnO	0.31	0.47	0.31	0.25	0.30	0.15
Total	100.65	100.28	100.33	100.28	100.52	100.76
	NUMBER OF IONS ON THE BASIS OF 6 OXYGENS					
Si	1.805	1.771	1.883	1.839	1.880	1.904
Al	.195	.229	.117	.161	.128	0.072
Ti	-	-	-	-	-	0.024
Al	.117	.092	.030	.036	.048	.000
Fe^{3+}	.036	.036	.052	.026	.031	.195
Fe^{2+}	.187	.186	.261	.238	.226	.189
Mg	.681	.725	.727	.781	.800	.646
Ca	.858	.859	.852	.843	.818	.817
Na	.036	.037	.033	.026	.031	.195
Ti	.059	.060	.037	.055	.038	.005
Mn	.010	.015	.010	.008	.009	.005
K	-	-	-	-	-	-
Mg	38.4	39.8	38.2	41.2	42.5	34.9
ΣFe(+Mn)	13.2	13.0	17.0	14.3	14.1	21.0
Ca	48.4	47.2	44.8	44.5	43.4	44.1
Z	2.000	2.000	2.000	2.000	2.000	2.000
X+Y+W	1.984	2.010	2.002	2.013	2.001	2.052

TABLE 1.3 (Contd.)

	13	14	15	16
SiO_2	51.02	50.32	48.58	50.50
Al_2O_3	1.68	3.17	4.23	2.93
ΣFe as FeO	12.45	8.80	8.18	8.30
Fe_2O_3	6.85	1.05	1.03	1.02
FeO	6.22	7.84	7.24	7.37
MgO	11.83	13.29	14.58	15.38
CaO	19.33	21.01	22.40	21.66
Na_2O	2.68	0.40	0.39	0.39
TiO_2	1.03	2.88	1.24	1.23
MnO	0.15	0.24	0.20	0.20
Total	100.79	100.20	99.89	100.52
	NUMBER OF IONS ON THE BASIS OF 6 OXYGENS			
Si	1.914	1.874	1.823	1.872
Al	.074	.126	0.177	0.128
Ti	.012	-	-	-
Al	.000	.013	.010	.000
Fe^{3+}	.193	.029	.028	.028
Fe^{2+}	.191	.243	.225	.226
Mg	.622	.738	.815	.850
Ca	.777	.838	.900	.860
Na	.195	.029	.028	.028
Ti	.013	.081	.035	.034
Mn	.005	.008	.006	.006
Mg	34.8	39.7	41.3	43.2
ΣFe(+Mn)	21.7	15.2	12.5	13.1
Ca	43.5	45.1	45.6	43.7
Z	2.000	2.000	2.000	2.000
W+X+Y	1.996	1.979	2.047	2.032

CALCULATED END MEMBER MOLECULES OF THE CLINOPYROXENES IN TABLE 1.3.

Analysis No.	1	2	3	4	5	6	7
1	4.6	6.0	1.1	0.1	39.3	34.5	14.4
2	5.0	6.2	-	0.9	39.8	34.6	13.5
3	5.4	6.1	4.2	0.1	36.8	37.5	9.9
4	17.6	2.2	-	4.6	33.5	27.6	14.5
5	4.0	7.3	1.5	7.9	33.7	34.9	10.7
6	3.8	6.1	1.9	5.3	35.2	36.5	11.3
7	3.7	6.0	1.8	8.1	35.8	35.2	9.5
8	3.6	5.9	0.9	9.1	34.6	36.6	9.3
9	3.3	3.5	1.1	3.1	38.5	36.2	14.3
10	2.6	5.2	0.5	4.2	36.8	39.0	11.8
11	3.1	3.8	-	4.6	36.7	40.4	11.4
12	11.8	2.7	6.1	1.7	37.8	31.6	8.3
13	11.8	2.8	6.3	1.6	36.2	32.6	8.7
14	3.0	5.9	0.9	0.3	39.3	38.1	12.5
15	2.8	3.7	2.6	0.5	38.4	41.2	10.8
16	2.7	3.3	2.9	0.2	38.6	41.5	10.8

Column 1: Acmite ($Na\ Fe^{3+}\ Si_2O_6$)
2: Ti-Tschermak ($Ca\ Ti\ Al_2O_6$)
3: Ferri-Tschermak ($Ca\ Fe^{3+}_2\ SiO_6$)
4: Ca-Tschermak ($Ca\ Al_2\ SiO_6$)
5: Wollastonite ($Ca_2\ Si_2O_6$)
6: Enstatite ($Mg_2\ Si_2O_6$)
7: Ferrosilite ($Fe_2\ Si_2O_6$)
8: Jadeite ($Na\ Al\ Si_2O_6$)

KEY TO ANALYSES OF TABLE 1.4 (OLIVINE)

1. Margin of phenocryst, Talisker (20; 1A).
2. Centre " " " " "
3. " " " " " "
4. Phenocryst in hawaiite, Roineval (18; 1B).
5. Phenocryst in alkali-olivine basalt (1; 1A).
6. " " " " " " "
7. Phenocryst in alkali-olivine basalt; Royal Park, Edinburgh.

TABLE 1.4

OLIVINE ANALYSES

	1	2	3	4	5	6	7
SiO_2	35.01	35.29	35.35	35.62	39.01	38.26	39.34
Al_2O_3	0.08	0.08	0.11	0.03	0.10	0.08	0.03
FeO	39.58	37.73	37.31	37.51	20.05	24.24	17.42
MgO	24.01	25.53	25.98	26.16	41.06	37.18	42.42
CaO	0.57	0.44	0.43	0.30	0.28	0.26	0.23
Na_2O	0.05	0.04	0.04	-	0.04	0.03	0.02
K_2O	-	-	-	-	0.05	0.02	-
TiO_2	0.14	0.07	0.08	0.09	0.03	0.02	0.02
MnO	0.80	0.65	0.66	0.71	-	-	
Total	100.24	99.83	99.96	100.42	100.62	100.09	99.48
	NUMBER OF IONS ON THE BASIS OF 4 OXYGENS						
Si	0.996	0.998	0.996	1.003	0.997	1.002	1.004
Al	0.003	0.003	0.004	0.001	0.003	0.002	0.001
Fe	0.942	0.892	0.879	0.883	0.428	0.531	0.372
Mg	1.018	1.076	1.091	1.098	1.564	1.452	1.613
Ca	0.017	0.013	0.013	0.009	0.008	0.007	0.006
Na	0.003	0.002	0.002	-	0.003	0.002	-
K	-	-	-	-	0.002	0.002	-
Ti	0.003	0.001	0.002	0.002	0.002	0.002	.0001
Mn	0.019	0.016	0.016	0.017	-	-	-
	END MEMBERS (MOL PERCENT)						
FO	51.9	54.7	55.4	55.4	78.5	73.2	81.3
FA	48.1	45.3	44.6	44.6	21.5	26.8	18.7

APPENDIX D

CORRELATION MATRICES
(in pocket at back cover)

CORRELATION MATRICES

A. Talisker composite flow.

B. Roineval composite flow.

C. Greenock composite flow with all specimens.

D. " " " minus specimens at junction of the two units.

E. Bras Rouge Sill.

CORRELATION MATRIX FOR DATA MATRIX TALISKER

	SiO_2 / H_2O / SR	Al_2O_3 / TiO_2 / RB	FE_2O_3 / P_2O_5 / HEIGHT	FEO / MNO / TOTFE	MGO / BA	CAO / Y	NA_2O / ZR	K_2O / ZN
SiO_2	1.000000 -0.351679 0.627602	0.803687 -0.283866 0.625430	-0.098489 -0.174029 0.856508	-0.210498 -0.575151 -0.316158	-0.837197 0.652919	-0.670169 0.252888	0.881635 0.392142	0.655583 -0.538354
Al_2O_3	0.803687 -0.270339 0.282181	1.000000 -0.237017 0.002694	0.390638 -0.309500 0.750202	-0.641227 -0.757468 -0.534683	-0.685178 0.612320	-0.378537 -0.267621	0.726415 0.370807	0.416501 -0.349828
FE_2O_3	-0.098489 -0.181443 -0.112854	0.390638 -0.210856 -0.231883	1.000000 -0.136519 0.042013	-0.572759 -0.284651 -0.067995	-0.075470 0.293918	0.088910 -0.786298	0.038583 0.160693	-0.249365 0.112821
FEO	-0.210498 -0.109488 0.398355	-0.641227 0.828291 0.403955	-0.572759 0.566823 -0.082304	1.000000 0.838794 0.856772	-0.006810 -0.000468	-0.354159 0.576681	-0.073712 -0.333873	0.257198 -0.132886
MGO	-0.837197 0.590425 -0.838981	-0.685178 0.452105 0.438442	-0.075470 -0.159938 -0.913466	-0.006810 0.273417 -0.055768	1.000000 -0.890728	0.842340 -0.157226	-0.952738 0.543838	-0.824186 0.557969
CAO	-0.670169 0.315324 -0.827636	-0.378537 0.700470 0.397252	0.088910 -0.158766 -0.797317	-0.354159 0.002578 0.375112	0.842340 -0.797789	1.000000 -0.309211	-0.854983 0.275340	-0.673055 0.718466
NA2O	0.881635 -0.397532 0.744488	0.726415 0.347851 0.307313	0.038583 -0.048750 0.554107	-0.073712 -0.423040 0.065442	-0.952738 0.873090	-0.854983 0.156645	1.000000 0.514696	0.725676 -0.607585
K_2O	0.655583 -0.538573 0.784561	0.416501 0.228735 0.426675	-0.249365 0.471435 0.741974	0.257198 0.045383 0.156158	-0.824186 0.671438	-0.673055 0.405840	0.725676 0.490189	1.000000 -0.330677
H_2O	-0.351679 1.000000 -0.658707	-0.270339 0.421052 -0.377798	-0.181443 0.556616 0.376021	-0.109488 0.112083 0.247405	0.590425 -0.581819	0.315324 -0.005063	-0.397532 -0.344992	-0.534573 0.027909
TiO_2	0.627602 -0.421052 0.693169	0.803687 1.000000 0.493832	-0.210856 0.657243 0.341571	0.828291 0.656102 0.875461	-0.452105 0.505449	-0.700470 0.398562	0.347851 -0.040042	0.528735 -0.325941
P_2O_5	-0.174029 -0.556616 0.382768	-0.309500 0.657243 0.245360	-0.136519 1.000000 0.010567	0.566823 0.717637 0.603994	-0.159938 0.200372	-0.158766 0.199330	-0.048750 0.102106	0.471435 0.212327
MNO	-0.575151 -0.112083 0.111541	-0.757468 0.056102 0.226586	-0.284651 0.717637 -0.385751	0.838794 1.000000 0.841820	0.273417 -0.175618	0.002578 0.267827	-0.423040 0.275687	0.045383 0.125725
BA	0.652919 -0.581819 0.680427	0.612320 0.505449 0.362441	0.293918 0.200372 0.892265	-0.000468 -0.175618 0.184336	1.000000	-0.090083	0.873090 0.480454	0.671438 -0.463057
Y	0.252888 -0.005063 0.452660	-0.267621 0.398562 0.226732	-0.786298 0.199330 0.118408	0.576681 0.267827 0.207211	-0.157226	-0.309211 -0.090083	0.156645 -0.002777	0.405840 -0.149359
ZR	0.392142 -0.344992 0.385961	0.370807 -0.040042 0.066297	0.160693 0.102106 0.434039	-0.333873 -0.275687 -0.305263	-0.543838 0.480454	-0.275340 -0.002777	0.514696 1.000000	0.490189 -0.093890
ZN	-0.538354 0.027909 -0.603455	-0.349828 -0.325941 -0.350336	0.112821 0.212327 -0.563788	-0.132886 0.125725 -0.090759	0.557969 -0.463057	0.718466 -0.149359	-0.607585 -0.093890	-0.330677 1.000000
SR	0.627602 -0.658707 1.000000	0.262181 0.693169 0.493867	-0.212854 0.382768 0.650767	0.398355 0.111941 0.350929	-0.838981 0.680427	-0.827636 0.452660	0.744488 0.385961	0.784561 -0.603455
RB	0.225480 -0.577708 0.648367	0.062694 0.493832 0.010300	-0.231883 0.245360 0.235664	0.403955 0.226588 0.345774	-0.438442 0.362441	-0.397252 0.226732	0.307313 0.066297	0.426675 -0.350336
HEIGHT	0.854508 -0.374021 0.450767	0.750202 0.341571 0.235664	0.042013 0.010567 1.000000	-0.082304 -0.385751 -0.073741	-0.913466 0.892265	-0.797317 0.118408	0.954107 0.434039	0.741974 -0.563788
TOTFE	-0.316158 -0.247405 0.350929	-0.534683 0.875461 0.345774	-0.067995 0.603994 -0.073741	0.856772 0.841820 1.000000	-0.055768 0.184336	-0.375112 0.207211	-0.065442 -0.305263	0.156158 -0.090759

CORRELATION MATRIX FOR DATA MATRIX BCINEVAL

	SiO_2 H_2O SR WBE	Al_2O_3 TiO_2 RB	Fe_2O_3 P_2O_5 HEIGHT	FEO MNO NI	MGO BA CU	CAO Y TOTFE	Na_2O ZR	K_2O ZN
SiO_2	1.000000 -0.370130 0.915214 0.368877	-0.884829 0.797836 0.412993	-0.746560 0.826753 0.075958	-0.300640 0.595733 -0.006100	-0.489083 0.902078 -0.107590	-0.413335 0.475434 -0.940426	0.512562 0.511580	0.851532 0.802039
Al_2O_3	-0.884829 0.126180 -0.584165 -0.406784	1.000000 0.588270 -0.736144	0.200438 -0.877022 0.646785	0.505578 -0.886105 0.683656	0.273364 -0.750298 0.220408	0.682730 -0.885147 0.511977	-0.622174 -0.667966	-0.867045 -0.575630
FE_2O_3	-0.746560 0.473421 -0.885363 -0.545678	0.200438 0.484223 0.242753	1.000000 -0.470349 -0.575998	-0.323565 -0.154839 -0.526891	0.447556 -0.627154 0.063890	-0.027213 -0.035218 0.816103	0.042298 -0.343819	-0.493743 -0.843986
FEO	-0.300640 -0.311405 -0.054716 0.299184	0.505578 0.427417 -0.773205	-0.323565 -0.397191 0.521635	1.000000 -0.212779 0.548007	-0.120857 -0.212779 -0.116930	0.344216 -0.612031 0.262757	-0.512366 0.060157	-0.325318 0.256332
MGO	-0.489083 0.086192 -0.312184 -0.420110	0.273364 0.761687 -0.368518	0.447556 -0.627154 -0.194993	-0.120857 -0.383128 -0.068909	1.000000 -0.696854 0.842671	0.625944 -0.884370 0.379883	-0.614508 -0.550145	-0.663809 -0.535938
CAO	-0.413335 -0.000282 -0.053831 -0.228481	0.682730 0.607811 -0.844852	-0.027213 -0.720806 0.563092	0.344216 -0.853712 0.688620	0.625944 -0.734572 0.742733	1.000000 -0.953335 0.182647	-0.897630 -0.827121	-0.789805 -0.366597
Na_2O	0.512562 -0.123919 0.156275 0.155705	-0.622174 0.753892 0.899277	0.042298 0.618096 -0.430829	-0.512366 0.756904 -0.560029	-0.614508 0.736876 -0.556893	-0.897630 0.292867 -0.270055	1.000000 0.596651	0.741769 0.279513
K_2O	0.851532 -0.101115 0.307146 0.688838	-0.867045 0.799198 0.687912	-0.493743 0.937983 -0.296663	-0.325318 0.851739 -0.399958	-0.663809 0.963888 -0.538226	-0.789805 0.590802 -0.699211	0.741769 0.800071	1.000000 0.762586
H_2O	-0.370130 1.000000 -0.352788 -0.355062	-0.126180 0.588369 0.215830	0.475421 -0.146722 -0.422292	-0.311405 -0.167629 -0.347779	0.086192 -0.349791 -0.190103	-0.000282 0.413513 0.291752	-0.123919 -0.258213	-0.101115 -0.441488
TiO_2	-0.797856 0.126366 -0.562316 -0.562102	0.588270 1.000000 -0.835689	0.464223 -0.652771 -0.089012	0.427417 -0.462608 0.039896	0.781687 -0.823529 0.494762	0.607811 -0.247520 0.731644	-0.753892 -0.410761	-0.799198 -0.483927
P_2O_5	0.826753 -0.146722 0.741459 0.619213	-0.877022 -0.652771 0.941521	-0.470349 1.000000 -0.374749	-0.397191 0.853208 -0.466154	-0.418181 0.896136 -0.331547	-0.720806 0.667610 -0.719393	0.618096 0.802722	0.937983 0.717181
MNO	0.595733 -0.167629 0.448165 0.382629	-0.886105 0.902638 0.723845	-0.154839 0.853208 -0.634062	-0.257333 1.000000 -0.714732	-0.383128 0.808871 -0.392942	-0.853712 0.603047 -0.338563	0.756904 0.680268	0.851739 0.617704
BA	0.902078 -0.349791 0.751700 0.556652	-0.750298 0.823529 0.582411	-0.607154 0.896136 0.115100	-0.212779 0.808871 -0.235930	-0.696854 1.000000 -0.459186	-0.734572 0.408391 -0.745444	0.736876 0.794487	0.963888 0.827102
Y	0.475434 0.413513 0.467001 0.176955	-0.884370 -0.247520 0.578117	-0.035218 0.667610 -0.678412	-0.612031 0.603047 -0.646757	0.884370 0.408391 0.079686	-0.953335 1.000000 -0.409507	0.292867 0.317418	0.590802 0.299918
ZR	0.511580 -0.258213 0.450344 0.160500	-0.667966 0.410761 0.474423	-0.343819 0.802722 -0.380545	0.060157 0.880268 -0.484743	-0.550145 0.794487 -0.618863	-0.827121 0.317418 -0.311796	0.596651 1.000000	0.800071 0.721241
ZN	0.802039 -0.441488 0.832303 0.939608	-0.533600 0.483927 0.981890	-0.843986 0.717181 0.122039	0.254332 0.617704 0.061070	-0.535938 0.827102 -0.254862	-0.366597 0.299918 -0.700232	0.279513 0.721241	0.762586 1.000000
SR	0.915214 -0.352788 1.000000 0.883153	-0.584165 0.342316 0.588994	-0.883163 0.741459 0.191186	-0.054716 0.448169 0.152245	-0.312184 0.751700 0.050549	-0.153831 0.467001 -0.928904	0.156275 0.450344	0.707146 0.872303
RB	0.412993 0.215830 0.688904 -0.038810	-0.739144 0.635836 1.000000	0.242753 0.641521 -0.680267	-0.773205 0.723845 -0.769286	-0.368518 0.582411 -0.430344	-0.844852 0.578117 -0.226160	0.899277 0.474423	0.687912 0.881890
HEIGHT	0.075958 -0.422292 0.193386 0.367552	0.646785 -0.869012 -0.680267	-0.575998 0.374749 1.000000	0.521635 -0.634062 0.585057	-0.194993 0.115100 0.127785	0.563092 -0.678412 -0.265309	-0.430829 -0.380545	-0.296683 0.122039
NI	-0.608300 0.347779 0.152245 0.303700	0.883656 -0.839896 -0.769286	-0.526891 0.466154 0.585057	0.548007 -0.714732 1.000000	-0.068909 0.235930 0.241329	0.688620 -0.646757 -0.199420	-0.560029 0.484743	-0.399958 0.061070
CU	-0.107590 0.190103 0.050596 -0.263236	0.220438 0.494752 -0.433344	0.063890 -0.331547 0.127785	-0.116930 0.392962 0.241329	0.842671 -0.459186 1.000000	0.742733 -0.079686 -0.006650	-0.556893 0.618863	-0.508226 0.254862
TOTFE	-0.940426 0.791752 -0.578504 -0.789477	0.821977 0.731644 -0.822080	0.816103 -0.719393 -0.265309	0.262757 -0.338563 -0.199420	0.379883 -0.745444 -0.006650	0.182647 -0.409507 1.000000	-0.270055 0.311796	-0.699211 -0.700232

CORRELATION MATRIX FOR DATA MATRIX GREENROCK 1

	SiO_2 H_2O SR	Al_2O_3 TiO_2 RB	FE_2O_3 K HEIGHT	FEO MNO NI	MGO BA CU	CAO Y ICTFE	NA_2O ZR	K_2O ZN
SiO_2	1.000000 -0.213037 -0.913623	-0.516215 -0.371394 0.362958	-0.461863 3.435339 0.210888	-0.577603 -0.043390 -0.319987	0.187938 0.728685 -0.657800	-0.686189 -0.214332 -0.575535	0.746224 0.863761	0.817254 0.607773
Al_2O_3	-0.516215 0.629744 0.649183	1.000000 -0.737990 -0.382200	-0.367402 -0.454560 0.530976	-0.726682 -0.120210 -0.322752	0.005247 -0.683282 0.785664	0.682785 -0.405586 -0.232159	-0.518113 -0.365874	-0.806437 -0.217785
FE_2O_3	-0.461863 -0.286522 0.343582	-0.367402 0.454560 -0.530976	1.000000 -0.008226 -0.582914	0.706784 0.032325 0.329458	-0.239788 -0.242181 -0.078060	-0.090955 0.764881 0.877388	-0.205549 -0.171981	-0.342353 0.046983
FeO	-0.577603 -0.169537 0.467140	-0.726682 0.714054 -0.416770	0.706784 -0.265722 -0.380507	1.000000 -0.134513 0.275384	-0.468733 -0.523619 0.160003	-0.098498 0.494208 0.959535	-0.422656 -0.265770	-0.120593 -0.261074
MgO	0.383538 0.217846 -0.411849	0.005247 -0.683282 -0.394878	-0.239788 0.786784 0.134439	-0.468733 0.454674 0.361639	1.000000 0.454674 0.171245	0.207955 -0.150023 -0.413343	-0.013658 0.169949	-0.129708 0.007000
CaO	-0.686189 0.129554 0.617554	0.682785 -0.405586 -0.463625	-0.090955 0.764881 -0.086940	-0.098498 0.494208 0.959535	0.207955 -0.384407 0.745804	1.000000 -0.110435 -0.103004	-0.701774 -0.062724	-0.791932 -0.590544
Na_2O	0.746224 -0.116476 -0.565205	-0.518113 0.714054 0.462187	-0.205549 0.300218 0.344977	-0.422656 0.131230 -0.141450	-0.013658 0.479209 -0.776824	-0.701774 0.062724 -0.368465	1.000000 0.562731	0.583235 0.409067
K_2O	0.817254 -0.511766 -0.021000	-0.806437 0.441683 0.214318	-0.342353 0.046983 -0.228938	-0.120593 -0.261074 0.275384	-0.129708 0.007000 -0.490088	-0.791932 0.183179 -0.098643	0.583235 0.409067	1.000000 0.493080
H_2O	-0.213037 1.000000 0.261770	0.924744 -0.737990 -0.399228	-0.288522 -0.026375 0.691252	-0.165937 0.634120 -0.240700	0.217846 -0.384407 0.295989	0.129554 -0.490672 -0.228384	-0.116476 -0.528156	-0.511766 0.051304
TiO_2	-0.071064 -0.539588 -0.071441	-0.707030 0.662030 0.288638	0.686432 0.386952 -0.669148	0.714054 0.041959 0.386332	-0.345024 0.095120 -0.315516	-0.436000 0.504458 0.757707	0.013761 0.382264	0.441683 -0.091454
Mg/z	0.435339 -0.026375 -0.620986	-0.924940 0.388952 0.473081	-0.006226 1.000000 0.307036	-0.245722 -0.634537 0.463267	0.488786 0.435654 -0.526435	-0.296277 0.300759 -0.169924	0.200218 0.496341	0.494980 0.224084
MnO	-0.047393 0.134120 0.111842	-0.123216 0.041939 0.154221	0.032329 -0.074537 -0.283938	-0.124513 1.000000 0.005698	-0.470465 0.137813 0.440517	-0.080806 -0.224825 -0.071577	0.131230 -0.209796	0.119053 -0.120745
BA	0.128685 -0.341405 -0.363854	-0.883236 0.393123 0.762799	-0.262181 0.435654 -0.802241	-0.523619 0.137813 0.159634	0.454674 1.000000 -0.576128	-0.384407 0.234117 -0.451519	0.479209 0.740079	0.965429 0.211901
Y	-0.214932 -0.490672 0.160269	-0.405596 0.389648 -0.267421	0.304881 0.300759 -0.318550	0.454238 -0.224825 0.456434	-0.150023 -0.234117 0.205049	-0.110435 1.000000 0.639631	0.062724 0.067154	0.131179 0.042893
ZR	0.863961 -0.528156 -0.621768	-0.763874 0.512364 0.339724	-0.171981 0.496341 -0.132411	-0.205770 -0.265796 0.295100	0.169949 0.740079 -0.668357	-0.706935 0.067154 -0.208010	0.562731 1.000000	0.906780 0.430796
ZN	0.607773 0.091364 -0.458187	-0.517781 -0.091499 0.311491	0.046983 0.211901 0.237209	-0.261074 -0.120745 -0.493788	0.007066 0.211961 -0.373203	-0.590544 0.042893 -0.156360	0.409067 0.430796	0.493080 1.000000
SR	-0.513653 0.261770 1.000000	0.449193 -0.399228 -0.808994	0.343582 -0.691252 0.020108	0.467140 0.111142 0.024366	-0.411849 -0.863854 0.638555	0.617554 0.160369 0.453517	-0.565205 -0.921768	-0.821000 -0.458187
RB	0.886959 -0.395223 -0.808994	-0.883200 0.662030 1.000000	-0.501500 0.775081 0.020108	-0.416770 0.134221 -0.146602	-0.041878 0.722969 -0.668390	-0.607629 -0.267421 -0.482274	0.682187 0.835724	0.814318 0.211491
HEIGHT	0.210888 0.691252 0.020108	0.539978 -0.691252 0.363632	-0.582914 1.000000 1.000000	-0.380537 -0.634120 -0.433703	0.134439 -0.302241 0.122163	-0.086940 -0.318550 -0.490088	0.344977 -0.132411	-0.228938 0.217238
NI	-0.319987 -0.240300 0.024366	-0.323734 0.386332 -0.268602	0.329458 0.446767 -0.433703	0.265384 0.005698 1.000000	0.361639 0.159634 -0.065803	0.273582 0.456434 0.270431	-0.141450 -0.639100	-0.089740 -0.637751
CU	-0.657800 0.295963 0.638555	0.785664 -0.863854 -0.668390	-0.078060 -0.302241 0.122163	0.160003 -0.576128 1.000000	0.171245 -0.576128 1.000000	0.745804 -0.205049 0.091007	-0.776824 -0.668357	-0.805187 -0.373203
ICTFE	-0.575575 -0.227384 0.453517	0.462187 0.399228 -0.482274	0.277388 -0.691252 -0.490088	0.955535 -0.071577 0.270431	-0.413343 -0.451519 0.091007	-0.103004 0.839631 1.000000	-0.368465 -0.208010	-0.098643 -0.158360

CORRELATION MATRIX FOR DATA MATRIX GREENOCK

	SiO_2 / H_2O / SR	Al_2O_3 / TiO_2 / RB	FE_2O_3 / FU / NI	FEO / MNO / CU	MGO / BA / HEIGHT	CAO / Y / TUFFS	NA_2O / ZR	K_2O / ZN
SiO_2	1.000000 -0.230086 -0.793451	-0.789722 -0.195498 0.860760	-0.330725 0.380674 -0.310960	-0.883725 0.191235 -0.315959	-0.361782 0.784336 -0.914531	-0.709304 0.319841 -0.630584	0.793334 0.951083	0.886336 0.622114
Al_2O_3	-0.789722 0.350338 0.873058	1.000000 0.303300 -0.570512	-0.147784 -0.447903 0.476455	0.400875 -0.397892 -0.619683	0.074649 -0.732239 0.828934	0.677384 -0.224151 0.231695	-0.745057 -0.791917	-0.656378 -0.289289
Fe_2O_3	-0.330725 -0.284325 0.219217	-0.147584 0.459112 -0.526414	1.000000 -0.101445 -0.156013	0.426437 -0.055815 0.107967	0.124640 -0.262980 0.120307	0.014641 0.351146 0.759824	-0.080317 -0.290029	-0.253041 -0.104411
FeO	-0.883725 0.126076 0.411156	0.400875 0.629629 -0.745360	0.426437 -0.771103 0.345203	1.000000 -0.254153 -0.193577	0.241652 -0.631359 0.730611	0.024026 -0.511737 0.491249	-0.338726 -0.663442	-0.716086 -0.572913
MnO	-0.361782 0.303641 -0.164350	0.074649 0.239613 -0.526017	0.124640 -0.099720 0.284702	0.241652 0.004936 0.611849	1.000000 0.076108 -0.280366	0.147957 -0.537612 0.230295	-0.205616 -0.373526	-0.551786 -0.540721
CaO	-0.709304 0.086725 0.719469	0.677384 -0.368897 -0.804810	0.014641 -0.147910 -0.164111	0.024026 -0.163774 0.467434	0.147957 -0.353625 0.848079	1.000000 0.079681 0.023905	-0.789263 -0.556384	-0.412384 -0.160831
Na_2O	0.793334 -0.262841 -0.857770	-0.745057 0.156108 0.536565	-0.080317 0.104002 -0.031565	-0.338726 0.327170 -0.330628	-0.205616 0.617061 -0.773076	-0.789263 0.108047 -0.278899	1.000000 0.636584	0.552459 0.301766
K_2O	0.886336 -0.221612 -0.540659	-0.656378 -0.394928 0.940051	-0.253041 0.697487 -0.812620	-0.716086 0.142608 -0.779170	-0.551786 0.722353 -0.810811	-0.412384 0.038822 -0.829424	0.552459 0.920187	1.000000 0.854080
H_2O	-0.230086 1.000000 0.279087	0.550358 -0.391234 -0.170833	-0.284305 0.166059 0.515451	0.126076 -0.208316 -0.029638	0.830641 -0.272399 0.760068	0.088725 -0.192907 -0.029055	-0.262841 -0.361830	-0.221612 0.072395
SiO_2	-0.193498 0.391234 -0.211091	-0.303369 1.000000 -0.525975	0.459112 -0.481296 0.124146	0.447626 0.396063 0.126855	0.236013 -0.135617 0.107841	-0.308892 -0.491029 0.660589	0.156108 -0.242933	-0.394928 -0.682336
Fe_2O_3	0.300674 0.126059 -0.963068	-0.447966 -0.481296 0.592663	-0.101445 1.000000 -0.402462	-0.771103 0.190879 0.268030	-0.055756 0.549801 -0.704496	-0.147910 0.584384 -0.601087	0.164002 0.602233	0.697487 0.638364
MnO	0.191235 -0.208316 -0.313942	-0.397852 0.396083 0.128091	-0.055815 0.190879 -0.106887	-0.254153 1.000000 0.938862	0.004936 0.339815 -0.421793	-0.163774 -0.124461 -0.208307	0.327170 0.058727	0.142608 -0.231356
BA	0.784336 -0.272399 -0.734270	-0.732239 -0.106817 0.724097	-0.262980 0.549801 -0.592291	-0.609359 0.339816 0.172931	0.076108 1.000000 -0.708267	-0.353625 0.153014 -0.557194	0.612061 0.796512	0.720053 0.443009
Y	0.319841 -0.147937 0.107355	-0.224151 -0.491029 0.451610	0.351146 0.584384 -0.538018	-0.511737 -0.124461 -0.147856	-0.537612 0.153314 -0.434564	0.079681 1.000000 -0.208884	0.108047 0.401509	0.609822 0.785841
ZR	0.951083 -0.301830 -0.764933	-0.791917 0.242933 0.884469	-0.290067 0.602233 -0.526859	-0.663442 0.058729 0.282559	-0.373526 0.796512 -0.828805	-0.556384 0.401509 -0.608327	0.636584 1.000000	0.920187 0.679588
ZN	0.822114 0.072093 -0.147080	-0.289289 -0.662336 0.779169	-0.104411 0.838309 -0.534320	-0.572913 -0.231356 -0.408148	-0.540721 0.443009 -0.920187	-0.160831 0.785841 -0.459179	0.301766 0.679588	0.854080 1.000000
SR	-0.793457 0.279087 1.000000	0.873058 -0.711091 -0.999636	-0.147417 0.923088 -0.212988	-0.911156 -0.313942 -0.061380	-0.187353 -0.734270 0.756226	0.715969 0.107355 0.349878	-0.657770 -0.764933	-0.540659 -0.147080
RB	0.886336 -0.170833 -0.999636	-0.520512 -0.525975 1.000000	-0.526414 0.594083 -0.501239	-0.795360 0.128091 -0.267976	-0.528817 0.724097 -0.734820	-0.334410 0.451610 -0.811355	0.538585 0.884469	0.940051 0.779169
NI	-0.210420 0.515451 0.712708	0.478455 0.124146 -0.501239	-0.196013 -0.402462 1.000000	0.345203 -0.108867 -0.150650	0.269702 -0.592291 0.278448	-0.104111 -0.536018 0.177527	-0.037565 -0.529859	-0.612620 -0.534320
CU	-0.315959 -0.626058 -0.061380	-0.019683 0.126855 -0.267976	0.107967 0.488033 -0.150650	-0.193577 0.538802 1.000000	0.611849 0.172931 0.052163	0.467434 -0.147856 -0.040275	-0.330608 -0.282559	-0.273270 -0.408148
HEIGHT	-0.914531 0.260068 0.756226	0.828932 0.107841 -0.734820	0.102307 -0.709495 0.278448	0.730811 -0.421793 0.052163	0.280366 -0.708267 1.000000	0.644824 -0.434549 0.579754	-0.773876 -0.828805	-0.610811 -0.526561
TUFFS	-0.630584 -0.029055 0.399451	0.231695 0.460589 -0.811355	0.759824 -0.601087 0.177527	0.492714 -0.208007 -0.040275	0.233295 -0.557194 0.579754	0.323905 -0.238884 1.000000	-0.279899 -0.408327	-0.629424 -0.459179

CORRELATION MATRIX FOR DATA MATRIX **BRAS ROUGE**

	SiO_2 H_2O SR	Al_2O_3 TiO_2 RB	FEE P_2O_5 HEIGHT	FEO MNO TOTFE	MGO BA	CAO Y	Na_2O ZR	K_2O ZN
SiO_2	1.000000	0.230332	-0.769855	-0.171920	-0.927667	-0.935313	0.952369	0.904050
H_2O	0.705789	-0.789148	0.462849	0.601596	0.586414	0.929946	0.929560	0.872508
SR	-0.834420	0.911621	-0.789069	-0.912540				
Al_2O_3	0.230302	1.000000	-0.063558	-0.321513	-0.010148	-0.044437	-0.046854	-0.031896
TiO_2	-0.128765	0.357549	0.528663	-0.055762	-0.299092	0.024122	0.075603	0.002757
RB	0.036692	0.060238	0.267440	-0.284999				
Fe_2O_3	-0.769855	-0.063558	1.000000	-0.377802	0.869891	0.645773	-0.739014	-0.645406
P_2O_5	-0.462849	0.464558	-0.160392	-0.488154	-0.896382	-0.671318	-0.662499	-0.572626
HEIGHT	0.475153	-0.092904	0.583559	0.775241				
FEO	-0.171920	-0.321513	-0.377802	1.000000	0.048169	0.262648	-0.137668	-0.201085
MNO	-0.367504	0.326196	0.456941	0.190449	0.469244	-0.275624	-0.365806	-0.198418
TOTFE	0.372226	-0.269860	0.262728	0.291963				
MGO	-0.927467	-0.010148	0.869891	0.048169	1.000000	0.883656	-0.925821	-0.883925
BA	-0.701102	0.830215	-0.390961	-0.576390	-0.762643	-0.915586	-0.894970	-0.810805
Y	0.739376	-0.886722	0.887121	0.931449				
CAO	-0.935313	-0.044437	0.645773	0.262648	0.883656	1.000000	-0.962274	-0.986970
MGO	-0.850306	0.850767	-0.314255	-0.628927	-0.479190	-0.882492	-0.892566	-0.905551
Y	0.921979	-0.827734	0.863474	0.846262				
Na_2O	0.952369	-0.046854	-0.739014	-0.137668	-0.925821	-0.962274	1.000000	0.937667
K_2O	0.834456	-0.828280	0.252484	0.571446	0.657799	0.938446	0.917553	0.885728
ZR	-0.920872	0.718320	-0.870954	-0.857314				
K_2O	0.904050	-0.031896	-0.645406	-0.201085	-0.883925	-0.986970	0.937667	1.000000
ZN	0.798979	-0.843832	0.328664	0.704015	-0.479315	0.851494	0.870599	0.904365
ZR	-0.867631	0.766547	-0.890964	-0.803882				
H_2O	0.705789	-0.128765	-0.462849	-0.367504	-0.701102	-0.850306	0.834456	0.798979
TiO_2	1.000000	0.357549	0.528663	0.208722	0.438282	0.716243	0.690251	0.657643
RB	-0.937188	0.744778	-0.750705	-0.732543				
TiO_2	-0.789148	0.357549	0.464558	0.526196	0.830215	0.850767	-0.828280	-0.843832
P_2O_5	-0.794487	1.000000	-0.495866	-0.353532	-0.438536	-0.864004	-0.801723	-0.726835
RB	0.810930	-0.826232	0.948478	0.838859				
P_2O_5	0.462849	0.528663	-0.160392	-0.456941	-0.390961	-0.314255	0.252484	0.328664
FEO	-0.038120	0.273135	1.000000	0.273135	-0.063684	0.428190	0.546833	0.306520
RB	-0.134820	0.374917	-0.383942	-0.477421				
MNO	0.601596	-0.055762	-0.488154	0.190449	-0.576390	-0.628927	0.571446	0.704015
BA	0.208722	-0.353532	0.273135	1.000000	0.284335	0.543836	0.559166	0.607645
RB	-0.358838	0.241832	-0.524860	-0.374328				
BA	0.586414	-0.299092	-0.896382	0.469244	-0.762643	-0.479190	0.657799	0.479315
MNO	0.438282	-0.903536	-0.063684	0.284335	1.000000	0.607109	0.505187	0.420256
RB	-0.414812	0.661073	-0.570118	-0.605821				
Y	0.929946	0.024122	-0.671318	-0.275624	-0.915586	-0.882492	0.938446	0.851494
MNO	0.716243	-0.864004	0.428190	0.543836	0.607109	1.000000	0.985101	0.893731
RB	-0.825318	0.869044	-0.870685	-0.881503				
ZR	0.929560	0.075603	-0.662499	-0.365806	-0.894970	-0.892566	0.917553	0.870599
MNO	0.690251	-0.801723	0.546833	0.559166	0.505187	0.985101	1.000000	0.888074
RB	-0.815855	0.935264	-0.888521	-0.871937				
ZN	0.872508	0.002757	-0.572626	-0.198418	-0.810805	-0.905551	0.885728	0.904365
MNO	0.657643	-0.726835	0.306520	0.607645	0.420256	0.893731	0.888074	1.000000
RB	-0.783262	0.772191	-0.782297	-0.726882				
SR	-0.834420	0.330892	0.475153	0.372226	0.739376	0.921979	-0.920872	-0.867631
RB	-0.937188	0.813930	-0.134820	-0.358838	-0.414812	-0.825318	-0.815855	-0.783262
TOTFE	1.000000	-0.826232	0.776158	0.744770				
RB	0.811621	0.826232	-0.092904	-0.269860	-0.827734	0.869044	0.935264	0.766547
HEIGHT	0.744778	-0.826232	0.374917	0.341832	0.863474	0.965044	0.935264	0.772191
RB	-0.836577	1.000000	-0.798004	-0.655930				
HEIGHT	-0.739069	0.267440	0.583559	0.262728	0.887121	0.863474	-0.870954	-0.890964
RB	-0.750705	0.962478	-0.383942	-0.524860	-0.573118	-0.870685	-0.888521	-0.782297
TOTFE	0.776158	-0.798004	1.000000	0.782050				
TOTFE	-0.512540	-0.084397	0.775241	0.291963	0.931449	0.846262	-0.857314	-0.803882
RB	-0.732543	0.328369	-0.477421	-0.374328	-0.605821	-0.881503	-0.871937	-0.726882
TOTFE	0.744770	-0.399930	0.782050	1.000000				

ABSTRACT OF THESIS

Name of Candidate WALTER WILLARD BOYD, Jr.

Address KAIVOSRINTEENTIE 2-G-55, 00440 HELSINKI 44, FINLAND

Degree Doctor of Philosophy *Date* February, 1974.

Title of Thesis GEOCHEMICAL INVESTIGATION OF COMPOSITE BODIES INVOLVING INTERMEDIATE MEMBERS OF THE ALKALI BASALT-TRACHYTE SUITE

The geochemistry of the intermediate members (hawaiites, mugearites, benmoreites) of the alkali-olivine basalt-trachyte suite occurring as composite bodies is reviewed.

Typically, but not invariably, the porphyritic unit is hawaiite and the nearly aphyric unit a mugearite or benmoreite.

The four suites studied represent composite flows in both Tertiary and Carboniferous volcanics as well as composite sills and dykes ranging in age from Pre Cambrian to Pleistocene.

The hawaiites members of the composite bodies contain a wide range of plagioclase phenocryst composition, from bytownite to andesine. They may be accompanied by phases interpreted as originating in the immediate parental liquids at higher pressures. At least part of the variability in trace element distribution may be attributed to the polybaric fractionation of the phases observed.

Mugearites and benmoreites show less variability in their phenocryst composition, but an equally variable trace element distribution. This is not inconsistent with their postulated origin by crystal fractionation at relatively low pressures from hawaiites, themselves displaying a highly variable trace element content.

Ba, Sr, Zr, Zn, and Y all increase in passing from hawaiites to the mugearites; Rb is highly variable in content, but also shows an increase. The content of Nb increases, but at a much slower rate. Ni shows a marked decrease.

The content of Ba, Zr and possibly Zn, rises in passing from the mugearites to the benmoreites; the content of Sr and Ni decreases. Rb, Y and Nb are highly variable; the content either rises very slowly or remains steady.

The field, mineralogical and geochemical data are consistent with the various crystal fractional models proposed to explain the genesis of such bodies. Most of the bodies are believed to have developed in high level, compositionally zoned magma chambers. The composite flows represent the relatively rapid extrusion of lavas from such chambers; the various intrusive bodies represent either the serial tapping of such chambers to fill high level subadjacent cavities, or planar sections through such chambers exposed by erosion.

Use other side if necessary.